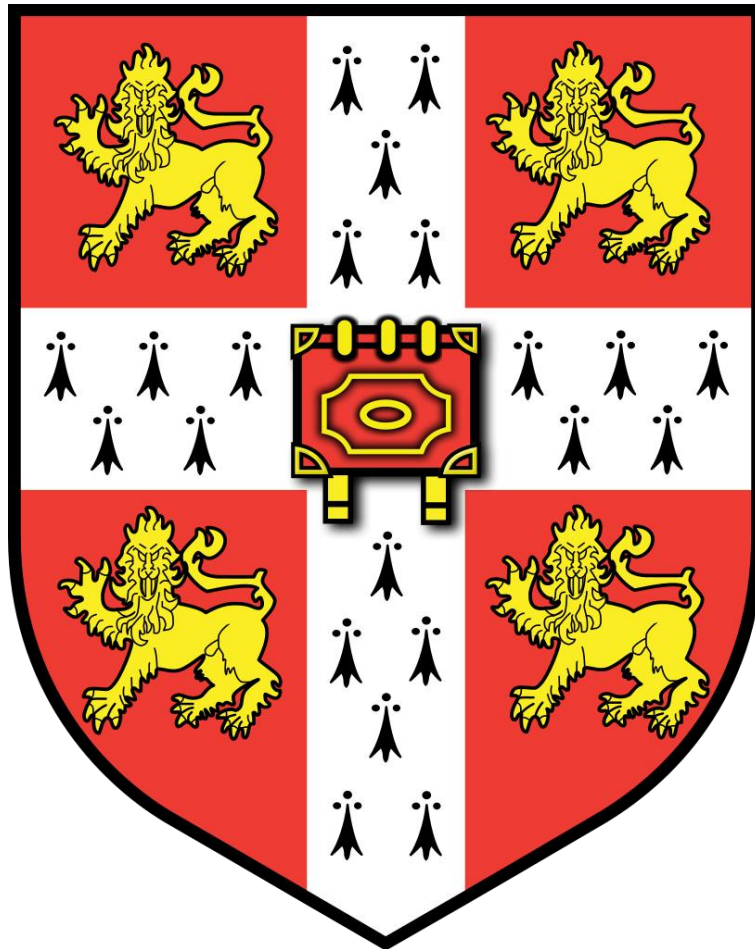


Imaging Correlates of Heterogeneity in the Syndromes Associated with Frontotemporal Lobar Degeneration



David John Whiteside

Corpus Christi College

University of Cambridge

This dissertation is submitted for the degree of Doctor of Philosophy

May 2023

Declaration

This thesis is the result of my own work and includes nothing which is the outcome of work done in collaboration except as declared in the Preface and specified in the text. It is not substantially the same as any that I have submitted, or, is being concurrently submitted for a degree or diploma or other qualification at the University of Cambridge or any other University or similar institution. The word count of does not exceed the prescribed word limit for the Degree Committee for the Faculties of Clinical Medicine and Veterinary Medicine.

Abstract

The syndromes associated with frontotemporal dementia are heterogeneous in their presentation and progression, with variable correlation between clinical phenotype and underlying proteinopathy. Single pathologies are associated with diverse clinical presentations, while the same clinical presentation can be caused by multiple pathological entities. Heterogeneity makes predicting underlying pathology and longitudinal outcomes challenging in clinical practice and in research settings. I propose that a multi-modal imaging approach, including structural and task-free functional magnetic resonance imaging, will provide mechanistic insight into how phenotypic variance arises and improve predictions of disease progression and survival.

In this thesis I draw from data for participants recruited at the University of Cambridge and from two multi-site collaborations, the Progressive Supranuclear Palsy Corticobasal Syndrome Multiple System Atrophy Longitudinal Study UK (PROSPECT-M-UK) and the Genetic Frontotemporal Dementia Initiative (GENFI). I describe characteristic differences in markers derived from task-free functional MRI and their relationship to patients' clinical manifestations. I relate these functional changes to imaging markers of neuronal loss, cell death and synaptic loss. I find that subcortical atrophy from structural MRI relates to cortical functional network disruption, and that synaptic loss measured through [^{11}C]UCB-J positron emission tomography affects behaviour in relation to changes in functional connectivity.

I investigate differences in functional connectivity across the disease course. In individuals with familial frontotemporal dementia, time-varying functional network abnormalities predict symptomatic conversion in presymptomatic mutation carriers and future cognitive decline in symptomatic participants. In progressive supranuclear palsy and corticobasal syndrome between-network connectivity explains variability in survival but does not improve predictive accuracy beyond clinical and structural imaging metrics.

Imaging-derived biomarkers in frontotemporal lobar degeneration need to be appropriately targeted at components of the neurodegenerative cascade. Task-free functional MRI is an objective and scalable neural marker of clinical syndrome, useful in detecting symptomatic onset and prognostication but limited by small effect sizes, poor signal-to-noise ratio, and moderate reliability. I discuss developments required in image acquisition and analysis to support clinical practice and trials of experimental treatments.

Acknowledgements

This work is only possible because of the combined efforts of a great many people at the Cambridge Centre for Frontotemporal Dementia and Related Disorders and the Cambridge Centre for Parkinson-plus. I have benefited from many years of patient recruitment and careful phenotyping. I am also lucky to have been able to call upon expertise in the clinical syndromes associated with frontotemporal lobar degeneration, neuroimaging, and statistical analysis. Particular thanks go to Simon Jones, Kamen Tsvetanov, Maura Malpetti, Alex Murley, and Negin Holland. I am grateful to all the research nurses, who have showed me how to treat patients with dignity and care. I am thankful to Professor James Rowe in giving me the wonderful opportunity to come to study in Cambridge and learn about neurodegenerative diseases. His constant enthusiasm to understand patients, pathology, and the workings of the brain are an inspiration. I am grateful for the support provided throughout my PhD by my supervisor Timothy Rittman, for his patient guidance on research methods and helping me to develop as a clinician scientist.

I thank the Cambridge Centre for Parkinson-plus for funding this research. I thank all the participants who have given their time to the various studies that support this study. Without them progress to curing these devastating illnesses would be impossible.

Lastly, I thank Sophia, who has, with great patience and love, put up with many hours of me prioritising my laptop over the very many other important things that constitute life.

Contents

Declaration.....	i
Abstract.....	ii
Acknowledgements.....	iii
Table of figures.....	vii
Abbreviations.....	ix
1 Introduction.....	1
1.1 The clinical syndromes associated with frontotemporal lobar degeneration	1
1.2 FTLN proteinopathies and the neuropathological cascade	10
1.3 Clinicoanatomical convergence and phenotypic diversity.....	13
1.4 Heterogeneity in progression in FTLN and the challenges of prognostication.....	15
1.5 Biomarkers of disease heterogeneity and progression in FTLN.....	18
1.6 Developments in clinical trials in FTLN.....	22
1.7 Structural magnetic resonance imaging in FTLN	23
1.8 Task-free functional magnetic resonance imaging.....	24
1.9 Positron emission tomography	28
1.10 Aims and hypotheses of this thesis.....	30
2 Study cohorts and methods	32
2.1 Cambridge Centre for Parkinson-plus and the Cambridge Centre for Frontotemporal Dementia.....	32
2.2 GENFI	35
2.3 PROSPECT-M-UK	37
2.4 Task-free functional MRI image pre-processing	39
2.5 Task-free fMRI analysis.....	42
2.6 Modelling clinical progression.....	48
3 Network dynamics in sporadic and familial frontotemporal dementia.....	52

3.1	Introduction	53
3.2	Methods.....	55
3.3	Results	60
3.4	Discussion	72
3.5	Supplementary materials for chapter 3.....	75
4	Network dynamics in progressive supranuclear palsy.....	79
4.1	Introduction	80
4.2	Methods.....	82
4.3	Results	86
4.4	Discussion	93
4.5	Supplementary materials for chapter 4.....	96
5	Functional connectivity and synaptic density in syndromes associated with Frontotemporal Lobar Degeneration.....	98
5.1	Introduction	100
5.2	Methods.....	102
5.3	Results	109
5.4	Discussion	118
5.5	Supplementary materials for Chapter 5.....	123
6	Imaging and clinical markers of survival in progressive supranuclear palsy and corticobasal syndrome	129
6.1	Introduction	130
6.2	Methods.....	132
6.3	Results	138
6.4	Discussion	148
6.5	Supplementary materials for chapter 6.....	152
7	Discussion.....	155
7.1	A summary of key findings.....	155
7.2	The utility of task-free fMRI in neurodegeneration	161

7.3	Towards precision medicine and supporting clinical trials	163
7.4	Conclusions	167
8	References	168
9	Appendix	223
9.1	Publications	223

Table of figures

Figure 1-1. A model of the pathophysiological cascade in neurodegenerative diseases.	12
Figure 1-2. Clinicopathological correlation in the syndromes associated with frontotemporal lobar degeneration.....	14
Figure 1-3. A conceptual framework for biomarker utility.	19
Figure 1-4. Two models of biomarker change through clinical disease stage.....	21
Figure 2-1. A schematic representation of the hidden Markov model pipeline used in chapters 3 and 4.....	47
Figure 2-2. A schematic representation of a linear mixed-effects model.....	49
Figure 3-1. Network dynamics in the Cambridge dataset.....	61
Figure 3-2. Network dynamics in GENFI.....	62
Figure 3-3. Principal component analysis loadings for state fractional occupancies	63
Figure 3-4. Fractional occupancy and neuropsychological assessments	65
Figure 3-5. Changes in network dynamics occur in the late presymptomatic phase.....	67
Figure 3-6. Cognitive decline in symptomatic participants	68
Figure 4-1 Network dynamics in PSP vs controls for the Cambridge cohort.....	87
Figure 4-2. Network dynamics in the PROSPECT cohort.	88
Figure 4-3. Complexity analysis	90
Figure 4-4. Significant areas of grey matter volume reduction in PSP v controls.....	91
Figure 4-5. Network dynamics, atrophy and network topology.	92
Figure 5-1. Regional differences between healthy controls and patients in A) [¹¹ C]UCB-J BP _{ND} and B) weighted degree.	110
Figure 5-2. Weighted degree and synaptic density	111
Figure 5-3. The effect of synaptic density, grey matter volume, and neurotransmitter receptors/transporter distributions on connectivity.....	112
Figure 5-4. Spatial variation in synaptic density and associated connectivity loss.	114
Figure 5-5. Functional connectivity, synaptic density, and clinical severity.....	116
Figure 6-1. Pipeline for assessment of relationship between large-scale network connectivity and severity, progression and survival.....	133
Figure 6-2. Between network connectivity in PSP and CBS.....	139
Figure 6-3. Differences in between-network connectivity between PSP and CBS.	140
Figure 6-4. Between network connectivity and clinical severity in PSP and CBS.....	141

Figure 6-5. Connectivity predicts longitudinal survival in PSP and CBS.	143
Figure 6-6. Identifying a transdiagnostic component predictive of outcome.	144
Figure 6-7. Partial least squares regression weights for a structural component predictive of survival.....	145
Figure 6-8. Connectome predictors of survival and regional atrophy	147
Figure 7-1. A schematic representation of personalised approach to medicine in FTLD.	164

Abbreviations

ACER	Addenbrooke's Cognitive Examination - Revised
AD	Alzheimer's disease
ALS	Amyotrophic lateral sclerosis
BET	Brain extraction tool
BOLD	Blood oxygen level dependent
BP _{ND}	Non-displaceable binding potential
BvFTD	Behavioural variant frontotemporal dementia
CBIR	Cambridge Behavioural Inventory - Revised
CBD	Corticobasal degeneration
CBS	Corticobasal syndrome
CCPP	Cambridge centre for Parkinson-plus
CSF	Cerebrospinal fluid
DVAR _S	Maximum spatial standard deviation of successive volume difference
FDG-PET	[18F]-fluorodeoxyglucose positron emission tomography
FDR	False discovery rate
FWE	Family-wise error
FWHM	Full width at half maximum
FAB	Frontal Assessment Battery
FIX	FMRIB's independent component analysis-based Xnoiseifier
fMRI	Functional magnetic resonance imaging
FMRIB	Oxford Centre for Functional Magnetic Resonance Imaging of the Brain
FSL	FMRIB Software Library
FTD	Frontotemporal dementia
FTLD	Frontotemporal lobar degeneration
FUS	Fused in sarcoma
GABA	Gamma-Aminobutyric acid
GENFI	Genetic frontotemporal dementia initiative
GIFT	Group independent component analysis of fMRIs
GRN	Progranulin
HMM	Hidden Markov modelling
ICA	Independent component analysis
JDR	Join dementia research
lvPPA	Logopenic variant primary progressive aphasia
MAPT	Microtubule associated protein tau
MDS	Movement disorders society
MMSE	Mini mental state exam
MND	Motor neuron disease
MNI	Montreal neurological institute
MPRAGE	Magnetization prepared rapid gradient echo
MRI	Magnetic resonance imaging
MRPI	Magnetic resonance parkinsonism index
nfvPPA	Non-fluent variant primary progressive aphasia
NHS	National health service
PALM	Permutation analysis of linear models

PCA	Principal Component Analysis
PET	Positron emission tomography
PIPPIN	Pick's disease and Progressive Supranuclear Palsy Prevalence and Incidence study
PLS	Partial least squares
PPA	Primary progressive aphasia
PREPARED	The Prospective Evaluation of Parkinson Plus and Related Disorders study
PROSPECT-M-UK	Progressive Supranuclear Palsy Corticobasal Syndrome Multiple System Atrophy Longitudinal Study UK
PSP	Progressive supranuclear palsy
PSP-RS	PSP Richardson's syndrome variant
PSPRS	PSP rating scale
SD	Standard deviation
SeNDER	Synaptic Evaluation in Neurodegenerative Research
SUVR	Standardised cortical uptake ratio
svPPA	Semantic variant primary progressive aphasia
TDP43	Transactive response DNA-binding protein 43 kDa
TE	Time to echo
TMTB	Trail making test B
TR	Time to repetition
[¹¹ C]UCB-J	((R)-1-((3-(methyl- ¹¹ C)pyridin-4-yl)methyl)-4-(3,4,5-trifluorophenyl)pyrrolidin-2-one)
UCL	University College London

1 Introduction

Neurodegenerative diseases are characterised by progressive loss of neuronal structure and function, resulting in decline in everyday function relative to premorbid performance (Dugger and Dickson, 2017; World Health Organization, 2019). Impairment can be in multiple cognitive domains, causing dementia, and in motor and physical well-being. Neurodegenerative diseases are common, with the number of people reaching diagnostic criteria for dementia globally estimated to increase from 57 million to over 150 million by 2050 (Nichols et al., 2022). These diseases come at great cost to the patient, their families, and to wider society, with an estimated \$263 billion global spending directly attributable to dementia in 2019 (Pedroza et al., 2022). Even in high income settings diagnosis is often delayed (Bradford et al., 2009; Department of Health, 2013; Livingston et al., 2020) and with variable correlation between clinical diagnosis and confirmed neuropathology at post-mortem (Beach et al., 2012). Delayed or missed diagnosis results in lost opportunities for timely and informed intervention (Hunter et al., 2015). There are currently no licensed disease modifying treatments for neurodegenerative diseases in the UK, with even therapeutics that successfully achieve their stated outcomes (van Dyck et al., 2022) challenging to implement in clinical practice and potentially not applicable to the majority of individuals with a relevant diagnosis (The Lancet, 2022; Walsh et al., 2022). There is therefore a pressing need to improve outcomes for people living with neurodegenerative diseases. Central to this is to understand how motor and cognitive impairments differ between individuals, variation in disease trajectory, and the causes of such heterogeneity.

Neurodegenerative syndromes arise from a spectrum of pathologies. In this thesis I focus on syndromes associated with frontotemporal lobar degeneration (FTLD), a neuropathological diagnosis characterised by progressive atrophy of the frontal and temporal lobes (Cairns et al., 2007; Mackenzie et al., 2010). FTLD as a neuropathological finding is associated with an umbrella of clinical syndromes: the behavioural variant frontotemporal dementia (bvFTD), progressive supranuclear palsy (PSP), corticobasal syndrome (CBS), the non-fluent/agrammatic variant of primary progressive aphasia (nfvPPA), and the semantic variant of primary progressive aphasia (svPPA). These clinically heterogeneous syndromes result in significant morbidity, reduced life expectancy, and include common causes of young onset dementia (Coyle-Gilchrist et al.,

2016). Given the overlap in symptomatology and neuropathology, there is benefit in considering the FTLD disorders together to understand shared neuropathological mechanisms and factors influencing disease progression.

In this chapter I introduce the syndromes and the primary pathological subtypes associated with FTLD, and the relationship between clinical diagnosis and pathological aetiology. I then explore the models of biomarker change in FTLD from presymptomatic accumulation of pathology to death. This provides a setting to discuss the role of neuroimaging biomarkers in FTLD in clinical practice, in supporting preclinical work, and in conducting trials of experimental treatments. The broad aim of this thesis is to understand how neuroimaging, particularly task-free functional magnetic resonance imaging, can be used to improve our understanding of heterogeneity in the symptom trajectory for individuals with FTLD and their families.

1.1 The clinical syndromes associated with frontotemporal lobar degeneration

In this section I will present the clinical syndromes associated with FTLD. Although they are described as distinct diagnostic entities it is important to recognise that they have overlapping clinical features, with patients often satisfying diagnostic criteria for more than one syndrome, while the most appropriate diagnosis may change through the disease course (Murley et al., 2020a).

1.1.1 Behavioural variant frontotemporal dementia

The behavioural variant frontotemporal dementia is a clinical syndrome of progressive changes in behaviour, personality, social conduct, and cognition (Rascovsky et al., 2011). Core behavioural features include marked apathy or inertia, impulsiveness, socially inappropriate behaviour, and loss of empathy (Boeve, 2022; Chow et al., 2009; Lansdall et al., 2017; Rascovsky et al., 2011; Snowden et al., 2001). Perseverative, stereotyped, compulsive or ritualistic behaviours may be observed in simple repetitive motor movements such as pacing or tapping, in stereotypy of speech, or in complex compulsive or ritualistic behaviours such as hoarding or walking fixed routes (Mateen and Josephs, 2009; Moheb et al., 2019; Rascovsky et al., 2011; Rosso et al., 2001). Changes in dietary behaviour and eating preferences are common, particularly in preferences for sweet foods and hyperorality (R. M. Ahmed et al., 2014; Ikeda, 2002; Miller et al., 1995). Oral exploration with ingestion of inedible objects may occur (Ikeda, 2002). These behavioural

changes have a profound impact on both the patient and their carers, with decline in caregiver health and healthcare related costs double that observed in Alzheimer's disease (Galvin et al., 2017).

The most prominent deficits on neuropsychological testing in bvFTD are typically in attention and executive function (Boeve, 2022; Rascovsky et al., 2011), although patients early in disease may perform within the normal range on many standard neuropsychological measures (Boeve, 2022; Piguet et al., 2017). Short executive batteries which incorporate measures of inhibitory control, verbal fluency and planning differentiate bvFTD from Alzheimer's disease (Leslie et al., 2016; Torralva et al., 2009). Nonetheless there is debate as to the specificity of impairments in executive functioning and attention for bvFTD, potentially reflecting the choice of testing modality used (Boeve, 2022; Hutchinson and Mathias, 2007; Ranasinghe et al., 2016). Part of the challenge is that patients with bvFTD may perform poorly on testing due to factors extrinsic to the cognitive domain intended to be tested, such as lack of motivation or concern with accuracy of answers (Mendez and Shapira, 2011; Ranasinghe et al., 2016).

Despite early proposals that the absence of akinesia and rigidity would support the diagnosis of frontotemporal dementia from Alzheimer's disease (Neary et al., 1988), motor signs and symptoms are commonly found in patients with bvFTD. In some series extrapyramidal features are observed in the majority of patients with bvFTD (Coyle-Gilchrist et al., 2016; Irwin et al., 2016), in keeping with neuropathological and imaging findings of striatal atrophy and loss of fronto-striatal connections (Bertoux et al., 2015; Irwin et al., 2016; Rowe, 2019). In contrast to idiopathic Parkinson's disease, rigidity is more likely to be predominantly axial, while limb akinesia may occur in the absence of rigidity (Rowe, 2019).

Approximately 20% to 40% of patients with bvFTD have a family history in keeping with a dominantly inherited familial disorder (Boeve, 2022; Greaves and Rohrer, 2019), with bvFTD the most common presentation of familial FTD (Moore et al., 2020). Mutations in three genes account for at least half of these cases: chromosome 9 open reading frame 72 (C9orf72), progranulin (GRN), and microtubule-associated protein tau (MAPT) (Greaves and Rohrer, 2019; Rohrer et al., 2009). Certain clinical characteristics show relative predominance depending on the causative mutation. Of particular note are the frequency of psychosis and anxiety in symptomatic patients with a C9ORF72 hexanucleotide expansion

(Ducharme et al., 2017), the association of this mutation with amyotrophic lateral sclerosis (DeJesus-Hernandez et al., 2011), and early parkinsonism in the MAPT mutation (Rowe, 2019).

Early and accurate diagnosis of bvFTD is important for families and carers but can be challenging, even for experienced clinicians. Many of the cardinal diagnostic features in bvFTD are observed in the behavioural/executive variant of Alzheimer's disease, with patients who ultimately have a pathological diagnosis of Alzheimer's disease tending to have a more restricted behavioural profile and co-existent memory impairment (Ossenkoppele et al., 2015). However memory impairment is well recognised in bvFTD (Hornberger et al., 2010) despite the inclusion of 'relative sparing of episodic memory' in the bvFTD diagnostic criteria (Rascovsky et al., 2011). A proportion of patients present with cognitive and behavioural impairment meeting the criteria for possible bvFTD, but without imaging abnormalities and whose symptoms do not progress (Hornberger et al., 2010, 2008; Kipps et al., 2009). The aetiology of this phenocopy syndrome of bvFTD is debated, with some cases likely due to late life decompensation of a psychiatric or neurodevelopmental disorder (Piguet et al., 2011b), although very slow evolution of symptoms has been observed in individuals with a C9ORF72 hexanucleotide expansion (Gómez-Tortosa et al., 2014).

1.1.2 Amyotrophic lateral sclerosis-frontotemporal dementia spectrum disorders

The co-existence of motor neurone diseases (particularly amyotrophic lateral sclerosis or ALS) and behavioural and cognitive impairment has long been recognised (Hudson, 1981), ranging from isolated dysexecutive function in at least half of patients with motor neurone disease, to symptoms meeting bvFTD criteria in up to a quarter of cases (Cividini et al., 2022; Strong et al., 2017). Strong and colleagues' consensus criteria set out the requirements for a diagnosis of ALS-FTD (Strong et al., 2017), which emphasises the spectrum of FTD-related deficits that arise in ALS. On these criteria individuals are classified as having ALS with normal cognition (ALS-cn), ALS with cognitive impairment (ALS-ci), ALS with behavioural impairment (ALS-bi), ALS with cognitive and behavioural impairment (ALS-cbi), and ALS with FTD (ALS-FTD).

The clinical heterogeneity and overlap between ALS and FTD is particularly recognised in patients with C9orf72, with expansions in the gene additionally associated with

parkinsonism and psychiatric features (Breevoort et al., 2022). Proposed pathogenic mechanisms for C9orf72 include loss of function (O'Rourke et al., 2016) or gain of toxicity from RNA expansion or via RNA translation products (Jiang et al., 2016; Nguyen et al., 2020). There may be synergistic and tissue specific effects of these processes which contribute to the variation in clinical presentation (Breevoort et al., 2022).

In ALS-FTD in general there is uncertainty as to whether cognitive/behavioural and motor symptom occur on a spectrum mirroring deposition of pathological protein, or if divergent phenotypes represent distinct diseases. The varying degree of cognitive and behavioural impairment is reflected in patterns of structural and functional changes observed on imaging (Cividini et al., 2022; Young et al., 2023). Both behavioural and executive dysfunction at baseline indicate poorer survival in ALS (Elamin et al., 2013; Hu et al., 2013), with relative stability of cognition in those who performed well on initial neuropsychological assessment.

1.1.3 Primary progressive aphasia

A clinical diagnosis of primary progressive aphasia (PPA) requires the presence from onset of a prominent, isolated and progressive language deficit caused by a neurodegenerative condition (Gorno-Tempini et al., 2011; Mesulam, 2003). Three variants of PPA are described, namely the semantic variant, non-fluent/agrammatic variant, and the logopenic variant. Logopenic variant primary progressive aphasia, characterised by impaired word retrieval and length-dependent difficulties with sentence repetition (Gorno-Tempini et al., 2008), is predictive of underlying Alzheimer's pathology (Spinelli et al., 2017). As such it is not considered a syndrome associated with frontotemporal lobar degeneration under current nosology (Mackenzie et al., 2010), and I will therefore focus on the other two variants here.

Speech in svPPA (also sometimes called semantic dementia) is fluent, but with impaired single-word comprehension and confrontational naming, indicating a profound loss in semantic knowledge (Hodges et al., 1992; Snowden et al., 1989). Speech production is often normal, particularly early in disease, such that a patient may be able to name an object without being able to define it (Hodges et al., 2008). Loss of object and concept knowledge begins with low frequency items, with progressive difficulties in more familiar objects as the disease develops. (Gorno-Tempini et al., 2008). Patients with svPPA will make regularisation errors, where atypical words are pronounced as they are spelt (Wilson et al.,

2009). Semantic variant PPA is relatively slowly progressing (Coyle-Gilchrist et al., 2016; Tastevin et al., 2021), with maintained performance in many cognitive domains until late in the illness. However behavioural dysfunction is common and may occur early in the condition, with symptoms including apathy, rigidity and clockwatching, and emotional withdrawal (Hodges and Patterson, 2007; Rosen et al., 2006). Bizarre food choices are more common than hyperorality (Hodges and Patterson, 2007) and may reflect food related semantic loss.

Imaging is important in the diagnosis of svPPA, with predominant and marked anterior temporal lobe atrophy (Gorno-Tempini et al., 2011; Hodges et al., 1992). Atrophy is normally asymmetrical, with more extensive atrophy in the left (language dominant) hemisphere in the majority of patients (Chan et al., 2009; Kumfor et al., 2016). There is currently a lack of consensus regarding terminology to describe the less commonly seen syndrome associated with focal right anterior lobe degeneration, with suggestions including *semantic behavioural variant frontotemporal dementia* (Younes et al., 2022), *right semantic dementia* (Mesulam et al., 2021), and *right temporal variant frontotemporal dementia* (Joubert et al., 2006). Characteristic clinical features of this syndrome are difficulty recognising familiar people and behavioural changes with early loss of empathy (Chan et al., 2009; Younes et al., 2022).

The core features of the non-fluent/agrammatic variant of primary progressive aphasia are effortful, halting speech and agrammatism, one of which must be present to meet published diagnostic criteria (Gorno-Tempini et al., 2011). Agrammatism is most commonly manifest as omission of short phrases such as function words (e.g. “of”, “it”, “to”) or inflections (Botha and Josephs, 2019; Gorno-Tempini et al., 2011). Speech may be slow and laboured, or with impairment in articulatory planning and programming (apraxia of speech). There is heterogeneity in the relative burden of agrammatism and apraxia of speech in patients with nfvPPA (Graham et al., 2016). Some individuals may present with only apraxia of speech and it has been argued that this should be considered a distinct diagnostic entity (Josephs et al., 2021), separate from the primary progressive aphasias due to lack of complaints of a language deficit. Patients may progress to develop signs and symptoms associated with corticobasal syndrome or progressive supranuclear palsy (Santos-Santos et al., 2016). A frontal cognitive syndrome may be found (Botha and Josephs, 2019; Rohrer and Warren, 2010), although the behavioural and socioemotional dysfunction tends to be less severe than in svPPA (Rosen et al., 2006).

There are a proportion of patients with primary progressive aphasia who cannot be classified into one of the three primary subtypes (Wicklund et al., 2014). While this may be due to the point on the disease course at which a patient is assessed, with either symptoms that are too mild to satisfy criteria or too severe to formally test, there are some patients who are unclassifiable throughout their illness (Botha and Josephs, 2019). Assessment and classification of patients with PPA is challenging, and modifications to the current criteria have been suggested to reduce the numbers of unclassified patients (Mesulam et al., 2021), although it is unclear yet if these changes improve ability to predict pathology and alter management.

1.1.4 Progressive supranuclear palsy

Progressive supranuclear palsy was first described in 1964 by Steele, Richardson and Olszewski as a progressive neurodegenerative condition characterised by supranuclear gaze palsy, axial predominant rigidity and early falls (Steele et al, 1964). The combination of postural instability and supranuclear gaze palsy has been subsequently termed Richardson's syndrome (Williams et al., 2005) as the most common of a range of PSP syndromes, in recognition of the varied clinical features associated with PSP pathology. A restriction in the range of voluntary vertical gaze, that can be at least partly overcome by the vestibulo-ocular reflex, is a cardinal diagnostic feature of PSP (Höglinger et al., 2017). Prior to development of a supranuclear gaze palsy slowing of vertical saccades or square wave jerks may be present (Chen et al., 2010). Patients with PSP often report visual disturbance, including diplopia (Hardwick et al., 2009), photophobia (Mohanty et al., 2021), and visual loss due to blepharospasm or apraxia of eye lid opening (Yoon et al., 2005) . Key motor features include parkinsonism, consisting of bradykinesia and rigidity. Typically, rigidity in PSP is predominantly axial and minimally responsive to levo-dopa (Höglinger et al., 2017; Litvan et al., 1996), although a proportion of patients present with a movement disorder that is initially clinically indistinguishable from Parkinson's disease (Williams et al., 2005). Postural instability in Richardson's syndrome occurs within three years of disease onset (Höglinger et al., 2017), with falls associated with significant morbidity and frequently necessitate careful weighting between encouraging mobilisation and reducing risk of injury (Brown et al., 2020).

Even in the initial nine cases of PSP presented by Steele and colleagues the majority had cognitive or behavioural impairment and included cases with severe dementia or where cognitive features were present at onset (Steele et al, 1964). Although the cognitive profile

of PSP had been described as a ‘subcortical dementia’ (Albert et al., 1974), with slowness of thinking (bradyphrenia) and executive dysfunction, subsequent work has shown that cortical pathology is common in PSP (Kovacs et al., 2020), with cortical features dominating the clinical presentation in a quarter of patients (Jabbari et al., 2020). Dementia occurs in approximately 70% of patients with PSP (Burrell et al., 2014; Pilotto et al., 2017), with the cognitive and behavioural symptoms overlapping with bvFTD (Kaat et al., 2007), including apathy, impulsiveness, hyperorality, social cognitive impairment, executive dysfunction, and language deficits (Bak et al., 2010; Burrell et al., 2014). Apathy and impulsivity commonly co-exist (Kok et al., 2021; Lansdall et al., 2017), with greater apathy and impulsivity predicting poorer survival and shorter time to requiring institutional care (Lansdall et al., 2019; Murley et al., 2021). Patients often lack insight into both their physical and cognitive deficits (O’Keeffe et al., 2007), with mismatches between carer- and patient-assessed rating scales of disability. Management of cognitive and behavioural symptoms in PSP is challenging (Bluett et al., 2021; Rittman et al., 2016a), with cognitive and behavioural change often causing significant distress to families and carers.

Impairments in speech, language and swallowing are also common in PSP. Speech in PSP has been described as an ‘adynamic dysarthrophonia’ (Peterson et al., 2019; Robinson et al., 2006), reflecting both a dysarthria arising from neurodegeneration to subcortical structures (Rusz et al., 2015) and impairment of executive function resulting in reduced verbal output (Peterson et al., 2019). A subset of patients who are ultimately found to have PSP pathology may present with a primary speech problem, including with non-fluent agrammatical speech or with apraxia of speech (Boeve et al., 2003a; Josephs, 2006; Josephs et al., 2021). Impaired swallow is evident on testing in the majority of patients with PSP (Clark et al., 2020) and is a poor prognostic sign (dell’Aquila et al., 2013).

Heterogeneity at the point of presentation is recognised in the most recent diagnostic criteria for PSP, which divides variant presentations by combinations of clinical features, with stratification based on sensitivity of these features for PSP pathology (Höglinger et al., 2017). These diagnostic criteria highlight the possibility of overlap with other FTLN syndromes, with possible variants including PSP with predominant corticobasal syndrome (PSP-CBS), PSP with a predominantly frontal presentation (PSP-F), and PSP with a speech and language disorder (PSP-SL). Patients will commonly satisfy more than one diagnostic category at the same time, and so rules have been designed to assist researchers in identifying a single predominant type per patient (Grimm et al., 2019), although these can

be challenging to apply and may fail to capture a patient's primary clinical manifestation (Shoeibi et al., 2019). Given that some variant presentations of PSP are rare, an additional stratification system has been proposed separating cases into three groups (PSP-Richardson's syndrome, PSP-subcortical and PSP-cortical) depending on the likely anatomical correlate of the dominant clinical features (Jabbari et al., 2020).

1.1.5 Corticobasal syndrome

The clinicopathological entity of corticobasal degeneration (CBD) was described by Rebeiz and colleagues (Rebeiz et al., 1968), with the clinical syndrome associated with the pathological diagnosis subsequently termed corticobasal syndrome (CBS) (Cordato et al., 2001). As I discuss below, CBS is associated with heterogenous underlying pathology (Boeve et al., 1999; Lee et al., 2011); through this thesis when using the term 'corticobasal syndrome' I refer only to the constellation of clinical features. CBS is a progressive asymmetric disorder with both cortical and extrapyramidal symptoms and signs (Constantinides et al., 2019). A diagnosis of probable corticobasal syndrome requires two of limb rigidity, limb myoclonus and limb dystonia, and also two of cortical sensory loss, alien limb phenomena, and apraxia (limb or orobuccal) (Armstrong et al., 2013). Asymmetrical rigidity and bradykinesia are common at presentation in CBS (Armstrong et al., 2013; Mathew et al., 2012), which rarely responds to dopaminergic therapy (Boeve et al., 2003b; Martin et al., 2021), although a trial of treatment is often warranted (Bluett et al., 2021). Dystonia is typically in the limbs rather than axial or cervical (Constantinides et al., 2019) and a postured hand may take a 'fisted' appearance or show finger hyperextension (Boeve et al., 2003b). Myoclonus is often prominent and may occur due to hyperexcitability of the motor cortex due to loss of inhibition from the sensory cortex (Lu et al., 1998), although subcortical structures have also been implicated (Di Stasio et al., 2019).

Apraxia is among the most common clinical features in CBS (Mathew et al., 2012), and may be observed in the limbs, face and mouth (orobuccal apraxia), eyelids (apraxia of eyelid opening) or eyes (ocular motor apraxia) (Armstrong et al., 2013; Boeve et al., 2003b; Mathew et al., 2012). In the alien limb phenomenon a patient's limb will act independently of the patient's reported intentions (Lewis-Smith et al., 2020), with reduced volitional control sense of agency (Wolpe et al., 2020), and must be more than simple levitation (Armstrong et al., 2013). Cortical sensory loss can be determined on examination by assessment for graphaesthesia, stereognosis or sensory extinction despite preservation of

primary sensory modalities, while patients may report numbness or tingling (Boeve et al., 2003b)

Clinical features associated with classical presentations of other FTLD syndromes can be found in individuals who develop corticobasal syndrome through their disease course. Frontal and executive dysfunction are common, including apathy, decreased verbal fluency, impaired reasoning, disinhibition and lack of empathy (Boeve et al., 2003b; Mathew et al., 2012). Aphasia in CBS is most frequently non-fluent, with both apraxia of speech and language deficits observed (Armstrong et al., 2013; Peterson et al., 2019). Other cognitive domains may also be affected, including episodic memory and visuospatial function (Bak et al., 2006; Day et al., 2017). Clinical overlap between CBS and PSP are recognised in diagnostic criteria for both syndromes (Armstrong et al., 2013; Höglinger et al., 2017), with variation in time to developing supranuclear gaze palsy potentially pointing to underlying pathological aetiology (Ling et al., 2010). In CBS, the clinical signs and symptoms appear to only weakly suggest underlying pathology (Lee et al., 2011), although clinical certainty may change through the disease course.

1.2 FTLD proteinopathies and the neuropathological cascade

Most neurodegenerative diseases are characterised by the accumulation of misfolded and aggregated proteins (reviewed in Soto and Pritzkow, 2018). FTLD can be subdivided into three primary sub-divisions based on the pathological protein (Mackenzie and Neumann, 2016), namely FTLD-tau, FTLD-TDP (TAR DNA-binding protein 43), and FTLD-FET (referring to the FET protein family). Below I discuss the first two subtypes, which account for approximately 95% of cases of FTLD (Irwin et al., 2015).

FTLD-tau can be considered within the broader framework of the *primary tauopathies*, a group of neurodegenerative conditions where the characteristic feature is abnormal intracellular accumulation of a hyperphosphorylated form of the microtubule-associated protein tau (Kovacs, 2015). Tau has an important role in maintaining neuronal integrity and axonal transport, with six isoforms of tau found in the adult human brain (Kovacs, 2015; Lee et al., 2001; Mackenzie and Neumann, 2016). These tau isoforms can be subdivided depending on whether they contain three (3R-tau) or four repeats (4R-tau) of the microtubule-binding domain. 4R predominant tauopathies include the pathological diagnoses of progressive supranuclear palsy and corticobasal degeneration. These are not synonymous with the clinical syndromes of PSP and CBS discussed above and in the next

section I consider further the associations between clinical syndrome and pathology. Characteristic features of PSP pathology include neuronal tau in the form of neurofibrillary tangles, tufted astrocytes, and oligodendroglial coiled bodies (Kovacs et al., 2020; Mackenzie and Neumann, 2016). Pathological change is often concentrated in subcortical structures (e.g. striatum, globus pallidus, subthalamic nucleus, midbrain tegmentum, substantia nigra, cerebellar dentate nucleus, and cerebellar peduncle) with variable cortical involvement (Kovacs et al., 2020; Mackenzie and Neumann, 2016). CBD is associated microscopically with a greater degree of cortical neuronal and astroglial tau, with more numerous neurophil threads and the pathognomonic finding of astrocytic plaques, although differentiating the two pathologically can be challenging in atypical cases (Kouri et al., 2011). In both CBS and PSP the distribution and load of tau pathology correlate with symptomatic burden (Kouri et al., 2011; Kovacs et al., 2020; Williams et al., 2005).

The term Pick's disease now refers to a predominantly 3R tauopathy with characteristic histological features of severe neuronal loss, swollen neurons and Pick bodies, a pathognomonic finding of large spherical argyrophilic neuronal cytoplasmic inclusions (Mackenzie and Neumann, 2016). The condition is named after Arnold Pick, who in 1892 described a 71 year old with progressive behavioural and language impairment (Berrios and Girling, 1994; Pick, 1892). The most common presentations of Pick's disease are with the behavioural variant FTD and nfvPPA (Piguet et al., 2011a). A proportion of patients with FTLT-tau have mutations in the MAPT gene (Hutton et al., 1998; Poorkaj et al., 1998; Spillantini et al., 1998), with clinical and pathological features overlapping with sporadic forms of FTLT-tau (Forrest et al., 2018).

TAR DNA-binding protein 43 is a ubiquitous protein important in regulation of RNA, including in alternative splicing and mRNA stabilisation (Jo et al., 2020). TDP-43 was identified as the pathological protein in most cases of FTLT without hyperphosphorylated tau in 2006 (Neumann et al., 2006; Sampathu et al., 2006), with subsequent work recognising four subtypes of FTLT-TDP (FTLT-TDP Types A-D) (Neumann et al., 2021). Differentiating the subtypes of FTLT-TDP can be challenging, with moderate interrater reliability, particularly between Types A and B (Alafuzoff et al., 2015). TDP-43 is also found in aging and in non-FTLT neurodegenerative conditions (including Alzheimer's disease and dementia with Lewy bodies) predominantly in limbic structures, with uncertainty as to whether these changes cause functional impairment (Neumann et al., 2021). TDP-43 Type A is found at post-mortem in patients with mutations in the

progranulin (GRN) gene, while hexanucleotide expansions in C9orf72 are associated with both Types A and B.

Full understanding of neurodegenerative diseases requires characterisation of a complex nexus of processes, from factors that increase the likelihood of protein misfolding and assembly, to determining how protein toxicity affects brain connections and thereby behaviour through cell death and synaptic dysfunction. This gives rise to the concept of a neurodegenerative cascade (Figure 1-1, Eimeren et al., 2019; Spires-Jones et al., 2017), with research methods from preclinical work to in vivo imaging studies aiming to shed light on distinct components of this cascade. Genetic (Chen et al., 2015; Ferrari et al., 2019) and environmental (Litvan et al., 2016; Rosso, 2003; Spencer et al., 1987) factors are important in increasing the chances of accumulation and propagation of misfolded proteins occurring. It is likely that multiple influences are important in shaping a patient’s pathology, clinical presentation, and disease course. Even in families with autosomal dominant mutations causing FTLD there is considerable within-family variation in age of disease onset and predominant symptoms (Cooper-Knock et al., 2014; Moore et al., 2020). Both tau and TDP-43 pathology accumulate with age, with brainstem tau found in most individuals by age 40 (Braak et al., 2011). It is possible that age related accumulation of protein is a prerequisite for neurodegeneration (Spires-Jones et al., 2017).

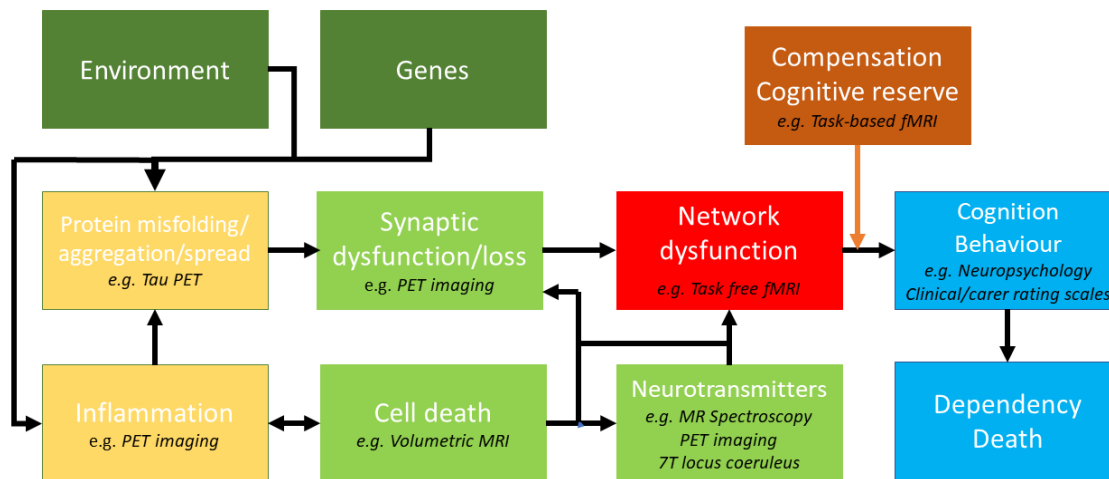


Figure 1-1. A model of the pathophysiological cascade in neurodegenerative diseases. Examples are given of imaging and other biomarkers and their utility in characterising respective components of this cascade.

In this thesis I predominantly focus on the lower part of the neurodegenerative cascade, to understand how changes in brain connections influence behaviour and the factors that determine maintenance or loss of connections. Pathological proteins may mediate

breakdown of connections in FTLD through direct toxic effects or indirectly through biological dysfunction to cellular processes that result in neuronal dysfunction or death (reviewed for FTLD-TDP and FTLD-tau in de Boer et al., 2021 and Yoshiyama et al., 2013). Brain connections may be functionally lost through synaptic dysfunction even without neuronal and cell death (Spires-Jones and Hyman, 2014). Inflammation and the presence of co-pathology (Spires-Jones et al., 2017) are important factors in the initiation and acceleration of FTLD pathogenesis and subsequent connectivity loss. There are also extensive neurotransmitter deficits found in FTLD (reviewed in Murley and Rowe, 2018), with performance on cognitive tasks and cortical physiology associated with in vivo measures of neurotransmitter levels (Adams et al., 2021; Murley et al., 2020b). Investigating the relationship between pathology, synaptic dysfunction, neurotransmitter deficits, connectivity and behaviour has the potential to detect important and reversible deficits in neurodegeneration.

1.3 Clinicoanatomical convergence and phenotypic diversity

Clinical syndrome in FTLD is often only moderately predictive of pathology (Figure 1-2). The strength of the association is variable depending on the syndrome in question and the disease stage. For instance, Richardson's syndrome is strongly associated with PSP 4R tauopathy (Litvan, 1997; Osaki et al., 2004), while most patients with svPPA have TDP-43 Type C (Spinelli et al., 2017). In contrast, bvFTD and CBS are highly pathologically heterogeneous. The disassociation between clinical syndrome and pathological findings gives rise to two key concepts when investigating heterogeneity in FTLD, namely *clinicoanatomical convergence* and *phenotypic diversity* (Seeley, 2017).

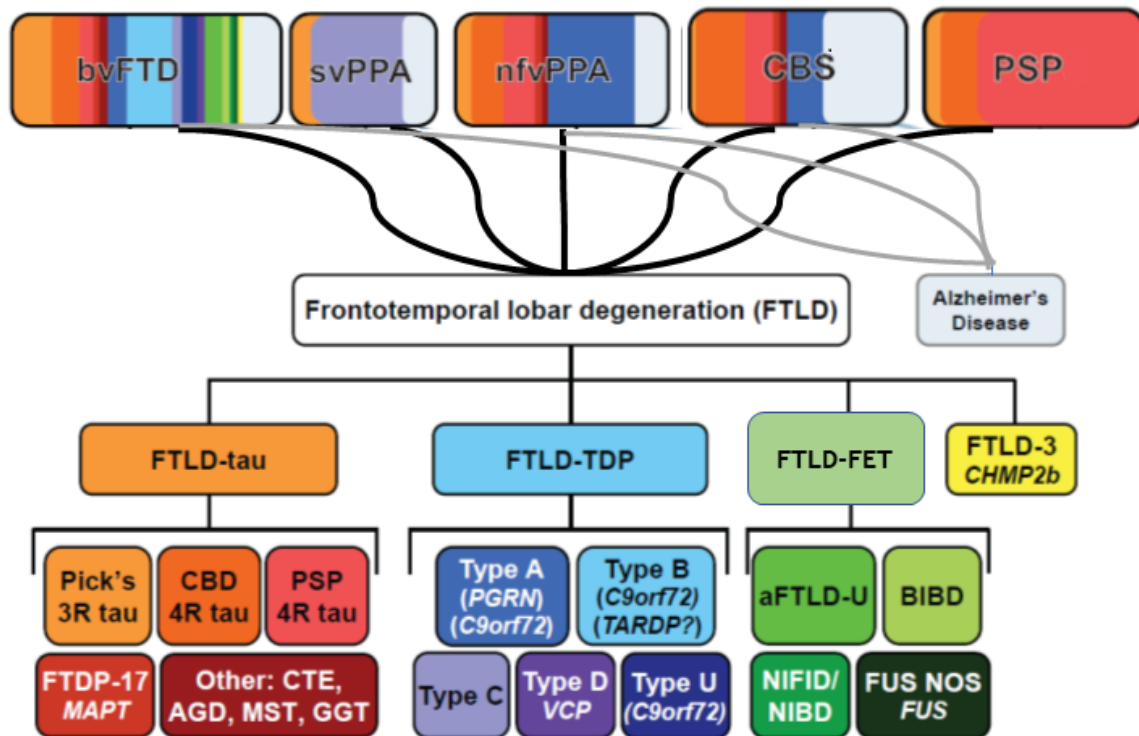


Figure 1-2. *Clinicopathological correlation in the syndromes associated with frontotemporal lobar degeneration.* Vertical colour stripes represent the proportion of patients with the corresponding pathological finding shown at the bottom. bvFTD, behavioural variant frontotemporal dementia; svPPA, semantic variant primary progressive aphasia; nvPPA non-fluent variant primary progressive aphasia; CBS, corticobasal syndrome; PSP, progressive supranuclear palsy; TDP, TAR DNA-binding protein; CBD, corticobasal degeneration; PGRN, progranulin; C9orf72, chromosome 9 open reading frame 72; BIBD, basophilic inclusion body disease; FTDP-17, frontotemporal dementia with parkinsonism linked with chromosome 17; MAPT, microtubule associated protein tau; CTE, chronic traumatic encephalopathy; VCP, valosin-containing protein; AGD, argyrophilic grain disease; MST, multiple system atrophy tauopathy with dementia; GGT, globular glial tauopathy; NIBD, neurofilament inclusion body disease; NIFID, neuronal intermediate filament inclusion disease; FUS, fused in sarcoma. Image adapted from Kim and colleagues (Kim et al., 2016), reprinted with permission from Cambridge University Press.

Clinicoanatomical convergence refers to the fact that the same clinical presentation can be caused by multiple pathological entities. This arises when distinct pathologies can affect the same region or neurons, or instead involve anatomically distinct components of a disparate brain network responsible for certain cognitive functions (Seeley, 2017). Various (non-exclusive) factors may be influential in allowing clinicoanatomical convergence to arise. Brain regions or a single brain network may have shared vulnerability due to common protein expression (Rittman et al., 2016b), greater metabolic demand (de Haan et al., 2012; Liang et al., 2013; Saxena and Caroni, 2011), or lack of trophic factors (Appel, 1981). Anatomical distribution of pathologies may be influenced by transneuronal spread of pathogenic protein from an initial ‘seed’ site, in a similar manner as occurs in prion disease (Clavaguera et al., 2009; Darricau et al., 2022; Frost and Diamond, 2010; Goedert, 2015; Jucker and Walker, 2018; Prusiner, 1984).

Phenotypic diversity describes the variety of clinical syndromes that may be associated with a single pathology. For instance, PSP pathology may present with Richardson's syndrome, corticobasal syndrome, nonfluent/agrammatical PPA, or with a behavioural and dysexecutive syndrome. This suggests that pathogenic proteins variably involve a finite set of brain regions, either as initial seeds or due their relative vulnerability for reasons outlined above, or instead that that each protein can be subtyped further into distinct sub-strains that correspond to different clinical syndromes (Seeley, 2017). Recent cryo-electron microscopy work characterising the structure of neurodegenerative proteins suggests that tau sub-strains may be an important contributor to heterogeneity, notably the finding that some variants of PSP have distinct tau filament structures (Shi et al., 2021).

1.4 Heterogeneity in progression in FTLN and the challenges of prognostication

Neurodegenerative diseases may show heterogeneity not only in clinical presentation but also in progression and outcome. Predicting progression and long-term outlook is important both to individuals at risk of dementia and to patients with neurodegenerative disease. The Lancet Commission on Dementia Prevention, Intervention and Care emphasises the importance of advanced care planning and early discussion of the future with patients and their families, with timely intervention potentially reducing distress in patients with advanced dementia and families' care burden (Livingston et al., 2020). Moreover with growing numbers of trials of disease modifying agents and the arrival of treatments that significantly reduce the rate of cognitive decline (Cummings et al., 2021; van Dyck et al., 2022), there is a pressing need to improve prognostication and to accurately risk-stratify trial participants. Yet predicting prognosis is challenging and clinician estimates of outcome may be imprecise.

Longitudinal observational studies of carriers of genetic mutations causing dementia have shown that neuropathological and structural change accumulate many years prior to symptom onset and a diagnosis of dementia. In autosomal dominant Alzheimer's disease changes in cerebrospinal fluid amyloid-beta are detectable 25 years before expected symptom onset, followed by amyloid-beta deposition on positron emission tomography and atrophy on structural magnetic resonance imaging 15 years before expected symptom onset (Bateman et al., 2012). In familial frontotemporal dementia atrophy may be observed up to four decades before expected symptom onset (Rohrer et al., 2015; Staffaroni et al., 2022),

with variation in the timing of biomarker change between mutation types. Less is known about the chronology of pathological change in individuals with sporadic dementias, with ongoing developments in this area possible due to large prospective cohort studies of healthy individuals such as the UK Biobank (Miller et al., 2016; Sudlow et al., 2015). Work led by colleagues in our group have found deficits on quality of life measures and neuropsychological testing many years prior to diagnosis in neurodegenerative disease, including in conditions that cause FTLD (Street et al., 2022; Swaddiwudhipong et al., 2022). Our group have also demonstrated that it is possible to use neuroimaging as a biomarker to identify patients at high risk of Alzheimer's disease before symptoms develop, raising the possibility of early intervention to stop or slow down the condition (Azevedo et al., 2022).

While in autosomal dominant Alzheimer's disease age of symptom onset can be accurately predicted from parental age of onset and mutation type (Ryman et al., 2014), this has not been found to be the case for non-MAPT carriers of mutations causing familial frontotemporal dementia (Moore et al., 2020). For instance, parental age of onset only explains 14% of variability in age of symptom onset in progranulin mutation carriers. Unlike in Huntington's disease there is no clear evidence that length of C9orf72 expansion size influences timing of conversion to symptomatic disease (Fournier et al., 2019). Neurofilament light chain (NfL), a non-specific fluid biomarker that is increased in a range of neurological conditions, may be a useful aid to identify mutation carriers on the cusp of symptom onset (van der Ende et al., 2019).

Variation is also seen in progression and survival in individuals with sporadic diseases causing FTLD. Survival is shortest in PSP and CBS, with average survival from symptom onset between six and eight years (Coyle-Gilchrist et al., 2016). While survival is longer in bvFTD, a greater proportion of time with disease is spent in care homes (Murley et al., 2021). In semantic variant PPA and the non-fluent/agrammatic variant PPA survival from disease onset is between nine and twelve years (Nunnemann et al., 2011). Divergence in outcome is seen not only across clinical syndromes but also in individual pathologies, with a subset of individuals with PSP showing exceptionally long survival (Lukic et al., 2022).

Clinical features and phenotypic variability are associated with heterogeneity in disease progression. The rate of progression is slower in the subcortical phenotypes of PSP (PSP-Parkinsonism and PSP-Progressive Gait Freezing) than in the classic PSP-Richardson's

form of the disease (Jabbari et al., 2020). In keeping with this, early falls and dysphagia are indicators of poor survival in PSP (Glasmacher et al., 2017). Features of motor neurone disease in FTD-ALS at initial presentation predict faster progression and shorter survival than those with presenting with a primarily cognitive syndrome (Ahmed et al., 2020). Clinical features may predict prognosis across diagnostic labels, with motor features in FTLD associated with short absolute survival, while greater behavioural impairment predicts time to care home admission (Murley et al., 2021). Apathy has been associated with both poor survival in FTLD (Lansdall et al., 2019) and with progression in presymptomatic mutation carriers in familial FTD (Malpetti et al., 2021a).

While understanding clinical predictors of prognosis assists accurate prognostication, it does not allow us to make direct mechanistic inferences about the neuropathological processes contributing to altered survival and phenotypic variation. In certain cases, longer survival from symptom onset may arise from the severity of clinical manifestation despite mild burden of pathology, perhaps due to impaired ability to compensate or to regional selective vulnerability to disease. This may be relevant to the long-standing observation that the prevalence of dyslexia is increased in the families of patients with primary progressive aphasia (Rogalski et al., 2008). Untangling the relative contributions of regional vulnerability versus factors that attenuate or accelerate the underlying pathological process is important when investigating potential targets for treatments that alter prognosis. Studies using imaging, fluid biomarker and genetic data provide insight into this. Greater neuroinflammation in PSP and Alzheimer's disease, as measured through positron emission tomography, is associated with increased rate of change in markers of clinical severity (Malpetti et al., 2021b, 2020). Genetic variation at the LRRK2 locus is associated with poorer survival in PSP (Jabbari et al., 2021), with LRRK2 potentially mediating proteostasis and the inflammatory response. Metabolic changes are common in FTD, with lower cholesterol associated with poorer survival in patients with FTD-ALS (Ahmed et al., 2017).

Accurate prognostication is relevant to patients from the development of presymptomatic pathological change to end-of-life care. Its importance is in supporting patients to make informed decisions about their care, in improving studies of experimental medicines, and in advancing our understanding of disease to identify novel therapeutic targets. In the next section I will discuss the range of biomarkers available to explain heterogeneity in

phenotype and survival in FTLD, and how variance explained by these biomarkers may vary through the disease course.

1.5 Biomarkers of disease heterogeneity and progression in FTLD

A biomarker is an objectively quantifiable measure that relates to underlying biology, a pathological process or response to a therapeutic intervention (NIH Biomarkers Definition Working Group, 2001). There are a wide array of putative applications for biomarkers, including in confirming diagnosis, disease monitoring, detecting or predicting treatment response, prognostication and for risk assessment before or after exposure to a therapeutic agent (FDA-NIH Biomarker Working Group, 2016). Biomarkers may therefore have a role not only in patient diagnosis, stratification, prediction and prognostication, but also as primary outcome measures for clinical trials.

In evaluating heterogeneity and progression in FTLD it is necessary to consider both the type of biomarker under consideration and its intended purpose. In this thesis much of the focus will be on clinical and imaging biomarkers. Clinical biomarkers can be derived from clinician history or examination, neuropsychological testing, or formalised rating scale (relevant examples discussed in further detail in chapter 2). Reliance on clinical data can be problematic when making predictions or assessing outcomes in neurodegenerative conditions (Eimeren et al., 2019). For instance, in presymptomatic FTLD there may be a significant time lag between the optimal point for intervention and the onset of clinical syndrome (Beach, 2017). Similarly in trials in symptomatic participants key outcomes, such as survival, require assessment over many years and as a result may be impractical (Strimbu and Tavel, 2010). As highlighted above, clinical assessments also show variable relationship with underlying neuropathology. Neuroimaging can potentially be used to augment assessments based on clinical data or instead be used as surrogates of a clinical outcome of interest. In the latter case, to provide benefit the effect size of the imaging biomarker must be at least equivalent to the related clinical measure over the same period (Eimeren et al., 2019). An imaging biomarker that demonstrates short-term change associated with long-term clinical outcome has the potential to improve and de-risk drug development (Cummings, 2019; Manyara et al., 2022). For a surrogate to be accepted as a trial endpoint, it requires a strong mechanistic rationale for the association between the biomarker and clinical outcome of interest (FDA-NIH Biomarker Working Group, 2016).

Eimeren and colleagues (2019) provide a conceptual framework to assess and categorise biomarkers (Figure 1-3). A biomarker may be useful in detecting a patient population *early* in disease, may be *specific* to underlying neuropathology, or be helpful in monitoring disease *progression*. When considering progression, they emphasise the difference between anticipation and correlation. A biomarker anticipates change if the effect size of the biomarker is associated with clinical progression at a late date, in contrast to biomarker change over time correlating with clinical progression. This framework clarifies that a biomarker may be useful even if it is not specific to neuropathology, and that a biomarker useful to detect early disease may not predict progression. Considering time dependent ordering of biomarker change within a model of disease progression leads to the concept of a cascade of biomarkers, a biomarker counterpart to the neurodegeneration cascade (Figure 1-4; Gordon et al., 2016; Jack et al., 2010; Sperling et al., 2011). For instance, cerebral atrophy, as detected by structural MRI, may be a relatively late phenomenon and represent the end process of neuronal and synaptic loss, axon degeneration and cell death (Fung et al., 2020; Planche et al., 2022). It may be hypothesised that in the presymptomatic phase of neurodegenerative diseases supra-normal function is required to maintain levels of performance given build-up of pathology, leading to biomarker specific models that directly characterise and allow testing for compensatory mechanisms (Figure 1-4; Gregory et al., 2018, 2017).

Grade	Early	Specific	Progression
A	Pre-symptomatic	Any variant of specific pathology	Anticipation and rationale
B	Before clinical criteria	Conclusive in a variant	Anticipation
C	After clinical criteria	Partial separation (e.g. tau v alpha-synuclein)	Correlation

Figure 1-3. A conceptual framework for biomarker utility. From Eimeren and colleagues (2019)

Decades of research into neuroimaging in FTLTD have so far resulted in limited validated imaging biomarkers (Whitwell et al., 2017), with only structural magnetic resonance

imaging markers currently used as secondary endpoints in FTLD clinical trials (Boxer et al., 2020; Dam et al., 2021; Höglinger et al., 2021; Vivash et al., 2020). The difficulties in part arise from moderate test-retest reliability for some modalities (Elliott et al., 2020; Noble et al., 2019). Reliability may be improved by brain-wide dimension-reduction techniques (Duff et al., 2022), but this potentially comes at a loss of anatomical and disease specificity. Although studies in FTLD have shown good group differentiation they may fail to generalise due to focus on specific phenotypes, small sample sizes from single centres, and lack of post mortem confirmation of pathology (Eimeren et al., 2019; Whitwell et al., 2017).

Research in potential neuroimaging biomarkers must also consider rapid developments in fluid biomarkers relevant to FTLD. Plasma neurofilament light chain has a potential role in differentiating people with Parkinson's disease from other neurodegenerative diseases with parkinsonism (Ashton et al., 2021), with higher levels predictive of more rapid progression in PSP (Rojas et al., 2016). The ratio between NfL and another plasma biomarker, glial fibrillary acidic protein, may be useful in discriminating FTLD-tau from FTLD-TDP (Cousins et al., 2022). New cerebrospinal fluid (CSF) biomarkers have been shown to differentiate corticobasal degeneration from other FTLD-tau (Horie et al., 2022). There has also been progress in using plasma biomarkers to distinguish people with Alzheimer's disease from other neurodegenerative diseases (Palmqvist et al., 2021; Thijssen et al., 2021, 2020), reducing cost and patient burden compared to current CSF or positron emission tomography biomarkers, and relevant for the FTLD syndromes where Alzheimer's disease is a possible underlying pathology.

Much of the development of biomarkers of heterogeneity and disease progression in FTLD has been in genetic forms of FTLD, given the possibility of identifying study participants for longitudinal modelling from the presymptomatic stage to disease onset. It is common to make the assumption that biomarker models in genetic dementias provide support for their sporadic comparators (Jack and Holtzman, 2013). Genetic and sporadic bvFTD show similar cross-sectional neuropsychological features (Capozzo et al., 2017; Heuer et al., 2020), suggesting that measures focused on key symptoms of genetic FTD might be applicable to both groups. However, we currently do not have sufficient comparable longitudinal data to ensure that longitudinal outcomes overlap. Moreover, pathophysiological differences exist between genetic and sporadic variants of FTD (Del Campo et al., 2022), and indeed between the genetic form of FTD. Therefore the

applicability of biomarker profiles in genetic FTLT to sporadic forms may depend on the biological or clinical mechanism being targeted.

In the next section I will place this conceptual framework for biomarker development in the context of the state of the art in treatment trials in FTLT. I will then discuss the current role, prospects, and challenges facing researchers of imaging biomarkers in FTLT.

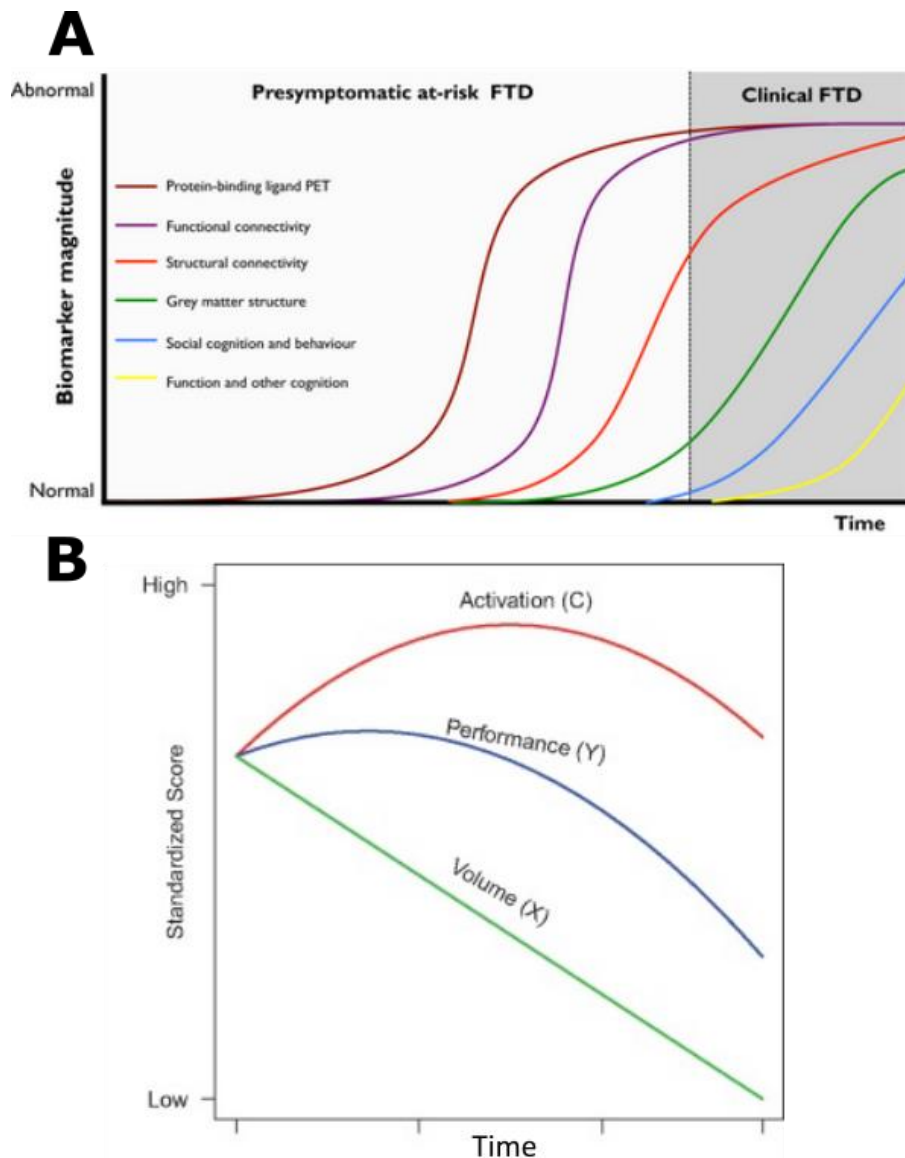


Figure 1-4. *Two models of biomarker change through clinical disease stage* A) Biomarker levels may change in the presymptomatic period in a time dependent manner, with detection of abnormal proteins possible before structural change and the development of clinical symptoms (From Gordon et al., 2016, reprinted with permission from Wiley). B) The brain may compensate in the early stages of disease to maintain performance despite build-up of pathology. This may be captured by biomarkers targeting these compensatory processes with supra-normal levels (from Gregory et al., 2018, with x-axis relabelled).

1.6 Developments in clinical trials in FTLD

There are currently no approved medications for FTLD, although symptomatic medications are often trialled and are beneficial in a proportion of patients (Bluett et al., 2021; Tsai and Boxer, 2014). While heterogeneity and comparative rarity of FTLD syndromes pose challenges for clinical trial design, the relatively high proportion of familial cases and existence of syndromes with rapid progression mean that phase 3 trials in certain cohorts are feasible (Boxer et al., 2020). The mechanism of action targeted in current trials in carriers of pathogenic FTLD-causing mutations vary, and include: monoclonal antibodies aimed at restoring progranulin protein levels in GRN mutation carriers (Jackson et al., 2021); gene therapy to replace the defective gene using viral mediated gene delivery (Arrant et al., 2018); and anti-sense oligonucleotides, which are small molecules designed to target messenger RNA and therefore modulate protein expression (Liu et al., 2022). One phase 3 trial for GRN mutation carriers recruits asymptomatic participants with raised levels of NfL, highlighting the importance of novel biomarkers in presymptomatic and early disease.

Most trials aimed at targeting tau in FTLD have been in PSP, an appealing condition for trialists given the high clinicopathological correlation in its classical form (Grossman, 2021). Candidate agents in trials have included monoclonal antibodies that bind tau (Dam et al., 2021; Höglinger et al., 2021), therapies that aim to reduce tau transcription and aggregation, and antisense oligonucleotides targeted at the MAPT gene (Przewodowska et al., 2021). These trials have so far failed to show clinical benefit, which may be a consequence not only of limitations of agents but also due to the clinical profile of the trial cohort (Grossman, 2021; Höglinger et al., 2021). One possibility is that the trials start too late, once neuropathology is well established. In sporadic neurodegenerative disease, particularly in PSP where diagnosis is delayed, there is therefore a need for biomarkers that assist early diagnosis to ensure that tau burden is sufficiently mild to respond to intervention. Biomarkers that accurately identify less common variants of PSP have the potential to increase the population eligible for trials (Street et al., 2021).

There are grounds for optimism for the prospect of new treatments in FTLD. We turn next to the role of different imaging modalities in supporting this progress, as well as their use in diagnosis and prognostication in clinical practice in FTLD.

1.7 Structural magnetic resonance imaging in FTLD

Structural MRI, using T1- and T2- weighted contrasts, are widely used in routine practice and in research settings in neurodegenerative diseases. Here I define structural imaging as referring to modalities that provide static anatomical information (Symms, 2004), with the focus in this thesis on measures of grey matter atrophy rather than structural connections, white matter degeneration or markers derived from quantitative susceptibility mapping. Atrophy, the loss of brain parenchyma relative to a control population or observed within an individual on longitudinal imaging, is a presumed marker of neuropathological change in neurodegenerative conditions (Kantarci and Jack, 2004). It is plausible that atrophy is the result of multiple complex interconnected processes in neurodegenerative disease. For instance, while tau pathology on post-mortem is associated with atrophy observed in vivo on structural MRI in PSP and CBS, the effect size of the association is only moderate (Spina et al., 2019).

Patterns of atrophy on structural imaging are associated with particular clinical syndromes in FTLD and may point to underlying neuropathology. PSP is associated with disproportionate midbrain atrophy, with imaging in the midsagittal plane resembling a hummingbird's beak and head (Kato et al., 2003). Other prominent sites of atrophy are the superior cerebellar peduncle, basal ganglia and frontal lobe (Whitwell et al., 2017). The structural imaging hallmark of corticobasal syndrome is asymmetric frontoparietal atrophy (Whitwell et al., 2017), observed across the different pathological aetiologies of the syndrome. The behavioural variant frontotemporal dementia atrophy is commonly found in the prefrontal cortex, anterior cingulate and in the insula cortex (Rosen et al., 2002; Whitwell, 2019). In semantic variant primary progressive aphasia, atrophy is found in the temporal lobes with an anteroposterior gradient and striking atrophy at the temporal poles (Hodges et al., 1992). Structural imaging in the non-fluent variant primary progressive aphasia is relatively normal, with mild inferior frontal and anterior temporal lobe atrophy in the dominant hemisphere (Grossman, 2012).

Atrophy in FTLD can be quantified to provide objective biomarkers to improve accuracy of diagnosis and assess neuropathological correlation. Examples in PSP include the ratio between midbrain and pons diameters (Cosottini et al., 2007), and the MR Parkinsonism Index (MRPI), which additionally takes into account the middle and superior cerebellar peduncles (Quattrone et al., 2008). The MRPI has shown good diagnostic accuracy in

differentiating PSP from other pathologies (Grijalva et al., 2022; Illán-Gala et al., 2022). The highest accuracy for differentiating PSP and CBD from other pathologies has been found with a combination of cortical and subcortical measures (Illán-Gala et al., 2022), with regional atrophy also differing between PSP phenotypes (Jabbari et al., 2020). Variable accuracy has been found when differentiating FTLN pathologies from Alzheimer's Disease (Bruun et al., 2019; McCarthy et al., 2018) without specific imaging markers of FTLN-tau or FTLN-TDP (Whitwell, 2019). Less is known how measures derived from structural MRI predict prognosis in FTLN. Brainstem measures have been found to be associated with worse outcome in PSP (Cui et al., 2020; Dutt et al., 2016), while diffuse atrophy predicts poorer survival in bvFTD (Lee et al., 2017).

Challenges remain in maximising the use of structural MRI in clinical practice in FTLN. Many structural imaging studies are in research cohorts and have focused on differentiating participants with neurodegenerative conditions from healthy controls, and therefore fail to address questions reflecting true clinical need. Instead, studies need real world cohorts on patients using hold out test sets, ideally collected from different sites, to ensure that structural biomarkers outperform current clinical practice. In addition, mechanistic inference is difficult, given the uncertainty as to the relative contribution of different pathological processes in driving atrophy in neurodegeneration.

1.8 Task-free functional magnetic resonance imaging

Magnetic resonance imaging can be used not only to map brain structure but also to capture activations associated with specific tasks or behaviours. In 1991 John Belliveau and colleagues presented work that showed localised increases in blood volume in the visual cortex associated with visual stimulation in patients given sequential injections of gadolinium (Belliveau et al., 1991). In the same year the first experiments were performed which demonstrated the potential utility of the blood-oxygen-level-dependent (BOLD) effect (Kwong et al., 1992; Ogawa et al., 1992), a change in neurovasculature in response to neural activity detectable as a result of the differential magnetic susceptibility of oxygenated and deoxygenated blood. This approach to imaging, termed functional MRI (fMRI), had the advantage of being non-invasive and relatively fast to acquire. The foundational work in the field was followed by a proliferation of novel applications, methodological advances and technical innovations (Bandettini, 2012).

One key development in functional MRI was the discovery that correlations in BOLD signal that recapitulate the topographic distribution of task-evoked responses could be observed without a stimulus (Biswal et al., 1995). This finding was in keeping with the longstanding observation that the brain accounted for a disproportionate amount of energy consumption, and that the brain's metabolic requirements differed little between a task and non-task state (Kety and Schmidt, 1948; Sokoloff et al., 1955). Functional MRI could therefore provide information about the intrinsic activity of the brain with whole-brain coverage and high spatial resolution. Using fMRI to study the brain 'at rest' has enabled identification of multiple networks of topographically distributed regions which show temporally correlated activity (Fox and Raichle, 2007; Yeo et al., 2011). These task-free or *resting state* networks are spatially consistent across subjects (Damoiseaux et al., 2006) and correspond to activation maps generated from task-based studies (Smith et al., 2009).

Multiple approaches have been used to investigate functional connectivity, the statistical dependencies (correlation or covariance) between timeseries derived from different regions of the brain. In seed-based functional connectivity investigators assess the cross-correlation between a chosen region of interest (the seed) and the rest of the brain. Instead data-reduction techniques may be used to identify large-scale networks (Beckmann et al., 2005; Shirer et al., 2012) followed by analysis of correlations within or between these networks. Graph theoretical approaches allow interrogation of functional imaging by describing the brain as a set of nodes (brain regions) linked by edges representing functional connections (Bullmore and Sporns, 2009).

While canonical approaches to functional connectivity have averaged over the scan acquisition time, time-varying fluctuations in connectivity can be also effectively captured by functional magnetic resonance imaging (fMRI) (Calhoun et al., 2014; Chang and Glover, 2010; Vidaurre et al., 2017). These approaches attempt to model the dynamical nature of mind wandering and internal models of the world (Deco et al., 2017; Lurie et al., 2019), in order to more fully capture the variance associated with task-independent brain activity (Killingsworth and Gilbert, 2010). The hypothesis that time-varying large-scale network activity is behaviourally important reflects evidence that temporal co-ordination of neurons occurs at the microscale (Berkes et al., 2011) and in non-human animal studies (Musall et al., 2019).

Understanding and mapping involvement of networks and connections in neurodegenerative diseases provides a potential explanatory bridge from pathology to clinical manifestation. Atrophy patterns in neurodegenerative diseases mirror patterns of functional connectivity to selected seed regions in the healthy brain (Seeley et al., 2009). Regions with greater numbers of connections are associated with greater atrophy (Crossley et al., 2014) and burden of pathological proteins (Cope et al., 2018; Franzmeier et al., 2022). One of the earliest identified resting state networks, the *default mode network*, has been suggested to be preferentially targeted in Alzheimer's Disease (Greicius et al., 2004; Yu et al., 2021). Connectivity of the *salience network*, with cortical hubs at the anterior insular and dorsal anterior cingulate cortices, is attenuated in behavioural variant FTD (Dopper et al., 2013; Zhou et al., 2010) and associated with the cardinal manifestations of the disease (Toller et al., 2018).

In the last two decades there have been a rapid growth in publications that have investigated resting state functional connectivity in neurodegeneration. Despite early optimism (Dickerson, 2006; Vemuri et al., 2012) this work has failed to result in direct clinical applications and has no proven utility in clinical trials of experimental medicines. Given this it is unsurprising that there is scepticism about the benefits of funnelling resources to studies of task-free functional MRI in clinical neuroscience (Kullmann, 2020). I will discuss three key challenges that limit the translation of task-free fMRI work in neurodegeneration into clinical practice.

In clinical studies using resting state functional MRI it is usually assumed that BOLD signal fluctuations correspond to neuronal activity, and that this activity contributes to brain function. Although resting state networks have been found to mirror intracortical neurophysiological recordings (Shmuel and Leopold, 2008), BOLD signal has neural and vascular determinates and is not a direct measure of neural activity (Logothetis, 2008; Tsvetanov et al., 2015). Networks derived from functional MRI show only moderate correspondence to structural networks (Mišić et al., 2016) with much of the intra- and inter-individual variation in functional connectivity unexplained. The opaqueness of the interpretability of the BOLD signal and connectivity differences is particularly important where inconsistent results have been found without a clear link to clinical syndromes, disease physiology or underlying pathology. For instance in PSP and CBS there are diffuse connectivity differences from healthy controls (Ballarini et al., 2020; Brown et al., 2017), but the direction of change is not consistent across studies (Bharti et al., 2017; Roskopf et

al., 2017). Moreover these differences have not been found to be predictive of regional pathological burden at post-mortem (Spina et al., 2019). Were results to be consistent, reproducible, and reliably related to other biomarkers it could be argued that the uncertainty regarding the neural origins of the BOLD signal could be ignored. Given that this is not case, the lack of an underlying ground truth accessible (or testable) by alternative methodologies is a concern.

The second difficulty facing task-free functional MRI research is that the effect sizes for associations between complex cognitive phenotypes and functional connectivity in healthy populations are small (Marek et al., 2022). The high dimensional datasets and analytic flexibility provided by task-free fMRI in the context of even moderate associations risks publication of false or inflated results (Ioannidis, 2008). In addition, effects that require large numbers of participants to demonstrate are unlikely to be relevant in uncommon conditions where imaging acquisition may be challenging. It is plausible to expect stronger associations in neurodegeneration than in health or in psychiatric illnesses as a result of the gross disruption to brain structure in the former. Choice of analytic technique is important, with increases in effect sizes by using multivariate methods (Marek et al., 2022; Yoo et al., 2019) and time-varying connectivity approaches (Moguilner et al., 2021).

Subject movement during scanner acquisition can have a substantial impact on measurements of task-free functional connectivity (Power et al., 2012; Satterthwaite et al., 2012), with even small movements affecting BOLD signal. This is of particular concern in conditions that cause FTLD, where impairment in attention, executive dysfunction and Parkinsonism mean that head motion is greater than in healthy controls. Metrics that measure in-scanner motion during fMRI acquisition have important neural correlates (Geerligs et al., 2017) and potentially relate to severity and clinical outcomes in neurodegenerative conditions. Therefore, simply regressing out motion from measures of functional connectivity risks removing important disease effects that are the focus of our investigation. A variety of standardised pre-processing pipelines are now available that include processes to remove sources of artefact in a principled manner (Esteban et al., 2019; Smith et al., 2013a), but these may fail to completely remove all head movement effects in high motion individuals.

These concerns can in part be addressed by rigorous methodology, including careful pre-processing of data, analysis and hypothesis preregistration, and replication of results in

different datasets. They also require considered use of task-free fMRI. Functional changes should closely align with changes of symptoms in neurodegeneration, and indeed functional network integrity is maintained in the presymptomatic phase in individuals at risk of dementia, with increased coupling between functional connectivity and cognition close to symptom onset (Rittman et al., 2019; Tsvetanov et al., 2020). This suggests that task-free fMRI would likely be poor at differentiating underlying pathologies where there is symptomatic convergence. Instead, it may act as an objective and scalable neural marker of clinical syndrome, useful in detecting symptomatic onset and prognostication. This is in keeping with the tight relationship between neuronal connectivity and cognition hypothesised in the neurodegenerative cascade in Figure 1-1. Understanding of the origin of functional connectivity patterns in neurodegeneration can be enhanced by comparison with other modalities, including markers of atrophy, synapse loss and neurotransmitter receptor distributions.

1.9 Positron emission tomography

Positron emission tomography (PET) is an imaging technique that uses an injection of a radiolabelled ligand to investigate molecular processes of interest in vivo, with a wide range of available ligands used both in clinical practice and research settings (Cope et al., 2021; Rittman, 2020). Targeted molecular processes in neurodegenerative diseases include quantifying regional metabolic activity through [18F]-fluorodeoxyglucose (FDG-PET), beta-amyloid (e.g. Pittsburgh compound-B, Klunk et al., 2004), tau neuropathology in both Alzheimer's disease and other tauopathies (e.g. AV-1451, Lowe et al., 2016), neuroinflammation, synaptic loss, and mapping neurotransmitter receptor densities (Hansen et al., 2022). The variety of potential targets for ligands enables assessment of the pathological cascade in neurodegenerative diseases and exploration of different disease mechanisms in determining phenotypic heterogeneity, disease progression and survival. While the use of PET imaging is most mature in Alzheimer's disease, with both beta-amyloid PET (van Dyck et al., 2022) and tau PET (Mintun et al., 2021) used in clinical trials, developments in PET imaging in FTLD dementias have shown promise in overcoming challenges facing the field, such as the reduced binding affinity and off-target binding in first-generation tau PET ligands (Leuzy et al., 2019). In this section I focus on radioligands assessed in this thesis, namely markers of synaptic density and neurotransmitter receptor distributions, and consider their role as part of multi-modal approach to characterising FTLD.

Synaptic dysfunction has been proposed as a key mid-stream component in models of development of neurodegenerative disease, with toxic proteinopathies and neuroinflammation leading to altered synaptic function and density, which in turn cause downstream functional effects, even prior to cell death. Synaptic health and plasticity have key roles in generating neurophysiological connections (Hebb, 1949; Ramon y Cajal, 1894), with preclinical and neuropathological studies showing widespread synaptic dysfunction and impaired plasticity to be key determinants of impaired brain network organisation in neurodegenerative diseases (DeKosky and Scheff, 1990; Spires-Jones and Hyman, 2014; Terry et al., 1991), including in FTLD (Bigio et al., 2001; Lipton et al., 2001). The PET radioligand [¹¹C]UCB-J quantifies synaptic density through selective binding to the presynaptic vesicle glycoprotein 2A (SV2A) (Finnema et al., 2016). [¹¹C]UCB-J binding has been found to be reduced in neurodegenerative diseases, including in Alzheimer's disease (Mecca et al., 2020), Parkinson's disease (Matuskey et al., 2020) and in FTLD syndromes (Holland et al., 2020; Malpetti et al., 2022). Combining this marker of synaptic density with imaging measures of function and structure promises therefore to provide insight into heterogeneity in FTLD, including the possibility of quantifying when therapeutic interventions are likely to be most successful.

A further factor that is potentially important in accounting for heterogeneity in FTLD syndromes is altered neurotransmitter systems, with variable reductions in receptor densities or in neurotransmitter levels observed in noradrenaline, dopamine, glutamate, γ -aminobutyric acid (GABA), serotonin and acetylcholine (Huber et al., 2022; Murley and Rowe, 2018). Post-mortem and fluid biomarker work have found mismatches between biochemical assays of neurotransmitter levels and receptor densities (for instance for serotonin in FTD, Vermeiren et al., 2016; Yang and Schmitt, 2001), potentially indicating compensatory mechanisms important in maintaining functional performance. Quantifying neurotransmitters and receptor populations with imaging markers of cell death, synaptic density and function enables detailed biophysical modelling across the course of disease and assessment of therapeutic interventions (Cope et al., 2021). PET radioligands for multiple receptors and neurotransmitter transporters have been used in healthy populations and in individuals with neurodegenerative diseases (Finnema et al., 2015; Hansen et al., 2022). Challenges in designing and interpreting PET imaging as an indirect measure of extracellular neurotransmitter levels include uncertainty about target specificity of radioligands, high cost of acquiring imaging, and the need to consider the neurotransmitter

intrinsic activity to the receptor as well as the possibility of receptor internalisation (Finnema et al., 2015). Multi-modal imaging studies have the potential to ensure findings from such studies are robust and produce biologically plausible results.

1.10 Aims and hypotheses of this thesis

In this thesis I aim to advance understanding of the utility of imaging biomarkers in explaining phenotypic heterogeneity and progression in frontotemporal lobar degeneration, assessing their use both for clinical practice and to support trials of experimental medicines. I focus primarily on task-free fMRI, exploring the determinants of functional connectivity and its role as a mediator of clinical syndrome. I explore imaging changes across the disease course in FTLD, from predicting symptomatic conversion in presymptomatic carriers of FTD-causing mutations to estimating survival in sporadic PSP and CBS.

I therefore set the following broad objectives:

- To determine whether task-free fMRI, as a marker of neural activity closely tied to cognition in neurodegenerative diseases, a) predicts disease progression and survival in FTLD, and b) explains phenotypic diversity in these conditions
- To determine the relative contribution of atrophy, synaptic change and neurotransmitter deficits in maintenance and loss of functional connectivity in FTLD, and the interaction between connectivity and its determinants in explaining clinical syndromes.

The specific hypotheses of my thesis are:

- 1) Measures derived from task-free fMRI differ between individuals with FTLD syndromes and cognitively normal controls, including time-varying network measures (chapters 3 and 4), graph metric approaches (chapters 4 and 5), and connectivity between large-scale networks (chapter 6).
- 2) Large-scale network differences, captured through fMRI, occur in presymptomatic individuals at risk of developing FTLD syndromes as they near disease onset and predict conversion to symptomatic disease (chapter 3).
- 3) fMRI derived time-varying network measures explain phenotypic diversity in FTLD syndromes (chapters 3 and 4).

- 4) Reduced synaptic density is associated with reduced functional connectivity in FTLN syndromes, with the effect of synaptic loss on cognition moderated by connectivity change (chapter 5).
- 5) Differences in functional connectivity and network activation in FTLN syndromes occur remotely from sites of atrophy and synaptic loss (chapters 4 and 5).
- 6) Atrophy, synaptic density loss and distribution of neurotransmitter receptors/transporters in combination explain a greater proportion of variance in connectivity in FTLN syndromes than individually (chapter 5).
- 7) Functional connectivity differences predict survival in FTLN syndromes (chapter 6).
- 8) Functional connectivity improves prediction of survival in FTLN syndrome over and above clinical measures, demographics and atrophy (chapter 6).

In the following chapter I describe the cohorts and neuropsychological and clinical assessments used to test these hypotheses. I then discuss image acquisition and pre-processing, before describing the fMRI analysis techniques used to address my hypotheses. I outline relevant data-reduction techniques and discuss statistical modelling of longitudinal change.

Given the limitations of fMRI as an imaging modality as set out above, I adopt various approaches to analysis to improve robustness and reliability:

- Replication of imaging findings from locally collected data in a second, multi-centre, cohort (Chapters 3 and 4).
- Preregistration of fMRI analysis pipeline and hypotheses prior to formal testing (Chapter 3).
- Multivariate and data-reduction techniques to identify a small number of features that explain variance in the outcome of interest (Chapters 3-6).
- Cross-validation comparing imaging and clinical biomarkers in their ability to predict patient outcome (Chapter 6).

2 Study cohorts and methods

This thesis uses data from participants recruited at the University of Cambridge and from two multi-site collaborations, the Progressive Supranuclear Palsy Corticobasal Syndrome Multiple System Atrophy Longitudinal Study UK (PROSPECT-M-UK) and the Genetic Frontotemporal Dementia Initiative (GENFI). In this chapter I describe participant recruitment, neuropsychological and clinical assessment, and imaging acquisition for each of these cohorts. A broad overview of the cohorts is provided in Table 2-1. I discuss methodological approaches I use in subsequent experiments, in pre-processing and analysis of task-free fMRI, and in modelling of longitudinal change in clinical severity and predicting survival. Additional methodological details relevant to individual projects are described in their respective experimental chapter (Chapters 3-6).

2.1 Cambridge Centre for Parkinson-plus and the Cambridge Centre for Frontotemporal Dementia

The Cambridge Centre for Parkinson-plus (CCPP) and the Cambridge Centre for Frontotemporal Dementia are research centres at the University of Cambridge which also provide National Health Service tertiary referral clinics for people suspected to have a clinical syndrome associated with frontotemporal lobar degeneration. In this thesis I draw on data from multiple studies at the University of Cambridge led by Professor James Rowe that have recruited patients since 2007. Key protocols include: *The Prospective Evaluation of Parkinson Plus and Related Disorders* (PrEPPAReD) study; *The Pick's disease and Progressive Supranuclear Palsy Prevalence and Incidence* study (PiPPIN) (Coyle-Gilchrist et al., 2016; Murley et al., 2020a); and *Synaptic Evaluation in Neurodegenerative Research* (SENDeR) (Holland et al., 2020). While there is variation in hypotheses and study designs of the different protocols, there is overlap in patient phenotyping, clinical and neuropsychological assessment, and imaging acquisition. In combination these patient cohorts make possible robust testing of the hypotheses set out in chapter 1.

2.1.1 Participants

All participants were reviewed by the clinical team at the Cambridge Centre for Parkinson-plus and the Cambridge Centre for Frontotemporal Dementia. In this thesis I consider participants with a diagnosis of a clinical syndrome associated with frontotemporal lobar

	CCPP (bvFTD)	CCPP (PSP/CBS)	GENFI (datafreeze 5)	PROSPECT	SENDeR
Diagnoses	bvFTD Control	PSP/CBS Control	Genetic FTD and first- degree relatives (mutation and non- mutation carriers)	PSP/CBS/ Control Also recruited MSA and atypical Parkinsonism	PSP/CBS/bvFTD Control
Chapters of this thesis	3	4 and 6	3	4 and 6	5
Years recruited	2008-2020	2007-2022	2012-2019	2015-2019	2018-2022
Imaging sites	Cambridge University (Wolfson Brain Imaging Centre)	Cambridge University (Wolfson Brain Imaging Centre)	25 research centres in Europa and Canada	Cambridge University, University College London, Oxford University	Cambridge University (Wolfson Brain Imaging Centre)
Modalities included in this thesis	Structural imaging, fMRI	Structural imaging, fMRI	Structural imaging, fMRI	Structural imaging, fMRI	Structural imaging, fMRI, UCB-J PET
Structural imaging					
Tesla	3	3	1.5-3	3	3
Echo time	2.86-2.93ms	2.86-2.93ms	Median 2.9ms	2.93ms	3.6ms
Repetition time	2-2.3s	2-2.3s	Median 2s	2s	9.2ms
Voxel-size	1.1mm- 1.25mm isotropic	1.1mm- 1.25mm isotropic	Median 1.1mm isotropic	1.1mm isotropic	0.55x0.55mm (interpolated to 1mmx1mm)
Functional imaging					
Tesla	3	3	1.5-3	3	3
Echo time	30ms	30ms	30ms	30ms	30ms
Repetition time	2-2.5s	2-2.5s (chapter 4 2s only)	Median 2.5s	2.5s	2.5s
Volumes	155-305	140-305 (305 volumes only in chapter 4)	122-305 (median 200)	200	200
Resolution	3x3x3.5mm/ 3x3x3.75mm	3x3x3.5mm/ 3x3x3.75mm (chapter 4 3x3x3.75mm only)	Median 3x3x3.5mm	3x3x3.5mm	3x3x3.5mm

Table 2-1. Overview of the clinical characteristics and imaging acquisition parameters in the cohorts studied in this thesis. Full details of the acquisition parameters for GENFI are provided in Supplementary Table 3.1. bvFTD behavioural variant frontotemporal dementia; PSP progressive supranuclear palsy; CBS corticobasal syndrome, MSA multiple system atrophy

degeneration, focusing on those who satisfy diagnostic criteria during the disease course for progressive supranuclear palsy (Höglinger et al., 2017; Litvan et al., 1996), corticobasal

syndrome (Alexander et al., 2014), and behavioural variant frontotemporal dementia (Rascovsky et al., 2011). A proportion of participants also registered for post-mortem brain donation to the Cambridge Brain Bank. I discuss findings at autopsy for these participants in the relevant chapters (chapters 4 and 6). In chapter 6 I also include participants who had a final neuropathological diagnosis of progressive supranuclear palsy or corticobasal degeneration but may have had an alternative clinical diagnosis at time of scanning. Given the heterogeneity in study protocol from which I acquired participant data there is variation in frequency and interval for follow-up from baseline scanning session, with most participants reviewed on repeat occasions. For analysis of survival in chapter 6 I recorded date of death from participants' NHS Summary Care Record.

2.1.2 Clinical and neurocognitive assessments

For the Cambridge cohort I focus in this thesis on widely used and well-validated clinical rating scales and carer-rated markers of severity, specifically the Progressive Supranuclear Palsy-Rating-Scale (PSPRS), the Addenbrooke's Cognitive Examination-Revised (ACE-R), and the Cambridge Behavioural Inventory-Revised (CBI-R). These outcome measures have the advantages of being collected for most participants at follow up visits and overlapping with the PROSPECT-M-UK assessment protocol.

The PSPRS (Golbe and Ohman-Strickland, 2007) is a clinician-assessed rating scale consisting of motor and non-motor features from participant history and physical examination. It shows high inter-rater reliability with linear progression through the disease course (Golbe and Ohman-Strickland, 2007) and has been the primary outcome measure in clinical trials of therapeutics in PSP (Dam et al., 2021; Höglinger et al., 2021). The first iteration of the Addenbrookes' Cognitive Examination (Mathuranath et al., 2000) was designed to provide a short, standardised neurocognitive assessment that overcame limitations in the Mini-Mental State Examination (MMSE) (Folstein et al., 1975), which is insensitive to early and non-Alzheimer's dementias (Devenney and Hodges, 2017). It has since been updated with the Addenbrooke's Cognitive Examination-Revised (ACE-R) (Mioshi et al., 2006) and the Addenbrooke's Cognitive Examination III (ACE-III) (Hsieh et al., 2013). The Cambridge Behavioural Inventory is an informant-based questionnaire that captures cognitive, behavioural, affective, and functional symptoms across 13 domains (Wedderburn et al., 2008). The CBI-R is a reduced 45-item version of the full questionnaire (Wear et al., 2008).

2.1.3 Neuroimaging acquisition

Participants included in this thesis were scanned at the Wolfson Brain Imaging Centre in the University of Cambridge between 2007 and 2022. There is some variation in scanner used and imaging acquisition parameters between study protocols, with standardisation from 2016 to align with imaging protocols used in the GENFI2 and PROSPECT-M-UK studies. All participants were imaged using a 3-Tesla scanner. High resolution T1-weighted Magnetization Prepared Rapid Gradient Echo (MPRAGE) structural images were acquired with repetition time (TR) of 2-2.3s, time to echo (TE) of 2.86-2.93ms, flip angle 8°-9°, voxel size 1.1mm-1.25mm isotropic. Echo-planar imaging was acquired with eyes open in a dark bore with TR 2-2.5 secs, TE 30ms, 3x3x3.5mm/3x3x3.75mm voxels, 140-305 volumes.

Note that in some chapters only participants scanned under selected protocols are included. In chapter 4 I only use images in the Cambridge cohort with 300 volumes, given the potential advantage of the longer scan (and therefore increased volume numbers) in estimating time-varying connectivity. In chapter 5 imaging acquisition parameters are identical to those in GENFI2, since recruitment for scanning with the PET ligand [¹¹C]UCB-J began in 2018. In chapter 6 I combine all available imaging data from the Cambridge cohort with PROSPECT-M-UK data, and use an empirical Bayesian framework called *ComBat* to account for site effects (Johnson et al., 2007, described further within the chapter).

I describe synthesis, image acquisition, image reconstruction and kinetic analysis of [¹¹C]UCB-J PET imaging in the methods section of chapter 5.

2.2 GENFI

The Genetic Frontotemporal dementia Initiative is a multi-site international longitudinal observational study of familial frontotemporal dementia, led at University College London (UCL) by Professor Jonathan Rohrer. The study co-ordinates research across multiple centres, recruiting large numbers of participants despite the rarity of genetic FTD, in order to provide mechanistic understanding and develop robust biomarkers of disease onset and progression (Rohrer and Boxer, 2021). Since the presence of an autosomal dominant mutation allows an individual at-risk of FTD to be identified long before symptom onset, participants can be studied both prior to and after disease onset. Given the clinical similarity

between sporadic and familial FTD it is plausible that biomarkers and therapies tested in GENFI would generalise to sporadic disease (Heuer et al., 2020). GENFI commenced with a pilot phase (GENFI1) in 2012, which was followed by an expanded five-year study (GENFI2) in 2015. Data is collated centrally at University College London and made available through periodic data freezes. In this thesis I use data from all participants included at datafreeze 5, with a latest date of assessment of 31st May 2019.

2.2.1 Participants

Participants were recruited from 25 research sites across Europe and Canada. Inclusion criteria were that participants must be aged over 18 and have a known pathogenic mutation in MAPT, C9ORF72, GRN or TANK-binding kinase 1 (TBK1) or were a first degree relative of a mutation carrier. Participants underwent testing for gene status, a standardised clinical and neuropsychological testing battery, MRI scanning, blood testing and lumbar puncture for cerebrospinal fluid. Where participants were unable or did not consent to all components of the full GENFI protocol (e.g., if they were unable to undergo MRI scanning), a partial assessment could be performed. Assessments were repeated yearly or biannually, with longitudinal data up to 7 years post baseline visit.

Participants were categorised on two axes: first, depending on their gene status as a mutation *carrier* or *non-carrier*; second as *symptomatic* or *asymptomatic*. If first-degree relatives of mutation carriers had not undergone predictive testing, the participant and clinical investigators were blinded to their genetic status, with mutation status known only to the GENFI team at UCL. Clinicians classified mutation carriers as either symptomatic or asymptomatic, with participants deemed symptomatic if symptoms were present, were progressive in nature and consistent with a diagnosis of an FTD-related degenerative disorder, including amyotrophic lateral sclerosis. Mutation carriers not considered symptomatic are termed *presymptomatic* mutation carriers.

For the analysis in chapter 3 I include all participants from GENFI datafreeze 5 with usable task-free fMRI (prior to exclusions for excess motion), consisting of 198 symptomatic mutation carriers, 341 presymptomatic mutation carriers and 329 family members without mutation. GENFI datafreeze 5 includes data from a total of 2,264 visits. I took the first assessment centre with task-free fMRI imaging to be the baseline visit with analysis of longitudinal data including follow-up from this point.

2.2.2 Clinical and neurocognitive assessments

The GENFI assessment consists of a standardised clinical history, physical examination, neuropsychological assessment, and informant-based questionnaires (Rohrer et al., 2015). Neuropsychological tests used in all stages of GENFI were taken from the Uniform Data Set (Morris et al., 2006) and included the Trail Making Tests A and B, Digit Symbol Test, Forwards and Backwards Digit Span from the Wechsler Memory Scale-Revised, Letter and Category Fluency, a short version of the Boston Naming Test, plus the Mini Mental State Examination (MMSE). The severity of behavioural symptoms and functional status was assessed using the Cambridge Behavioural Inventory-Revised (CBI-R) and the Frontotemporal Dementia Rating Scale (Mioshi et al., 2010).

The large number of neuropsychological tests performed creates a potential multiple comparison problem when comparing imaging-derived metrics with clinical severity. I therefore pre-registered neuropsychological tests (Backwards Digit Span, Digit Symbol, Trail Making Test B) as outcomes of interest in presymptomatic mutation carriers, and focused on these tests plus the MMSE and CBI-R in analysis of longitudinal change in severity.

2.2.3 Neuroimaging acquisition

Imaging was acquired at each of the GENFI sites, with imaging sequences developed by the GENFI Imaging Core team. GENFI imaging acquisitions were standardised from GENFI 2 onwards, with some variation in imaging acquisition parameters in the first GENFI iteration. In chapter 3 I utilise all images performed up to and including GENFI datafreeze 5. Echo-Planar Imaging and MPRAGE were acquired at each site at 3T or 1.5T where no 3T scanner was available. Echo-Planar Imaging was acquired with a median TR 2500ms, TE 30ms, median volume number 200 (range 122-305, upper and lower bound of interquartile range 200), in-plane resolution of 3x3mm and slice thickness of 3.5mm. T1 weighted MPRAGE structural images had a median isotropic resolution of 1.1mm, median TR 2s and median TE 2.9ms. Detailed task-free fMRI acquisition parameters for the dataset analysed in chapter 3 are provided in the supplementary materials for chapter 3.

2.3 PROSPECT-M-UK

The Progressive Supranuclear Palsy Corticobasal Syndrome Multiple System Atrophy Longitudinal Study UK (PROSPECT-M-UK) is an ongoing UK-based multi-site

longitudinal observational study of people with progressive supranuclear palsy, corticobasal syndrome, multiple system atrophy, and with disorders in which parkinsonism is a feature but where there is diagnostic uncertainty (atypical parkinsonian syndromes). The study aims to improve understanding and diagnosis in these conditions, supporting biomarker development and characterising the disease course to inform therapeutic trials. The chief investigator for the study is Professor Huw Morris at University College London. Recruitment began in 2015 from 7 participating centres in England and Wales. Data is collated centrally at University College London and made available through periodic data freezes. In chapters 4 and 6 I use data from participants included at datafreeze 2, with a latest imaging assessment date of 8th October 2019. Baseline cross-sectional data for PROSPECT-M-UK is described by Jabbari and colleagues (Jabbari et al., 2020).

2.3.1 Participants

Participants were eligible for inclusion in PROSPECT-M-UK providing they satisfied the relevant criteria for PSP (Litvan et al., 1996), CBS (Armstrong et al., 2013), MSA (Gilman et al., 2008), or had clinical parkinsonism but with atypical features for a diagnosis of idiopathic Parkinson's disease. Similarly-aged healthy controls were recruited either from relatives or friends of cases or through the Join Dementia Research volunteer registry. Patients with PSP, CBS or indeterminate cases were also classified according to the 2017 Movement Disorders Criteria (Grimm et al., 2019; Höglinger et al., 2017). Those satisfying at least 'possible' PSP diagnostic criteria were stratified into three broader categories as PSP Richardson's syndrome (PSP-RS), PSP-subcortical (PSP-P with predominant parkinsonism, PSP-PGF with progressive gait freezing, or PSP-OM with oculomotor features) or PSP-cortical (PSP-F with frontal presentations, PSP-CBS with corticobasal features or other focal cortical syndromes) (Jabbari et al., 2020). Assessments were carried out at baseline and at 6, 12, 24, and 36 months, with an abbreviated assessment virtually or face-to-face at 48 and 60 months. Full assessment included clinical history and physical examination, a neuropsychological testing battery, carer-rated questionnaires assessing functional and behavioural severity, MRI scanning, eye movement testing, and collection of biological samples (blood and cerebrospinal fluid).

2.3.2 Clinical and neurocognitive assessments

PROSPECT-M-UK participants underwent extensive clinical and neurocognitive assessment. In chapter 4 I use the PROSPECT-M-UK as a replication cohort for results

obtained from participants recruited in Cambridge, and in chapter 6 I combined the Cambridge and PROSPECT-M-UK cohorts to increase study power. Therefore, in this thesis I focus on assessments available for most participants in both study cohorts to reduce missing data, namely the PSP-rating-scale, the Addenbrooke's Cognitive Examination III, and the Cambridge Behavioural Inventory-Revised.

2.3.3 Neuroimaging acquisition

The imaging protocol across the three imaging centres in PROSPECT-MR mirrors the standardised protocol used in GENFI2, with acquisition of volumetric T1, volumetric T2, diffusion tensor imaging, task-free fMRI and arterial spin labelling. Imaging was collated centrally and released in sequential data freezes. Participants underwent high resolution 3T T1-weighted MPRAGE structural imaging (TR 2s, TE 2.93ms, flip angle 8°, voxel size 1.1mm isotropic). Parameters for echo-planar imaging were TR 2.5 secs, TE 30ms, 3x3x3.5mm voxels, and 200 volumes.

2.4 Task-free functional MRI image pre-processing

Prior to analysis task-free fMRI must be pre-processed. Pre-processing has two primary aims: to limit the effect of artefactual sources on the data so that analyses are driven predominantly by neural signal, and to allow signal localisation and comparison across participants through image registration and normalisation (Caballero-Gaudes and Reynolds, 2017; Esteban et al., 2019). The blood-oxygen-level-signal detected in fMRI is a combination of neuronal and non-neuronal sources. Non-neuronal factors affecting fMRI signal include scanner hardware and environment related noise, such as slow changes in low frequency signal over time (drift) due to scanner instabilities (Smith et al., 1999). Cardiac and respiratory physiology induces signal changes through effects on head motion (Power, 2019; Power et al., 2019, 2017), due to pulsatile changes in cerebrospinal fluid and large arteries (Liu, 2016), and through indirect effects including modulation of carbon dioxide levels (Wise et al., 2004). Subject head motion creates spurious correlations in a distance-dependent manner (Power et al., 2012; Satterthwaite et al., 2012).

Motion artefact is a particular concern in the cohort of patients I study in this thesis, since cognitive impairment and physical disability increase the chance of head motion. However propensity to move during scan acquisition has neural correlates (Geerligs et al., 2017) and plausibly relates to severity and heterogeneity in neurodegenerative conditions, a

hypothesis I test directly for in PSP and CBS in chapter 6. Therefore, removal of movement artefact must be done in a principled manner and caution taken over regressing metrics of motion (either at the pre-processing stage or during higher level analyses) because of the risk of removing the effect of disease on neural-derived signal.

Through this thesis I use an adapted form of FMRIB Software Library's (FSL) task-free fMRI pre-processing pipeline (Jenkinson et al., 2012; Smith et al., 2013a), based on scripts written by my supervisor Dr Timothy Rittman. Dr Rittman pre-processed the images used for analysis in chapter 4. I chose this pipeline as it is well validated, widely used (Alfaro-Almagro et al., 2018; Smith et al., 2013a), and has been applied prior to running analytic techniques used in this thesis (Vidaurre et al., 2018, 2017). We extended the pipeline with the addition of wavelet despiking to reduce motion artefact (Patel et al., 2014) given higher in-scanner movement in participants with neurodegenerative diseases. For initial fMRI preprocessing the T1 structural images were cropped to remove non-brain tissue followed by brain extraction using FSL's Brain Extraction Tool (Smith, 2002). I then used FSL's FMRI Expert Tool (Woolrich et al., 2001) with the following steps: motion correction using MCFLIRT (Jenkinson et al., 2002); spatial smoothing using a Gaussian kernel of 5mm FWHM; grand-mean intensity normalisation of the 4D dataset by a single multiplicative factor; and 100Hz high-pass temporal filtering.

Structured artefacts were removed using independent component analysis (ICA, discussed further below) denoising using FSL's MELODIC together with FMRIB's ICA-based noise reduction tool (*FIX*, Griffanti et al., 2014; Salimi-Khorshidi et al., 2014). *FIX* classifies the components as either neural signal or artefactual, based on labels applied to a training set. *FIX* hand training was performed separately for each chapter in this thesis. I hand-trained *FIX* using a set of at least 10 subjects from each disease group (or mutation in GENFI in chapter 3), based on principles and examples outlined by Griffanti and colleagues (Griffanti et al., 2017). Registration to high resolution structural and/or standard space images was carried out using FLIRT. Registration from high resolution structural to MNI space was then further refined using FNIRT nonlinear registration (Jenkinson et al., 2012). I did not use global signal regression, given the potential to remove neural signal and introduce anti-correlations (Murphy and Fox, 2017). Wavelet despiking was used for further removal of motion artefact. This is an algorithmic approach which identifies and removes spikes (Patel et al., 2014) in the fMRI timeseries which arise due to brief head movements.

2.4.1 Removing participants with increased motion

Where in-scanner movement is high it may be the case that artefactual correlations and activations cannot be removed even with stringent pre-processing. Depending on the analytic technique used these participants may bias the whole analysis. One approach that has been adopted in high movement populations is to eliminate scans with gross motion (Marek et al., 2019; Nebel et al., 2022; Nielsen et al., 2019; Parkes et al., 2018). The extent to which this is possible may depend on the number of participants and expected effect size. Excluded individuals may be phenotypically different, and so results would not generalise to the entire patient population (Nebel et al., 2022; Wylie et al., 2014). However even if artefact could be reliably removed the scans likely have such a poor signal-to-noise ratio that they contribute little to a group level analysis (Wylie et al., 2014).

Various thresholds have been suggested for exclusion of participants or individual volumes (Nebel et al., 2022; Parkes et al., 2018). In this these I used thresholds based on mean and standard deviation in 408 scans of patients with neurodegenerative conditions and healthy aged-matched controls recruited at the Cambridge Centre for Parkinson-plus for four data quality indices. These are median and maximum spike percentage (Patel et al., 2014), maximum framewise displacement (Power et al., 2012), and maximum spatial standard deviation of successive volume difference or DVARS (Smyser et al., 2010). Values are set out in Table 2-2. I then used thresholds of between 1 and 1.2 standard deviations above the mean, depending on the scan protocol, disease population, and analysis method and purpose. In chapters 3 and 6 I use only the three maximal statistics since these appear to capture most high movement participants. I additionally perform a sensitivity analysis in the GENFI cohort in chapter 3 excluding individuals above a threshold defined within the cohort (1.2 standard deviations from the whole group mean for mean framewise displacement, giving a value of 0.35mm).

fMRI motion metric	Mean	Standard deviation
Median spike percentage	4.24%	4.06%
Maximum spike percentage	20.33%	17.10%
Maximum DVARS	8.17	1.79
Maximum framewise displacement	2.11mm	5.51mm

Table 2-2: Mean and standard deviation for metrics of in-scanner motion for task-free fMRI used to derive thresholds for excluding high motion participants.

2.5 Task-free fMRI analysis

2.5.1 Identification of large-scale networks through independent component analysis

Temporally correlated large-scale brain networks are a consistent finding in healthy adults, across the lifespan, and can be identified by functional magnetic resonance imaging at rest (Damoiseaux et al., 2006; Fox and Raichle, 2007; Smith et al., 2009; Yeo et al., 2011). Analysis of functional MRI in FTLD syndromes in chapters 3, 4 and 6 depends on identification of large-scale networks before further analysis. One way in which this can be achieved is to assess correlations across the brain with the BOLD timeseries from predefined regions of interest or seeds (Bijsterbosch, 2017). An example would be identification of the default mode network using a seed in the posterior cingulate cortex (Greicius et al., 2003). The primary disadvantage of this approach is dependency on the choice of seeds, risking exclusion of important signals from analysis (Bijsterbosch, 2017). Instead, in this thesis I use group independent component analysis as a data-driven means to derive components that represent the different brain networks.

Independent component analysis models a multivariate signal as a linear combination of statistically independent components (Beckmann and Smith, 2004; Bijsterbosch, 2017). The statistical independence used to ‘unmix’ the original data can be defined and measured in multiple ways. In this thesis components are said to be independent where they maximise non-Gaussianity, since by the central limit theorem signals become more Gaussian after mixing (Beckmann and Smith, 2004; Bijsterbosch, 2017). Independent component analysis can be applied to a single fMRI dataset, for instance to separate artefactual from neuronal signal, or to data combined from the whole study group.

Spatial group independent component analysis in chapters 3, 4, and 6 was performed using FSL’s MELODIC tool (Beckmann and Smith, 2004). Pre-processed and normalised MRI were first cut to the minimum number of volumes of any participant used in the study. I then conducted independent component analysis on participants’ temporally concatenated datasets. The number of components for analysis can either be chosen a priori or determined through an algorithmic method (Beckmann and Smith, 2004). Higher model orders give greater fragmentation of networks and the optimal choice of number of components varies by study question. In this thesis I use a model order of 30 as a balance between excessive network fragmentation (Ray et al., 2013) and predetermining analysis output. To label

components I use a semi-supervised method, comparing with template network maps provided by other groups (Shirer et al., 2012; Yeo et al., 2011) using cross-correlation and goodness of fit measures and subsequent visual inspection.

While independent component analysis is well recognised as an approach to identify networks in analysis of task-free fMRI, it can be applied to other data sources where decomposition of multivariate signal into components can aid analysis (see for instance Fang et al., 2021; Passamonti et al., 2019). In chapter 5 I use a version of independent component analysis on spatially concatenated maps of [¹¹C]UCB-J positron emission tomography binding potential to capture patterns of spatial variance in synaptic density (further details of methods within chapter 5). Independent component analysis can also be applied to higher level features derived from fMRI, such as on correlations between networks (Elliott et al., 2018), an approach I use in chapter 6 and discuss further below.

2.5.2 Within- and between-network connectivity

To understand the organisation of functional brain networks, it is helpful to examine both the strength and configuration of connections within networks and interactions across networks. This can be achieved using ICA derived network components. Once components have been identified it is possible to derive participant-specific time courses and spatial maps for each component. One method to achieve this is dual regression (Filippini et al., 2009; Kelly, Jr. et al., 2022). In the first stage of dual regression the group component maps from the independent component analysis are regressed against each participant's pre-processed fMRI to obtain a time course for each subject per component. In chapters 3 and 4 I use these timeseries as inputs into a time-varying network analysis (see Dynamic network analysis below). In chapter 6 I calculated connectivity between components using full Pearson correlation between networks time series (normalised for each subject) followed by Fisher r-to-Z transformation using FSLNets (Smith et al., 2013b). I then performed a further independent component analysis on these connections (Hyvarinen, 1999) to identify a small number of components capturing between-network connectivity patterns (Elliott et al., 2018). I compared these between-network connectivity components with baseline clinical severity, longitudinal rate of change in severity and survival. Further methodological details, including processes to account for site differences and selecting number of components, are set out in the methods section in chapter 6.

In the second stage of dual regression subject normalised timeseries for each component are regressed against each participant's pre-processed fMRI, this time obtaining participant-specific spatial maps per component consisting of beta values. These subject maps can then be compared to assess how the size or shape of a network differs between groups or covaries with measures of disease severity (*within-network covariance*). I applied dual regression in chapter 5 against [¹¹C]UCB-J positron emission tomography independent components (rather than fMRI components) to derive participant-specific maps of spatial covariance with the PET maps.

2.5.3 Graph metric analysis

Graph theory is a mathematical tool that can be used to characterise structural and functional brain networks (Bullmore and Sporns, 2009). Within a graph theoretical framework, a brain network consists of *nodes* or *vertices* representing brain regions and the *edges* that link them. The edges may be synaptic or axonal connections observed on structural imaging or be statistical dependencies between brain regions derived from functional imaging. Graph theory has been used to describe disruption to functional brain organisation in neurodegenerative conditions (Bullmore and Sporns, 2009; Crossley et al., 2014; Stam, 2014; Yu et al., 2021) and in combination with other modalities offers mechanistic insight into disease pathogenesis and progression (Cope et al., 2018; Franzmeier et al., 2022; Rittman et al., 2016b).

Frequently a threshold is applied to the graph to reduce the effect of weak correlations that may be artefactual (Bullmore and Sporns, 2009; Zalesky et al., 2012). However the characteristics of the network vary depending on the threshold used (van Wijk et al., 2010), and so caution is needed in interpreting between-group differences in graph metrics (Yu et al., 2021). I adopt three approaches in this thesis to assist interpretation and to avoid the perils of arbitrary choices. First, I calculate weighted graph metrics, where the connections between nodes are weighted by their strength, which avoids the need to pick arbitrary thresholds but does not prevent some measures being affected by overall connectivity strength (van den Heuvel et al., 2017; Yu et al., 2021). Second, I report results across a range of thresholds, recognising that interpretation can be challenging where there is variation. Third, I used normalised graph metrics; thresholded graph metrics are normalised relative to random graphs with the same degree distribution, which reduces but does not entirely remove results being biased by connectivity strength (van Wijk et al., 2010; Yu et al., 2021).

Graph metric approaches form part of analysis in chapters 4 and 5 using the Maybrain software built by Timothy Rittman (<https://github.com/RittmanResearch/maybrain>) and dependent on Networkx (<https://networkx.org/>). First, the participants' pre-processed fMRI is parcellated using the relevant atlas. In chapter 4 my analysis uses the Brainnetome parcellation (Fan et al., 2016), a data-driven atlas that provides good cortical and subcortical coverage. In chapter 5 I used a modified Hammers atlas (Gousias et al., 2008; Hammers et al., 2003) with cortical regions masked by a grey matter mask. The Hammers atlas is widely used in PET imaging studies and was selected here to allow comparisons across modalities. I calculated associations between regions in chapter 4 by taking the wavelet cross-correlation between each region using a maximal overlap discrete wavelet transform and Daubechies filter performed using the waveslim package in R. I used the second band of 4, corresponding to a frequency range of 0.0675-0.125Hz (Achard and Bullmore, 2007). In chapter 5 I calculated Pearson correlations between regions, followed by Fisher's r-to-Z transformation. I then derive an association matrix of all region-by-region associations for each participant, from which graph metrics can be calculated. The two methods to quantify associations between regions have relative merits. Graph metrics from Pearson correlations have been extensively studied and have been found to be statistically robust, but may be more affected by confounds affecting the whole brain and capture non-neuronal information (Smith et al., 2011). Wavelet cross-correlation allows selection of a band known to have neuronal origins, although neuronal signal may occur at higher frequencies (Smith et al., 2013a).

A large set of metrics can be used to characterise a graph. In this thesis I focus on the following metrics: *weighted degree*, measuring the number and strength of nodal functional connections; *clustering coefficient*, the proportion of triangular connections formed by each node over the proportion of all possible such connections; and *path length*, the average shortest topological distance between nodes of the graph. The combination of path length and clustering coefficient defines randomness or regularity of the graph, with random graphs exhibiting short path length and small clustering coefficient (Watts and Strogatz, 1998).

2.5.4 Dynamic network analysis

Functional connectivity and network activation is most commonly assessed by averaging over the scan acquisition time. However the last decade has seen increasing interest in approaches that capture time-varying fluctuations in connectivity from functional MRI

(Calhoun et al., 2014; Chang and Glover, 2010; Vidaurre et al., 2017). The clinical syndromes of FTLD, deficits in inhibitory and excitatory neurotransmitters integral for network integration and segregation (Murley and Rowe, 2018), and imaging and pathological features suggest that temporal dynamics are disrupted in these diseases. Time-varying or *dynamic* approaches have been found to be more sensitive to capturing variation in clinical syndrome than traditional *static* connectivity analyses (Moguilner et al., 2021).

Therefore in chapters 3 and 4 I use Hidden Markov modelling (HMM) as a highly articulated data-driven approach to directly model the blood-oxygen-level-dependent signal of fMRI and characterise transitions between large scale networks (Meer et al., 2020; Vidaurre et al., 2018, 2017). Hidden Markov models posit the existence of a finite number of hidden states that describe the sequential evolution of observed data (Eddy, 2004; Rabiner and Juang, 1986) with the Markovian assumption that the probability of an event depends only on the state at the previous time point. Generative modelling of time series avoids difficulties associated with alternative sliding window approaches, notably large sampling variability from small window size and autocorrelation from overlapping windows (Hindriks et al., 2016; Leonardi and Van De Ville, 2015; Lurie et al., 2019). This is particularly important when studying temporal dynamics in neurodegeneration, where obtaining imaging with acquisition times required for adequate time windows can be challenging. Each time point is classified as being in a single state, although the assumption of state mutual exclusivity is adjusted through soft probabilistic inference. While the states and probability of transitioning between them are defined at the group level, a state time course can be estimated for each participant.

A hidden Markov model can be derived for a set of task-free fMRI time courses provided core underlying assumptions are met. In chapter 3 and 4 I adopted an approach presented by Vidaurre and colleagues (Vidaurre et al., 2018, 2017, Figure 2-1), where time courses for brain networks (or network components) derived from an independent component analysis are used as input into the HMM. First, I performed an independent component analysis using FSL's MELODIC tool from the relevant cohort. Participant specific time courses for each component were generated by regression of the template maps into each subject's preprocessed fMRI. I assessed components as representing neuronal or artefactual signal using the same classification methods outlined in the pre-processing section (Griffanti et al., 2017) with reference to canonical network maps (Shirer et al., 2012). From standardised per participant non-artefactual component timecourses a multivariate

Gaussian HMM (Vidaurre et al., 2017) with six-eight brain states was inferred for each cohort using the HMM-MAR toolbox (<https://github.com/OHBA-analysis/HMM-MAR>). All states shared a common covariance matrix, so that network dynamics were primarily driven by changes in signal variance and amplitude (Vidaurre et al., 2021).

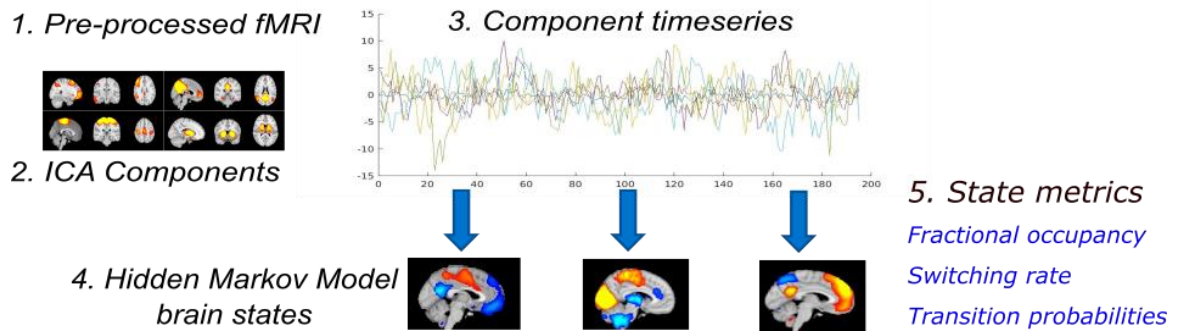


Figure 2-1. A schematic representation of the hidden Markov model pipeline used in chapters 3 and 4. Pre-processed fMRI were concatenated in an independent component analysis of model order 30. Participant specific time courses for non-artefactual components were then used to estimate brain states in a hidden Markov model. Model metrics were taken forward for further analysis.

Both number of components from the independent component analysis and number of brain states from the HMM must be determined a priori. I chose an independent component analysis model order of 30 in chapters 3 and 4. In previous work using HMMs from task-free fMRI, between 6 and 12 states have been selected for analysis (Meer et al., 2020; Quinn et al., 2018; Vidaurre et al., 2018), although as the number of states increases their reliability falls (Vidaurre et al., 2018). In chapter 3 I specified six states would be derived in registration prior to analysing the GENFI dataset (<https://osf.io/27ajq/>), and in chapter 4 I replicated analysis across two datasets using the same number of states.

The temporal dynamics of HMM states can then be characterised through a small set of metrics, namely switching rate (the frequency with which states transitions occur), fractional occupancy (the proportion of time a state is active) and the transition matrix consisting of transition probabilities (the chance of between state transitions) and persistence probabilities (the chance of remaining in the same state). These metrics are then taken to higher order analysis to compare between groups, with clinical severity, and with longitudinal outcomes. For illustrative purposes I generated mean activation maps by weighting component maps by the mean of the state Gaussian distribution.

2.6 Modelling clinical progression

In chapters 3 and 6 I test the hypotheses that imaging collected at a baseline assessment predicts longitudinal outcomes in frontotemporal lobar degeneration syndromes. Longitudinal outcomes of interest were: first, trajectories of change in neuropsychological assessments and clinical and carer-based severity ratings; second, survival time from baseline assessment. In this thesis I used linear mixed-effects modelling to derive the former, a univariate regression-based model that simultaneously models intercept and trajectory at an individual and whole group level (Ghisletta et al., 2015; McNeish and Matta, 2018). These models are able to handle incomplete data or where there is variation in time points for follow-up assessments (Ghisletta et al., 2015). Analysis of survival time requires statistical techniques that can handle *censored* data, where the outcome in question (death) has not occurred in the follow up period (Clark et al., 2003). Cox proportional hazard regression (Cox, 1972) is the most commonly used form of survival modelling and can be considered analogous to multiple regression. I discuss mixed-effects and Cox proportional hazard modelling in turn in the following sections.

2.6.1 Linear mixed-effects models

A mixed-effects model allows simultaneous estimation of intercepts and coefficients at the whole-sample and individual level (Ghisletta et al., 2015; Laird and Ware, 1982). The two forms of parameter distinguished by the models can be termed fixed effects and random effects, although the statistical literature is not consistent in defining these terms (Gelman, 2005). In this thesis, when analysing longitudinal change, fixed effects are the mean slopes and intercepts for the whole sample, while random effects capture individual variation in slopes or intercepts (McNeish and Matta, 2018). Modelling data in this way allows for improved estimates for repeat sampling, explicitly estimating variation and avoiding the need for averaging (McElreath, 2020). A schematic representation of a linear mixed-effects model in Figure 2-2.

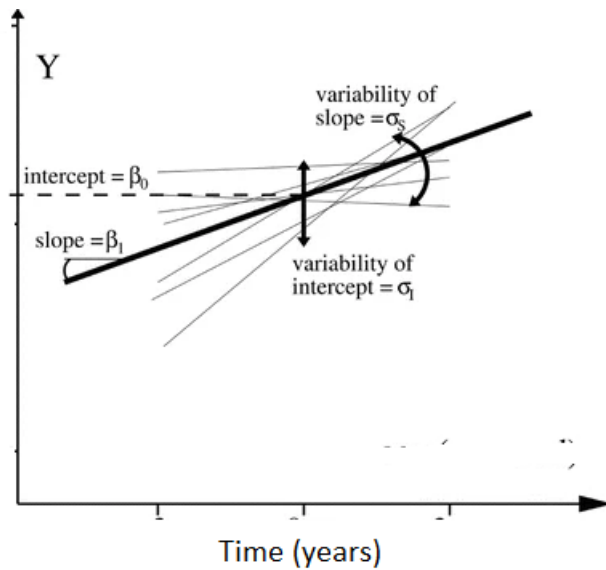


Figure 2-2. A schematic representation of a linear mixed-effects model. Fixed effects are represented by the thick line and thin lines individual variation in estimated slope and intercept (adapted from Ghisletta et al., 2015)

In this thesis all linear mixed-effect model were derived using the R package lme4 (Bates et al., 2015). I calculated patient specific yearly rates of change in the relevant clinical and neurocognitive scores in each chapter. Neurocognitive assessment was the dependent variable in the model, with years from baseline assessment as an independent variable and with estimation of individual intercepts and individual change in neurocognitive assessment over time (slope), which can be written in Wilkinson-style notation (Wilkinson and Rogers, 1973) as follows:

$$\text{Neurocognitive assessment} \sim \text{time} + (\text{time} \mid \text{participant}) + \varepsilon$$

These models were calculated using all participants for each project.

To assess whether baseline neuroimaging marker (dynamic network component in chapter 3, between-network connectivity component in chapter 6) predicts neurocognitive decline individual estimates of disease progression were taken to a second model as a dependent variable, with baseline imaging marker as an independent variable and relevant covariates of no interest.

Including random effects provides a powerful modelling option wherever data is pooled across clusters (McElreath, 2020) and therefore can be applicable to cross-sectional as well as longitudinal data. In chapter 3 I use scanner site for the GENFI cohort as a random effect to improve estimation of site-related variation. In chapter 5 when comparing a graph

measure of functional connectivity (weighted degree) with regional synaptic density measured with the PET ligand [¹¹C]UCB-J I use a mixed-effects model with crossed random effects for region and participant and an effect of [¹¹C]UCB-J binding potential slope within each region. This approach captures the effect of individual and regional variability in the weighted degree-[¹¹C]UCB-J binding potential relationship. When deriving complex models it is important to justify the added complexity by assessing model fit (McNeish and Matta, 2018). Therefore I compared models using the anova function in R to ensure that inclusion of a random slope for [¹¹C]UCB-J BP_{ND} per region improved model fit .

2.6.2 Survival modelling

Survival data can be formulated in terms of the *survival function* and the *hazard rate* (Clark et al., 2003). The survival function $S(t)$ is the probability that an individual has avoided the event of interest at time t after baseline assessment. The hazard $h(t)$ is the probability that an individual has the event at time t . These functions are interrelated such that one can be derived once the other is known. Cox proportional hazard modelling is a regression-based approach to survival data that models the relationship between the hazard function and covariates (Bradburn et al., 2003), and can be formulated as follows:

$$h(t) = h_0(t) \times \exp\{B_1x_1 + \dots + B_px_p\}$$

where h_0 is the baseline hazard, $\{x_1, \dots, x_p\}$ are a set of p covariates and $\{B_1, \dots, B_p\}$ their respective coefficients. The $\exp(B_i)$ terms are the *hazard ratios*, with a value greater than one indicating that survival time increases with greater covariate value. Cox modelling estimates the hazard function nonparametrically, so that no particular statistical distribution is assumed for survival times (Bradburn et al., 2003).

In chapter 6 I used a Cox proportional hazards regression analysis to assess the relationship between between-network component score and time from scan until death with age and sex as covariates using the R packages *survival* (Therneau, 2023) and *survminer* (Kassambara et al., 2021) for analysis and visualisation. Given the importance of scanner motion as a potential confounder in quantifying connectivity, I additionally report the relationship between mean framewise displacement and time from scan until death.

2.7 Correcting for multiple comparisons

At various points in this thesis, I perform multiple statistical tests related to a single independent variable. This occurs when comparing to multiple clinical and neuropsychological measures of clinical severity (for instance in chapters 3, 4, and 6), when performing analysis across large numbers of brain regions (such as comparing UCB-J values by region in chapter 5), and when comparing group differences in multiple derived imaging measures such as ICA components (chapters 3 and 4).

As the number of comparisons increases there is greater risk that incorrect rejection of the null hypothesis occurs. It is important to complete some form of controlling procedure to account for the possibility of these *Type I* errors. However, the relevant outcomes measures are typically not statistically independent, and therefore correction for the family-wise error rate with the Bonferroni method (where the *alpha* is divided by the number of comparisons) is too strict. In this thesis broadly I use two methods of multiple comparison correction. Wherever permutation testing is used it is possible to determine the distribution of the maximal statistic and therefore control the family-wise error (FWE) rate (Winkler et al., 2014), without the requirement for the observations to be independent. For other statistical tests I use false-discovery rate (FDR) adjusted p-values using the Benjamini-Hochberg method (Benjamini and Hochberg, 1995). Further details are provided in the relevant experimental chapters, with p-values denoted FDR/FWE depending on the method of correction.

3 Network dynamics in sporadic and familial frontotemporal dementia

Preface

This results from this chapter have been published in *Alzheimer's and Dementia* as 'Temporal dynamics predict symptom onset and cognitive decline in familial frontotemporal dementia' (<https://doi.org/10.1002/alz.12824>). Data collection was from the research team at the Cambridge Centre for Frontotemporal Dementia over a decade, and by a large group of researchers across 25 sites in Europe and Canada for GENFI. I designed the analysis strategy with Professor Rowe and Dr Timothy Rittman. I performed all preprocessing and analysis. I wrote the manuscript with input from the co-authors of the paper.

Summary

In this chapter I test the hypothesis that dynamic changes in functional networks predict cognitive decline and conversion from the presymptomatic prodrome to symptomatic disease in familial frontotemporal dementia. For hypothesis generation I use data from 36 participants with behavioural variant frontotemporal dementia and 34 controls were recruited from the Cambridge Centre for Frontotemporal Dementia. For hypothesis testing, I studied 198 symptomatic frontotemporal dementia mutation carriers, 341 presymptomatic mutation carriers and 329 family members without mutations. I identified a characteristic pattern of dynamic network changes in frontotemporal dementia, which correlated with neuropsychological impairment. Among presymptomatic mutation carriers, this pattern of network dynamics was found to a greater extent in those who subsequently converted to the symptomatic phase. Baseline network dynamic changes predicted future cognitive decline in symptomatic participants, and older presymptomatic participants. These findings show that dynamic network abnormalities in frontotemporal dementia predict cognitive decline and symptomatic conversion, suggesting a potential role of functional MRI in stratification and prognostication.

3.1 Introduction

Neuropathological and structural changes accumulate over many years prior to the onset of symptoms in neurodegenerative diseases (Oxtoby et al., 2018; Rohrer et al., 2015). Understanding the timing and consequence of such changes for clinical syndromes is key to accounting for heterogeneity in progression and risk-stratifying asymptomatic individuals for preventative clinical trials. Our group has previously shown that functional network integrity is important in maintaining cognitive performance in individuals at risk of dementia (Rittman et al., 2019; Tsvetanov et al., 2020), with the corollary that loss of network integrity may herald symptom onset and predict cognitive decline. Genetic Frontotemporal Dementias (FTD) provides an opportunity to characterise functional networks throughout the course of the disease. Approximately one-third of patients with FTD have a family history in keeping with an autosomal dominant inheritance (Greaves and Rohrer, 2019). Mutations in three genes account for the majority of these cases: chromosome 9 open reading frame 72 (C9orf72), granulin (GRN) and microtubule-associated protein tau (MAPT) (Greaves and Rohrer, 2019; Rohrer et al., 2009). The resulting phenotypes are heterogeneous, with behavioural variant FTD (bvFTD) the most common clinical presentation (Greaves and Rohrer, 2019).

The co-ordination of neural activity across distributed spatial and temporal scales is dynamic (Breakspear, 2017; Shine et al., 2019; Tognoli and Kelso, 2014). Such connectivity underpins cognition in health and is affected in psychiatric and neurodegenerative diseases (Filippi et al., 2019; Fu et al., 2021; Liégeois et al., 2019). While functional connectivity is typically determined by averaging over the scan acquisition time, time-varying fluctuations in connectivity can also be captured by functional magnetic resonance imaging (fMRI) (Calhoun et al., 2014; Chang and Glover, 2010; Vidaurre et al., 2017). In the clinical syndromes of FTD, there are deficits in inhibitory and excitatory neurotransmitters required for network integration and segregation (Murley and Rowe, 2018) which I propose to contribute to changes in temporal dynamics in the disease. Subtle changes in time-varying functional connectivity occur in presymptomatic mutation carriers (Premi et al., 2019), although their longitudinal significance and evolution into the symptomatic phase have not been studied.

I examined resting state brain dynamics in presymptomatic and symptomatic carriers of pathogenic mutation carriers in the Genetic Frontotemporal Initiative (GENFI) using fMRI

to determine whether disruption to network dynamics predicts cognitive decline. I used Hidden Markov modelling as a highly articulated data-driven approach to model the blood-oxygen-level-dependent signal of fMRI, an approach which posits the existence of a finite number of hidden states that describe the sequential evolution of observed data (Vidaurre et al., 2018, 2017).

I investigated brain state dynamics using hidden Markov models with a two-stage approach to ensure replication and refine analytic choices. Hypothesis generation used a cohort of patients with mainly sporadic behavioural variant FTD and control participants recruited at the Cambridge Centre for Frontotemporal Dementia. I repeated the methodology in GENFI, following preregistration of my cross-sectional analysis plan (<https://osf.io/k64gh/wiki/home/>), with the following hypotheses: 1) brain state dynamics differ between symptomatic mutation carriers and cognitively normal non-mutation carriers; 2) changes in network dynamics correlate with a) neuropsychological deficits and b) carer assessed measures of impairment; 3) presymptomatic mutation carriers (versus non-mutation carriers) have abnormal network dynamics as a function of proximity to onset as denoted by age; and 4) altered network dynamics predict conversion from the presymptomatic to symptomatic phase and subsequent cognitive decline in gene mutation carriers. In assessing the relationship between network dynamics and age, I considered non-linear models given evidence that non-linearity is found between disease age and other biomarkers (including clinical, neuropsychological, structural imaging, and blood based biomarkers) (Staffaroni et al., 2022) in genetic FTD.

3.2 Methods

3.2.1 Participants

I used datasets from 36 participants with behavioural variant frontotemporal dementia (bvFTD) and 34 healthy controls recruited at the Cambridge University Centre for Frontotemporal Dementia for hypothesis generation. Clinical assessment included the Addenbrooke's Cognitive Examination-Revised (ACE-R) (Mioshi et al., 2006), Mini-Mental State Examination (MMSE) (Folstein et al., 1975), Frontal Assessment Battery (Dubois et al., 2000), and Cambridge Behavioural Inventory-Revised (CBI-R) (Wear et al., 2008).

The Genetic Frontotemporal dementia Initiative (GENFI) includes participants from 25 research sites across Europe and Canada. Participants were included if they were over 18 and had a known pathogenic mutation in MAPT, C9ORF72, GRN or TBK1, or were a first degree relative of a mutation carrier. 198 symptomatic mutation carriers, 341 asymptomatic mutation carriers and 329 family members with usable fMRI (datafreeze 5) were included in this study. Details of the GENFI clinical and cognitive assessments are set out in chapter 2.

3.2.2 Image acquisition and preprocessing

Image acquisition for the two cohorts and fMRI preprocessing are described in detail in chapter 2. Given the potential sensitivity of estimates of network dynamics to motion (Laumann et al., 2017; Power et al., 2012), I excluded participants 1.2 standard deviations above thresholds as defined in chapter 2 for three data quality indices (maximum spike percentage (Patel et al., 2014), maximum framewise displacement (Power et al., 2012), maximum spatial standard deviation of successive volume difference (Smyser et al., 2010)). I excluded 9 participants with bvFTD and 2 healthy controls from the Cambridge cohort, and 103 scans from 89 participants in GENFI (20 non-carriers, 21 presymptomatic mutation carriers, 48 symptomatic participants). I performed an additional analysis excluding participants above 1.2 standard deviations from the whole group mean for mean framewise displacement but included in the primary analysis.

3.2.3 Hidden Markov Models

I assessed network dynamics in both cohorts through hidden Markov modelling (Rabiner and Juang, 1986), as introduced in chapter 2. I performed an independent component

analysis using MELODIC (fMRIB Software Library, FSL) from preprocessed fMRI of all participants to allow comparison between cohorts. I chose a model order of 30 as a balance between excessive network fragmentation (Ray et al., 2013) and predetermining HMM outputs. Six component maps were identified as artefact. Participant specific timecourses for each component were generated by regression of the component maps into each subject's preprocessed fMRI. From standardised per participant non-artefactual component timecourses a multivariate Gaussian HMM (Vidaurre et al., 2017) with six brain states was inferred for each cohort using the HMM-MAR toolbox (<https://github.com/OHBA-analysis/HMM-MAR>). All states shared a common covariance matrix (Vidaurre et al., 2021). Model order was specified in registration prior to analysing the GENFI dataset; it has previously been shown that robust behavioural inferences can be made through a six-state model (Quinn et al., 2018).

The temporal dynamics of HMM states can be characterised through a small set of metrics, namely switching rate (the frequency with which states transitions occur), fractional occupancy (the proportion of time a state is active), and the transition matrix consisting of transition probabilities (the chance of between-state transitions) and persistence probabilities (the chance of remaining in the same state). Mean activation maps were generated by weighting component maps by the mean of the state Gaussian distribution. For illustrative purposes I compared these maps with templates maps of canonical static functional networks (Shirer et al., 2012). I calculated the mean score within both a binarised template map and within a binarised inverse, with goodness of fit being the difference between the two. Higher scoring networks were taken to be matching resting state networks of positive areas of activation for that state, and strongly negative scores to be the corollaries of the negative state activations.

3.2.4 Statistical analyses

I adopted a two-stage approach to the analysis, with hypothesis generation in the Cambridge dataset followed by full hypothesis testing in GENFI. Prior to the analysis of the GENFI dataset I registered the plan for processing and cross-sectional analysis using the Open Source Framework (<https://osf.io/k64gh/wiki/home/>, see appendices), All statistical analyses were performed in R (R Core Team, 2018) with the exception of permutation testing using FSL's PALM ("Permutation Analysis of Linear Models") (Winkler et al., 2014). P-values throughout were corrected across relevant tests for a false

discovery rate of 5%, except permutation testing where family-wise error correction to 5% was performed across all tests and contrasts.

3.2.4.1 Descriptive statistics

I compared continuous variables between groups using independent sample t-tests and categorical variables with the Chi-Squared test. In GENFI I calculated effect sizes (Cohen's d) for t-test comparisons, since given larger group sizes may result in small differences that may be statistically but not clinically significant.

3.2.4.2 Cambridge

I compared fractional occupancy and switching rates between groups using a one-way analysis of covariance, with age and sex as covariates. For each participant I extracted matrices of the 36 transition and persistence probabilities. Given the interdependence of these probabilities, I assessed for group differences in a permutation test (5000 permutations) using FSL's PALM. Age and sex were included as covariates of no interest.

3.2.4.3 GENFI

In GENFI cross-sectional analysis was performed using participants' latest scan that passed motion thresholding, maximising per-participant volume number. Differences in fractional occupancy rates and switching rates were assessed using mixed-effects linear models with diagnostic group as the main effect, age and sex as dependent variables, and scan site as a random intercept using the lme4 package (Bates et al., 2015). Significance values were calculated using the Satterwaithe estimate of effective degrees of freedom. Switching rates were adjusted to account for small differences in repetition time. Group differences in transition/persistence probabilities were calculated as per the Cambridge cohort.

For contrasts with clinical scores and longitudinal analysis I performed a principal component analysis on state fractional occupancies using the *alfa.pca* ($\alpha=1$) function from the Compositional package in R (Tsagris et al., 2016), followed by varimax rotation. I selected number of components for analysis using MacArthur's 'broken-stick' criterion (MacArthur, 1957).

3.2.4.4 Network dynamics by age

In previous GENFI studies, mean family age at symptom onset has been used to estimate years until symptom onset, but only in MAPT mutations does this explain a significant proportion of variability in age of onset (Moore et al., 2020). Given that component scores

did not differ by mutation type, I explored component scores by age as a marker of proximity to onset (comparing to family members without mutations, over a similar age range). I compared component scores and state occupancies between non-carriers and presymptomatic mutation carriers as a function of age, assessing the group by age (linear or quadratic) interaction.

3.2.4.5 Presymptomatic mutation carriers and neuropsychological correlates

I compared component scores in presymptomatic mutation carriers with pre-registered neuropsychological tests (backwards digit span, digit symbol, trail making test) as a function of age within a mixed-effects linear model.

3.2.4.6 Converters

Mutation carriers who were assessed during longitudinal follow up as moving from the presymptomatic to symptomatic phase were classified as *converters*. I compared component scores, state occupancies and neuropsychological scores between converters and non-converting presymptomatic mutation carriers at their latest presymptomatic scan in mixed-effects linear models with group as the main effect, age and sex as covariates, and scan site as a random variable.

3.2.4.7 Longitudinal cognitive data in symptomatic patients

A mixed linear model was used to calculate patient specific yearly rates of change in clinical and neurocognitive scores (MMSE, CBI-R, backwards digit span, digit symbol, trail making test B), as described in chapter 2. Neurocognitive assessment was the dependent variable in the model, with years from baseline assessment as an independent variable and with estimation of intercept and slope (neurocognitive assessment ~ time + (time | ID)). These models were calculated using all GENFI participants.

To assess whether baseline component scores predict neurocognitive decline individual estimates of disease progression (slope) were taken to a second model as a dependent variable, with baseline component scores as an independent variable and baseline age, sex, and site as covariates of no interest.

3.2.4.8 Longitudinal cognition in presymptomatic mutation carriers

I repeated the two-step model for presymptomatic mutation carriers, additionally assessing the interaction between baseline component scores and age given that proximity to

symptom onset increases the probability that small fluctuations in neurocognitive assessment are important.

3.3 Results

3.3.1 Descriptive statistics

Demographic and clinical characteristics for the two cohorts for participants with a sub-motion threshold scan are included in Table 3-1 and Table 3-2. In the Cambridge cohort no significant differences were observed in age or sex. In GENFI symptomatic participants were older than asymptomatic participants and showed marked deficits in neuropsychological and informant-based assessment of severity.

	NC	PSC	Symp	NC v Symp			NC v PSC		
				Stat (χ^2/t)	P	d	Stat (χ^2/t)	P	d
	n=309	n=320	n=150						
Age (y)	48 (13)	45 (12)	63 (8.2)	t=-15	<0.0001	1.3	t=2.5	0.01	0.2
Gender (F/M)	179/197	197/123	67/83	$\chi^2=0.26$	0.6		$\chi^2=11$	<0.001	
Mutation (n)	C9orf72 109 GRN 133 MAPT 60 TBK1 7	C9orf72 119 GRN 141 MAPT 58 TBK1 2	C9orf72 71 GRN 53 MAPT 26	$\chi^2=5$	0.06		$\chi^2=0.3$	0.9	
MMSE	29 (1)	29 (1)	21 (7)	t=13	<0.0001	1.9	t=-0.1	0.92	0
CBIR Total	5 (7)	6 (9)	62 (32)	t=-21	<0.0001	-3	t=-1.5	0.1	-0.13
Trial making test B	67 (37)	67 (40)	211 (92)	t=-16	<0.0001	-2.4	t=0.13	0.99	0
Digit Symbol	58 (14)	58 (14)	25 (14)	t=22	<0.0001	2.3	t=0	1	0
Backwards Digit Span Score	4.8 (1.2)	4.8 (1.2)	3.1 (1.5)	t=13	<0.0001	1.4	t=-0.54	0.6	-0.04
Boston naming	28 (2)	28 (3)	19 (8)	t=13	<0.0001	1.8	t=0.84	0.4	0.07
Letter fluency	41 (13)	41 (13)	17 (12)	t=18	<0.0001	1.9	t=0.84	0.4	0.07
Category fluency	23 (6)	24 (6)	11 (6)	t=20	<0.0001	2.2	t=-1.5	0.14	-0.12

Table 3-1 Demographic and clinical characteristics for the GENFI participants. Scores are mean (SD). P values minimum threshold of < 0.0001. (NC Non carrier, PSC presymptomatic mutation carrier, Symp symptomatic, CBIR Cambridge Behavioural Inventory-Revised, MMSE Mini-Mental State Examination)

	Control (n=32)	FTD (n=27)	Statistic (t/ χ)
Age	67.2 (8.5)	64.3 (7.3)	$t(57)=1.4$, $P=0.16$
Sex (M/F)	14/18	17/11	$\chi=1.5$, $P=0.23$
ACER		65 (20)	
FAB		9.3 (4.4)	
CBIR		74.3 (22.3)	

Table 3-2 Demographic and clinical characteristics for the participants recruited at the Cambridge Centre for Frontotemporal Dementia and Related Disorders. Scores are mean (SD). (ACER Addenbrookes Cognitive Examination-Revised, CBIR Cambridge Behavioural Inventory-Revised, FAB Frontal Assessment Battery)

3.3.2 Network dynamics in frontotemporal dementia

For the Cambridge data, I used temporally concatenated participant timeseries from ICA components to fit an HMM with 6 brain states (Figure 3-1A, with labelling in Supplementary Figure 3-1 to indicate the most closely matching canonical static network for positive and negative activations). Participants with FTD had increased fractional occupancy of state 2, whose positive activations constituted the salience network ($F=7.8$, FDR $P=0.043$). Switching rates between states were reduced in FTD (Figure 3-1C $F=6.5$, $P=0.014$). A permutation test of persistence and transition probabilities found no group differences following correction for multiple comparisons.

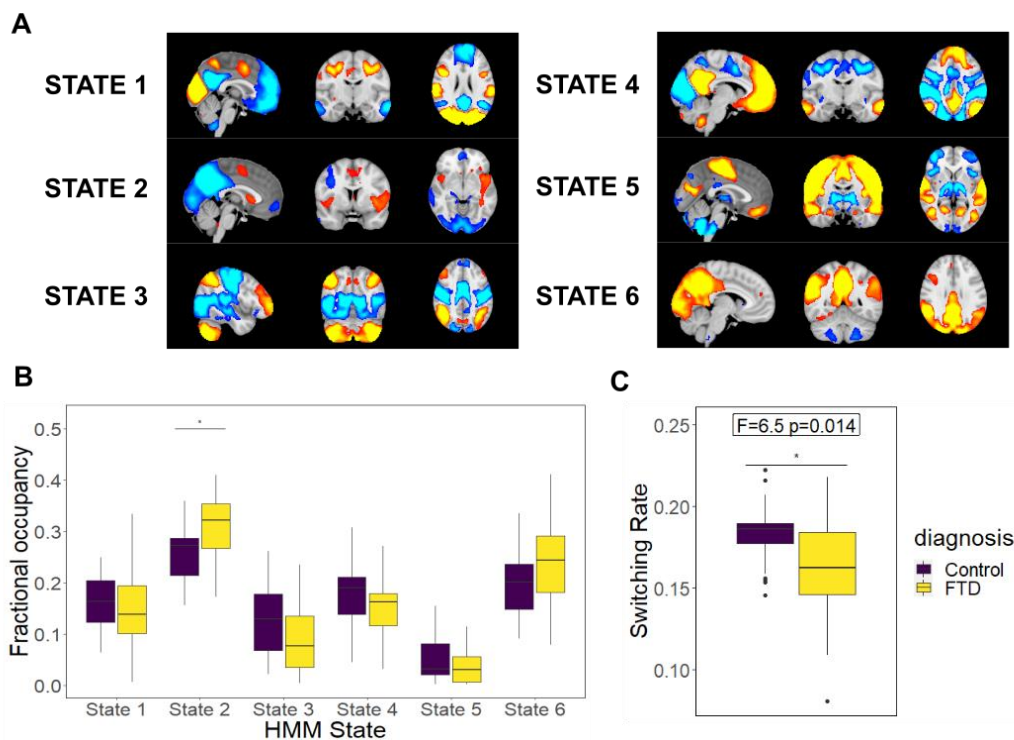


Figure 3-1. Network dynamics in the Cambridge dataset (A) Mean activation maps for the six modelled states. (B) Fractional occupancy by state, with a post-correction increase in state 2 occupancy in frontotemporal dementia (FTD). (C) Switching rates are reduced in FTD in this cohort.

For GENFI data, I used temporally concatenated participant component timeseries to fit an HMM with 6 brain states (Figure 3-2A-C, Supplementary Figure 3-1). Comparing symptomatic participants with mutation non-carriers, I found that participants with FTD had increased fractional occupancy of the state overlapping with the salience network (state 2, $F=32$, FDR $P=2 \times 10^{-7}$) and of state 4 overlapping with the default mode network ($F=8$, FDR $P=0.008$). Participants with FTD spent less time than non-carriers in two states with inverse activation patterns: state 3 with positive activations in sub-cortical regions ($F=17$, FDR $P=1 \times 10^{-4}$); and state 5 with positive activations in motor and sensory (somatic, visual and auditory) regions ($F=15$, FDR $P=2 \times 10^{-4}$). In this cohort switching rates did not differ in FTD ($F=3.1$, $P=0.08$).

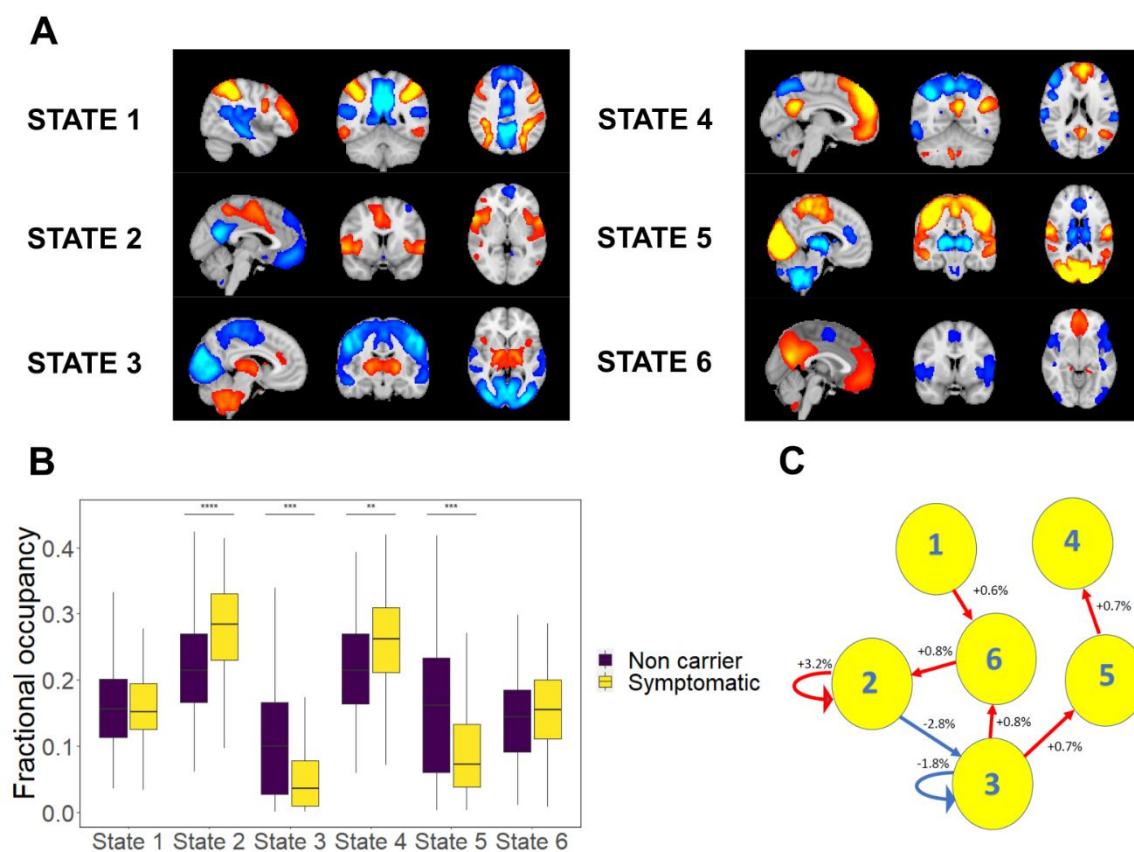


Figure 3-2. *Network dynamics in GENFI.* (A) Mean activation maps for the six modelled states. (B) Fractional occupancy by state, with increased occupancy in states 2 and 4, and decreased occupancy in states 3 and 5. (C) Altered transition and persistence probabilities in FTD using a permutation test. Blue lines represent significantly decreased transitions in FTD, and red lines significantly increased transitions. The figures show the absolute percentage increase or decrease in probability in FTD.

A permutation test of persistence and transition probabilities found a decreased transition probability in FTD from state 2 (salience) to state 3 (subcortical) ($t(455)=4.5$, FEW

$P=0.0002$, Figure 3-2C), and decreased persistence probability for state 3 ($t(455)=3.7$, FWE $P=0.007$). I found an increased persistence probability in FTD for state 2 ($t(455)=4.2$, FWE $P=0.002$), and increased transition probabilities from state 6 (default mode) to state 2 ($t(455)=4.3$, FWE $P=0.0008$), from state 5 to state 4 ($t(455)=3.2$, FWE $P=0.046$), from state 3 to both state 5 ($t(455)=4.5$, FWE $P=0.0002$) and state 6 ($t(455)=3.3$, FWE $P=0.04$) and from state 1 to state 6 ($t(455)=4.5$, $P=0.0002$).

I performed a principal component analysis with varimax rotation on state occupancies for each cohort. For the Cambridge dataset two components were selected by MacArthur's criterion, which explained 87% of the variance (Figure 3-3A). Higher scores in the first component were associated with more time in states 2 and states 6, and less time in states 3 and states 5. Higher scores in the second component were associated with less time in states 1 and 4, and more time in state 6. Scores were significantly increased for the first component in FTD ($F=4.1$, $P=0.046$), with the group difference in second component scores were not significant ($F=3.2$, $P=0.078$). In GENFI one component was selected, which explained 68% of the variance (Figure 3-3B). Higher component scores were associated with greater time in states 2, 4 and 6, and decreased time in states 3 and 5. Component scores were increased in symptomatic participants ($F=21$, $P=4 \times 10^{-7}$). There was no relationship between component scores and motion assessment indices in symptomatic participants (maximum framewise displacement Pearson's $R=0.047$, $P=0.57$; maximum DVARS $R=0.042$, $P=0.61$; maximum spike percentage $R=0.1$ $P=0.1$).

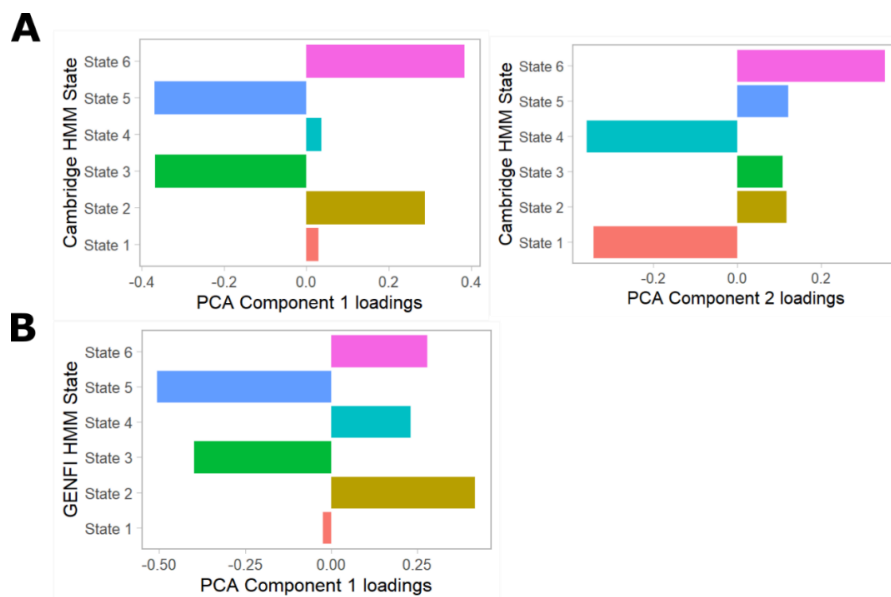


Figure 3-3. Principal component analysis loadings for state fractional occupancies for the A) Cambridge and B) Genfi datasets. The number of components was chosen by MacArthur's criteria (PCA: Principal component analysis, HMM hidden Markov modelling)

3.3.3 Network dynamics and clinical correlates in symptomatic FTD

From Cambridge data, I found that scores for the first component in participants with FTD showed an uncorrected association with Addenbrooke's Cognitive Examination-Revised (Figure 3-4A, Std Beta=-0.41, uncorrected $P=0.039$, FDR $P=0.069$) and Mini-Mental State Examination (Std Beta=-0.43, uncorrected $P=0.035$, FDR $P=0.069$). There were no significant associations with Frontal Assessment Battery score (Std Beta=-0.55, FDR $P=0.069$) or Cambridge Behavioural Inventory-Revised (Std Beta=-0.01, FDR $P=0.96$). No significant associations were observed with the second component.

For GENFI I found fractional occupancy component scores for symptomatic participants correlated with neuropsychological assessment (Figure 3-4B): digit symbol (Std Beta -0.21, FDR $P=0.019$); trail making test B (Std Beta 0.22, FDR $P=0.019$); backwards digit span (Std Beta -0.21, FDR $P=0.019$); letter fluency (Std Beta -0.22, FDR $P=0.019$); Boston naming test (Std Beta -0.19, FDR $P=0.034$); and category fluency (Std Beta -0.21, FDR $P=0.019$). No relationship was found with the Cambridge Behavioural Inventory-Revised (Std Beta=0.02, FDR $P=0.79$) and MMSE (Std Beta -0.15, FDR $P=0.082$)

Assessing for differences in slope between non-carriers and symptomatic patients using the interaction between component scores and group found significantly steeper slopes in trail making test B (interaction Std Beta -0.3, FDR $P=0.0004$); MMSE (interaction Std Beta 0.27, FDR $P=0.007$); and Boston naming (interaction Std Beta 0.25, FDR $P=0.011$). The interaction was not significant for letter fluency (interaction Std Beta 0.14, FDR $P=0.14$); category fluency (interaction Std Beta 0.17, FDR $P=0.059$); backwards digit span (interaction Std Beta 0.13, FDR $P=0.18$); digit symbol (interaction Std Beta 0.13, FDR $P=0.11$); and Cambridge Behavioural Inventory-Revised (interaction Std Beta -0.01, FDR $P=0.86$)

In GENFI the behavioural variant frontotemporal dementia and primary progressive aphasia accounted for 83% of symptomatic patients, with the remaining patients split between twelve other diagnostic labels. Considering three groups (non-carriers, behavioural variant FTD and primary progressive aphasia) I found that fractional occupancy component scores were higher in both disease groups than in non-carriers (post-hoc Tukey PPA $t=3.4$, $P=0.0019$; bvFTD $t=4.5$ $P<0.0001$) but did not differ between the clinical phenotypes ($t=0.68$, $P=0.78$).

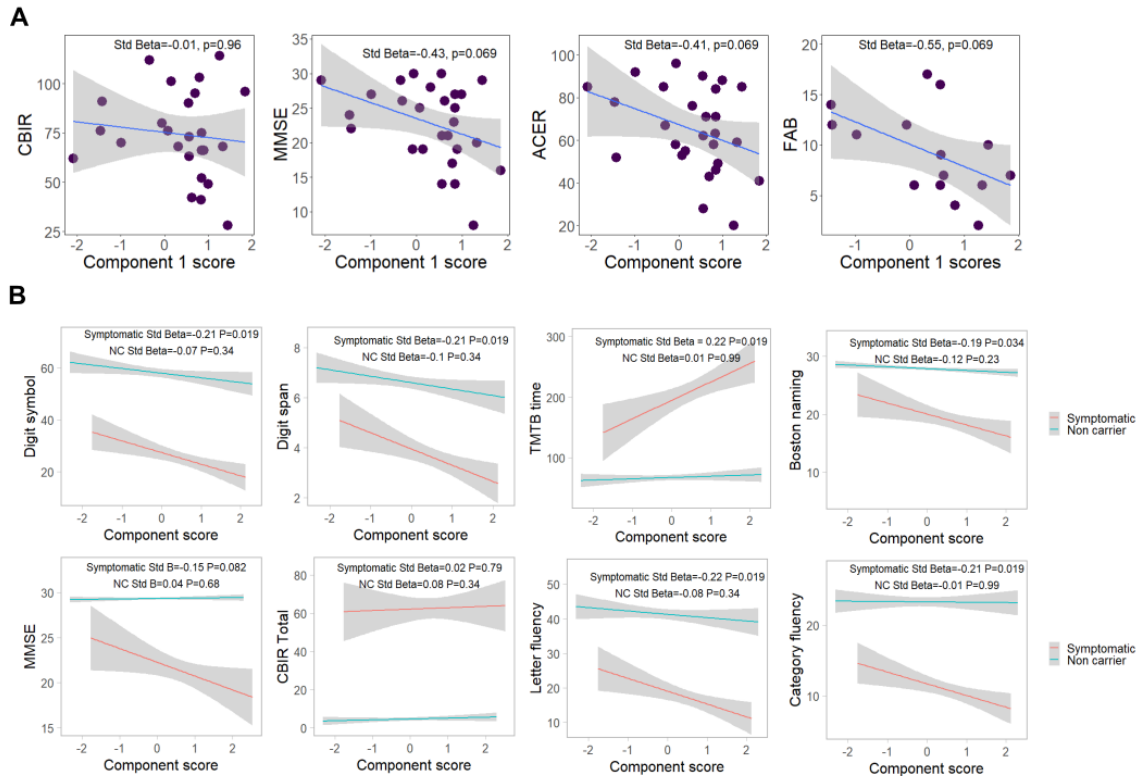


Figure 3-4. Fractional occupancy and neuropsychological assessments Component scores showed uncorrected association (A) with MMSE and Addenbrookes Cognitive Examination-Revised (ACE-R) in the Cambridge dataset and (B) with associations with neuropsychological measures in GENFI. Single subject data not plotted to protect genetic anonymity. Significant differences in slope were seen for TMTB, Boston naming, and MMSE. (CBIR Cambridge Behavioural Inventory-Revised, TMTB Trail Making Test B, MMSE Mini-Mental State Examination, FAB Frontal Assessment Battery)

3.3.4 Network dynamics and neuropsychological testing in presymptomatic mutation carriers

I assessed whether fractional occupancy component scores correlated with preregistered neuropsychological assessments (trail making test B, digit symbol, backwards digit span) in presymptomatic mutation carriers. In presymptomatic mutation carriers component scores correlated with trail making test B (Std Beta=0.15, FDR $P=0.015$) with no relationship found in non-carriers (Std Beta=0.01, FDR $P=0.92$). Moreover, the relationship in presymptomatic mutation carriers was modified by age (interaction Std Beta=0.13, FDR $P=0.043$). I found no relationship with component scores and either backwards digit span or digit symbol score.

3.3.5 Network dynamics in mutation carriers

I investigated temporal dynamics across all mutation carriers. I hypothesised that fractional occupancy could show a non-linear relationship with age, as a proxy marker of proximity to symptom onset. I therefore included a quadratic term for age using orthogonalised polynomials. Model comparison found that inclusion of a quadratic age term to a linear model significantly improved fit for state 2, but not for component scores or other states (Table 3-3, Figure 3-5C).

State	All carriers		Presymptomatic carriers		Non carriers	
	ChiSq	P	ChiSq	P	ChiSq	P
State 1	0.03	0.96	0.15	0.70	0.14	0.91
State 2	8.7	0.020	7.2	0.043	0.03	0.91
State 3	2.5	0.35	1.3	0.70	0.29	0.91
State 4	0.0	0.96	0.24	0.70	1.6	0.62
State 5	1.7	0.39	0.74	0.70	0.01	0.91
State 6	0.01	0.96	0.23	0.70	1.6	0.62
PCA	3.5	0.061	3.2	0.073	0.05	0.83

Table 3-3. *Linear v Quadratic model comparison for age against state occupancy and component scores for all carriers, presymptomatic carriers and non-carriers. PCA: Principal component analysis component. State P values corrected for false discovery rate across states.*

Within a mixed model including age as a quadratic term and with sex and site as covariates of no interest, state 2 occupancy showed an uncorrected difference between non-carriers and presymptomatic mutation carriers as a function of age (Interaction $F=3.8$, uncorrected $P=0.022$, Figure 3-5D), results that were not replicated in a purely linear model ($F=1.7$, uncorrected $P=0.19$). No differences were observed for other states or components scores.

3.3.6 Network dynamics predict symptomatic conversion

Fourteen presymptomatic carriers became symptomatic during follow up. I compared these converters at their latest presymptomatic visit with imaging with other presymptomatic carriers. Converters had significantly worse performance on neuropsychological assessment at this visit (backwards digit span $F=5.7$, $P=0.017$; backwards digit span score $F=6.9$, $P=0.009$; trial making test B $F=28$, $P=2 \times 10^{-7}$). I found that component scores ($F=6.1$, $P=0.014$) and state 2 occupancy ($F=7.7$, FDR $P=0.035$) were increased in converters (Figure 3-5C-D).

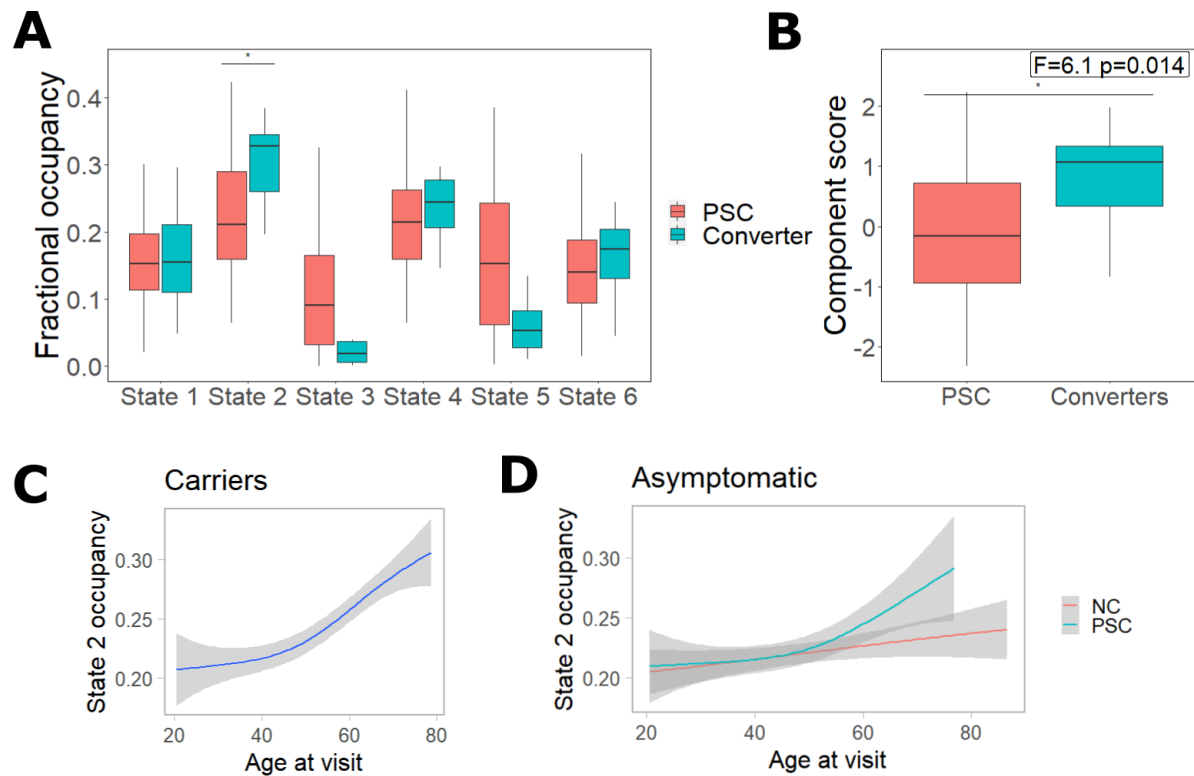


Figure 3-5. *Changes in network dynamics occur in the late presymptomatic phase.* A) State 2 (salience) occupancy and (B) component scores significantly increased in converters (at their latest presymptomatic scan) in contrast to those who have not converted to the symptomatic phase during longitudinal follow up. A non-linear relationship was observed in state 2 occupancy in (C) all carriers and in (D) presymptomatic mutation carriers, in contrast to non-carriers. Regression lines fitted with a generalised additive model, with individual data points removed to protect genetic anonymity.

3.3.7 Network dynamics predict cognitive decline

I assessed whether higher baseline component scores in symptomatic patients were associated with subsequent neurocognitive decline using pre-registered assessments (trail making test B (TMTB), digit symbol, backwards digit span) and measures of global cognitive and behavioural decline (CBI-R, MMSE). Patients at floor scores for assessments were removed prior to deriving linear mixed models (TMTB $n=20$, backwards digit span $n=2$, digit symbol $n=2$). Linear mixed models on longitudinal clinical and neurocognitive scores indicated an effect of time for all measures in symptomatic participants (Supplementary Table 3-2).

Correcting for age at baseline scan, sex and site, baseline component scores were related to the annual rate of clinical progression for MMSE (Figure 3-6A, Std Beta=-0.43, $P=0.001$). The associations with backwards digit span (Std Beta=-0.26, uncorrected $P=0.021$, FDR $P=0.054$) and TMTB (Std Beta=0.35, uncorrected $P=0.035$, FDR $P=0.059$) were not significant after correction for multiple comparisons. No significant relationship was found with digit symbol (Std Beta=-0.21, FDR $P=0.089$) or carer-rated severity using the CBI-R

(Std Beta=0.16 FDR $P=0.18$). I found a significant difference in slope between symptomatic mutation carriers and non-carriers for MMSE, TMTB and CBI-R (group x baseline component score interaction: MMSE Std Beta=-0.66, FDR $P=2 \times 10^{-10}$; backwards digit span Std Beta=-0.23 FDR $P=0.11$; digit symbol Std Beta=-0.12 FDR $P=0.18$; trail making test B Std Beta=0.58 FDR $P=5 \times 10^{-5}$; CBI-R Std Beta=0.12 FDR $P=0.041$).

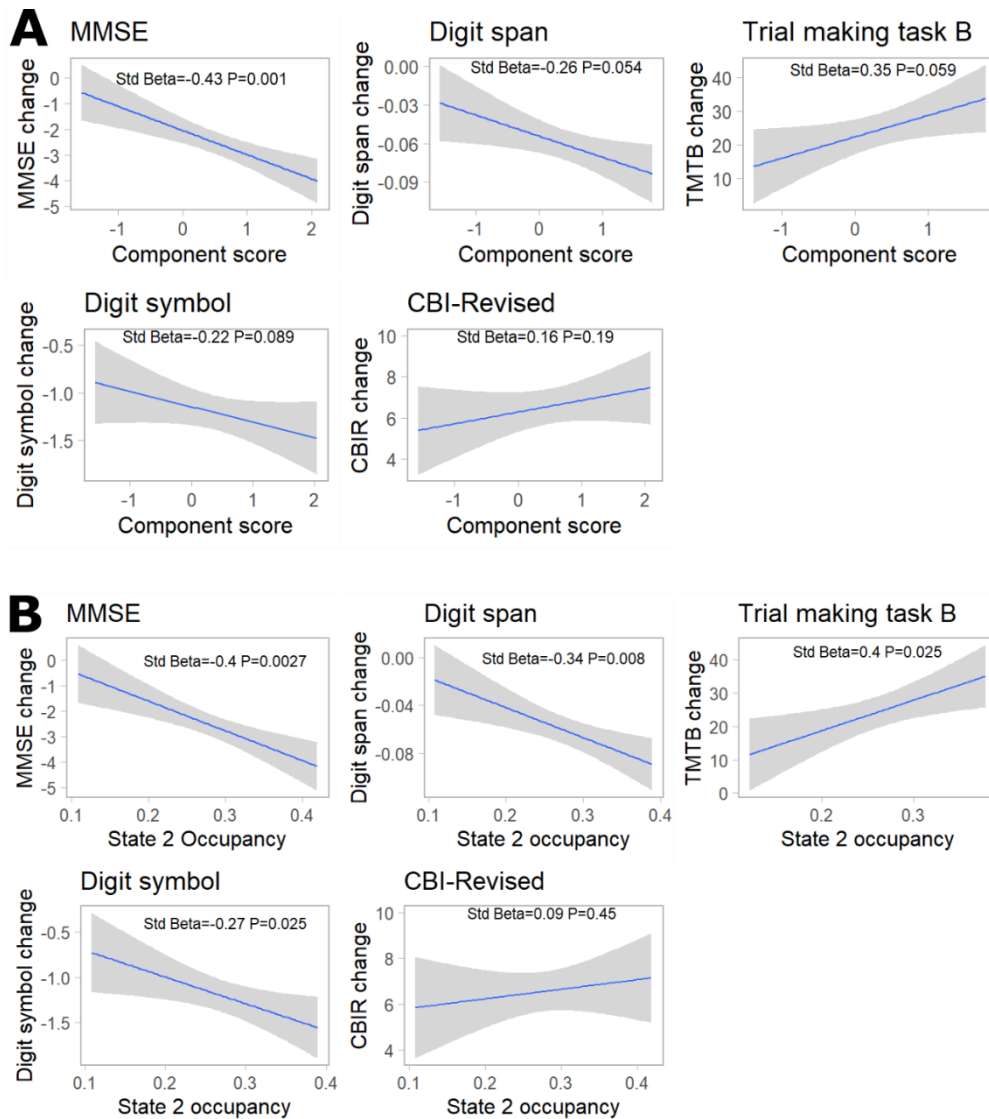


Figure 3-6. Cognitive decline in symptomatic participants (A) Baseline component scores predict subsequent cognitive decline in symptomatic participants in the MMSE, with an uncorrected association with digit span and trail making test B. Annualised rates of change in cognitive scores are derived from a mixed linear effect model, and taken to a second model to compare with component scores while partialling out covariates. (B) Baseline state 2 occupancy predicts subsequent cognitive decline in symptomatic patients in a range of clinical and neuropsychological tests. All p-values are false discovery rate corrected (CBIR Cambridge Behavioural Inventory-Revised, TMTB Trail Making Test B, MMSE Mini-Mental State Examination)

I proceeded to investigate whether baseline network dynamics predicted cognitive and clinical decline in presymptomatic mutation carriers, hypothesising that the relationship

between annualised rate of change in neurocognitive measure and component scores would depend on age as a marker of proximity to symptom onset.

I found that age significantly modified the relationship between annualised rate of clinical progression and baseline component scores for TMTB (Interaction Std Beta=0.21 FDR $P=0.002$), and MMSE (Interaction Std Beta=-0.14 FDR $P=0.048$). For the TMTB, a significant three-way interaction (group x age x component score) implied that baseline component score increased the rate of clinical deterioration in older presymptomatic mutation carriers, relative to non-carriers or younger carriers (Table 3-4). I did not find any significant relationships with digit symbol, backwards digit span or CBI-R.

Model	Slope ~ comp + cov			Slope ~ comp*age + cov			Slope ~ comp*age*group + cov		
	Std Beta	t	P	Std Beta	t	P	Std Beta	t	P
TMTB	-0.13	-1.0	0.75	0.22	3.9	0.0006	0.43	5.1	2×10^{-6}
Digit span	0.02	0.37	0.75	0.09	1.5	0.17	0.12	1.3	0.19
Digit symbol	-0.02	-0.31	0.75	-0.02	-0.45	0.66	-0.12	-1.6	0.15
MMSE	-0.05	-0.76	0.75	-0.14	-2.4	0.048	-0.19	-2.1	0.072
CBI-R	0.03	0.50	0.75	0.11	1.7	0.15	0.20	2.0	0.072

Table 3-4. **Two step prediction models for presymptomatic mutation carriers.** comp Fractional occupancy component, TMTB Trail Making Test B, CBI-R Cambridge Behavioural Inventory-Revised, MMSE Mini-Mental State Examination

Given the difference in state 2 occupancies both in converters and between non-carriers and pre-symptomatic mutation carriers, together with the known role of the salience network in FTD, I also investigated the relationship between baseline state 2 occupancy and longitudinal cognitive decline. Correcting for age at baseline scan, sex and site, baseline state 2 occupancy was related to the annual rate of clinical progression for MMSE (Figure 3-6, Std Beta=-0.4, FDR $P=0.003$), backwards digit span (Std Beta=-0.34, FDR $P=0.008$), digit symbol (Std Beta=-0.27, FDR $P=0.025$) and trail making test B (Std Beta=0.4, FDR $P=0.025$). No relationship was found with carer-rated severity using the CBI-R (Std Beta=0.09 FDR $P=0.45$). I found a significant difference in slope between

symptomatic mutation carriers and non-carriers for all measures except digit symbol and CBI-R (group x baseline state 2 interaction: MMSE Std Beta=-0.6, FDR $P=3 \times 10^{-9}$; backwards digit span Std Beta=-0.27 FDR $P=0.0498$; trail making test B Std Beta=0.57 FDR $P=6 \times 10^{-6}$, CBI-R Std Beta=0.12 FDR $P=0.17$; digit symbol Std Beta=-0.17 FDR $P=0.079$).

I found that age significantly modified the relationship between annualised rate of clinical progression and baseline salience network occupancy for trail making test B (Interaction Std Beta=0.21 FDR $P=0.002$), MMSE (Interaction Std Beta=-0.16 FDR $P=0.023$) and the CBI-R (Interaction Std Beta=0.16 FDR $P=0.030$). For these three measures, significant three-way interactions (group x age x state 2 occupancy) implied that baseline state 2 increased the rate of clinical deterioration in older presymptomatic mutation carriers, relative to non-carriers or younger carriers (Table 3-5). I did not find any significant relationships with digit symbol or backwards digit span.

Model	Slope ~ state 2 + cov			Slope ~ state 2*age + cov			Slope ~ state2*age*group + cov		
	Std Beta	t	P	Std Beta	t	P	Std Beta	t	P
TMTB	0.12	1.9	0.26	0.21	3.6	0.002	0.38	4.4	0.0008
Digit span	0.01	0.16	0.87	0.07	1.2	0.30	0.1	1.1	0.27
Digit symbol	-0.05	-0.97	0.55	0	0.08	0.93	-0.09	-1.2	0.27
MMSE	-0.07	-1.2	0.55	-0.16	-2.6	0.024	-0.24	-2.7	0.022
CBIR	0.05	0.8	0.55	0.16	2.4	0.030	0.22	2.2	0.032

Table 3-5. *Two step prediction models for presymptomatic mutation carriers v baseline state 2 (salience state) occupancy. TMTB Trail Making Test B, CBIR Cambridge Behavioural Inventory-Revised, MMSE Mini-Mental State Examination*

3.3.8 Impact of higher average motion participants on network dynamics

To ensure that the results of the GENFI cohort were not distorted by participants who showed higher motion but were not excluded by the maximum-statistic based criteria, I repeated the analyses excluding 28 scans from 27 participants (10 non-carriers, 9 presymptomatic mutation carriers, 8 symptomatic carriers) who were above 1.2 standard deviations from the whole group mean for mean framewise displacement but included in the primary analysis.

I found that component scores differed between symptomatic participants and non carriers ($F=24.8$ $P=9 \times 10^{-7}$). In symptomatic participants higher component scores were associated with digit symbol, trail making test B, backwards digit span and category fluency (Digit Symbol Std Beta -0.21 FDR $P=0.029$; Trail making test B Std Beta 0.21 FDR $P=0.029$; Digit span Std Beta -0.23 FDR $P=0.029$; Category fluency Std Beta -0.21 FDR $P=0.029$; MMSE Std Beta -0.18 FDR $P=0.062$; CBI-R Std Beta 0.05 FDR $P=0.56$; Letter Fluency -0.18 FDR $P=0.062$, Boston naming Std Beta -0.17 FDR $P=0.062$). Component scores were increased in converters at their latest presymptomatic scan ($F=6.2$ $P=0.013$). Baseline component scores in symptomatic participants were associated with longitudinal decline in MMSE (Std Beta -0.46, FDR $P=0.0006$) and with uncorrected change in digit span (Std Beta -0.28 uncorrected $P=0.020$, FDR $P=0.051$) and trail making test B (Std Beta 0.35, uncorrected $P=0.035$, FDR $P=0.058$). Baseline component scores were associated with cognitive decline in older presymptomatic mutation carriers for the MMSE and trial making test B (MMSE Interaction Std Beta -0.14 FDR $P=0.045$; TMTB Std B 0.23 FDR $P=0.0004$).

3.4 Discussion

This study demonstrates that the temporal dynamics of large-scale brain networks are disrupted by sporadic and familial Frontotemporal Dementia, with characteristic changes in both the symptomatic and late pre-symptomatic phases of disease. There is an increase in salience and default mode network occupancy, and a decrease in proportion of time spent in the primary cortices and subcortical regions: a change which correlates with clinical and neuropsychological markers of disease severity. Changes in temporal dynamics occur near to disease onset and predict the onset and deterioration of the clinical syndrome as evidenced by i) the increased component scores of those who subsequently converted to the symptomatic phase during follow up, and ii) increased rates of cognitive and clinical decline in both symptomatic and older presymptomatic participants with higher component scores.

Functional networks provide an intermediate phenotype to investigate the compensatory changes that account for the dissociation between neuropathological progression and maintained cognitive performance in presymptomatic neurodegeneration (Gregory et al., 2017), with coupling between functional connectivity and cognition increasing close to disease onset (Klöppel et al., 2015; Tsvetanov et al., 2020). Changes in time-varying connectivity predict behavioural traits beyond static functional connectivity or structure alone (Liégeois et al., 2019; Vidaurre et al., 2021), suggesting that investigating network dynamics can inform our understanding of the transition from the presymptomatic to symptomatic phase of neurodegenerative disease. Here I found that while the dynamic repertoire is unchanged through much of the presymptomatic period, the onset of change indicates future symptomatic decline. This suggests that network dynamics can potentially be used both to guide prognosis and as an intermediate marker of success for interventions in presymptomatic mutation carriers, adding to existing clinical, blood and other imaging biomarkers (Meeter et al., 2017).

Given that the salience network is selectively targeted in behavioural variant FTD, with atrophy of network hubs and reduced functional connectivity (Seeley et al., 2009; Zhou et al., 2010; Zhou and Seeley, 2014), the finding of increased salience network occupancy in FTD in both cohorts is perhaps unexpected. The salience network is integral to accessing other large-scale networks, including executive (Sridharan et al., 2008) and default mode networks (Bonnelle et al., 2012). Neuropathological disruption to salience network

connectivity may undermine its ability to coordinate network switching, perturbing global network dynamics, resulting in increased time spent in a state with positive activations in the default mode network and increased time within the salience network itself. Assessment of between group differences in transition probabilities provides a potential explanation for these changes. I found a reduced frequency of transition from the salience state to the subcortical (primarily thalamic) state. Subcortical atrophy is well recognised in FTD, notably in the thalamus, and occurs in both sporadic and genetic FTD (Bocchetta et al., 2018; Lee et al., 2014) including in the presymptomatic phase (Rohrer et al., 2015). These findings could suggest that subcortical network integrity influences cortical salience network dynamics, echoing previous work describing the role of thalamic degeneration in disrupting salience network connectivity in genetic FTD (Lee et al., 2014).

I found that switching rates were reduced in sporadic behavioural variant FTD, but not in familial FTD. While the results from the Cambridge cohort may be a type I error, there are important between-cohort differences that potentially account for this divergence: resting state scans in the Cambridge cohort had on average longer timeseries, enabling more precise modelling of network dynamics; increased severity in participants with sporadic FTD as demonstrated by higher CBI-R; and variation in clinical phenotypes between the two groups. I also found that higher salience network occupancy in older presymptomatic mutation carriers predicted decline in trail making test B scores, but not digit symbol or digit span. This may be because the trail making test captures distinct aspects of executive function (such as set-shifting (Misdraji and Gass, 2010)) that are better predicted by disrupted network dynamics, or that the rapid rate of deterioration in trail making test over time (Rohrer et al., 2015) mean that changes are more easily captured.

There are limitations to this study, despite the advantages of cross-sectional replication and longitudinal follow-up in GENFI. The hidden Markov model provides a data-driven explanation of the data without biological assumptions (Lurie et al., 2019), with resulting constraints to its explanatory power. It is possible that a time-varying connectivity approach with additional biologically informed constraints could provide further group differentiation and refined longitudinal predictions. My approach was not optimised to find differences in brain state dynamics between mutation types or by phenotype. Alternative methodological choices may reveal such differences, according to different a priori numbers of states, focusing on different large-scale networks and modelling subsets of patients. In the GENFI cohort the study design necessarily results in a significant age

difference between non-carriers and symptomatic participants. That similar patterns of state occupancies were observed in the Cambridge cohort suggests that the results are not primarily driven by age differences. This study was also limited by the length of scans compared to studies in healthy populations, for example from resting state fMRI using Human Connectome Project data where use of hidden Markov modelling shows high levels of test-retest reliability (Vidaurre et al., 2017). The imaging protocols in GENFI were designed to ensure that they could be tolerated by patients; however the acquisition times make assessment of longitudinal subject-specific network patterns inappropriate (Gordon et al., 2017).

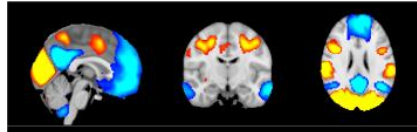
In this study I preregistered the use of age as a proxy marker for disease onset, since parental/familial age of onset explains little additional variance age at symptom onset in GRN and C9orf72 (Moore et al., 2020). There has been growing interest in using latent disease age (Staffaroni et al., 2022), which combines clinical measures, fluid biomarker data, and atrophy to predict disease onset in presymptomatic mutation carriers. I compared the functional disease markers with pre-registered neuropsychological markers given my hypothesis that these changes would be most closely associated with markers of executive function, to focus on markers available in almost all participants, and to increase comparability from the hypothesis generating sporadic cohort to the genetic group. In future work it will be important to assess the relationship in time between temporal network changes and fluid biomarkers (such as NfL), atrophy, and other clinical measures, such as the FTLD-modified CDR.

I conclude that network dynamics are a critical link between neuropathology and symptomatology, heralding symptom onset and correlating with key measures of clinical severity. Network dynamics are a promising tool for stratification and prognostication in frontotemporal dementia.

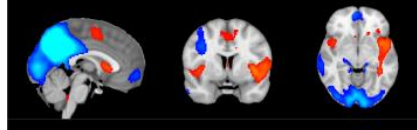
3.5 Supplementary materials for chapter 3

Cambridge

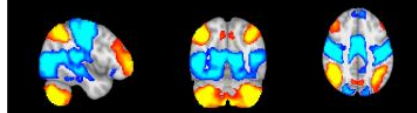
STATE 1
+VE ATT
-VE DMN



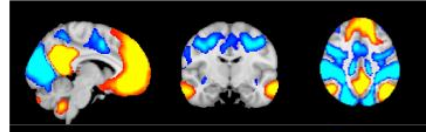
STATE 2
+VE SN
-VE DMN/VIS



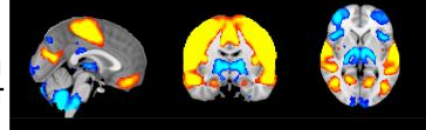
STATE 3
+VE EX
-VE MOT/SEN



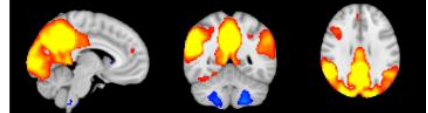
STATE 4
+VE DMN
-VE ATT



STATE 5
+VE MOT/SEN
-VE SUBCORT

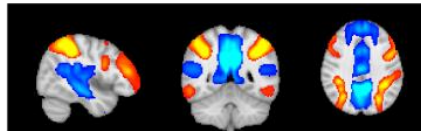


STATE 6
+VE DMN/VIS

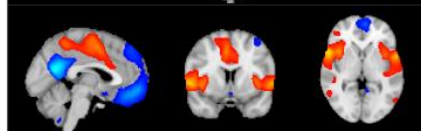


GENFI

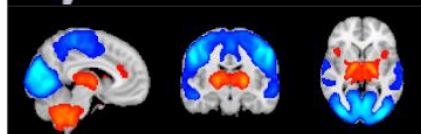
STATE 1
+VE ATT/EX
-VE DMN



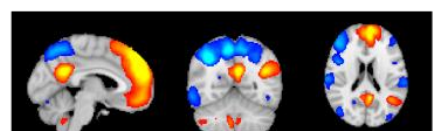
STATE 2
+VE SN
-VE DMN



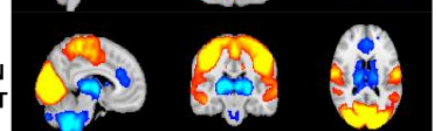
STATE 3
+VE SUBCORT
-VE MOT/SEN



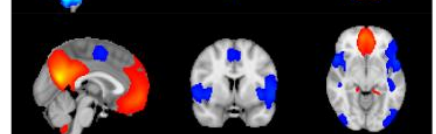
STATE 4
+VE DMN
-VE ATT



STATE 5
+VE MOT/SEN
-VE SUBCORT



STATE 6
+VE DMN
-VE SN



Supplementary Figure 3-1. Mean activation states for the two cohorts. Mean activation maps for the six modelled states in each cohort, with reference to their closest canonical static functional network (DMN default mode network, SN salience network, EX Executive, ATT Attention, MOT motor, SEN sensory, VIS visual).

Scans (n)	Scanner	TR (s)	TE	Vols	Volume slices	Slice thickness	Pixel spacing	FOV	T
88	Philips Achieva	2.2	30	140	36	3.3	2.65\2.65	80*80	3
197	Philips Achieva	2.2	30	200	38	2.72	2.75\2.75	80*80	3
73	Philips Achieva	2.5	30	200	42	3.5	3\3	64*64	3
58	Philips Achieva	2.5	30	200	42	3.5	3\3	64*64	3
15	Philips Achieva	2.2	30	140	33	3.5	2.3\2.3	96*96	3
2	Philips Achieva	2.2	30	140	36	3.3	2.5\2.5	96*96	3
1	Philips Achieva	2.2	30	140	42	3.3	2.5\2.5	96*96	3
9	Siemens Aera	3	30	200	29	3	3.4\3.4	64*64	1.5
3	Siemens Allegra	2.2	30	140	36	3.4	3.4\3.4	64*64	3
36	Siemens Avanto	2.2	30	200	29	3.5	3.5\3.5	64*64	1.5
1	Siemens Avanto	2.2	30	200	29	3.5	3.7\3.7	64*64	1.5
47	GE Discovery	2.2	30	140	39	3.3	3.4\3.4	64*64	3
329	Siemens Prisma	2.5	30	200	42	3.5	3\3	64*64	3
38	Siemens Prisma	2.5	30	200	42	3.5	3\3	64*58	3
14	Siemens Prisma	2.2	30	140	36	3.3	3.3\3.3	64*58	3
1	Siemens Prisma	2.5	30	200	42	3.5	3.3\3.3	64*64	3
1	GE Signa	2.5	30	200	36	3.5	3\3	64*64	3
8	GE Signa	3	30	200	40	3.5	3.4\3.4	64*64	1.5
1	GE Signa	2.5	30	200	45	3.5	3\3	64*64	3
1	GE Signa	3	30	200	39	3.5	3.4\3.4	64*64	1.5
123	Simens Skyra	2.5	30	200	42	3.5	3\3	64*64	3
86	Simens Skyra	2.5	30	200	42	3.5	3\3	64*58	3
16	Simens Skyra	2.25	30	140	36	3.3	3.3\3.3	64*58	3
2	Simens Skyra	2.5	30	200	45	3.5	3\3	64*58	3
2	Simens Skyra	2.5	30	200	42	3.5	3\3	64*60	3
1	Simens Skyra	2.5	30	200	46	3.5	3\3	64*60	3
3	Simens Skyra	2.5	30	200	42	3.5	3.4\3.4	64*64	3
2	Simens Skyra	2.5	30	200	42	3.5	3.4\3.4	64*58	3
2	Simens Skyra	2.5	30	200	42	3.5	3.1\3.1	64*58	3
3	Siemens Triotrim	2	30	300	32	3	3\3	64*64	3

137	Siemens Triotrim	2.2	30	140	42	3.3	3.3\3.3	64*58	3
254	Siemens Triotrim	2.5	30	200	42	3.4	3\3	64*64	3
2	Siemens Triotrim	2.5	30	200	46	3.4	3\3	64*64	3
1	Siemens Triotrim	2.2	30	140	36	3.3	3.3\3.3	64*60	3

Supplementary Table 3-1. **MRI acquisition parameters of all included GENFI scans.** TR=Repetition time, TE=Echo time, FOV=Field-of-view, T=Tesla/Field strength

Neurocognitive/clinical assessment	Annualised rate of change		
	Symptomatic	Presymptomatic mutation carriers	Non-carriers
Group			
TMTB	20 (16)	0.65 (5.6)	0.33 (4.7)
Digit span	-0.05 (0.06)	0.02 (0.06)	0.01 (0.05)
Digit symbol	-1.1 (0.79)	0.54 (0.79)	0.61 (0.69)
MMSE	-2.1 (1.9)	-0.04 (0.22)	-0.02 (0.18)
CBI-revised	5.9 (3.7)	0.68 (1.5)	0.52 (0.89)

Supplementary Table 3-2. *Annualised rates of change in clinical assessments. Scores are mean (SD). (TMTB Trail Making Test B, CBIR Cambridge Behavioural Inventory-Revised, MMSE Mini-Mental State Examination)*

4 Network dynamics in progressive supranuclear palsy

Preface

The work that forms this chapter has been published in *Neurobiology of Aging* as ‘Altered network stability in progressive supranuclear palsy’ (<https://doi.org/10.1016/j.neurobiolaging.2021.07.007>). Data collection was from the research team at the Cambridge Centre for Parkinson-plus, and by a large group of researchers across England and Wales for PROSPECT-M-UK. Task-free functional MRI preprocessing was performed by my supervisor Dr Timothy Rittman, who also calculated regional graph metric and atrophy measures. I designed the analysis strategy and completed the analysis. I wrote the manuscript with input from the publication’s co-authors.

Summary

In this chapter I test the hypothesis that differences in network dynamics explain phenotypic diversity in progressive supranuclear palsy, and that these differences relate to signal complexity, atrophy, and network topology. I used data from 94 participants with PSP and 64 healthy controls from the Cambridge Centre for Parkinson-plus and PROSPECT-M-UK. In both cohorts, I found that PSP increased the proportion of time in networks associated with higher cognitive functions. This effect correlated with clinical severity as measured by the PSPRS, and with reduced neural signal complexity. Regional atrophy influenced abnormal brain-state occupancy, but abnormal network topology and dynamics were not restricted to areas of atrophy. These findings show that a single pathological entity can cause variable and remote changes in neural temporal dynamics, leading to a greater proportion of time in inefficient brain-states.

4.1 Introduction

The human brain optimises efficiency by balancing integration and segregation of information transfer among neural assemblies. The activity and connectivity of regional specialisation is dynamic (Deco et al., 2017; Friston et al., 2012; Honey et al., 2007; Shine, 2019; Tognoli and Kelso, 2014), even on the suprasecond timescale of functional magnetic resonance imaging (Calhoun et al., 2014; Hindriks et al., 2016; Vidaurre et al., 2017). The co-ordination of such state transitions depends on the divergent topological properties of cortical and subcortical regions (Gu et al., 2015), and may be moderated by the principal inhibitory and excitatory neurotransmitters, GABA and glutamate. In the neurodegenerative tauopathies, the pattern of spread of tau-pathology is dictated in part by the brain's topology and connectivity (Z. Ahmed et al., 2014; Clavaguera et al., 2009; Seeley et al., 2009), leading to reductions in effective information processing and cognition.

In this chapter I propose that alterations in large-scale network dynamics contribute to phenotypic heterogeneity in progressive supranuclear palsy (PSP). I focus on this tau-associated disease as a demonstrator condition because of its high clinicopathological correlation. I extend the work in chapter 3 by testing how regional atrophy, abnormal network topology, and signal complexity relate to network dynamics. To quantify signal complexity and network dynamics I use task-free functional MRI (fMRI) from the Cambridge Centre for Parkinson-plus and PROSPECT-M-UK.

The clinical features of PSP, together with its established imaging and pathological findings, qualify it as a model disease to investigate network dynamics. PSP has prominent cognitive and behavioural features, including a dysexecutive frontal syndrome, apathy, impulsivity and language impairment, in addition to the movement disorder of axial akinetic-rigidity and impaired postural reflexes (Burrell et al., 2014; Steele et al., 1964). The disruption to static functional connectivity in PSP (Brown et al., 2017; Gardner et al., 2013; Roskopf et al., 2017; Whitwell et al., 2011) affects frontal cortical regions associated with cognitive control and behaviour, alongside striatal degeneration and loss of dopaminergic and noradrenergic projections from the brainstem to forebrain (Murley and Rowe, 2018). The latter are critical to balancing network integration and segregation (Shine, 2019), with catecholaminergic deficits related to dynamic connectivity, cognitive performance and disease severity (Eldar et al., 2013; Kaalund et al., 2020; Shine et al., 2018).

Network dynamics need to be interpreted in the context of neural complexity (Honey et al., 2007; McDonough and Nashiro, 2014). Complexity varies with the timescale analysed, with the potential for scale dependent relationships between integrative or synchronous activity, state switching and complexity (McDonough and Nashiro, 2014; McIntosh et al., 2014; Wang et al., 2018). This relationship may be due to interference between neural complexity and regional phase relationships, decreasing the likelihood of synchrony between brain regions (Ghanbari et al., 2015). Alternatively, sufficient signal complexity may be required to establish long range dependencies, leading to a positive relationship between connectivity and complexity conditional on timescale (McDonough and Nashiro, 2014; Wang et al., 2018).

Entropy measures have been successfully applied to assess complexity in the relatively short, non-linear and noisy time series typical of fMRI (Grandy et al., 2016; Pincus and Goldberger, 1994; Turkheimer et al., 2015). Sample entropy measures the likelihood that repeated patterns are present in data: signals with a repetitive structure have lower entropy (Richman and Moorman, 2000). Multiscale entropy (MSE) extends sample entropy by assessment at multiple timescales, with the advantage that random noise can be differentiated from complex signal; random fluctuations increase entropy at fine time scales, but with increasing the timescale entropy decreases (Costa et al., 2005).

Large-scale network dynamics can be quantified by hidden Markov modelling (HMM), as described in chapters 2 and 3, in terms of a finite number of mutually exclusive states between which the brain switches over time (Vidaurre et al., 2017).

I used these methods to investigate the impact of PSP on network dynamics, as a function of changes in signal complexity, brain structure and functional reorganisation. I examined two contemporary but independent cohorts of PSP, and controls, from the Cambridge Centre for Parkinson-plus (CCPP) and the UK national PSP Research Network (PROSPECT-MR). In each cohort, I analysed HMM and MSE of task-free functional magnetic resonance. I then tested whether the network properties in PSP varied as a function of disease severity (PSP rating scale) and PSP phenotype (Richardson's syndrome, cortical- and sub-cortical variants).

4.2 Methods

4.2.1 Participants

Forty-five participants with PSP (possible or probable, according to MDS-PSP criteria (Höglinger et al., 2017)) and 27 controls were recruited at the Cambridge University Centre for Parkinson Plus (CCPP). 49 study participants with PSP and 37 controls were recruited to Progressive Supranuclear Palsy-Corticobasal Syndrome-Multiple System Atrophy-UK (PROSPECT-MR) study (Jabbari et al., 2020). Thirty-four participants (28 PSP, 6 controls) were removed following assessment of motion and image quality. For both cohorts clinical assessment included the PSP rating scale (PSPRS) (Golbe and Ohman-Strickland, 2007) and Addenbrooke's Cognitive Examination (ACE: Addenbrooke's Cognitive Examination-Revised for CCPP (Mioshi et al., 2006), Addenbrooke's Cognitive Examination-III for PROSPECT-MR (Hsieh et al., 2013)). Summary scores and demographic details are outlined in Table 4-1.

PSP is a heterogeneous syndrome with variant presentations other than the classical Richardson's syndrome (Jabbari et al., 2020). The clinical phenotype is related to the distribution of tau and focal grey matter loss, allowing us to test whether variation in the topographical distribution of disease burden (Ling et al., 2014; Sakae et al., 2019; Tsuboi et al., 2005) or atrophy (Jabbari et al., 2020) results in distinct changes in network dynamics. In keeping with Jabbari et al, clinical phenotype was categorised as PSP Richardson's syndrome (PSP-RS), PSP-subcortical (i.e. PSP-P with predominant parkinsonism or PSP-PGF with progressive gait freezing) or PSP-cortical (PSP-F with frontal presentations, PSP-CBS with corticobasal features or other focal cortical syndromes). Clinical phenotypes for both cohorts are included in Table 4-1.

4.2.2 MRI acquisition and preprocessing

Image acquisition and preprocessing for the two cohorts was as described in chapter 2. For the Cambridge cohort I only used echo planar imaging with 305 volumes, given the benefits of longer time series in describing time-varying network activity. Given the sensitivity of estimates of network dynamics to participant motion (Laumann et al., 2017; Leonardi and Van De Ville, 2015; Power et al., 2012), I excluded thirty-three participants (27 PSP, 6 Control) with greater than 1 standard deviation from the whole sample mean the four data quality indices described in chapter 2, and one participant with PSP for incomplete data.

Summary measures by group are in Supplementary Table 4-1. I took the average of the four metrics post standardization as covariate of no interest in further analyses.

4.2.3 Structural MRI

I extracted cortical thickness and subcortical grey matter volumes for 246 nodes of the Brainnetome Atlas (Fan et al., 2016) and volumes for four brainstem substructures (midbrain, pons, medulla and superior cerebellar peduncle) (Iglesias et al., 2015) using Freesurfer 6.0 (Dale et al., 1999). I compared differences between participants with PSP and controls in thicknesses and volumes with permutation testing, family-wise error correction for multiple comparisons, and a statistical threshold of $p < 0.05$. Age and total intracranial volume were included as nuisance variables. I compared network dynamic metrics with atrophy measures, focusing on subcortical volumes and frontal cortical thicknesses given that neuropathological changes occur earlier and sequentially in these regions (Kovacs et al., 2020).

4.2.4 Hidden Markov Modelling

To investigate changes in network dynamics in PSP using hidden Markov modelling I followed the methodology set out in chapter 2. I chose a model order of 30 for the initial independent component analysis. From standardised per participant component timecourses a multivariate Gaussian HMM with 8 brain states was inferred using the HMM-MAR toolbox (Vidaurre et al., 2017); it has previously been shown that 8 states capturing large scale networks can be robustly and reliably inferred (Vidaurre et al., 2018). I assessed between-group differences in switching rate and fractional occupancy. Given the interdependence of fractional occupancy rates I performed a principal component analysis (PCA) to compare with severity measures.

4.2.5 Multiscale entropy

To investigate changes in complexity I calculated MSE for the same component timeseries used to infer the HMM, adapting LOFT's Complexity toolkit (Smith et al., 2013b). I averaged over a fixed number of timescales (3 scales PROSPECT-MR, 4 for CAPP due to the longer time series), and calculated sample entropy on the time series constructed for each scale (Costa et al., 2005). MSE is then sum of sample entropy across all timescales. I selected pattern length of 1 and pattern matching threshold of 0.35 given evidence that these parameters provide robust results (Yang et al., 2018). I took the average MSE calculated across the 30 component timeseries for further analyses. I assessed between-group

differences and the correlation across-subjects between complexity and fractional occupancy.

4.2.6 Graph measures

I performed graph theoretical analysis using Maybrain software (<https://github.com/RittmanResearch/maybrain>) and NetworkX (Hagberg et al., 2008), with the Brainnetome parcellation, as outlined in chapter 2. In brief, association matrices were constructed by taking the wavelet cross-correlation between each region using a maximal overlap discrete wavelet transform and Daubechies filter performed using the waveslim package in R. The second band of 4 was used corresponding to a frequency range of 0.0675-0.125Hz (Achard and Bullmore, 2007).

To test the hypothesis that changes in network dynamics were related to cortical network topological remodelling in PSP in response to subcortical tau burden, I focused on graph metrics that quantify regional connectivity and small world properties (Bassett and Bullmore, 2016; Watts and Strogatz, 1998). I therefore derived the following metrics: *weighted degree*, measuring the number and strength of nodal functional connections; *clustering coefficient*, the proportion of triangular connections formed by each node over the proportion of all possible such connections; and *path length*, the average shortest topological distance between nodes of the graph. Small world properties of cortical topology enable segregation and integration while minimising the biological costs of maintaining connections (Bassett and Bullmore, 2016). If the brain networks lose small world characteristics to become more random, it is plausible that network dynamics would be altered.

Path length and clustering coefficient were assessed across the brain, and weighted degree in cortical and subcortical regions and between groups. Metrics except for weighted degree were binarised after thresholding and normalised against 1000 random graphs with identical degree distribution and random connections. A network density threshold of 5% was used. I also report results at density thresholds of 1-10% for significant results to ensure robustness.

4.2.7 Statistical approach

I conducted initial analysis in the two cohorts separately. This was to allow analysis of MSE at higher scales in the CCPP cohort, thereby increasing the ability to differentiate complex signal from randomness and to contrast with HMM metrics, given that with fewer

than 50 timepoints error of sample entropy estimates may increase (Yang et al., 2018, 2013). Replication can ensure that results are robust, an important factor given concerns that apparent changes in network dynamics from resting state fMRI are attributable to analysis techniques, head motion and sleep (Laumann et al., 2017).

Statistical tests used a general linear model with permutation testing (10000 permutations), with family-wise error correction for multiple comparisons and contrasts using FSL's PALM (Winkler et al., 2014) and a statistical threshold of $p < 0.05$. The exceptions were moderation analysis, comparisons with graph metrics and direct tests of slope, which were performed in R (R Core Team, 2018). Participant motion, age and sex (estimated total intracranial volume for contrasts involving measures of volume) were included as nuisance variables.

4.3 Results

4.3.1 Demographics

There were 24 participants with PSP and 22 controls from CCPP with sufficient length fMRI (305 volumes) who were not removed following assessment of motion parameters, and 42 participants with PSP and 36 controls from PROSPECT-MR. Demographic details are outlined in Table 4-1. There were significant differences in age in both cohorts and in gender in PROSPECT-MR.

	CCPP: Control	CCPP: PSP	t/ χ (p)	PROSPECT: Control	PROSPECT: PSP	t/ χ (p)
Number	22	24		36	42	
Age (years)	64.9 (9.9)	70.1 (6.5)	t=2.1 p=0.038	67.3 (7.1)	71.1 (7.3)	t=2.4 p=0.021
Gender (F/M)	14/8	11/13	χ =1.5 p=0.23	26/10	15/27	χ =10.4 p=0.001
PSP clinical phenotype (n)		PSP-RS = 16 PSP-subcortical= 0 PSP-cortical=8			PSP-RS = 25 PSP-subcortical= 11 PSP-cortical=6	
ACE		82 (11.4)		95.7 (3.4)	81.3 (11.6)	t=6.9 p<0.0001
PSPRS		34.9 (12.5)			33.9 (14.2)	

Table 4-1. *Demographic and clinical characteristics of study participants.* ACE: Addenbrooke's Cognitive Examination, PSPRS Progressive supranuclear palsy rating scale

4.3.2 Network dynamics

CCPP: I used temporally concatenated participant timeseries from ICA components to fit an HMM with 8 brain states. Mean activation maps for these states are shown in Figure 4-1A.

There was no difference in switching rate between controls and participants with PSP (t=0.37, p=0.59). I performed a PCA of fractional occupancy rates, which are collinear and compositional. Three components with eigenvalues greater than 1 explained 75% of the variance and were taken forward for further analysis. The first component was significantly

more negative in PSP than controls ($t=4.0$, FWE $p=0.0008$) (Figure 4-1B). States with the highest positive loadings (states 5 and 7) had prominent subcortical and posterior activation, while states with the most negative loadings (states 1, 4 and 6) largely constituted the executive control and salience networks.

CCPP A

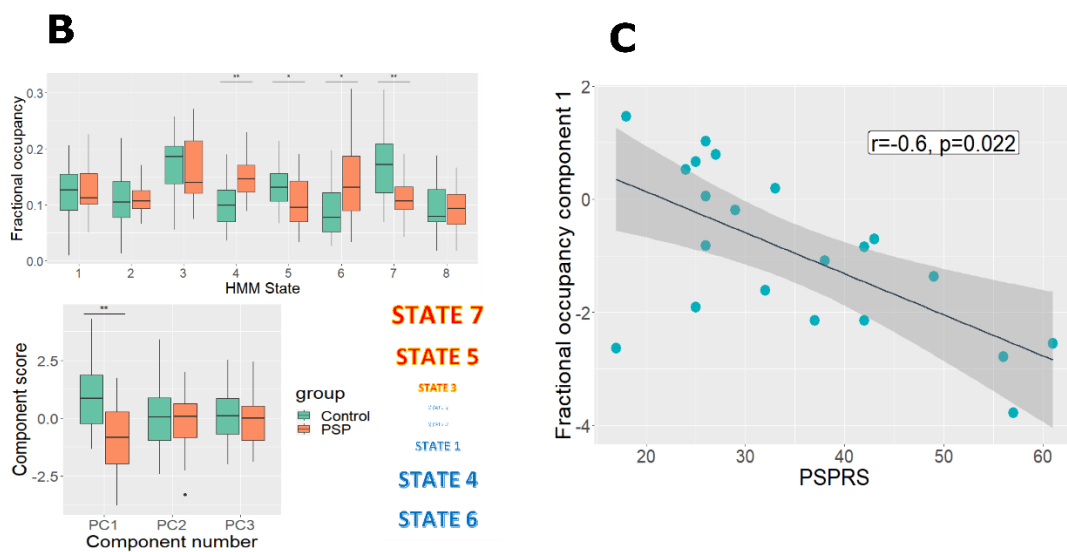
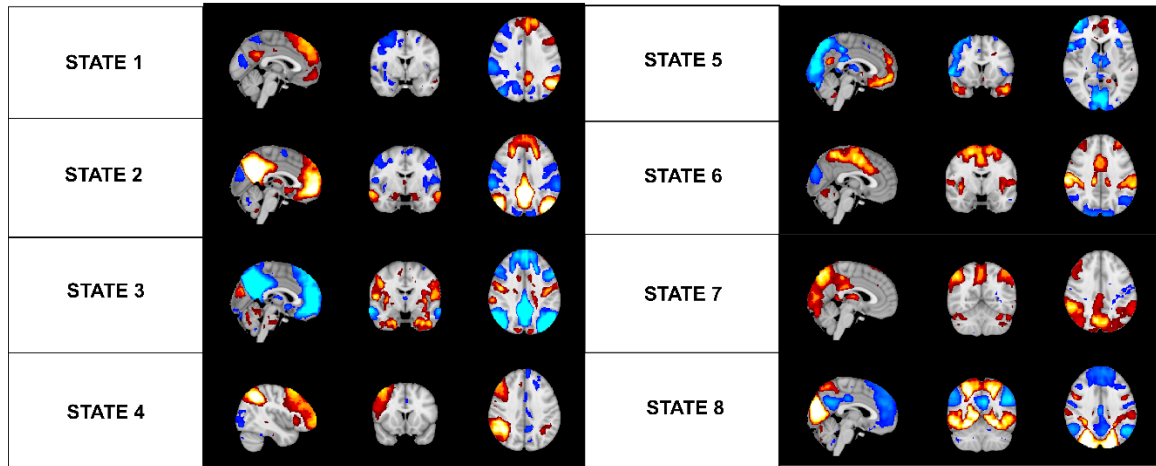


Figure 4-1 Network dynamics in PSP vs controls for the Cambridge cohort A) Mean activation maps for the 8 inferred brain states from hidden Markov modelling for the Cambridge cohorts. B) Altered fractional occupancy rates in PSP. Results are shown both by differences in states computed within a general linear model with a single permutation test and family-wise error correction, and in a principal component analysis of fractional occupancy rates. Participants with PSP spent less time in states with subcortical and posterior activation, and more time in frontoparietal and salience states. Colours of state names indicate direction of principal component loading, and font size scales with their magnitude. C) The component that differed between PSP and controls correlated with PSP rating scale among patients

PROSPECT-MR: Mean activation maps for the 8 HMM inferred PROSPECT-MR brain states are shown in Figure 4-2A. States 1-4 were the closest Dice coefficient matches (Supplementary Figure 4-1) for both positive and negative maps. There were anatomical differences in the mean activation maps between the two cohorts, particularly in identified

anti-correlations, resulting in divergence between designations for positive and negative maps. Therefore, I adjudicated matching for the remaining states by visual inspection.

PROSPECT A

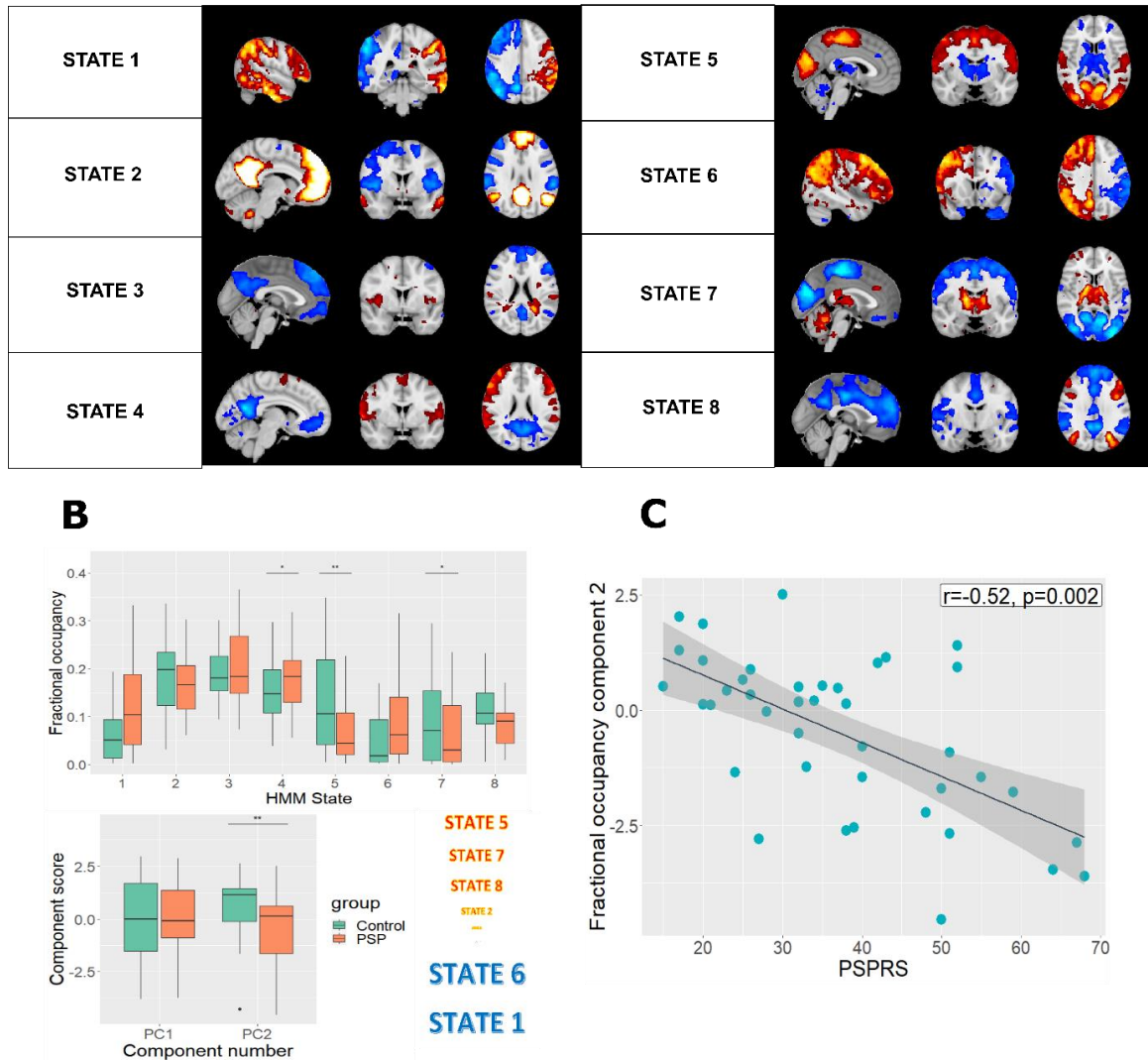


Figure 4-2. Network dynamics in the PROSPECT cohort. A) Mean activation maps for the 8 inferred brain states from hidden Markov modelling. B) Altered fractional occupancy rates in PSP. As in the Cambridge Figure cohort participants with PSP spent less time in states with subcortical and in motor and sensory (somatic, visual) regions activation, and more time in frontoparietal states. C) The component that differed between PSP and controls correlated with PSP rating scale among patients.

There was no difference in switching rate between the two groups, but participants with PSP had altered fractional occupancy (see Figure 4-2B). Two components with eigenvalues greater than 1 explained 74% of the variance and were taken forward for further analysis. Component scores for the second component were significantly lower in PSP ($t=3.1$, FWE $p=0.006$). States with the most positive loadings (states 5 and 7) had prominent subcortical, posterior and motor region activations, while states with negative loadings overlapped with executive networks (states 1 and 6).

In summary, in both groups participants with PSP spent a greater proportion of time in states of activity in executive networks, and away from states of activity in networks with posterior and subcortical activations.

4.3.3 Network dynamics and clinical severity.

I tested whether the distinct changes in network dynamics in PSP were related to clinical severity, as measured by the PSPRS and ACE.

CCPP: The first fractional occupancy component negatively correlated with the PSPRS ($r=-0.60$, $t=-3.1$, FWE $p=0.022$, see Figure 4-1C). There was also a relationship between principal component 3 and ACE which was not significant after correction for multiple comparisons ($r=0.47$, $t=2.4$, uncorrected $p=0.03$).

PROSPECT-MR: Component scores for the second fractional occupancy component correlated with PSPRS ($r=-0.52$, $t=-3.7$, FWE $p=0.002$, Figure 4-2C). There was also a relationship between the second fractional occupancy component and ACE which was not significant after correction for multiple comparisons ($r=-0.34$, $t=-2.1$, uncorrected $p=0.046$).

4.3.4 Complexity

I investigated whether complexity differed between PSP and Controls, to provide further insight into temporal dynamics in the disease.

CCPP: I calculated MSE for each participant at 4 timescales using the same component timeseries used to infer the HMM. MSE was significantly reduced in PSP ($t=2.3$, $p=0.022$, Figure 4-3A).

PROSPECT-MR: MSE was calculated over 3 rather than 4 timescales, due to shorter time series. In contrast to our locally collected data, I did not find the reduction in MSE in PSP to be significant ($t=1.1$, $p=0.27$, Figure 4-3D)

4.3.5 Network dynamics and complexity

I investigated the relationship between signal complexity and network dynamics. I asked whether a) the distinct changes in fractional occupancy were related to complexity and b) switching rate related to complexity, and whether these relationships interacted with diagnosis.

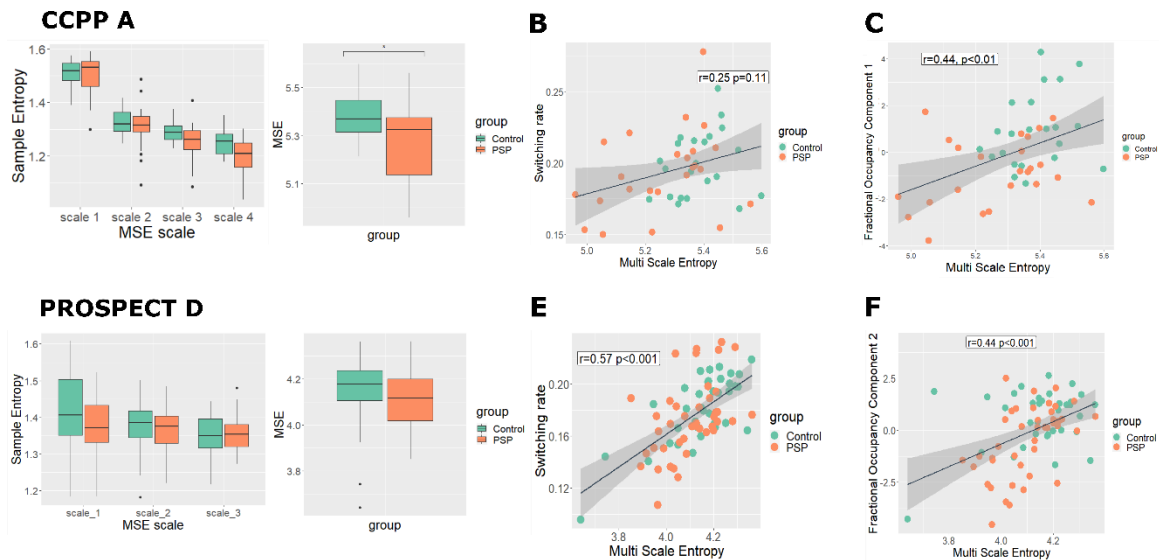


Figure 4-3. **Complexity analysis** A) and D) I found complexity to be reduced in PSP in the CCPP, but not in PROSPECT-MR. B) and E) In PROSPECT-MR but not CCPP multiscale entropy (MSE) correlated significantly with switching rate. C) and F) MSE correlated with the fractional occupancy component that differed between PSP and controls in CCPP.

Fractional occupancy and MSE. In both groups there was a significant relationship between MSE and the fractional occupancy component that differed between people with PSP and Controls (CCPP $r=0.44$, $t=3.2$, $p=0.004$, Figure 4-3C; PROSPECT-MR $r=0.44$, $t=4.2$, $p=0.0003$, Figure 4-3F). We performed a moderation analysis by including an interaction between diagnosis and MSE. This did not show any significant differences in these relationships by diagnosis. In PROSPECT-MR the slope in controls was driven by a single outlier; following outlier removal the relationship between component and complexity differed by diagnosis (PROSPECT-MR $\Delta r^2 = 0.08$, $F=9.8$, $p=0.003$).

Switching rates and MSE: In the CCPP group MSE did not correlate significantly (Figure 4-3) with switching rate ($r=0.25$, $t=1.6$, $p=0.11$). In the PROSPECT-MR group a significant relationship was found ($r=0.57$, $t=6$, $p=0.0001$, Figure 4-3E). Moderation analysis did not show any significant group differences in these relationships.

4.3.6 Network dynamics in PSP versus structure, topology, and clinical presentation

I tested the hypothesis that people with PSP spend a greater proportion of time in inefficient states due to cortical remodelling in response to focal disease. Given that distribution of atrophy and pathology differ by phenotype, I tested whether network dynamics vary by clinical phenotype. Since the two datasets showed overlapping changes in brain state occupancy in PSP, I performed a combined analysis to investigate these hypotheses,

focusing on fractional occupancy. I assessed whether fractional occupancy components: i) relate to frontal cortical thickness and subcortical volumes; ii) relate to regional topological remodeling; and iii) differed depending on PSP clinical phenotype.

I first sought to investigate the distribution of atrophy across the two cohorts. For participants with PSP I found significant areas of grey matter atrophy compared to controls in the midbrain and subcortical regions defined by the Brainnetome Atlas (Figure 4-4). I found cortical atrophy primarily in the frontal lobe and peri-Rolandic regions, but also in the temporal and parietal cortex. There were no regional differences when comparing participants with PSP between the Cambridge and PROSPECT cohorts.

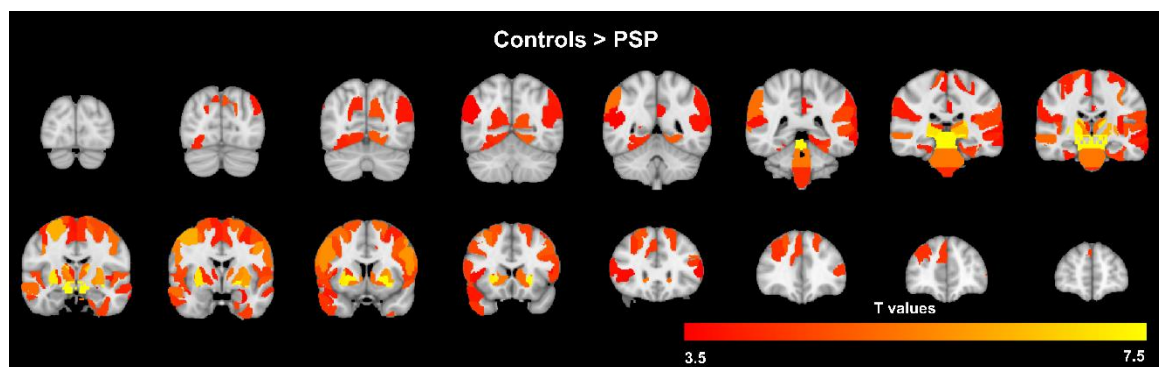


Figure 4-4. Significant areas of grey matter volume reduction in PSP v controls. Differences in a combined analysis across the two cohorts, where regions are nodes of the Brainnetome Parcellation. $p < 0.05$ after family-wise error correction for multiple comparisons. There were no regional differences in direct comparison of participants with PSP from the two cohorts.

The two principal components derived from HMM analysis (Figure 4-5A and Figure 4-5D) that were taken forward for analysis differed between PSP and controls (component 1 $t=2.6$, $p=0.023$; component 2 $t=-2.8$, $p=0.014$).

Looking at the PSP group only, component 1 correlated with subcortical volume ($r=0.30$, $\Delta r^2 = 0.08$, $t=2.4$, $p=0.038$), but not frontal cortical thickness ($r=0.03$, $t=0.24$, $p=0.96$, figure 4C). Steiger's Z-test of the partial correlation coefficients did not find a significant difference between the strength of the correlations with component 1 (Steiger's $Z=1.9$, $p=0.06$). Component 2 did not correlate with either frontal cortical thickness ($r=-0.20$, $t=-1.6$, FWE $p=0.22$), or subcortical grey matter volume ($r=-0.19$, $t=-1.5$, $p=0.26$, Figure 4-5D).

I then tested whether changes in brain state occupancy were driven by randomisation of the network and connectivity changes in subcortical and cortical regions in response to focal atrophy. Component 2 scores correlated negatively with clustering coefficient ($r=-0.23$, $t=-$

2.6, $p=0.012$, Figure 4-5F, replicated between thresholds 2-10%) suggesting increasing randomness of the brain's network topology. No significant correlation was found with path length ($r=-0.14$, $t=-1.4$, $p=0.14$). The relationship between weighted degree and component 2 differed between people with PSP and controls in both cortical and subcortical regions (cortical $F=4$, $\Delta r^2 = 0.03$, $p=0.047$; subcortical $F=4$, $\Delta r^2 = 0.03$, $p=0.048$) and was steeper in participants with PSP (cortical $r=-0.31$, $t=-2.5$ $p=0.014$; subcortical $r=-0.34$ $t=-2.8$ $p=0.006$) than in controls (cortical $r=0$, $t=-0.02$ $p=0.98$; subcortical $r=-0.06$ $t=-0.44$ $p=0.66$). No significant relationships were found with component 1.

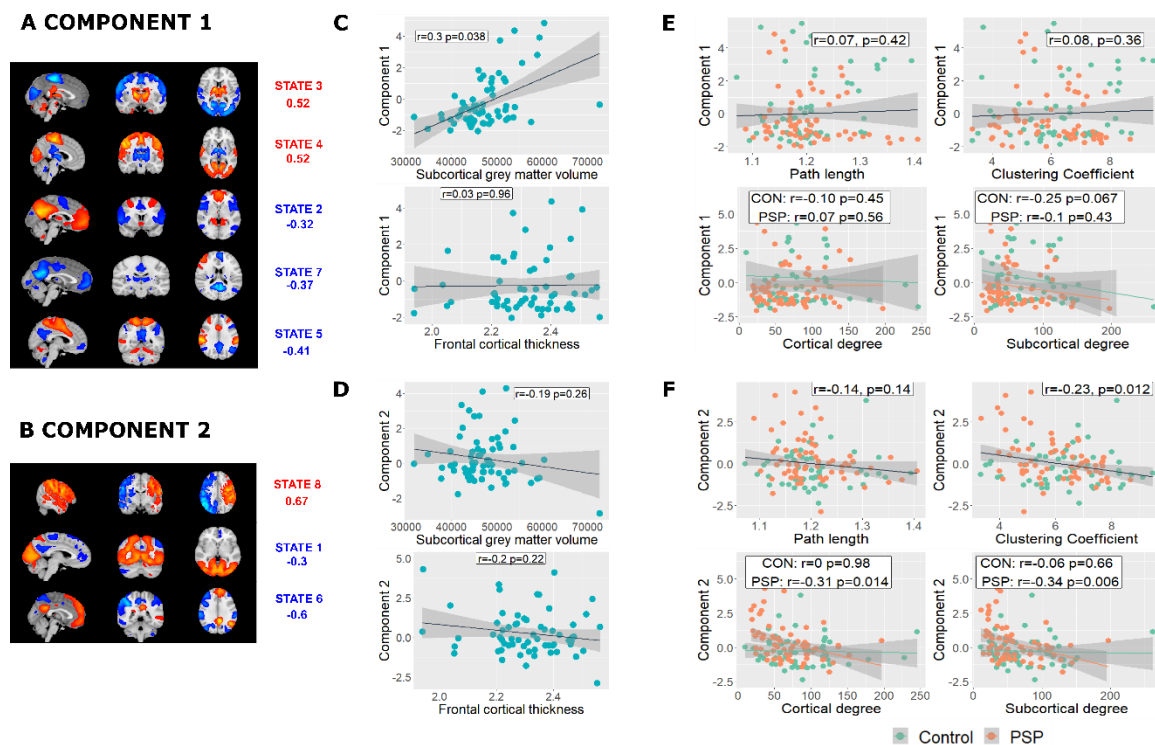


Figure 4-5. *Network dynamics, atrophy and network topology.* A) and B) In a combined analysis of the two cohorts the first two principal components differed between PSP and controls. Mean activation states with PCA loadings $>|0.3|$ are shown. C) and D) Component 1 correlated with subcortical volume but not frontal cortical thickness, although with no significant difference in slope. Component 2 did not correlate significantly with either frontal cortical thickness or subcortical volume. E and F) Loadings in component 2 were associated with reduced clustering coefficient and reduced weighted degree in PSP but not controls. No relationships were found with component 1.

Despite the relationships between network dynamics, focal atrophy and topological changes, I found no significant difference by clinical phenotype (component 1 $F=3.4$ $p=0.083$; component 2 $F=0.57$, $p=0.82$).

4.4 Discussion

The principal results of this study are that (i) the exemplar tauopathy of PSP changes network dynamics, with a higher proportion of time spent in frontoparietal activation states; (ii) these changes in network dynamics are related to complexity as measured by multi-scale entropy, (iii) the changes in network dynamics correlated with clinical severity and regional atrophy; and (iv) altered network dynamics occur in the context of widespread changes to network topology. The effect of PSP phenotypic variance is expressed in terms of the relationship between network dynamics, clinical severity and focal atrophy, in cortical *versus* subcortical regions.

In two independent datasets, people with PSP spent more time in states whose spatial distributions mirror executive control networks. Given that in health, occupancy of networks associated with higher order cognition correlates positively with cognitive function (Vidaurre et al., 2017), these results may seem surprising. Time in these networks did not correlate with frontal atrophy but did show a negative relationship with clustering coefficient and weighted degree only in PSP. This suggests a loss of small-world properties towards greater network randomness (Bassett and Bullmore, 2016; Watts and Strogatz, 1998), with occupancy of a remodelled and more random network no longer relating to its effective functioning.

PSP causes severe disruption to connectivity between the subcortex/brainstem and cortical regions (Brown et al., 2017; Whitwell et al., 2011), changes that may account for my finding of reduced time in states with activity in subcortical regions, which correlated with subcortical atrophy. So, why do participants with PSP spend more time in executive control networks and less time in states representing the default mode network with negative activations in regions of the task-positive network? Regional structural network properties influence brain state transitions, with access to frontoparietal cognitive control networks depending on nodes within weakly connected regions (Gu et al., 2015). These key nodes in a dysfunctional random network may no longer effectively determine state transitions, causing altered network dynamics in regions remote from the primary pathology. Specifically, the results shed light on the interplay in disease between atrophy, remodelling of network topology and network dynamics.

I found that network dynamics in PSP varied by disease severity, both in terms of relationship to atrophy and to the PSPRS: the latter is sensitive to disease progression and

predicts survival (Bang et al., 2016; Golbe and Ohman-Strickland, 2007). I did not find that this dependency translated into differences between PSP phenotypes, although this study was powered to only detect large subgroup differences. Nonetheless, given that the intrinsic network architecture of the brain present at rest shapes that seen during tasks (Cole et al., 2014; Smith et al., 2009), and that network structure predict behavioural traits (Arbabshirani et al., 2017; Beaty et al., 2018; Meer et al., 2020; Rosenberg et al., 2016), I hypothesise that the observed changes in brain state transitions in PSP underpin cognitive symptoms of the disease.

I have shown that measuring complexity provides a complementary method to assess temporal dynamics in disease. In the CCPP dataset I found reduced complexity in PSP, with the greatest differences seen at the highest scale, indicating a true reduction in complexity and not randomness. This result was not seen in PROSPECT-MR, perhaps because these images were acquired with fewer time points. I found that complexity correlated with both switching rate and fractional occupancy, suggesting that changes in global signal influence network dynamics in PSP. This raises the possibility of additional aetiological factors to those outlined above, such as the profound neurotransmitter deficits which occur early in PSP (Murley and Rowe, 2018) and alter global fMRI signal (Turchi et al., 2018) and dynamic connectivity (Shine et al., 2018) in health.

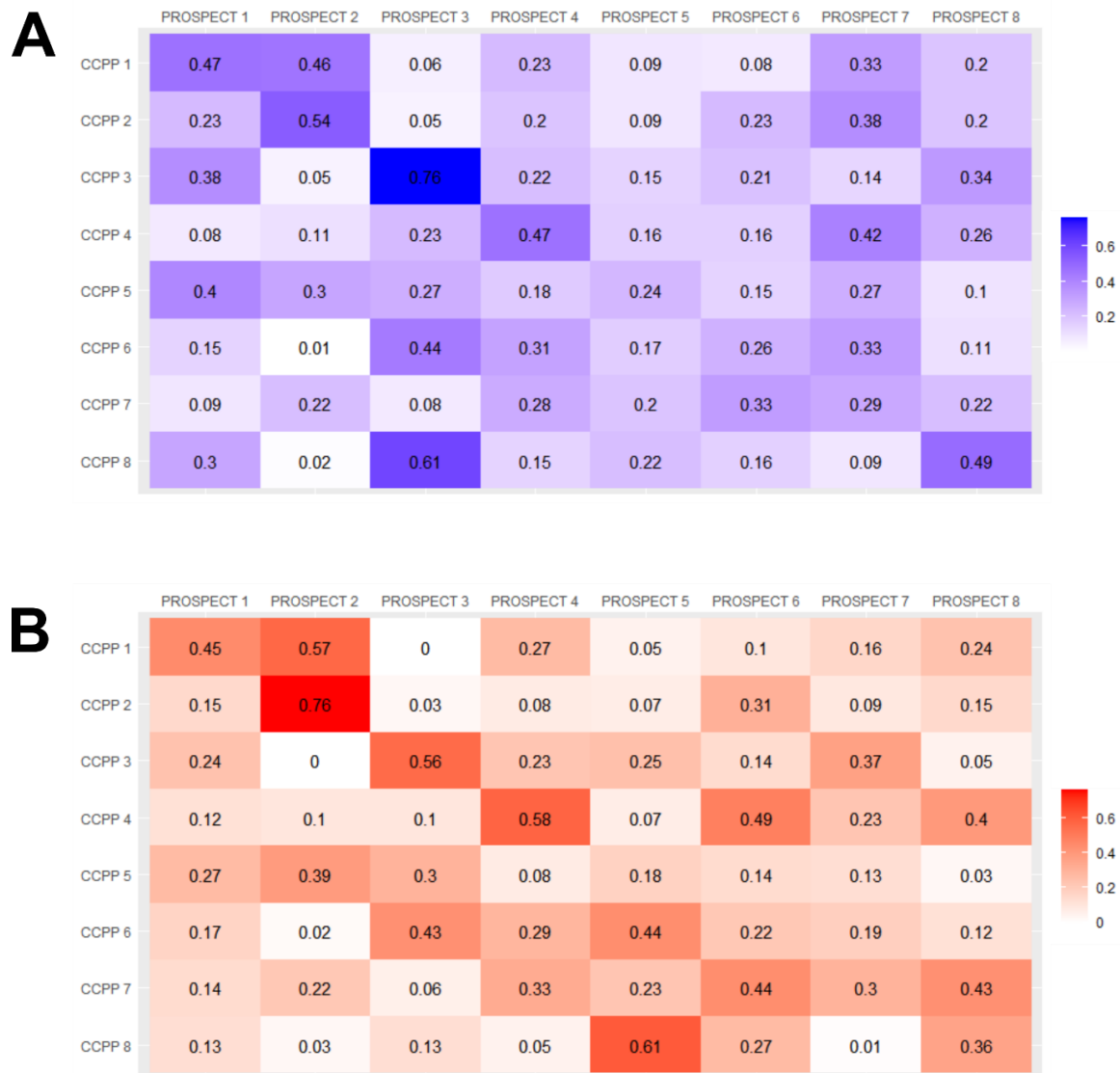
I used a different model order to infer each HMM for this chapter, with eight states chosen rather than six in Chapter 3. This was chosen in order to capture phenotypic variation across a single diagnostic entity, rather than identify broad changes that align most closely with general cognition as when investigating genetic FTD. This limits the ability to make direct comparisons between the HMMs for the different diagnostic entities, including for fractional occupancies of individual states. Note however that in performing a principal component analysis allows scores from multiple states to be collapsed to a small number of scores. Here I observed similar findings, with greater time spent in higher cortical states and away from sub-cortical regions.

There has been controversy as to whether variability in dynamic functional connectivity in task-free fMRI represents more than motion (Laumann et al., 2017). I used stringent exclusion criteria to limit the impact of movement artefact. A key advantage of this study is that results are replicated in two datasets, an important part of the solution to non-generalizable results in neuroimaging due to low statistical power and analytic flexibility

(Poldrack et al., 2017). My approach did however result in significant numbers of exclusions, particularly from the CCPP dataset (due to the longer time series). It may be that these excluded participants have distinct clinical phenotypes, and therefore the conclusions would not apply to all individuals with PSP. Modelling network dynamics via an HMM requires forced choices in analysis, notably the number of states inferred. If brain states consist of a hierarchy of structures (Vidaurre et al., 2017) it is likely that HMMs can provide multiple related solutions. Indeed, this may account for some of the anatomical differences observed in the two datasets. I believe that this challenge is best tackled by independent replication and relating findings to clinical scores. The findings that properties of dynamic connectivity were related to clinical measures is reassuring in this regard.

Investigating dynamics of large-scale resting state networks offers an intermediate phenotype with which to understand clinical syndromes. Through hidden Markov modelling I have shown that changes in network dynamics relate to neural signal complexity and to phenotypic variance in progressive supranuclear palsy. This approach demonstrates how abnormalities in regional atrophy and topological changes correlate with brain state transitions, and provides a means to directly test the causes and consequences of altered network dynamics.

4.5 Supplementary materials for chapter 4



Supplementary Figure 4-1. Dice coefficients between binarised A) negative and B) positive CCPP and PROSPECT-MR states

	Control included	PSP included	t (p)	Control excluded	PSP excluded
Maximum spike percentage	9.8 (5.9)	13.7 (7.9)	-3.2 (0.002)	27.9 (13)	41.6 (16)
Median spike percentage	2.5 (1.3)	2.5 (1.4)	-0.02 (0.98)	6 (3.9)	5.6 (4.3)
Maximum framewise displacement	0.54 (0.45)	1 (0.95)	-3.3 (0.001)	2.1 (2.3)	5.1 (7.1)
Maximum DVARS	7.3 (1.1)	7.5 (1.1)	-0.84 (0.41)	9.7 (0.8)	10.4 (2.3)

Supplementary Table 4-1. Motion quality metrics for participants. Values are mean (SD)

5 Functional connectivity and synaptic density in syndromes associated with Frontotemporal Lobar Degeneration

Preface

This chapter forms part of a manuscript that is currently in revision. Patient recruitment and data collection was a collaborative effort by a group of researchers at the Cambridge Centre for Parkinson-plus and the Cambridge Centre for Frontotemporal Dementia, particularly Negin Holland, George Savulich, Maura Malpetti, and Michelle Naessens. Positron emission tomography data was pre-processed by Tim Fryer and Young Hong, who provided regional values and non-displaceable [^{11}C]UCB-J binding potential maps. Analysis of locus coeruleus integrity was performed by Rong Ye. I designed and executed the analysis strategy with help from Simon Jones and Kamen Tsvetanov. I wrote the text, with input from co-authors of the manuscript.

Summary

In this chapter I investigate how *in vivo* synaptic loss in FTLD syndromes, measured using the PET ligand [^{11}C]UCB-J, affects behaviour in relation to functional connectivity. I further test the contributions of synaptic density, atrophy and neurotransmitter receptor and transporter distributions in explaining regional variation in functional connectivity. I show that the anatomical distribution of synaptic loss partially overlaps in FTLD syndromes but with syndrome-specific effects. I also demonstrate that; [^{11}C]UCB-J binding potential is associated with reduced connectivity, with synaptic density predicting measures of connectivity over and above grey matter volume; functional connectivity adds to and moderates the relationship between synaptic density and clinical severity; neurotransmitter receptor/transporter distributions from control populations explain significant additional variance in weighted degree in all patients and in PSP alone. For a subset of patients with 7-Telsa imaging, the relationship between noradrenaline transporter distribution and weighted degree is associated with whole locus coeruleus integrity. This work demonstrates

the benefit of multi-modal quantification of the biomarker cascade in investigating the determinants of clinical heterogeneity in FTLD.

5.1 Introduction

Frontotemporal lobar degeneration (FTLD) pathologies cause heterogenous syndromes with partially overlapping clinical features and highly variable correlations between neuropathology and phenotypic expression (Murley et al., 2020a; Respondek et al., 2014; Rohrer et al., 2011; Seeley, 2017). These conditions are associated with early loss of functional independence, considerable care burden and reduced life expectancy (Coyle-Gilchrist et al., 2016; Murley et al., 2021). There is a pressing need for new therapeutic interventions, based on better characterisation and *in vivo* analysis of the pathogenic cascade leading to clinical presentation and progression (Eimeren et al., 2019; Jack et al., 2010). This cascade includes severe synaptic loss (Holland et al., 2020; Malpetti et al., 2022), which integrates the toxicity of protein aggregation and inflammation (Hong et al., 2016; Hoover et al., 2010; Liddelow et al., 2017; Spires-Jones and Hyman, 2014).

I propose that the severe synaptic loss arising from frontotemporal lobar degeneration would impair local and long-range functional connectivity, and consequently affect cognition and behaviour. I test this hypothesis with three clinical syndromes associated with different types of frontotemporal lobar degeneration; progressive supranuclear palsy (PSP), corticobasal syndrome (CBS) and behavioural variant frontotemporal dementia (bvFTD). These phenotypic entities show molecular heterogeneity, with 3-repeat and 4-repeat tauopathies and TDP-43 pathology. By studying these distinct syndromes from the FTLD-spectrum, I capture variations in anatomical distribution of synaptic loss to better assess its consequence for connectivity and clinical severity.

The radioligand [¹¹C]UCB-J quantifies synaptic density through selective binding to the presynaptic vesicle glycoprotein 2A (SV2A). When used in positron emission tomography scanning, it demonstrates a reduction in non-displaceable binding potential in bvFTD (Malpetti et al., 2022), CBS and PSP (Holland et al., 2020). [¹¹C]UCB-J non-displaceable binding potential correlates with clinical severity and validates the post mortem studies (Bigio et al., 2001; Lipton et al., 2001). [¹¹C]UCB-J binding potential is primarily a measure of synaptic density rather than synaptic function (Serrano et al., 2022) and is directly related to changes in cortical neurophysiological generators in FTLD (Adams et al., 2022). Functional connectivity dysfunction may also be explained by cell death and the extensive neurotransmitter deficits in FTLD (Murley and Rowe, 2018). Disruption to functional

connectivity and network integration in FTLD-disorders aligns closely with symptom onset and progression (Rittman et al., 2019; Tsvetanov et al., 2020).

I therefore aimed to test the overarching hypothesis that differences in synaptic density are related to disruption of large-scale brain connectivity and network organisation as measured from resting state functional MRI (fMRI). I undertook a multimodal neuroimaging study to combine [¹¹C]UCB-J non-displaceable binding potential with resting state functional MRI in participants with FTLD-associated disorders and similarly-aged healthy controls. I quantified functional connectivity using the graph metric of weighted degree. I predicted that synaptic loss would be associated with reduced connectivity, and that reductions in synaptic density would explain connectivity loss that is not accounted for by atrophy. To further understand the role of neurotransmitter changes in connectivity changes over and above synaptic loss, I used (i) PET derived maps of neurotransmitter receptor/transporter distributions, and (ii) ultrahigh field MRI imaging of locus coeruleus integrity. To examine disease-specific differences in the effect of synaptic loss, I reduced data dimensionality by independent component analysis. I predicted that reduced synaptic density would be associated with connectivity loss of the same region and the region to which it is connected, in such a way as predicts individual differences in cognition.

5.2 Methods

5.2.1 Participants

Twenty-nine participants with probable progressive supranuclear palsy, Richardson's syndrome (Höglinger et al., 2017), 16 participants with probable corticobasal syndrome and probable corticobasal degeneration (Armstrong et al., 2013), and 8 participants with behavioural variant Frontotemporal Dementia (Rascovsky et al., 2011) were recruited from tertiary clinics at the Cambridge Centre for Parkinson-plus, the Cambridge Centre for Frontotemporal Dementia, and National Hospital for Neurology and Neurosurgery at Queen Square, London (Holland et al., 2020; Malpetti et al., 2022). 24 healthy volunteers were recruited from the UK National Institute for Health Research Join Dementia Research (JDR) register. The research protocol was approved by the Cambridge Research Ethics Committee and the Administration of Radioactive Substances Advisory Committee. All participants provided written informed consent in accordance with the Declaration of Helsinki.

Participants underwent study-specific clinical and neuropsychological assessment including the Mini-mental State Exam (MMSE) (Folstein et al., 1975), revised Addenbrooke's Cognitive Examination (ACE-R) (Mioshi et al., 2006), Progressive Supranuclear Palsy Rating Scale (PSPRS) (Golbe and Ohman-Strickland, 2007), and the Cambridge Behavioural Inventory-Revised (Wear et al., 2008).

All participants underwent brain imaging with 3-Tesla MRI, including echo-planar imaging sequences sensitive to the blood-oxygen-level-dependent signal, and PET scanning with [¹¹C]UCB-J ((R)-1-((3-(methyl-¹¹C)pyridin-4-yl)methyl)-4-(3,4,5-trifluorophenyl)pyrrolidin-2-one) (Milicevic Sephton et al., 2020). The median interval between scanning sessions was 72 days in patients (inter-quartile range 19-181 days) and 194 days in control participants (inter-quartile range 32-284 days). Participants with CBS also underwent amyloid PET using Pittsburgh compound B ([¹¹C]PiB). Cortical standardized uptake value ratio (SUVR; 50–70 minutes post injection; whole cerebellum reference tissue) was determined using the Centiloid Project methodology (Klunk et al., 2015). Only participants with corticobasal syndrome and a negative amyloid status, as characterized by a cortical [¹¹C]PiB SUVR <1.21 (obtained by converting the Centiloid cut-off of 19 to SUVR using the Centiloid-to-SUVR transformation (Jack et al., 2017)) are included in the subsequent analysis. A subset of 10 participants with PSP also had 7-Tesla imaging including sensitive

3D magnetization transfer weighted sequence for imaging of the locus coeruleus (Ye et al., 2022).

5.2.2 Image acquisition and processing

Our group have previously reported our protocol for [¹¹C]UCB-J synthesis, image acquisition, image reconstruction and kinetic analysis (Holland et al., 2020). In short, dynamic PET analysis was performed on a GE SIGNA PET/MR (GE Healthcare, Waukesha, USA) for 90 minutes following [¹¹C]UCB-J injection, with attenuation correction including the use of a multisubject atlas method (Burgos et al., 2014) and improvements to the MRI brain coil component. Each emission image series was aligned to a T1 weighted MRI acquired during the same session (TE = 3.6 ms, TR = 9.2 ms, 192 sagittal slices, in-plane resolution 0.55×0.55 mm [interpolated to 1.0×1.0 mm]; slice thickness 1.0 mm). A [¹¹C]UCB-J BP_{ND} map was derived for each participant from dynamic images with correction for partial volume effects using the iterative Yang method (Erlandsson et al., 2012). Regional analysis used a modified version of the n30r83 Hammersmith atlas (<http://brain-development.org>) with inclusion of segmentation of brainstem and cerebellar structures, and non-rigid registration to the T1-weighted MRI of each participant. Regions of interest with sufficient grey matter coverage in all participants were multiplied by a binary grey matter mask thresholded at >50% smoothed to PET resolution. Cerebrospinal fluid partial volume correction was applied to each image of the dynamic series. [¹¹C]UCB-J non-displaceable binding potential (BP_{ND}) was calculated both at the regional and voxelwise level using a basis function implementation of the simplified reference tissue model (Wu and Carson, 2002), with centrum semiovale as the reference tissue (Koole et al., 2019). For independent component analysis (see below) [¹¹C]UCB-J BP_{ND} maps were warped to the FSL MNI152 6th generation atlas using parameters from the spatial normalisation of the co-registered T1 image with FSL's FLIRT and FNIRT. Normalised maps were smoothed with an 8mm Gaussian kernel.

Functional MRI imaging was performed with 3-Tesla Siemens Prisma (Siemens Healthcare) using echo-planar imaging sensitive to the blood-oxygen-level-dependent signal (TR 2.5 secs, TE 30ms, whole brain acquisition, 3x3x3.5mm voxels, 200 volumes). fMRI preprocessing followed the pipeline described in chapter 2. I hand-trained FIX using a set of 20 subjects. For dual regression analysis data was further smoothed with a 6mm FWHM Gaussian kernel.

From volumetric T1-weighted MRI images grey matter volumes were extracted for the same regions of the Hammersmith Atlas using SPM12 (SPM12 v7771, Institute of Neurology, London, UK) segmentation. Total intracranial volume was calculated via direct segmentation using Sequence Adaptive Multimodal SEGmentation (Puonti et al., 2016). The Cambridge Centre for Parkinson-plus protocol for 7-Tesla imaging and integrity estimation of the locus coeruleus for this cohort of patients is described by Ye et al (Ye et al., 2022). In short, the locus coeruleus was imaged using a magnetization transfer weighted sequence at high resolution ($0.4 \times 0.4 \times 0.5 \text{ mm}^3$). Locus coeruleus integrity was measured using an atlas-based segmentation approach from a 5% probabilistic locus coeruleus atlas from 29 healthy older adults. The contrast-to-noise ratio was calculated with reference to the central pons.

5.2.3 Statistical analysis

I tested the relationships between [^{11}C]UCB-J, functional connectivity, grey matter volume and cognition in regional and voxelwise analyses. First, I tested whether regional [^{11}C]UCB-J BP_{ND} explains regional variation in connectivity beyond that accounted for by grey matter volume. I then investigated whether including maps of neurotransmitter receptor and transporter distribution from publicly available healthy controls would further improve prediction of regional connectivity. As a *post-hoc* analysis, in a subset of participants with PSP I tested whether variation in regional functional connectivity explained by the distribution of noradrenaline transporters is associated with another *in vivo* marker of noradrenergic function, locus coeruleus integrity.

I used voxelwise [^{11}C]UCB-J maps to identify patterns of [^{11}C]UCB-J BP_{ND} that were differentially expressed in neurodegeneration using an independent component analysis (Fang et al., 2021). I identified participants-specific maps of functional spatial covariance with the [^{11}C]UCB-J components through seed-based dual regression (Filippini et al., 2009; Kelly, Jr. et al., 2022). I tested whether variability in functional connectivity to regions showing group differences in synaptic density: a) improves modelling of clinical severity as assessed through the ACE-R and PSPRS; b) moderates the effect of [^{11}C]UCB-J differences on cognition.

5.2.4 Weighted degree

Participants' preprocessed fMRI was parcellated using the modified Hammersmith atlas, with cortical regions masked with a grey matter mask. Given the variation in parcel size in

the Hammersmith atlas, I sub-parcellated the masked Hammersmith atlas with 163 regions of approximately equal volume, such that each sub-parcel could be uniquely identified with an atlas region. Pearson correlations were calculated between nodes, followed by Fisher's r-to-Z transformation. Weighted degree was derived from association matrices using Maybrain software (<https://github.com/RittmanResearch/maybrain>) and Networkx. I then calculated mean weighted degree across the sub-parcellations for each Hammersmith atlas region to compare with regional [¹¹C]UCB-J BP_{ND}.

I compared regional values for [¹¹C]UCB-J BP_{ND} and weighted degree between participants with FTLD-associated syndromes and controls in a linear model with age and sex as covariates (plus mean DVARS for weighted degree and total intracranial volume for volumetric measures). I further compared differences in these modalities between patient groups in a linear model with the same covariates. For both analyses P values were adjusted for the false discovery rate across regions.

I compared regional z scores for weighted degree and [¹¹C]UCB-J BP_{ND} using mean values and standard deviation from the control participants. P-values (denoted P_{SA}) were calculated using a permutation test with 5000 spatial autocorrelation-preserving null models (Burt et al., 2020).

To capture the effect of individual variability in the relationship between weighted degree and synaptic density as measured by [¹¹C]UCB-J BP_{ND}, I then derived mixed linear effects models (separately for patients and control participants) using the lme4 package in R (Bates et al., 2015) with crossed random effects for region and participant and an effect of [¹¹C]UCB-J BP_{ND} slope within each region. I compared models using the *anova* function in R to ensure that inclusion of a random slope for [¹¹C]UCB-J BP_{ND} per region improved model fit. Age, sex and a marker of fMRI motion (DVARS, Power et al., 2012) were included as covariates of no interest. I also included a covariate denoting whether a region was cortical or subcortical, to ensure that the relationship between [¹¹C]UCB-J BP_{ND} and weighted degree was not driven by differences due to the average lower [¹¹C]UCB-J BP_{ND} in subcortical regions, and a group by cortical/subcortical interaction in the model with all participants. We further tested whether inclusion of regional grey matter volume and total intracranial volume in the model in patients altered the [¹¹C]UCB-J BP_{ND}-weighted degree relationship.

5.2.5 Neurotransmitter receptor and transporter maps

To further understand the nature of residual variation in cortical weighted degree (i.e. variation not accounted for by grey matter atrophy or synaptic density), I further tested whether neurotransmitter receptor and transporter distributions would account for additional variance. I followed the methodology set out by Hansen and colleagues (Hansen et al., 2022) using the neuromaps toolbox (<https://netneurolab.github.io/neuromaps> (Markello et al., 2022)). I performed a multiple linear regression with mean weighted degree z score averaged from all patients as the dependent variable, with mean [¹¹C]UCB-J BP_{ND} and grey matter volume z scores as independent variables together with regional values for the cortical parcels of the Hammersmith Atlas from publicly available neurotransmitter receptors and transporter PET maps. Neurotransmitter receptor and transporter maps were for the noradrenaline transporter (Ding et al., 2010), D₁ receptor (Kaller et al., 2017), D₂ receptor (Sandiego et al., 2015), GABA_{A/BZ} receptors (Nørgaard et al., 2021), mGluR₅ receptor (Smart et al., 2019), 5-HT_{1A} receptor (Savli et al., 2012), 5-HT_{2A} receptor (Beliveau et al., 2017), and the vesicular acetylcholine transporter (Aghourian et al., 2017).

I assessed significance of the model using a permutation test with 5000 spatial autocorrelation-preserving null models for each neurotransmitter receptor/transporter map (Burt et al., 2020). I then performed a dominance analysis to assess the contribution of each neurotransmitter using the R package *yhat* (Nimon et al., 2008). A dominance analysis calculates the incremental validity of each predictor across all submodels of a multiple linear regression. The *general dominance weights* represent an independent variable's average R² across all submodels, allowing the effect size to be partitioned across the predictors (Laguerre, 2021; Nimon and Oswald, 2013). I repeated the analysis for each diagnostic group (PSP, CBS and bvFTD) in turn.

I fitted the same model for each participant with a neurodegenerative disease, to derive participant specific standardised coefficients for the noradrenaline transporter. For the 10 participants with PSP I compared these standardised coefficients with 7-T derived locus coeruleus integrity in a linear model with age and total intracranial volume as coefficients of no interest.

5.2.6 Source-based synaptometry

I then proceeded to independent component analysis (referred to here as *source-based synaptometry*, analogous to “volumetry”) to identify a small number of statistically independent components capturing spatial variation in [¹¹C]UCB-J BP_{ND}. Spatially concatenated [¹¹C]UCB-J BP_{ND} maps were submitted to source-based synaptometry using the GIFT toolbox (Fang et al., 2021; Xu et al., 2009) with a model order of 10. Components were discarded if they represented artefact, captured regions known to be sensitive to artefact in fMRI acquisition or were driven by outliers identified using Grubbs’ test (Grubbs, 1969). Component loading values, which represent the degree to which an individual expresses a [¹¹C]UCB-J BP_{ND} component map, were taken forward to estimate association with connectivity providing they were differentially expressed by participants with neurodegenerative diseases and controls after correction for false discovery rate with $p < 0.05$. Five components satisfying these criteria were included. In the primary analysis presented here partial volume corrected [¹¹C]UCB-J BP_{ND} maps were used, with repeat source-based synaptometry with uncorrected maps performed to ensure robustness of spatial distribution of components to atrophy correction. Independent component analysis model order was chosen *a priori*, with additional analysis that components of interest with similar spatial distributions could be extracted at alternative model orders.

5.2.7 Connectivity of [¹¹C]UCB-J BP_{ND} components

I then sought to investigate subject functional spatial covariance with the identified [¹¹C]UCB-J BP_{ND} components, using a seed-based dual regression approach (Filippini et al., 2009; Kelly, Jr. et al., 2022). In the first stage of dual regression I regressed the selected [¹¹C]UCB-J BP_{ND} components maps into each participant’s fMRI 4-dimensional dataset to give participant specific timecourses per component. These timecourses were taken to a second regression with the [¹¹C]UCB-J BP_{ND} component maps to obtain participant spatial maps per component. I assessed the association between [¹¹C]UCB-J BP_{ND} loadings values and functional covariance per component in a general linear model with age, sex and mean DVARS as covariates of no interest using threshold free cluster enhancement with 5000 permutations using FSL’s *randomise* tool (Winkler et al., 2014) with family-wise error significance level $p < 0.05$. I then calculated mean beta for each participant’s spatial maps from the second stage of dual regression (within a mask defined as regions in controls showing significant mean covariance with each [¹¹C]UCB-J BP_{ND} component map at family-wise error $p < 0.01$) using FSL’s *fslmeans* function. I compared the association

between [¹¹C]UCB-J BP_{ND} loadings and functional covariance scores for each component in the whole group and in patients alone using the same covariates of no interest.

5.2.8 Comparison with clinical scores

Our group and others have previously shown that [¹¹C]UCB-J BP_{ND} values are strongly related to markers of clinical severity in neurodegenerative diseases. I sought to understand connectivity moderates this relationship and improves prediction of total ACE-R and total PSPRS. I therefore performed model selection using stepwise regression with the Bayesian information criteria from a baseline model of:

*ACE-R/PSPRS ~ [¹¹C]UCB-J component 1 * fMRI component 1 + ... + [¹¹C]UCB-J component 5 * fMRI component 5 + Age + Sex + Mean DVARS.*

Age, sex and mean DVARS were considered covariates of no interest and were not stepped out of the model.

5.3 Results

5.3.1 Participants

Demographic details and clinical characteristics for participants are set out in Table 5-1. No significant group differences were observed for age or sex. Clinical and neuropsychological assessments showed impairment in all patient groups, with expected higher average scores on the CBI-R in bvFTD and greater impairment on the PSPRS in PSP than bvFTD. Participants with bvFTD had increased in-scanner motion during fMRI acquisition, and therefore I included a metric of motion as a covariate of no interest throughout.

	Control	PSP	CBS	bvFTD	Statistic (F/ χ^2)	P/Post-hoc tests
N	24	29	16	8		
Age at fMRI	70.0 (8.4)	70.7 (8.4)	67.1 (5.7)	65.6 (10.3)	1.2	0.31
Sex (M/F)	16/8	15/14	7/9	6/2	3.5	0.33
Mean DVARS	5.0 (0.4)	5.2 (0.5)	4.9 (0.4)	5.8 (0.9)	6.0	0.001 bvFTD < Control p=0.004 bvFTD < PSP p=0.025 bvFTD < CBS p=0.0006
ACE-R	95.8 (2.6)	79.5 (12.9)	77.8 (16.9)	65.2 (25.5)	12.5	1×10^{-6} bvFTD < Control p<0.0001 PSP < Control p=0.0004 CBS < Control p=0.001
PSPRS	-	33.2 (10.3)	27.2 (11.1)	17.5 (12.5)	5.7	0.006 PSP < bvFTD p=0.006
CBI-R	-	52.4 (34)	37.7 (19.8)	90.8 (32.6)	8.3	0.0008 bvFTD > CBS p=0.0005 bvFTD > PSP p=0.0072

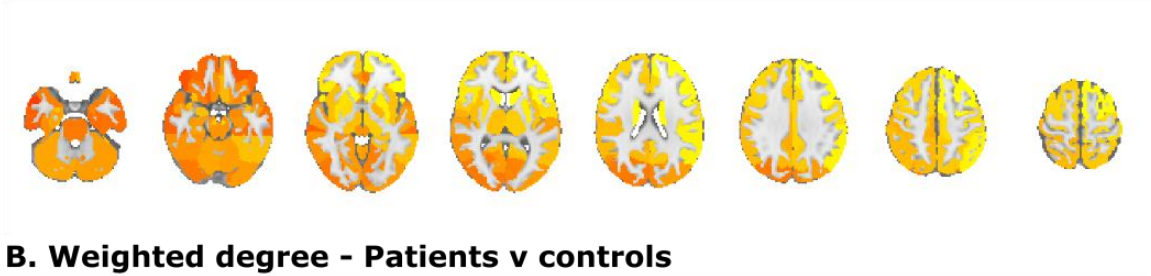
Table 5-1. *Demographic and clinical characteristics for participants.* Scores are mean (SD). fMRI functional magnetic resonance imaging, DVARS spatial standard deviation of successive images, ACE-R Addenbrooke's Cognitive Examination-Revised, PSPRS Progressive Supranuclear Palsy Rating Scale, CBI-R Cambridge

5.3.2 Synaptic density, connectivity, and grey matter

1.1.1.1 Synaptic density

There were widespread significant reductions in [^{11}C]UCB-J BP_{ND} in patients compared to control participants in cortical and subcortical regions, with the largest effect sizes in the frontal lobe and basal ganglia (Figure 5-1A). There were no regional differences between-patient groups, after correcting for multiple comparisons. Uncorrected differences, including the frontotemporal cortex for bvFTD vs CBS, are described in Supplementary Table 5-1.

A. UCBJ - Patients v controls



B. Weighted degree - Patients v controls

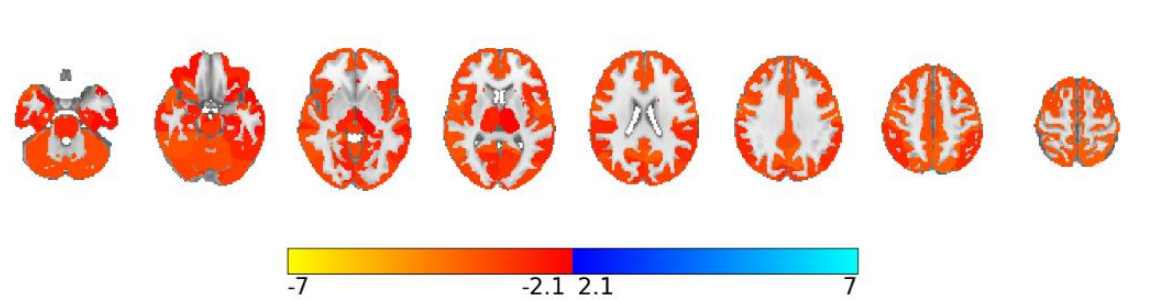


Figure 5-1. Regional differences between healthy controls and patients in A) [^{11}C]UCB-J BP_{ND} and B) weighted degree. All parcels shown are significantly different after FDR-correction for multiple comparisons across regions.

5.3.2.1 Weighted degree

There were widespread significant reductions in weighted degree in patients compared to control participants in cortical and subcortical regions, with smaller effect sizes than [^{11}C]UCB-J BP_{ND} (Figure 5-1B). There were no regional differences between-patient groups, after correcting for multiple comparisons. Uncorrected differences (Supplementary Table 5-2) were observed in the cerebellar dentate, presubgenual frontal cortex, and the anterior temporal lobe.

5.3.2.2 Weighted degree and synaptic density

I calculated regional [^{11}C]UCB-J BP_{ND} and weighted degree z scores in patients standardized to control data. For cortical regions, mean weighted degree z scores correlated with mean [^{11}C]UCB-J BP_{ND} z scores (Pearson's $r=0.41$ $P_{\text{SA}}=0.026$, Figure 5-2A). There was no such relationship in subcortical regions (Pearson's $r=-0.02$ $P_{\text{SA}}=0.96$).

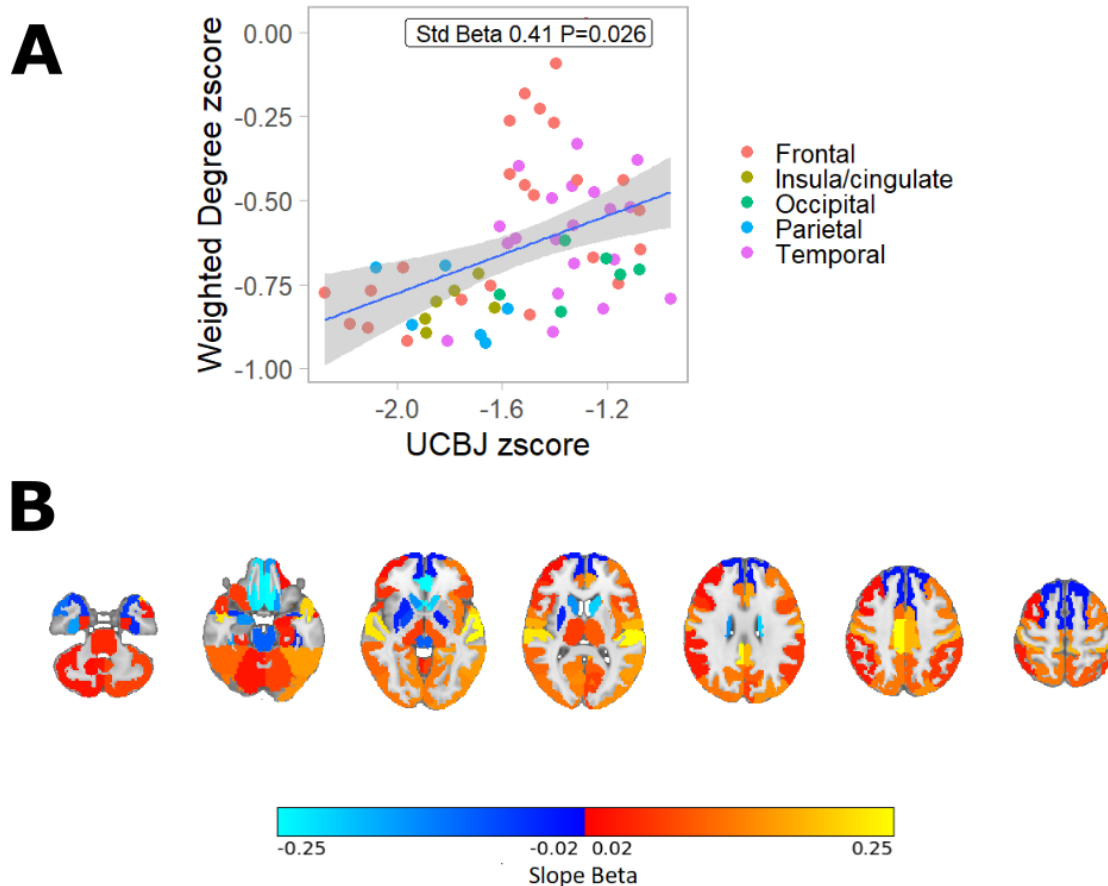


Figure 5-2. *Weighted degree and synaptic density in frontotemporal lobar degeneration syndromes* Mean [^{11}C]UCB-J binding potential in cortical regions in patients is associated with mean weighted degree, with z scores calculated relative to control values. B) Variation in strength of the weighted degree-[^{11}C]UCB-J relationship in patients derived from the effect of [^{11}C]UCB-J BP_{ND} slope within each region, with a stronger relationship observed across the cortex and away from inferior frontal, anterior temporal and striatal regions.

I fitted linear mixed-effects models to account for individual variation in the regional relationship between [^{11}C]UCB-J BP_{ND} and weighted degree. Inclusion of an effect of [^{11}C]UCB-J BP_{ND} slope within each region improved model fit ($\chi^2=36$, $P=2 \times 10^{-8}$). Weighted degree was associated with [^{11}C]UCB-J BP_{ND} in patients (Standardised Beta 0.20, $P=1 \times 10^{-9}$) but not in control participants (Standardised Beta 0.0 $P=0.96$). The group-by-[^{11}C]UCB-J BP_{ND} interaction in a refitted model with all participants was significant ([^{11}C]UCB-J BP_{ND} *Group Standardised Beta 0.054, $P=0.008$), with unchanged effect size and significance with scanning interval included as a covariate of no interest. In patients, assessing the [^{11}C]UCB-J BP_{ND} effect within region showed stronger weighted degree-[^{11}C]UCB-J BP_{ND} relationships in temporal, parietal, cingulate and superior frontal regions (Fig. 1B). The relationship between [^{11}C]UCB-J BP_{ND} and weighted degree remained significant (Standardised Beta 0.18, $P=2 \times 10^{-8}$) with inclusion of regional grey matter volumes and total intracranial volume.

5.3.3 Synaptic density, connectivity, and neurotransmitter receptor/transporter distributions

I tested whether maps of neurotransmitter receptors and transporters distributions explain additional variance in cortical weighted degree beyond synaptic density and grey matter volume. For weighted degree, averaged for each region across all patients, the inclusion of neurotransmitter receptor and transporter maps to synaptic density and grey matter volume in a multiple regression model improved fit above spatial autocorrelation-preserving null models (adjusted $R^2=0.59$, $P_{SA}=0.031$, Figure 5-3A). Assessing each diagnosis group in turn, neurotransmitter receptor and transporter maps significantly improved fit for PSP (adjusted $R^2=0.59$, $P_{SA}=0.0058$), with no significant improvement above null models for CBS (adjusted $R^2=0.48$, $P_{SA}=0.44$) and bvFTD (adjusted $R^2=0.55$, $P_{SA}=0.10$).

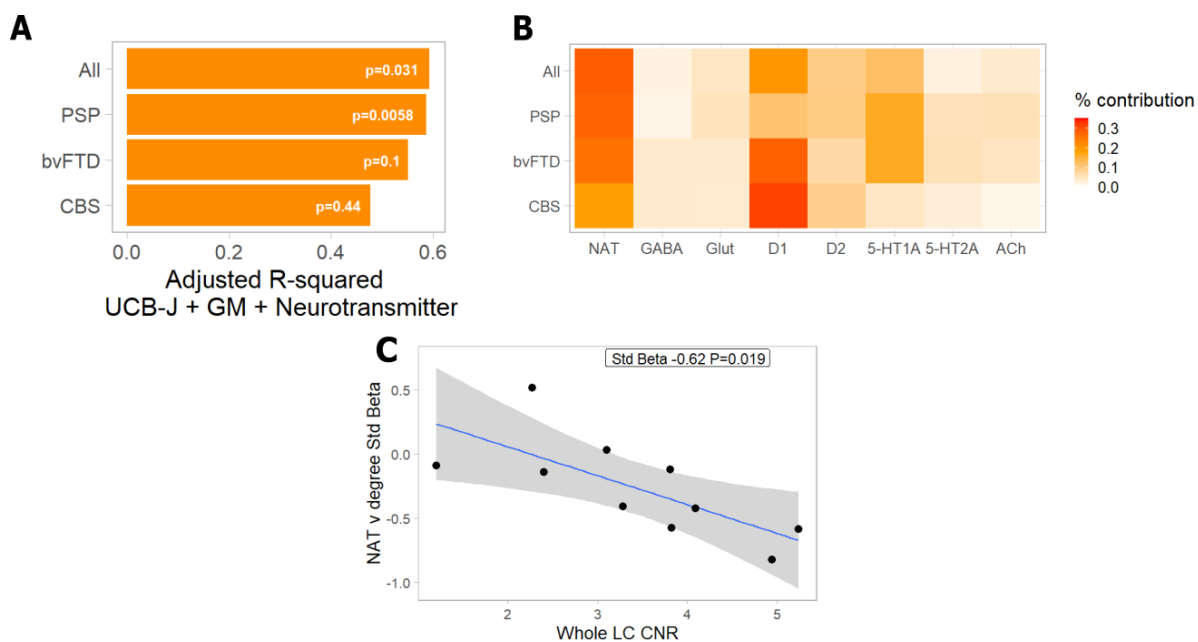


Figure 5-3. The effect of synaptic density, grey matter volume, and neurotransmitter receptors/transporter distributions on connectivity. Using a multiple regression model, neurotransmitter receptors/transporter distributions from control populations were fit to weighted degree, partialling out [^{11}C]UCB-J and grey matter volumes. **A)** The significance of the addition of neurotransmitter receptors/transporter distributions above [^{11}C]UCB-J and grey matter volume is assessed against null models preserving spatial autocorrelation **B)** Dominance analysis assessing the percentage contribution to the fit of each model, defined as the variable's dominance over the total model R-squared. **C)** The relationship between noradrenaline transporter distribution and weighted degree in the whole model is associated with whole locus coeruleus CNR

I performed a dominance analysis (Figure 5-3B) to assess the contribution of individual maps to model fit. For weighted degree derived from all patients I found that the noradrenaline transporter (29% of total explained R^2) and D1 receptor (20% of total explained R^2) were the most important contributors to cortical connectivity. For PSP the

strongest contributors were the noradrenaline transporter (28% of total explained R^2) and the 5-HT1A receptor (17% of total explained R^2).

Given the leading contribution of noradrenaline transporter maps, I took advantage of a complementary imaging modality relevant to noradrenergic function available in a subset of patients. Specifically, I tested *post hoc* whether standardised coefficients for noradrenaline transporter distribution from the same regression model, fitted for individuals with neurodegenerative diseases, was associated with locus coeruleus integrity estimated from ultra-high field 7-Tesla MRI. I found that increasing locus coeruleus contrast-to-noise ratio was associated with more negative coefficient for noradrenaline transporter distribution derived from the multiple regression model (Standardised Beta - 0.62, $P=0.019$, Figure 5-3C). Given the predominantly presynaptic action of the noradrenaline transporter, this direction of effect is consistent with the hypothesis that the relationship between functional connectivity and extracellular noradrenaline depends on functioning forebrain noradrenergic input related to the integrity of the locus coeruleus.

5.3.4 Synaptic density, connectivity, and clinical severity

5.3.4.1 Source-based synapometry

To investigate how variation in synaptic density influences functional connectivity and cognition, I first performed an independent component analysis on concatenated participant [^{11}C]UCB-J BP_{ND} partial volume corrected maps. One component was discarded as representing CSF and another where derivation of the component was not robust to removal of an outlier (Grubb's test G 7.0 $P=0.0005$). Two further components were not taken forward for further analysis as they incorporated regions particularly prone to artefact. Five of the remaining components differed between groups (Figure 5-4A-B): component 1 covering left frontoparietal regions ($F(3,71)=8.1$ FDR $P=0.0006$; post-hoc Tukey bvFTD < Control $P=0.0014$, CBS < Control $P=0.043$, PSP < Control $P=0.0005$); component 2 with high values in the caudate and anterior cingulate ($F(3,71)=6.9$ FDR $P=0.002$; PSP < Control $P=0.0002$); component 3 with spatial extent incorporating the superior frontal lobe ($F(3,71)=5.8$ FDR $P=0.002$; bvFTD < Control $p=0.0008$); component 4 covering the medial parietal lobe and adjacent parts of the frontal lobe ($F(3,71)=5.5$ FDR $P=0.002$; post-hoc Tukey CBS < Control $P=0.005$, CBS < PSP $P=0.017$); and component 5 with peak values at the right superior parietal lobule ($F(3,71)=6.8$ FDR $P=0.001$; post-hoc Tukey bvFTD < Control $P=0.0014$, CBS < Control $P=0.001$, CBS < PSP $P=0.0004$).

Component identification was robust to alternative model order choices (9-14 components, mean spatial cross-correlation of matched component: component 1 0.76, component 2 0.92, component 3 0.95, component 4 0.87, component 5 0.97) and to partial volume correction (uncorrected maps with model order 10, cross-correlation of matched component 0.87-0.98).

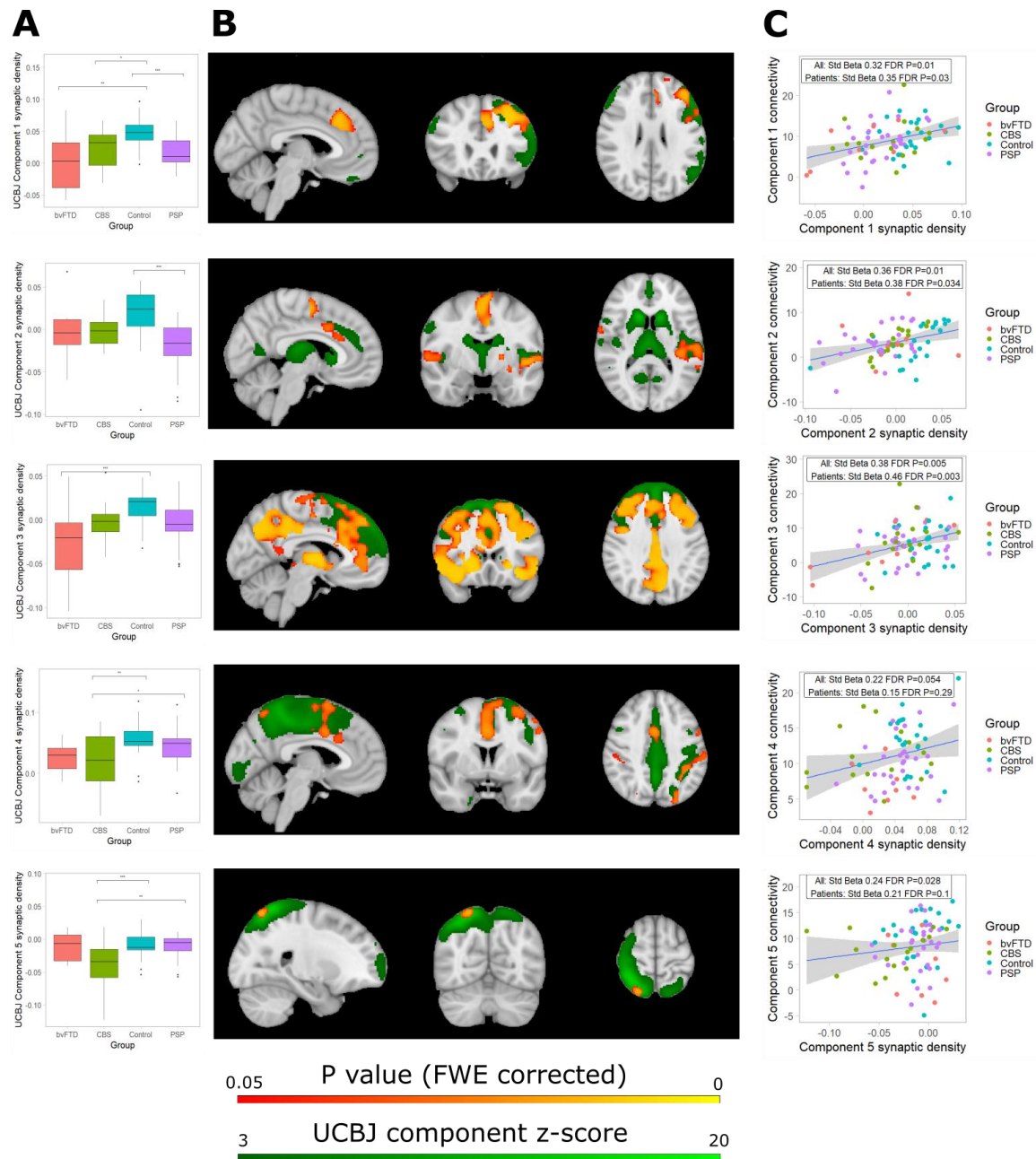


Figure 5-4. Spatial variation in synaptic density and associated connectivity loss. A) [¹¹C]UCB-J independent component analysis loadings by group for the five components that show differential expression in neurodegeneration. B) [¹¹C]UCB-J component maps (in green) with areas of increased functional covariance (in red-orange) significantly associated with increased [¹¹C]UCB-J component loadings. C) Connectivity scores, derived from participant-specific functional covariance maps per component, are associated with [¹¹C]UCB-J independent component analysis loadings

5.3.4.2 *Connectivity of UCB-J BPND components*

Dual regression identified participant specific patterns of spatial covariance to each [¹¹C]UCB-J BP_{ND} component map. Participant covariance maps per component were taken forward to assess for voxel-wise associations with [¹¹C]UCB-J BP_{ND} component loadings in a general linear model with permutation testing. There were significant associations between increased [¹¹C]UCB-J BP_{ND} loadings and increased functional covariance for all components (Figure 5-4B, $P < 0.05$ with family-wise error correction across voxels). I found that connectivity differences were observed both at the site of synaptic loss and remotely from it. For instance, greater [¹¹C]UCB-J BP_{ND} loadings in a component (component 3) with high values in superior frontal regions were associated with increased functional covariance in the precuneus, posterior cingulate and right angular gyrus.

I extracted participant component scores by taking the mean *beta* from participants' component covariance maps within a mask defined as significant areas of average control functional covariance with each component. Four of the five components showed associations between [¹¹C]UCB-J BP_{ND} loadings and functional covariance score (Figure 5-4C: component 1 Standardised Beta 0.32 FDR $P = 0.01$, component 2 Standardised Beta 0.36 FDR $P = 0.01$, component 3 Standardised Beta 0.38 FDR $P = 0.005$, component 4 Standardised Beta 0.23 FDR $P = 0.054$, component 5 Standardised Beta 0.24 FDR $P = 0.028$). This association remained significant for the first three components when patients alone were included in the model (component 1 Standardised Beta 0.35 FDR $P = 0.03$, component 2 Standardised Beta 0.38 FDR $p = 0.034$, component 3 Standardised Beta 0.46 FDR $P = 0.003$, component 4 Standardised Beta 0.15 FDR $P = 0.29$, component 5 Standardised Beta 0.22 FDR $P = 0.1$).

5.3.4.3 *UCB-J BP_{ND}, connectivity and clinical severity*

I tested whether inclusion of connectivity component scores to [¹¹C]UCB-J BP_{ND} loadings improved modelling of clinical severity as measured by the ACE-R and PSPRS. Individual functional component scores were not significant predictors of either the ACE-R or the PSPRS, whereas [¹¹C]UCB-J BP_{ND} component 3 (Standardised Beta 0.65 FDR $P = 1 \times 10^{-6}$) and UCB-J BP_{ND} component 4 (Standardised Beta 0.38 FDR $P = 0.017$) were significantly associated with total ACE-R. Stepwise regression using Bayesian Information Criteria determined whether combinations of predictors improved model fit. The final model for ACE-R included [¹¹C]UCB-J BP_{ND} component 3 and fMRI components 2 and 5 (Figure 5-5A and Table 5-2), suggesting that participants with frontal synaptic loss and reduced

connectivity to frontal, posterior and subcortical regions had greater cognitive impairment. The final model for the PSPRS included the fMRI-[11C]UCB-J BP_{ND} interaction terms for components 2 and 3 (Figure 5-5B and Table 5-3). For both components I found that the relationship between UCB-J BP_{ND} loading and PSPRS was only present in those with higher connectivity scores.

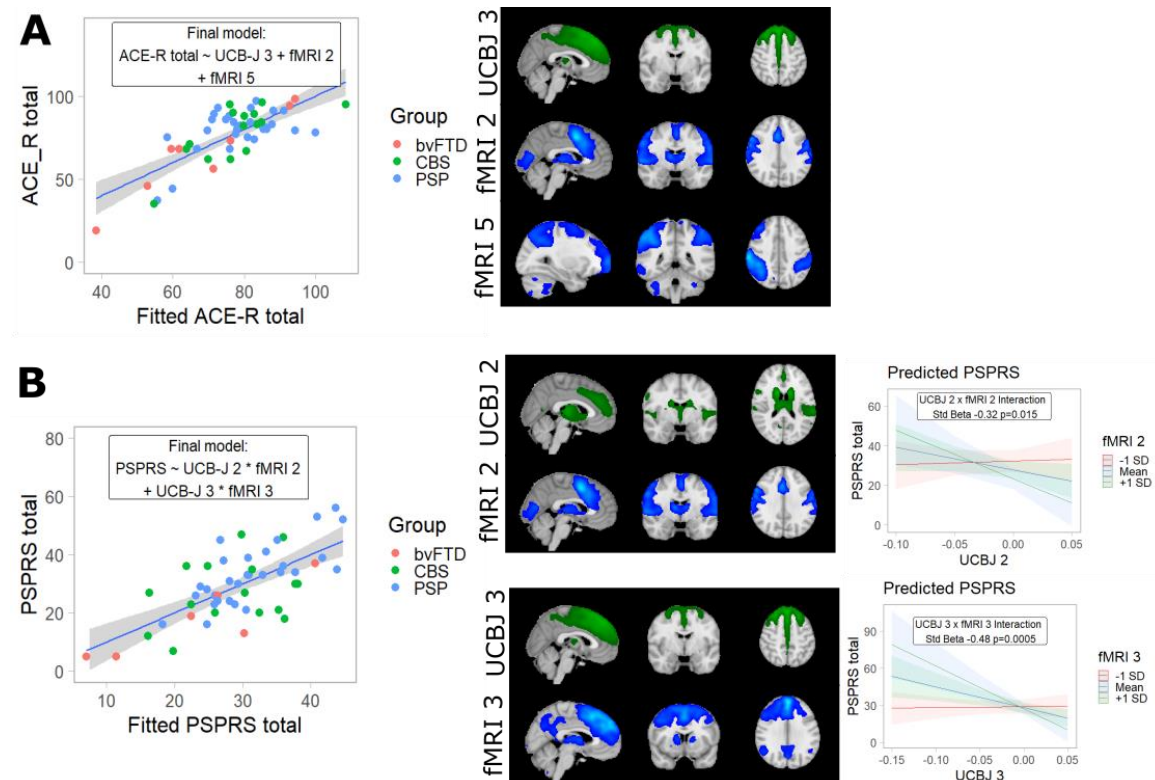


Figure 5-5. *Functional connectivity, synaptic density, and clinical severity.* [¹¹C]UCB-J components (in green) and distribution of functional covariance (in blue) for components included in final model selected using stepwise regression for A) Addenbrooke's Cognitive Examination-Revised and B) Progressive Supranuclear Palsy Rating Scale. The relationship between [¹¹C]UCB-J component loading and PSPRS was seen only in those with higher connectivity scores.

	Std Beta	Std Error	T value	P
Intercept	-0.25	0.15	-1.7	0.1
fMRI 2	0.29	0.12	2.4	0.019
fMRI 5	0.29	0.1	2.8	0.007
UCB-J 3	0.65	0.1	6.6	3x10 ⁻⁸
Mean DVARS	0	0.12	0	0.99
Age	-0.1	0.1	-0.7	0.47
Sex	0.47	0.21	2.2	0.03

Table 5-2. *Final model for stepwise regression for ACE-R total.* ACE-R: Addenbrooke's Cognitive Examination-Revised, DVARS the spatial standard deviation of successive difference images.

	Std Beta	Std Error	T value	P
Intercept	0.76	0.19	3.9	0.0004
fMRI 2	-0.25	0.13	-1.9	0.06
fMRI 3	0.03	0.13	0.2	0.81
UCB-J 2	-0.28	0.16	-1.8	0.08
UCB-J 3	-0.45	0.15	-2.9	0.006
Mean DVARs	0.32	0.14	2.3	0.03
Age	-0.28	0.16	-1.8	0.075
Sex	-0.73	0.25	-2.9	0.006
fMRI 2 * UCB-J 2	-0.32	0.13	-2.5	0.015
fMRI 3 * UCB-J 3	-0.48	0.13	-3.8	0.0005

Table 5-3. Final model for stepwise regression for PSPRS total. PSPRS -Progressive supranuclear palsy rating scale, DVARs the spatial standard deviation of successive difference images.

In summary, reductions in synaptic density were associated with reduced functional connectivity, and connectivity both adds to and moderates the explanatory effect of synaptic density on clinical severity.

5.4 Discussion

There are three principal results of this study. First, lower synaptic density as measured by [^{11}C]UCB-J BP_{ND} is associated with lower functional connectivity. Second, functional connectivity augments and moderates the relationship between synaptic density and clinical severity. Third, the [^{11}C]UCB-J BP_{ND} predicts connectivity over and above grey matter volume. The profound reductions in synaptic density in frontotemporal lobar degeneration occur in partially overlapping distributions, but with disease specific effects. The corresponding reductions in functional connectivity are observed both at the site of the synaptic loss and remotely from it. The majority of regional variation in functional connectivity could be explained by synaptic density, grey matter volume, and neurotransmitter receptor/transporter distributions. Leveraging information from multiple modalities allows us to estimate the relative contribution of individual determinants of connectivity. In my example case, I have found that estimates of noradrenaline contribution to connectivity correspond to direct assessment of the locus coeruleus noradrenergic system, using a neuromelanin-sensitive sequence at 7T. This study therefore provides important mechanistic insights into the multiple and interacting pathogenic processes of FTLD that result in diverse clinical syndromes.

Progressive supranuclear palsy, corticobasal syndrome and behavioural variant frontotemporal dementia are severely disabling progressive conditions that significantly reduce life expectancy (Coyle-Gilchrist et al., 2016; Murley et al., 2021). To improve patient outcomes we require models of the human neurodegenerative pathogenesis as a bridge between preclinical studies and experimental medicines in people. This approach complements mesoscale mechanistic models of cortical function (Adams et al., 2022, 2021) and macroscale whole-brain models of neurodegeneration (Jones et al., 2013; Khan et al., 2022; Shafiei et al., 2023). Such transitional markers may facilitate the selection and design of trials of potential disease modifying agents (Eimeren et al., 2019) .

The primary finding of an association between lower synaptic density and reduced functional connectivity accords with the ubiquitous role of synaptic health and plasticity in generating neurophysiological connections, with synaptic change mediating information storage and contributing to learning (Hebb, 1949; Ramon y Cajal, 1894). In neurodegeneration preclinical and neuropathological studies have shown that synaptic dysfunction and impaired plasticity are key determinants of impaired brain network

organization and cognitive dysfunction (Spires-Jones and Hyman, 2014), and occur before neuronal degeneration (Kaniyappan et al., 2017; Yoshiyama et al., 2007). The *in vivo* associations between synaptic density and markers of connectivity derived are strengthened by the concordance across imaging and analytical methodologies.

The variances in functional connectivity explained by [¹¹C]UCB-J BP_{ND} is independent of and in addition to that accounted for by grey matter atrophy, demonstrated through partial volume correction and by direct inclusion of grey matter volumes in linear models. This highlights the distinct contribution [¹¹C]UCB-J PET offers over and above T1-weighted MRI in capturing aspects of the neurodegenerative cascade. The histopathological processes that cause atrophy on structural imaging are incompletely characterised, with evidence for neuronal and synaptic loss, axon degeneration and cell death being important contributory factors (Fung et al., 2020; Planche et al., 2022). Synaptic dysfunction and loss may occur without cell death or atrophy (Hoover et al., 2010; Kaniyappan et al., 2017). Since [¹¹C]UCB-J BP_{ND} is an independent predictor of connectivity and function, measuring synaptic density has the potential to improve our understanding of the individual role of synaptic loss in cognitive symptoms.

The distinct proteinopathies underlying frontotemporal lobar degeneration show overlap in clinical syndromes and anatomical distribution, while the same pathological entity can result in heterogeneous clinical presentations (Murley et al., 2020a; Seeley, 2017). Despite the heterogeneity and pleiotropy, synaptic loss and dysfunction is a common feature (Taoufik et al., 2018; Wareham et al., 2022) associated with the direct and indirect toxic effects of multiple proteins' aggregates. I found patterns of synaptic density loss that were differentially expressed across the diagnostic labels in a manner in keeping with typical neuropathological distributions post-mortem findings (Dickson et al., 2011; Kovacs et al., 2020), but with regional synaptic loss occurring in a continuum across participants with neurodegeneration. For instance I found lower [¹¹C]UCB-J BP_{ND} loadings in CBS for posterior components, with frontal synaptic loss in all conditions with the largest effect sizes in bvFTD. Synaptic dysfunction results in altered cognition and behaviour through loss of connectivity, with synaptic loss strongly predicting cognitive function and decline (DeKosky and Scheff, 1990; Terry et al., 1991). Here I have shown that functional connectivity loss may occur remotely from sites of reduced synaptic density, and that connectivity improves prediction and moderates the effect of synaptic density on clinical

severity. Indeed, worse cognitive performance was found in those with frontal synaptic loss and reduced connectivity with frontal, subcortical and posterior regions.

Together, these findings provide indirect support for three key hypotheses; first, heterogeneous proteinopathies may result in overlapping clinical syndromes due to the cognitive effects of connectivity loss resulting from synaptic dysfunction at a single site; second, synaptic dysfunction may cause connectivity change at sites of minimal atrophy, potentially contributing to the behavioural prodrome in presymptomatic dementias; third, brain regions may be implicated in cognitive symptoms in neurodegeneration that are remote from atrophy or synaptic loss.

This work advances on recent studies of fMRI and synaptic PET in psychiatric disease (Holmes et al., 2019) and neurodegeneration (Zhang et al., 2023). It is novel in investigating a cohort with a heterogeneous distribution of synaptic loss, through adopting a whole-brain approach to demonstrate the anatomical effects of synaptic loss on connectivity, by combining synaptic density, connectivity and clinical severity in a single model, and in testing the additional role of neurotransmitter dysfunction in determining functional connectivity to synaptic loss and atrophy.

There are several limitations to this study. Interpreting connectivity from resting state fMRI is made challenging by the low signal to noise ratio, the impact of movement and other artefact on measures of connectivity (Power et al., 2012), the indirect neuronal interpretability of the BOLD signal (Kullmann, 2020), and the small effect sizes of brain-behaviour studies in a healthy population (Marek et al., 2022). Yet it is a scalable and widely available modality with good spatial localization that provides a neural correlate closely connected to behaviour, with network integrity closely aligned with symptom development in neurodegeneration (Rittman et al., 2019; Tsvetanov et al., 2020). It is therefore a potential outcome biomarker of the consequences of upstream neuropathological change. I found that the relationship between connectivity and [¹¹C]UCB-J BP_{ND} showed regional heterogeneity. The variance in functional connectivity not explained by synaptic density raises the possibility for a role for other factors, such as the extensive neurochemical deficits observed in FTLD (Murley and Rowe, 2018). This is supported by my findings that neurotransmitter receptor/transporter distributions improve fit of weighted degree and that derived coefficients of noradrenaline transporter distribution are associated with 7-T measured locus coeruleus integrity. These hypothesis generating

results do not necessarily mean that noradrenaline is depleted, and are not direct evidence that replacement would restore connectivity, as a single neural system has multiple and interacting determinants (Hansen et al., 2022) that may be only partially characterised in our modelling. They do highlight how combining PET, fMRI and structural imaging modalities with clinical and other data allows individualised modelling of pathophysiological pathways with implications for developing personalised treatments (Iturria-Medina et al., 2020, 2018).

I leverage the heterogeneity in FTLD to capture variation in the anatomical distribution of synaptic loss and explore its consequences but recognise that the small-to-moderate and varied group sizes mean that this study may be underpowered to detect small differences between disease groups. High motion has a well-recognised confounding effect on functional connectivity (Power et al., 2012; Satterthwaite et al., 2012) and was observed in participants with bvFTD during resting state fMRI scanning. Despite careful pre-processing, including ICA denoising and wavelet despiking, together with inclusion of an in-scanner movement related parameter as a covariate of no interest in relevant models, it remains possible that residual artefact influences the findings. I acknowledge that longitudinal and interventional studies are required to demonstrate causality between synaptic dysfunction, brain network organisation and clinical severity, and cannot be assumed from the statistical associations observed here. Although SV2A expression is closely related to synaptic activity and function (Rizzoli and Betz, 2005), [¹¹C]UCB-J BP_{ND} is considered a measure of synaptic density rather than synaptic function (Serrano et al., 2022). Given that functional connectivity in fMRI is defined as a statistical dependency, with functional activation only indirectly related to neuronal activity, any inferences in my study made about synaptic function are necessarily implicit. Nonetheless the findings are as expected given the interplay between synaptic loss and dysfunction observed in preclinical studies (Spires-Jones and Hyman, 2014). Lastly, this study uses reference tissue modelling rather than arterial blood sampling given the challenges of scanning in this patient cohort. Our group have previously performed sensitivity analyses to ensure that group differences cannot be explained by any bias introduced through reference tissue selection (Holland et al., 2020).

To conclude, I report that reduced synaptic density in multiple frontotemporal lobar degeneration syndromes is associated with lower functional connectivity, with connectivity moderating the relationship between synaptic density and clinical severity. Synaptic

density independently explains variance in connectivity beyond measuring atrophy from structural MRI. This study provides in vivo support for preclinical findings and pave the way for individualised pathogenic models and personalised treatments.

5.5 Supplementary materials for Chapter 5

Region	F value	P	FDR P	Post-hoc tests
Cingulate gyrus anterior part L	6.40	0.003	0.17	bvFTD < CBS P=0.0027
Anterior temporal lobe medial part L	4.73	0.013	0.17	bvFTD < CBS P=0.011 bvFTD < PSP P=0.033
Pallidum R	4.73	0.013	0.17	PSP < CBS P=0.0175
Straight gyrus R	4.60	0.015	0.17	bvFTD < CBS P=0.013
Nucleus Accumbens R	4.60	0.015	0.17	bvFTD < CBS P=0.012
Posterior orbital gyrus	4.55	0.016	0.17	bvFTD < CBS P=0.011
Straight gyrus L	4.45	0.017	0.17	bvFTD < CBS P=0.014
Middle frontal gyrus	4.32	0.019	0.17	bvFTD < CBS P=0.014
Nucleus Accumbens L	4.30	0.019	0.17	bvFTD < CBS P=0.015
Cingulate gyrus anterior part L	3.94	0.026	0.21	bvFTD < CBS P=0.023
Superior frontal gyrus L	3.85	0.028	0.21	bvFTD < CBS P=0.023
Subgenual frontal cortex R	3.49	0.038	0.22	bvFTD < CBS P=0.031
Hippocampus R	3.42	0.041	0.22	bvFTD < CBS P=0.045
Subgenual frontal cortex L	3.37	0.043	0.22	bvFTD < CBS P=0.033
Insula R	3.28	0.046	0.22	bvFTD < CBS P=0.037
Presubgenual frontal cortex L	3.27	0.047	0.22	bvFTD < CBS P=0.036
Lateral orbital gyrus	3.23	0.048	0.22	
Superior temporal gyrus central part L	3.21	0.049	0.22	bvFTD < CBS P=0.038
Parahippocampal and ambient gyri R	3.07	0.056	0.22	
Fusiform gyrus	3.04	0.057	0.22	
Fusiform gyrus	3.03	0.058	0.22	
Inferior frontal gyrus L	2.83	0.069	0.25	
Substantia nigra R	2.76	0.073	0.25	
Anterior temporal lobe medial part R	2.72	0.076	0.25	
Superior temporal gyrus anterior part L	2.65	0.081	0.25	
Anterior orbital gyrus	2.60	0.084	0.25	

Middle and inferior temporal gyrus	2.56	0.087	0.25	
Anterior temporal lobe lateral part R	2.56	0.088	0.25	
Amygdala R	2.49	0.094	0.25	
Subcallosal area L	2.48	0.094	0.25	
Posterior orbital gyrus	2.45	0.097	0.25	
Presubgenual frontal cortex L	2.41	0.10	0.25	
Superior temporal gyrus central part R	2.37	0.10	0.26	
Superior frontal gyrus R	2.30	0.11	0.26	
Cuneus L	2.30	0.11	0.26	
Anterior temporal lobe lateral part R	2.26	0.12	0.26	
Posterior temporal lobe L	2.23	0.12	0.26	
Superior parietal gyrus L	2.14	0.13	0.26	
Subcallosal area R	2.09	0.14	0.26	
Midbrain	2.07	0.14	0.26	
Medial orbital gyrus	2.06	0.14	0.26	
Inferior frontal gyrus R	2.05	0.14	0.26	
Anterior orbital gyrus	2.03	0.14	0.26	
Middle frontal gyrus	2.03	0.14	0.26	
Medial orbital gyrus	2.02	0.14	0.26	
Lateral remainder of occipital lobe L	2.00	0.15	0.26	
Insula L	1.94	0.15	0.27	
Thalamus R	1.78	0.18	0.29	
Caudate Nucleus L	1.77	0.18	0.29	
Medulla	1.77	0.18	0.29	
Caudate Nucleus R	1.75	0.18	0.29	
Cingulate gyrus posterior part L	1.74	0.19	0.29	
Middle and inferior temporal gyrus	1.59	0.21	0.33	
Thalamus L	1.49	0.24	0.35	
Putamen R	1.42	0.25	0.37	
Superior parietal gyrus R	1.41	0.25	0.37	
Postcentral gyrus R	1.37	0.26	0.37	

Inferiolateral remainder of parietal lobe	1.34	0.27	0.38	
Postcentral gyrus L	1.31	0.28	0.39	
Pallidum L	1.28	0.29	0.39	
Cuneus R	1.18	0.32	0.42	
Superior temporal gyrus anterior part R				
Cingulate gyrus posterior part L	1.16	0.32	0.42	
Lingual gyrus L	1.07	0.35	0.45	
Inferiolateral remainder of parietal lobe	0.94	0.40	0.50	
Putamen L	0.92	0.41	0.50	
Pons	0.90	0.41	0.50	
Precentral gyrus L	0.82	0.45	0.54	
Posterior temporal lobe R	0.80	0.45	0.54	
Lateral orbital gyrus	0.76	0.47	0.56	
Substantia nigra L	0.67	0.52	0.60	
Lateral remainder of occipital lobe R	0.65	0.53	0.60	
Lingual gyrus R	0.58	0.57	0.64	
Hippocampus L	0.56	0.57	0.64	
Parahippocampal and ambient gyri L	0.52	0.60	0.65	
Cerebellum gm L	0.50	0.61	0.66	
Cerebellum dentate L	0.47	0.63	0.67	
Precentral gyrus R	0.42	0.66	0.69	
Amygdala L	0.41	0.67	0.69	
Cerebellum dentate R	0.34	0.71	0.73	
Cerebellum gm R	0.15	0.86	0.87	

Supplementary Table 5-1. Regional differences in [^{11}C]UCB-J BP_{ND} between progressive supranuclear palsy, corticobasal syndrome and behavioural variant frontotemporal dementia. Post-hoc tests only performed where there is an uncorrected group difference in an ANCOVA with age and sex as covariates of no interest. Only significant results after Tukey adjusted p-values are shown. There were no post-correction significant differences between groups.

Region	F value	P	FDR P	Post-hoc tests
Presubgenual frontal cortex L	3.69	0.032	0.85	
Cerebellum dentate L	3.62	0.034	0.85	CBS < PSP P=0.045
Anterior temporal lobe lateral part R	3.33	0.044	0.85	
Inferior frontal gyrus L	2.81	0.070	0.85	
Caudate Nucleus L	2.74	0.075	0.85	
Substantia nigra R	2.52	0.091	0.85	
Anterior temporal lobe lateral part R	2.22	0.12	0.85	
Middle and inferior temporal gyrus	2.11	0.13	0.85	
Inferior frontal gyrus R	1.99	0.15	0.85	
Subgenual frontal cortex L	1.92	0.16	0.85	
Medial orbital gyrus	1.84	0.17	0.85	
Anterior temporal lobe medial part L	1.78	0.18	0.85	
Anterior orbital gyrus	1.72	0.19	0.85	
Caudate Nucleus R	1.48	0.24	0.85	
Straight gyrus L	1.46	0.24	0.85	
Cingulate gyrus anterior part L	1.44	0.25	0.85	
Posterior orbital gyrus	1.44	0.25	0.85	
Lateral orbital gyrus	1.36	0.27	0.85	
Superior temporal gyrus anterior part L	1.33	0.27	0.85	
Presubgenual frontal cortex L	1.31	0.28	0.85	
Anterior temporal lobe medial part R	1.30	0.28	0.85	
Superior frontal gyrus L	1.29	0.28	0.85	
Fusiform gyrus	1.27	0.29	0.85	
Superior temporal gyrus central part R	1.25	0.30	0.85	
Lateral orbital gyrus	1.22	0.30	0.85	
Anterior orbital gyrus	1.20	0.31	0.85	
Posterior orbital gyrus	1.16	0.32	0.85	
Subcallosal area L	1.16	0.32	0.85	

Insula R	1.13	0.33	0.85	
Middle and inferior temporal gyrus	1.04	0.36	0.85	
Subgenual frontal cortex R	0.99	0.38	0.85	
Posterior temporal lobe L	0.98	0.38	0.85	
Cingulate gyrus posterior part L	0.97	0.39	0.85	
Medial orbital gyrus	0.93	0.40	0.85	
Precentral gyrus R	0.89	0.42	0.85	
Cerebellum dentate R	0.87	0.43	0.85	
Middle frontal gyrus	0.86	0.43	0.85	
Superior frontal gyrus R	0.85	0.43	0.85	
Pons	0.85	0.43	0.85	
Hippocampus L	0.81	0.45	0.85	
Putamen R	0.80	0.46	0.85	
Superior temporal gyrus central part L	0.79	0.46	0.85	
Cingulate gyrus anterior part L	0.77	0.47	0.85	
Precentral gyrus L	0.77	0.47	0.85	
Straight gyrus R	0.76	0.47	0.85	
Cerebellum gm L	0.62	0.54	0.87	
Putamen L	0.62	0.54	0.87	
Cuneus R	0.59	0.56	0.87	
Postcentral gyrus L	0.58	0.57	0.87	
Middle frontal gyrus	0.56	0.58	0.87	
Cuneus L	0.47	0.63	0.87	
Midbrain	0.47	0.63	0.87	
Posterior temporal lobe R	0.46	0.64	0.87	
Lingual gyrus R	0.45	0.64	0.87	
Inferiolateral remainder of parietal lobe	0.45	0.64	0.87	
Insula L	0.45	0.64	0.87	
Superior parietal gyrus L	0.44	0.65	0.87	
Cerebellum gm R	0.43	0.66	0.87	
Hippocampus R	0.42	0.66	0.87	
Amygdala L	0.40	0.67	0.87	

Inferiolateral remainder of parietal lobe	0.38	0.69	0.87	
Lateral remainder of occipital lobe R	0.36	0.70	0.87	
Substantia nigra L	0.35	0.71	0.87	
Cingulate gyrus posterior part L	0.35	0.71	0.87	
Nucleus Accumbens L	0.30	0.75	0.87	
Lingual gyrus L	0.29	0.75	0.87	
Pallidum L	0.29	0.75	0.87	
Lateral remainder of occipital lobe L	0.29	0.75	0.87	
Postcentral gyrus R	0.26	0.77	0.87	
Superior parietal gyrus R	0.25	0.78	0.87	
Medulla	0.25	0.78	0.87	
Amygdala R	0.23	0.80	0.87	
Parahippocampal and ambient gyri L	0.22	0.80	0.87	
Thalamus L	0.22	0.80	0.87	
Fusiform gyrus	0.21	0.81	0.87	
Nucleus Accumbens R	0.20	0.82	0.87	
Superior temporal gyrus anterior part R	0.17	0.85	0.89	
Pallidum R	0.11	0.90	0.93	
Thalamus R	0.08	0.93	0.95	
Subcallosal area R	0.06	0.94	0.95	
Parahippocampal and ambient gyri R	0.02	0.98	0.98	

Supplementary Table 5-2. Regional differences in weighted degree between progressive supranuclear palsy, corticobasal syndrome and behavioural variant frontotemporal dementia. Post-hoc tests only performed where there is an uncorrected group difference in an ANCOVA with age, in-scanner motion and sex as covariates of no interest. Only significant results after Tukey adjusted p-values are shown. There were no post-correction significant differences between groups.

6 Imaging and clinical markers of survival in progressive supranuclear palsy and corticobasal syndrome

Preface

This chapter is adapted from a manuscript that is in press in *Human Brain Mapping* as ‘Network connectivity and structural correlates of survival in progressive supranuclear palsy and corticobasal syndrome.’ Data was collected by a large number of researchers at the Cambridge Centre for Parkinson-plus and across the United Kingdom for the PROSPECT-M-UK study. I preprocessed the imaging data, designed and executed the analysis strategy, and wrote the manuscript with input from co-authors.

Summary

In this chapter I test the hypothesis that the magnitude and distribution of connectivity changes in PSP and CBS predict the rate of progression and survival time, using data from the Cambridge Centre for Parkinson-plus and PROSPECT-M-UK. In PSP and CBS, I identify between-network connectivity components that (i) differ from controls, (ii) are associated with disease severity, and (iii) predict survival and rate of change in clinical severity. A transdiagnostic component predicts survival beyond demographic and motion metrics, but with lower accuracy than an optimal model that included clinical and structural measures. Cortical atrophy enhances the connectivity changes that were most predictive of survival.

6.1 Introduction

Progressive supranuclear palsy (PSP) and corticobasal syndrome (CBS) are characterised by short average survival, but with significant variability in individual outcome (Chiu et al., 2010; Coyle-Gilchrist et al., 2016). There is a pressing need to accurately predict survival time, to aid clinical management, assist stratification for clinical trials and to identify potential protective factors associated with better prognosis (Eimeren et al., 2019). Functional connectivity is a promising candidate to improve prognostication given the close association between functional organisation and changes in cognition with aging and neurodegeneration (Chan et al., 2014; Rittman et al., 2019; Tsvetanov et al., 2020).

I tested the overarching hypothesis that widespread changes in connectivity predict a poor prognosis in PSP and CBS. Large-scale brain networks can be identified by functional magnetic resonance imaging at rest (Beckmann et al., 2005; Biswal et al., 1995; Damoiseaux et al., 2006; Yeo et al., 2011). Altered functional organisation, representing dysfunctional neurons and networks, may be a more sensitive measure of underlying disease state than regional atrophy or cross-sectional performance on standardised clinical tasks. In neurodegenerative conditions network segregation is associated with maintained cognitive performance in the presence of pathology (Ewers et al., 2021; Tsvetanov et al., 2020), with loss of network integrity and large scale network change occurring at the point of symptom onset (Rittman et al., 2019). It is therefore plausible that greater network disruption would imply poor longitudinal outcome. Resting state connectivity in neurodegeneration is influenced by inflammation (Passamonti et al., 2019), synaptic loss (Zhang et al., 2023), pathological protein (Cope et al., 2018; Franzmeier et al., 2022), white matter disease (McColgan et al., 2017), neurotransmitter deficits (Borchert et al., 2019; Klaassens et al., 2019), metabolism (Sheline and Raichle, 2013), and cell death (Hampton et al., 2020). Identifying connectivity markers of survival would enable *in vivo* mechanistic testing of the importance of different components of the neurodegenerative cascade for outcome.

A challenge when assessing the impact of connectivity on survival is that even in healthy controls, individual connections show poor reproducibility and vary on repeat scanning (Lynch et al., 2020; Noble et al., 2019). However, multivariate data-driven approaches to identify a small number of features, such as independent component analysis, significantly improve robustness of connectivity estimates (Elliott et al., 2018; Marek et al., 2022). This

is important when considering the clinical syndromes of PSP and CBS, which are heterogenous with overlapping clinical features (Höglinger et al., 2017; Murley et al., 2020a) that explain only a proportion of variability in outcome (Murley et al., 2021). Connectivity changes in these conditions are diffuse (Ballarini et al., 2020; Brown et al., 2017), in keeping with brain-wide synaptic loss observed in vivo (Holland et al., 2020) and at post-mortem (Bigio et al., 2001; Lipton et al., 2001). I therefore investigated the utility of functional connectivity to predict outcome for individual diagnostic groups and transdiagnostically, adopting a whole brain approach rather than focusing on individual connections.

Data reduction techniques to identify common patterns of connectivity change may not give the most sensitive survival predictors. Machine learning approaches may be more successful in identifying predictors, but standard machine learning tools need to be modified when estimating time to death given the presence of censored data resulting from including individuals alive at the end of a follow-up period (Spooner et al., 2020). The Partial Least Squares regression for Cox models (Bastien, 2008; Bastien et al., 2015, 2005; Bertrand and Maumy-Bertrand, 2021) provides a promising approach that is adapted to explain maximal variance in survival, identifies patterns using all features, and is suitable for high dimensional data.

I therefore used these methods to test whether connectivity changes are associated with poorer prognosis in PSP and CBS. I quantify connectivity through resting state functional MRI and compare the predictive value of connectivity with clinical metrics and structural imaging. To assess generalisation, I used k-fold cross validation for data from two cohorts of PSP, CBS, and controls: from the Cambridge Centre for Parkinson-plus (CCPP) and the UK national PSP Research Network (PROSPECT-MR). I tested the following hypotheses: i) between-network connectivity differs between participants with neurodegeneration and controls; ii) more extensive changes in connectivity predict faster clinical deterioration and shorter survival; and iii) changes in connectivity provide additive information to predict prognosis beyond clinical and structural imaging measures.

6.2 Methods

6.2.1 Participants

I recruited 146 participants with MDS-PSP criteria probable or possible PSP (Höglinger et al., 2017), 82 participants with the clinical phenotype of corticobasal syndrome (Armstrong et al., 2013), and 90 age-matched healthy controls from the Cambridge Centre for Parkinson-plus (CCPP) and the Progressive Supranuclear Palsy-Corticobasal Syndrome-Multiple System Atrophy-UK (PROSPECT-MR) study (Jabbari et al., 2020). Clinical assessments for the two cohorts included the PSP rating scale (PSPRS) (Golbe and Ohman-Strickland, 2007), the Cambridge Behavioural Inventory-Revised (CBIR) (Wear et al., 2008) and the Addenbrooke's Cognitive Examination-Revised (ACER) (Mioshi et al., 2006). 49 participants with PSP, 11 participants with CBS and 9 healthy controls were excluded following assessment for motion (see below). I recorded survival and longitudinal neurocognitive assessments for participants up to 12 years from baseline imaging, with date of death recorded from participants' NHS Summary Care Record. Demographic details and summary scores for included participants are described in Table 6-1.

27 included participants with a clinical diagnosis of PSP proceeded to autopsy, with a predominant neuropathological diagnosis of PSP in 26, and 1 predominant argyrophilic grain disease. 16 of the included participants with corticobasal syndrome donated their brain. As expected in CBS, the underlying neuropathology was heterogenous with a final pathological diagnosis of corticobasal degeneration (n=6), Alzheimer's disease (n=5), mixed corticobasal degeneration/progressive supranuclear palsy (n=1), progressive supranuclear palsy (n=2), Pick's disease (n=1) and multiple system atrophy (n=1).

6.2.2 MRI acquisition and preprocessing

MRI acquisition and preprocessing were as outlined in chapter 2. A subset of 48 participants (20 PSP, 17 CBS, 11 Controls) also had repeat imaging during the disease course (Table 1), with primary analysis from the baseline visit. Since in-scanner participant motion in resting state fMRI has the potential to bias connectivity estimates (Power et al., 2012), I excluded individuals above thresholds taken as 1.2 standard deviations above the whole sample mean as defined in chapter 2 (maximum spike percentage (Patel et al., 2014) maximum framewise displacement (Power et al., 2012), and maximum spatial standard deviation of successive volume differences (Smyser et al., 2010)). Given that motion has relevant neural correlates (Geerligs et al., 2017) and likely relates to severity and survival

in PSP and CBS, I did not include it as a covariate of no interest in the primary analysis but additionally report the effect of adding mean framewise displacement to predictions of survival and progression, included it in the baseline model when comparing predictors of survival in disease, and report the association of in-scanner motion with survival. Summary motion indices by group for included participants are in Supplementary Table 6-1.

6.2.3 Structural parcellation

I derived subcortical volumes and cortical thickness for parcels of the Brainnetome Atlas (Fan et al., 2016) using Freesurfer 7.1.0 (Dale et al., 1999). Subcortical volumes were adjusted for total intracranial volume by deriving residuals from linear regression between parcel volume and total intracranial volume (Voevodskaya et al., 2014). Volumes and thicknesses were averaged over the forty-eight larger regions and gyri to reduce number of features for model fitting. I additionally calculated volumes for four brainstem structures (medulla, pons, midbrain, and superior cerebellar peduncle) (Iglesias et al., 2015).

6.2.4 Between-network connectivity

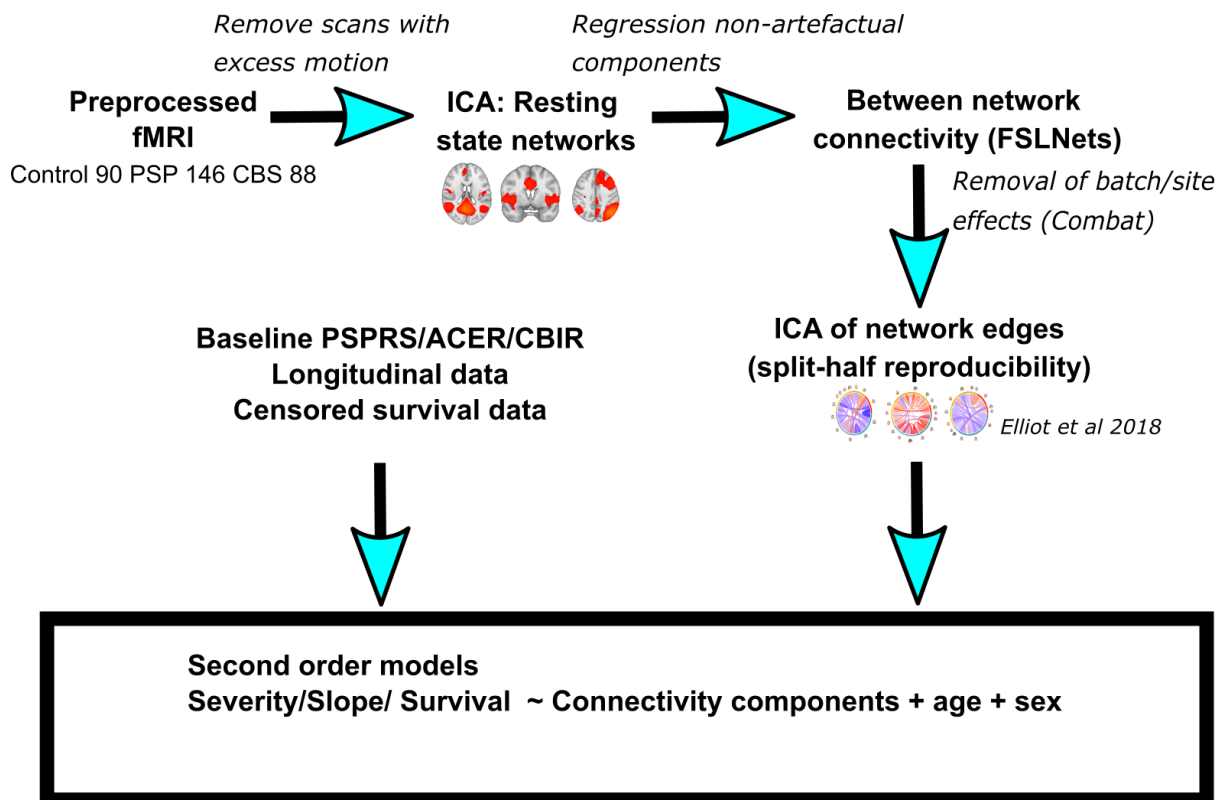


Figure 6-1. Pipeline for assessment of relationship between large-scale network connectivity and severity, progression and survival. Schematic representation of pipeline to derive independent components of between-network connectivity to compare with outcome measures in PSP and CBS (PSP: Progressive Supranuclear Palsy, CBS: Corticobasal Syndrome, fMRI: functional Magnetic Resonance Imaging, ICA: Independent Component Analysis, ACER: Addenbrooke’s Cognitive Examination-Revised, PSPRS: Progressive Supranuclear Palsy Rating Scale, CBIR – Cambridge Behavioural Inventory Revised).

To identify between-network connectivity patterns I employed the pipeline used by Elliott and colleagues (Elliott et al., 2018) (Figure 6-1). I adopted this approach as it captures multivariate large-scale connectome patterns with improved test-retest reliability, which is important in these heterogenous conditions where widespread connectivity change and synaptic loss (Holland et al., 2020) suggest that isolated connections are unlikely to be reliably related to survival. I performed independent component analysis with a model order of 30 using FSL's MELODIC on preprocessed fMRI from patients and controls. These components were matched with their closest Yeo network (Yeo et al., 2011) using cross-correlation against template maps and subsequent inspection. Components were selected if they were non-artefactual and were a constituent of a Yeo network or overlapped with the thalamus. I did not include the Yeo limbic network given the influence of artefact and similarity to noise signal at 3-Tesla fMRI (Omidvarnia et al., 2021), and excluded inferior and ventral visual cortical regions due to the challenges in this region of differentiating BOLD signal from venous artefact (Boyd Taylor et al., 2019; Kay et al., 2019; Tsvetanov et al., 2015; Winawer et al., 2010). I then extracted component time series by regression of participant's preprocessed fMRI against the component maps, with time series for the chosen components taken forward for further analysis. Connectivity between components was calculated by full Pearson correlation between networks followed by Fisher r-to-Z normalization using FSLNets (Smith et al., 2013b). I adjusted for scanner and site differences through an empirical Bayes framework using ComBat (Johnson et al., 2007; Yu et al., 2018). I compared the adjusted between-component connectivity between patient groups and healthy controls in a linear model with age and sex as covariates of no interest, using the Benjamini-Hochberg method (Benjamini and Hochberg, 1995) to control the false discovery rate.

I then performed a further independent component analysis (Hyvarinen, 1999) to identify a small number of components capturing between-network connectivity patterns. I set a maximum model order of four since even in a large dataset only four components could be robustly inferred (Elliott et al., 2018), using split-half reproducibility of imaging component weights across subjects to determine the final number of components (Elliott et al., 2018).

6.2.5 Statistical approach - Severity, progression and survival

I took baseline imaging component scores for further analysis to compare between groups and correlate with severity, progression and survival. Age and sex were included as

covariates of no interest in all models. Cross-sectional analyses were performed using assessments at the earliest scanning date. P values were adjusted for multiple comparisons adjusted across components and neuropsychological tests (false discovery rate $p < 0.05$), with the corrected P value reported unless stated otherwise. All statistical analyses and visualization were performed in R (version 4.1.0) ([Gu et al., 2014](#); [Mowinckel, 2018](#); [R Core Team, 2018](#)).

To compare component scores between groups I performed a multivariate analysis of covariance. I compared clinical and neuropsychological markers of severity with scores for components of interest within a linear model, and test whether the disease groups differ in their component-neuropsychological measure relationship through a refitted model including a group-by-component interaction.

A linear mixed-effect model was used to calculate annual rates of changes in clinical and neuropsychological scores for participants with longitudinal data using the R package lme4 (Bates et al., 2015), as described in chapter 2. Neuropsychological score was the dependent variable with years from baseline assessment as an independent variable. The model estimated a random intercept and slope to account for individual variability. The individual estimated slopes were included as a dependent variable in a second model with baseline connectivity component scores as predictors. Models were repeated with mean framewise displacement as a covariate of no interest. To assess whether connectivity components improve model fit for clinical progression (for PSPRS, CBIR and ACER) beyond baseline severity, I performed stepwise regression using the Akaike information criteria (AIC). In the initial model estimated slope was the dependent variable, with the two connectivity components, baseline clinical score, and total grey matter volume as independent variables. Age, sex, motion, and total intracranial volume were covariates of no interest, and not stepped out of the model.

I used a Cox proportional hazards regression analysis to assess the relationship between component score and time from scan until death with age and sex as covariates, an approach that enabled me to include participants alive at the end of the assessment period. Given the importance of scanner motion as a potential confounder in quantifying connectivity, I additionally report the relationship between mean framewise displacement and time from scan until death.

6.2.6 Partial Least Squares for Cox Models

I proceeded to compare different potential predictors of survival in PSP and CBS. An independent component analysis finds statistically independent connectivity changes, but these may not be the best survival predictors. I therefore used partial least squares for Cox models (Bastien et al., 2015, 2005; Bertrand and Maumy-Bertrand, 2021) to maximize covariance of the predictor to censored survival data. This finds broad connectomic patterns most predictive of survival and likely to improve reliability beyond focusing on individual connections.

I used a transdiagnostic approach with partial least squares regression for Cox models performed with all baseline patient scans as a single group. I derived models with different predictors to determine indicators of survival: connectivity patterns; structural imaging measures; and clinical scores. The partial least squares for Cox models approach also allows component scores to be calculated where there is missing data for clinical assessments, based on a modified non-linear partial least squares algorithm where iterative regressions are performed with the available data (Bastien et al., 2005; Bertrand and Maumy-Bertrand, 2021).

To determine the best survival predictors, I used 20 repeats of 5-fold cross-validation comparing: a baseline model (age, sex and mean framewise displacement); the baseline model combined with connectivity; the baseline model with structural measures of atrophy; the baseline model together with clinical scores (PSPRS, CBIR, ACER); the baseline model with clinical scores and structural measures; the baseline model with clinical scores and connectivity; and a full model with all predictors. For each model the number of components was chosen which maximised cross-validation performance. I compared models using i) concordance index (Harrell, 1982), the proportion of pairs of participants where the hazards predicted by the model accord with observed survival and ii) area under the curve for survival data (Heagerty et al., 2000).

On a *post-hoc* basis I repeated model comparison with PSP and CBS individually. I compared the same models as in our transdiagnostic assessment, with the addition of a combination of the baseline model with clinical scores and a composite of thalamic, pontine and midbrain volume, given the risk of overfitting with higher feature number to participant ratio in these subgroups.

6.2.7 Baseline atrophy and longitudinal connectivity change

I tested whether baseline focal atrophy influenced the longitudinal change in connectomic predictors of survival for the subset of patients with repeat imaging. I first derived partial least squares connectivity component scores for scans after the baseline visit. I tested the relationship between connectivity and time from baseline imaging session in a linear mixed-effect model with partial least squares connectivity component score as the dependent variable, time from baseline scan as a fixed effect and a random intercept for each participant. I then refitted the model including an interaction term with time from baseline imaging and focal atrophy (mean cortical thickness or subcortical volume).

I proceeded to perform mediation analysis using the *mediation* (Tingley et al., 2014) package in R using bootstrapping with 100,000 draws, with the partial least squares connectivity component as mediator, mean cortical thickness or mean subcortical volume as predictors and age, sex and the remaining atrophy marker as covariate of no interest.

6.3 Results

6.3.1 Participants

I report results from the analysis from 97 participants with PSP, 71 participants with CBS and 81 healthy controls, after data quality control. Demographic details at the baseline scan are in Table 6-1. There were no significant differences in age or sex, with mean time to death under 3 years from baseline imaging in both diseases.

	Control (n=81)	PSP (n=97)	CBS (n=71)	F/t/χ^2	p
Scans (n)	94	118	88	--	--
Longitudinal imaging (n)	11	20	17		
Age (years)	68.5 (6.4)	70.1 (7.2)	67.9 (6.4)	2.1	0.12
Sex (F/M)	46/35	43/54	42/29	4.5	0.11
Number deceased	--	70	40	--	--
Time to death (years)	--	2.8 (1.8)	2.8 (2.0)	0.07	0.95
3-year survival (from scan)	--	42/87 (48%)	28/53 (53%)	0.12	0.73
PSPRS n (%)	--	35.3 (14.9) 85 (88%)	33.2 (15.8) 50 (70%)	-0.74	0.46
CBIR n (%)	--	44.4 (33.2) 67 (69%)	42.9 (25.8) 62 (87%)	-0.30	0.76
ACER n (%)	--	80.5 (14.3) 84 (87%)	75.2 (17.2) 66 (93%)	-2.0	0.048

Table 6-1. Demographic details for participants at baseline scan. Continuous values are mean (SD). Group comparison used F or t-test for groups with continuous data and chi-squared for binary variables. (ACER: Addenbrooke's Cognitive Examination-Revised, PSPRS: Progressive Supranuclear Palsy Rating Scale, CBIR: Cambridge Behavioural Inventory Revised)

6.3.2 Between-network connectivity

Between-network connectivity differences between patient groups and healthy controls are presented in Figure 6-2A-B. Connectivity was lower in patients than controls for most

between-network connections, with significant reductions in connectivity in patients between sensorimotor and dorsal attention network regions and between default mode network and frontoparietal network components after correction for multiple comparisons. Connectivity was significantly increased from the ventral attention network to dorsal attention and sensorimotor components.

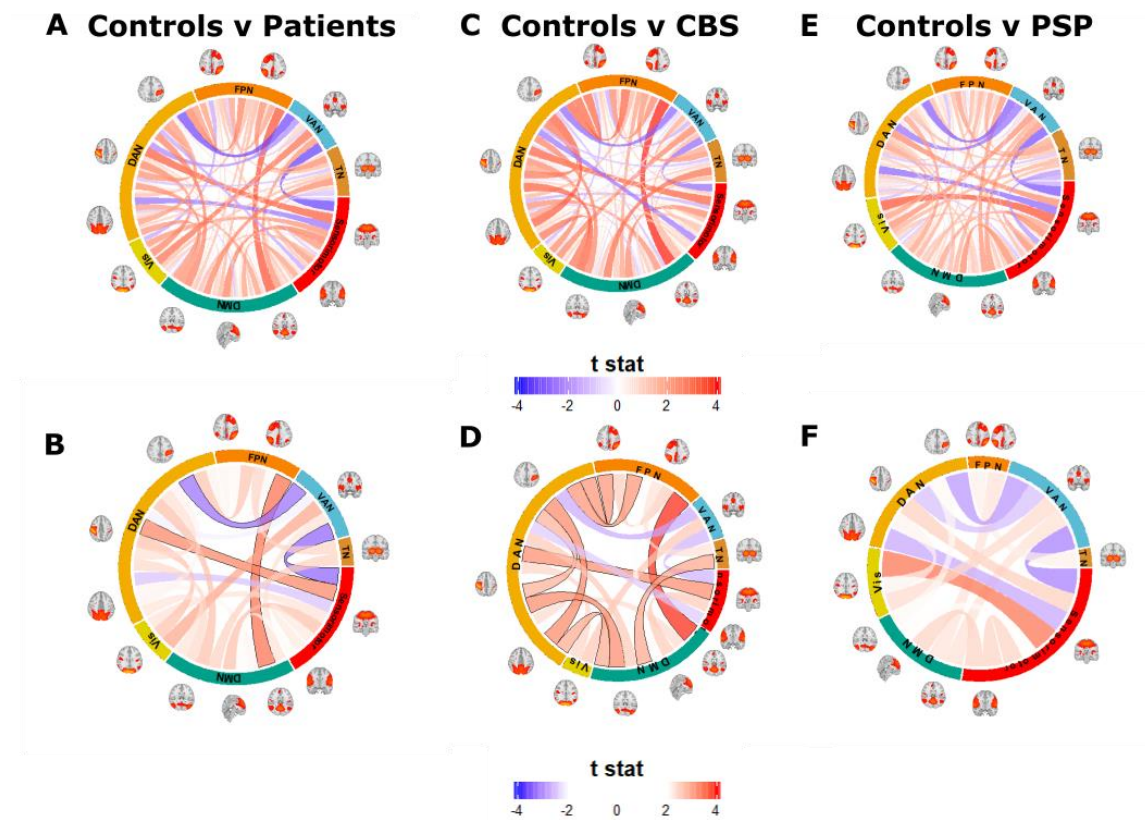


Figure 6-2. Between network connectivity in PSP and CBS. Differences in between-network connectivity between all patients and controls (A and B), CBS and controls (C and D) and PSP and controls (E and F). Red links represent lower connectivity in patient groups, and blue links relatively increased connectivity versus controls. The bottom figures show only connections that show uncorrected significant differences ($p < 0.05$) between group differences beyond age and sex, with connections that remain significant after correction for multiple comparisons outlined in black.

Broadly similar connectivity differences from controls were observed in CBS (Figure 6-2C-D) and PSP (Figure 6-2E-F). Comparing the disease groups, I found uncorrected greater reductions in connectivity in CBS predominantly in posterior components (including to regions of the dorsal attention network), with lower connectivity in PSP between the thalamus and a dorsal attention network component and between sensorimotor and visual regions (Figure 6-3). There were no significant differences between PSP and CBS after correction for multiple comparisons.

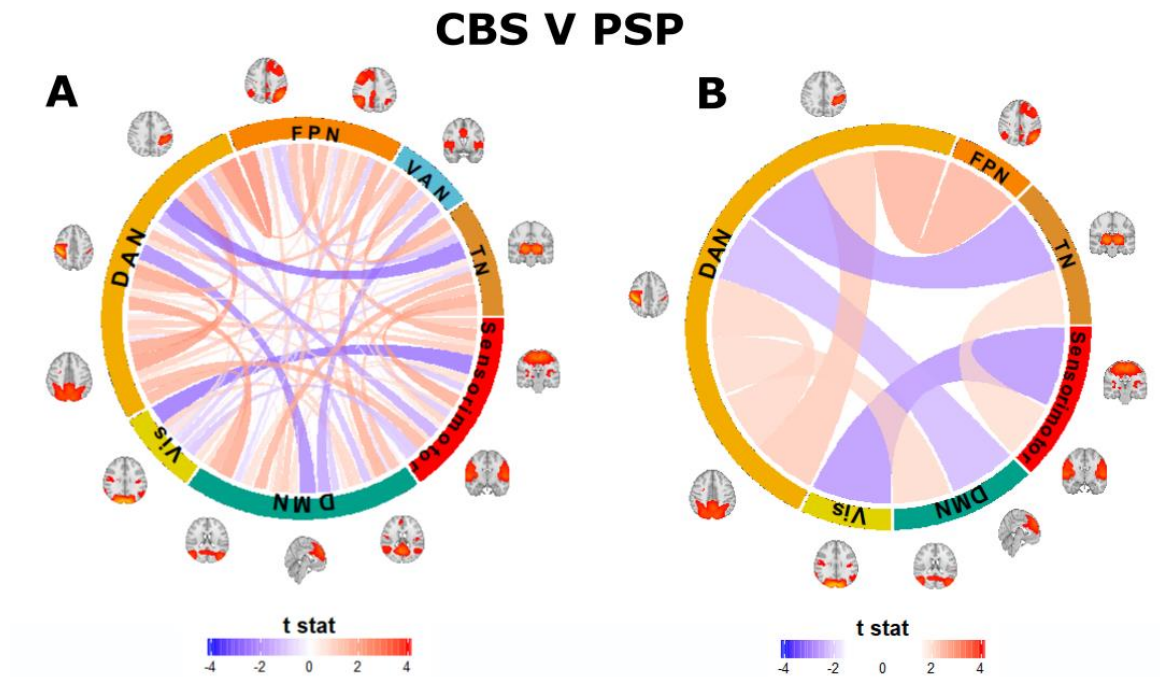


Figure 6-3. Differences in between-network connectivity between PSP and CBS. Red links represent lower connectivity in CBS, and blue links lower connectivity in PSP. B) Only connections that show uncorrected significant differences ($p < 0.05$) between group differences, after adjusting for age and sex, are shown

6.3.3 Connectivity relates to clinical severity

I took the between-network connections to an independent component analysis to capture broad patterns of connectivity to compare with clinical severity and progression. I found that using 4 components maximised split-half reproducibility of component weights. Scores for the first component were decreased in both participants with PSP and CBS versus controls (Figure 6-4A $F=12.9$ $FDR P=2 \times 10^{-5}$; PSP v Control Tukey-adjusted $P=2 \times 10^{-5}$; CBS V Control Tukey-adjusted $P=0.0002$). Scores for the second component were decreased in CBS compared to controls, with no significant difference between either PSP and controls or between disease groups ($F=8.1$ $FDR P=0.01$; PSP v Control Tukey-adjusted $P=0.2$; CBS V Control Tukey-adjusted $P=0.014$). In Component 1 the disease state was associated with predominantly decreased connectivity but with increased connectivity between task-positive, motor and subcortical regions (Figure 6-4C). Lower scores in component 2, as observed in CBS, were associated with relatively increased connectivity between the default mode, dorsal attention and motor networks and decreased connectivity within these networks.

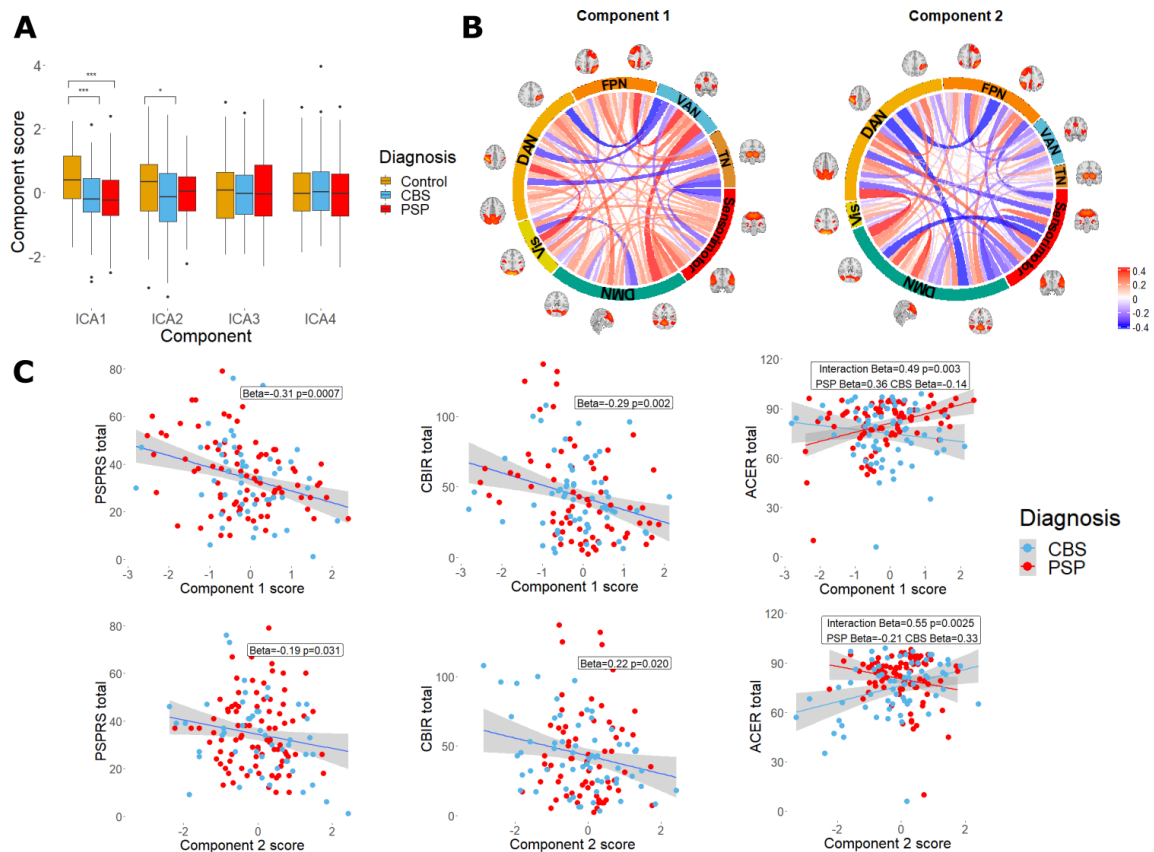


Figure 6-4. **Between network connectivity and clinical severity in PSP and CBS.** A) Components were identified in PSP and CBS which differ between patients and controls, shown in B. Connections represent the correlation between component score and edge, so that for higher scoring subjects red indicates stronger connections and blue weaker. C) Component scores correlate with clinical severity (DMN: Default Mode Network, DAN Dorsal Attention Network, VAN Ventral Attention Network, FPN Frontoparietal Network, TN Thalamic Network, Vis Visual, ACER: Addenbrooke's Cognitive Examination-Revised, PSPRS: Progressive Supranuclear Palsy Rating Scale, CBIR – Cambridge Behavioural Inventory Revised)

I considered the components that differed from controls in either disease group in subsequent analysis. Component 1 scores were associated with the PSP rating scale (Figure 2C Std Beta=-0.31 FDR P=0.0007) and the CBIR (Std Beta=-0.29 FDR P=0.002), with similar but weaker associations found with component 2 (PSPRS Std Beta=-0.19 FDR P=0.031; CBIR Std Beta=-0.22 FDR P=0.020). The relationship between ACER and component scores differed between disease group, with a significant interaction (Component 1xdiagnosis Interaction Std Beta=0.49 FDR P=0.003, PSP Std Beta=0.36 CBS Std Beta=-0.14, Component 2xdiagnosis Interaction Std Beta=0.55 FDR P=0.0025, PSP Std Beta=-0.21 CBS 0.33), demonstrating the cognitive profile associated with greater posterior network involvement in CBS.

6.3.4 Connectivity and disease progression

I tested whether baseline component scores were associated with subsequent decline in neuropsychological assessments. Linear mixed-effect models indicated an effect of time

for all measures (Supplementary Table 6-2). I found that baseline component 1 score was associated with rate of progression in the PSPRS (Figure 6-5A Std Beta=-0.36 FDR P=0.0006) and that baseline component 2 score was associated with greater rate of decline in the ACER (Std Beta=0.26 FDR P=0.015). The implications of lower baseline component 1 score on ACER varied by disease, with lower scores associated with faster decline only in PSP (Component x diagnosis interaction Std Beta=0.57 FDR P=0.008, PSP Std Beta=0.36 CBS Std Beta=-0.23). The relationships with component 1 remained significant when mean framewise displacement was included in the model (PSPRS-Component 1 Std Beta=-0.36 FDR P=0.003; ACER-Component 2 Std Beta=0.22 FDR-corrected P=0.060 uncorrected P=0.030; ACER-Component 1 x diagnosis interaction FDR P=0.014). Lower component 2 scores were also associated with an uncorrected increase in the rate of change of CBIR, including with adjustment for motion and baseline severity (Std Beta=-0.21 uncorrected P=0.046 FDR corrected P=0.091).

I used stepwise regression to investigate if connectivity components were included in the best model of progression when incorporating baseline severity and total grey matter volume. For the PSPRS, component 1 was included in the final model, with component 2 in the final model for ACER, and both components for the CBIR. Between-network connectivity differences were associated with more rapid decline in severity beyond baseline clinical scores and global atrophy.

6.3.5 Connectivity and survival

I found that lower component 1 score was a significant predictor of survival using Cox proportional hazards regression (Figure 6-5B Component 1 hazard ratio 0.72 CI 0.58-0.88 P=0.001; Component 2 hazard ratio 0.83 CI 0.68-1.0 P=0.052) in a model including age and sex as covariates. Component 1 remained a significant predictor with mean framewise displacement included in the model (Component 1 hazard ratio 0.72 CI 0.59-0.89 P=0.002; Component 2 hazard ratio 0.87 CI 0.71-1.1 P=0.19), an important consideration given that increased mean framewise displacement was associated with poorer survival in the whole cohort prior to exclusion for data quality (Supplementary Figure 6-1). Significance remained with further addition of total grey matter volume and total intracranial volume to the model (Component 1 hazard ratio 0.74 CI 0.60-0.91 P=0.005; Component 2 hazard ratio 0.89 CI 0.72-1.1 P=0.26). The diagnosis by component interaction was not significant for either component.

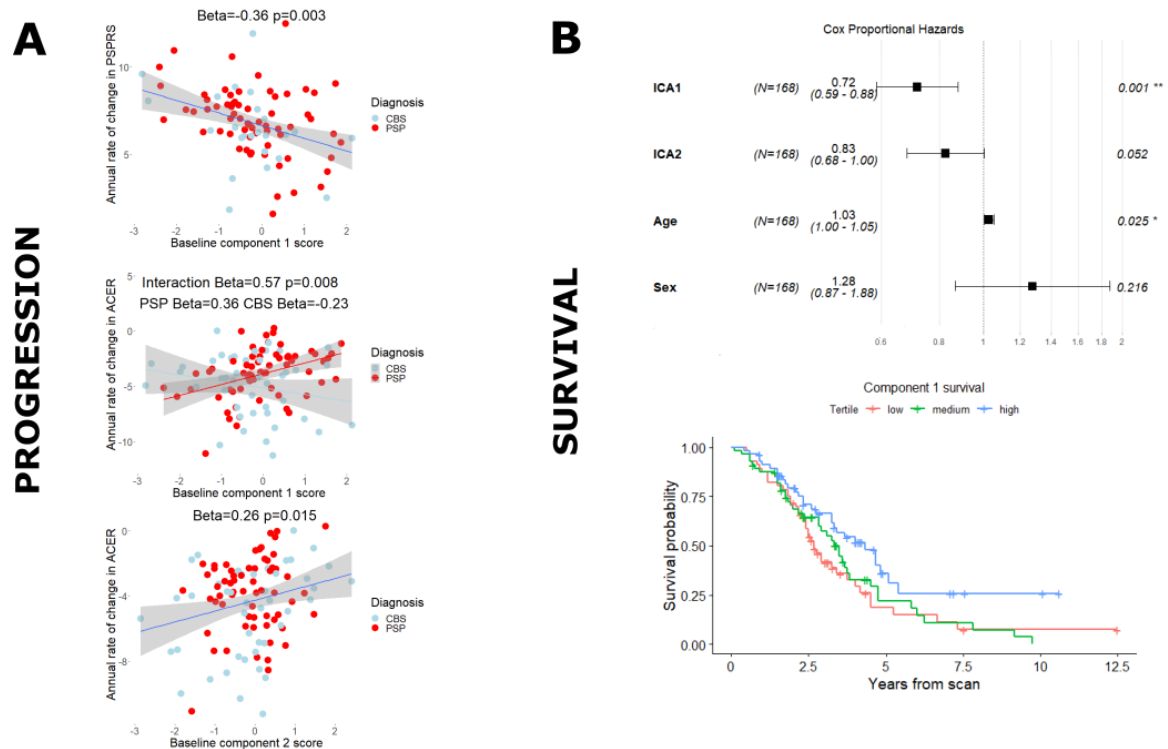


Figure 6-5. Connectivity predicts longitudinal survival in PSP and CBS. Component scores at baseline scan are associated with rate of change of severity (A) and are significantly associated with survival in a Cox proportional hazards model (B). For illustration survival curves are shown by component score divided into high, medium and low scoring tertiles.

6.3.6 Comparing transdiagnostic models to predict survival

I proceeded to investigate the optimal predictors of survival in patients with PSP and CBS. Since the most important connectivity changes for determining outcome may differ from the patterns of changes most common in disease, I used partial least squares (PLS) for Cox models to maximise covariance between predictor and survival.

I identified a connectivity component with covariance maximised to predict survival (Figure 6-6A), with worse survival related to relatively increased connectivity between task-positive regions, from the thalamus to sensorimotor regions and from the default mode network to visual regions, representing loss of segregation between these large-scale networks, with decreased connectivity elsewhere. I found component scores differed between patient groups and controls (PSP v Controls $t=3.8$ Tukey-adjusted $P=0.0006$; CBS v Control $t=3.6$ $P=0.001$), with no difference between PSP and CBS (Figure 6-6C $t=0.1$ $P=0.99$). I also identified two structural components predictive of survival (Figure 6-7). The highest absolute weights for the first component were for the thalamus, pons and midbrain, with significant contributions from limbic and frontotemporal cortical regions. Lower scores in the second component, associated with worse survival, were for

participants with thalamic and brainstem atrophy but relatively preserved cortical thickness. The highest component weight in a clinical component was for the PSPRS (Supplementary Table 6-3).

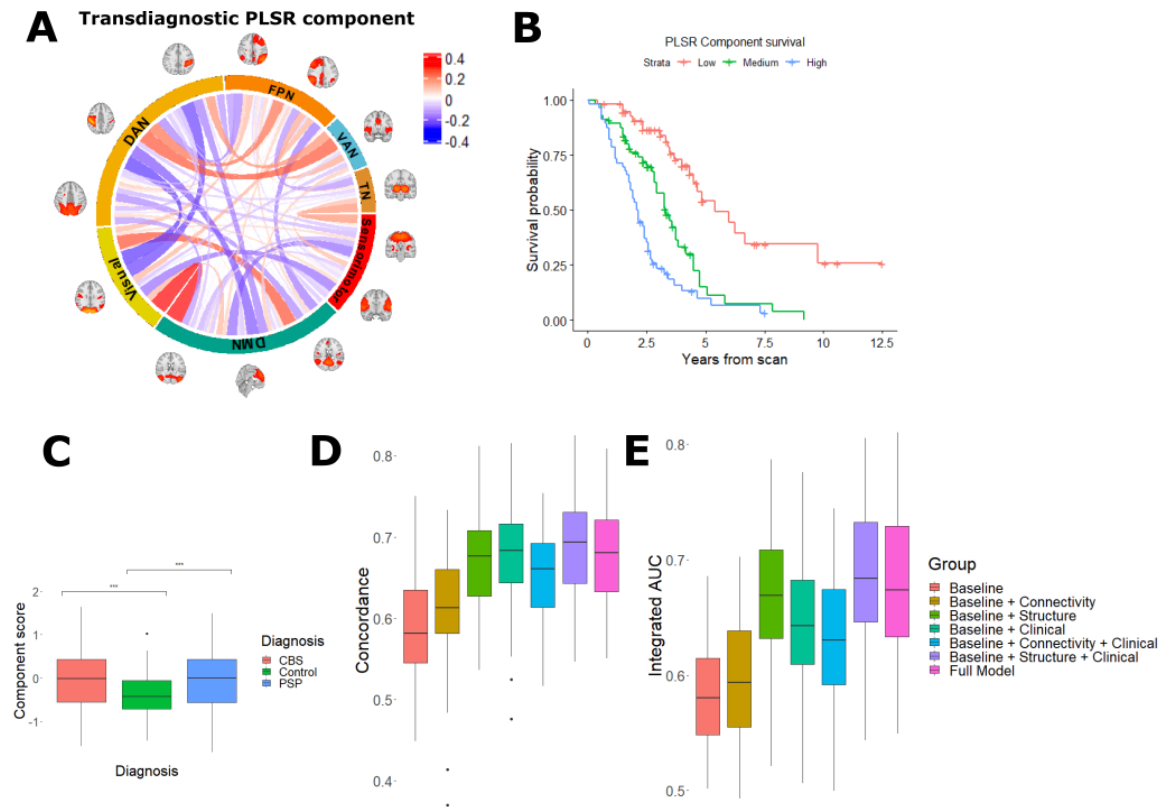


Figure 6-6. Identifying a transdiagnostic component predictive of outcome. I used Partial Least Squares Regression for Cox Models to find a component (A) that maximised the covariance between connectivity and censored time to death. Connections represent PLSR weights, so that for higher scoring subjects red indicates stronger connections and blue weaker. This component did not differ between participants with PSP and those with CBS (C). Using 5-fold cross-validation with outcome assessed using concordance analysis, I found that connectivity provided additional information above patient's demographic information and inpatient motion, but with a combination of structural, clinical and baseline metrics providing the best predictive accuracy (D). (DMN: Default Mode Network, DAN Dorsal Attention Network, VAN Ventral Attention Network, FPN Frontoparietal Network, TN Thalamic Network, SM Sensorimotor)

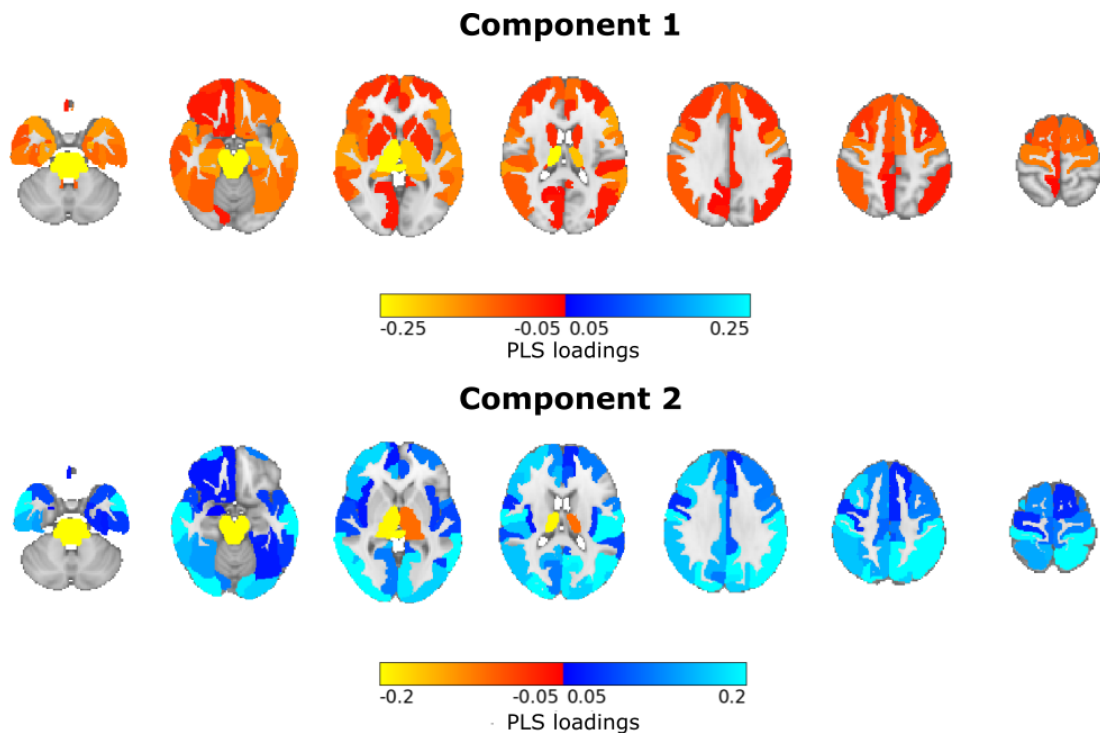


Figure 6-7. Partial least squares regression weights for structural components predictive of survival. Map thresholded so that all coloured parcels are significant predictors of survival (FDR adjusted $P < 0.05$).

I compared transdiagnostic predictive models of survival using repeat 5-fold cross-validation to a baseline model consisting of age, sex and mean framewise displacement from the fMRI scanning session, since the latter is predictive of survival (Supplementary Figure 6-1). I found that combining connectivity with the baseline model showed moderate improvement in predictive power, but that this was outperformed by both the combined baseline and structural model and the baseline and clinical models (Figure 6-6D-E Baseline: mean concordance 0.59, mean iAUC 0.58; Baseline + Connectivity: mean concordance 0.61, mean iAUC 0.59; Baseline + Structure mean concordance 0.67, mean iAUC 0.67; Baseline + Clinical mean concordance 0.68, mean iAUC 0.64). The best performing model combined baseline, structural and clinical metrics, while including all predictors in a single model worsened concordance (Baseline + Structural + Clinical mean concordance 0.68, mean iAUC 0.69; Baseline + Connectivity + Clinical mean concordance 0.65, mean iAUC 0.63; Full model mean concordance 0.68, mean iAUC 0.68). In all models including structural features best performance was with two PLS components, with one component for all other models.

To consider the potential impact of multiple collinear structural features we tested a further model with baseline and clinical measures, and the sum of volumes from the thalamus, pons and midbrain. We chose this model on a post-hoc basis to test whether cross-validation

performance is potentially substantially reduced by overfitting given the moderate-large number of collinear structural features. However, this post-hoc model showed only a modest improvement in performance over other models (mean concordance 0.7; mean iAUC 0.69).

We further tested survival predictors in each diagnostic group individually. In PSP, for a component derived using PLS regression with all predictors, highest weights were for the PSPRS, pons, midbrain, and thalamic volumes and bilateral superior temporal gyri thicknesses. In CBS largest component weights were for the PSPRS, right thalamus, pons, midbrain, with hippocampal atrophy also predictive of poor survival. In addition, in CBS connectivity between posterior networks (posterior default mode network, dorsal attention, and visual) were also weighted highly. In both PSP and CBS best model performance was with baseline and clinical predictors, together with the composite thalamic, pons and midbrain volume (PSP mean concordance 0.68, mean iAUC 0.68; CBS mean concordance 0.72 mean iAUC 0.69).

6.3.7 Focal atrophy and its relationship to connectivity

Since connectivity was only a moderate survival predictor, I investigated whether connectivity change may be driven by focal pathology. I considered the relationship with connectivity and cortical and subcortical atrophy, given that subcortical parcels had high loadings in the best survival model.

For individuals with longitudinal scanning, I found PLS component connectivity score increased over time ($t=2.7$ $P=0.01$), with higher component scores indicating worse survival. The rate of increase was greater in those with low cortical thickness (Figure 6-8A Cortical x years interaction $t=-4.9$ $P=0.0002$), but not those with reduced subcortical volume (Figure 6-8B interaction $t=1.3$ $P=0.20$). I then considered whether connectivity changes as identified in the partial least squares regression may mediate the effect of atrophy on survival. I found that the connectivity component was a significant mediator of the effect of cortical atrophy on survival (average direct effect -0.15 years $P=0.51$, average mediated effect -0.30 years $P=0.012$, proportion mediated 67%), in contrast to the significant average direct effect of subcortical atrophy (average direct effect -0.84 years $P=0.0007$, average mediated effect -0.26 years $P=0.057$, proportion mediated 24%).

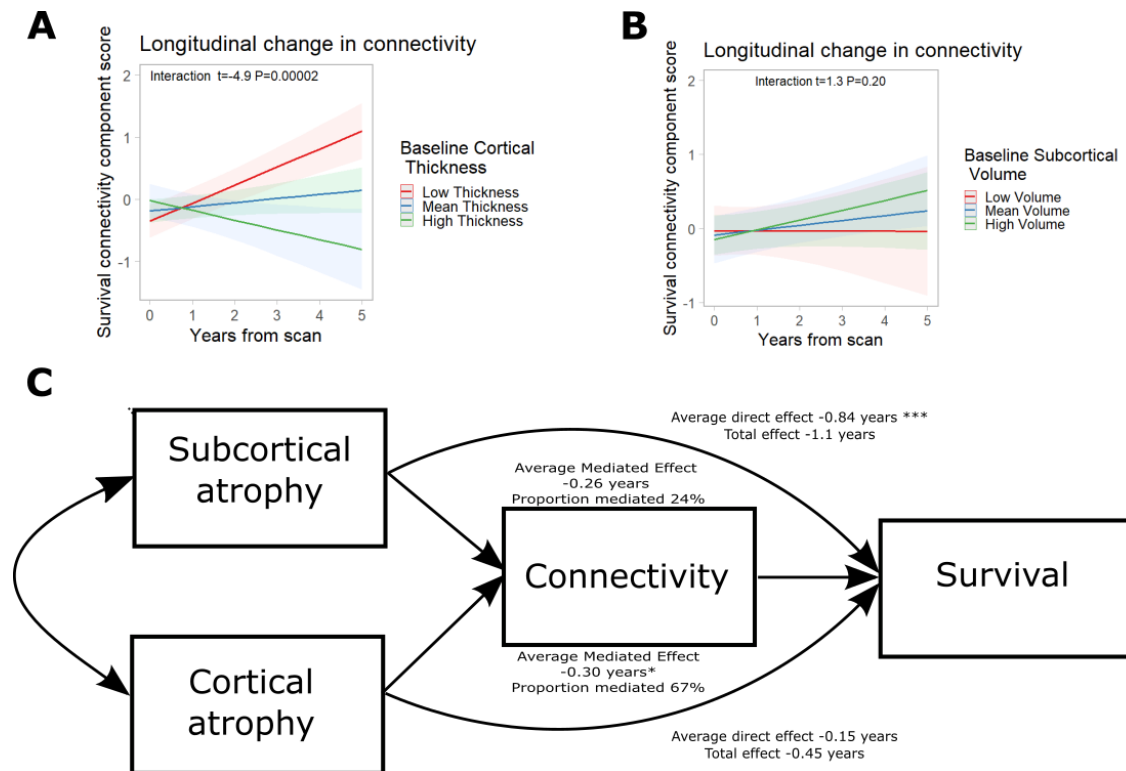


Figure 6-8. *Connectome predictors of survival and regional atrophy* Baseline cortical atrophy (A) and not subcortical volume (B) is associated with longitudinal changes in connectivity predictive of survival. C) Connectivity may mediate a significant proportion of the survival effect of cortical atrophy, while subcortical atrophy has a significant direct effect not mediated by connectivity. (* $P<0.05$, ** $P<0.01$)

In summary I have found that cortical rather than subcortical atrophy accelerates the connectivity changes most predictive of survival. However, the effects of subcortical atrophy on survival (primarily thalamic, pontine and midbrain) are predominantly not mediated by changes in between-network connectivity.

6.4 Discussion

In this study of two independent cohorts, I have found that functional connectivity and focal atrophy predict disease trajectory for people with PSP and CBS, including their rate of progression and survival. There are connectivity changes associated with shorter time to death that are shared between the diseases, but these provide less robust predictions than simple clinical and structural imaging metrics. In the most accurate model for survival prediction, the greatest weights were for the PSPRS and thalamic, midbrain and pontine volume. Cortical rather than subcortical volume at baseline was associated with subsequent progressive change in the functional connectivity that was predictive of survival. In contrast, the prognostic value of subcortical atrophy on survival is largely independent of the changes in network connectivity.

I found patterns of connectivity and structural change associated with poor survival that were shared between PSP and CBS. This is in keeping with the clinical, molecular, and pathological overlap between the diseases (Höglinger, 2018; Murley et al., 2020a), and implies the existence of common pathways important in determining survival. Commonality in survival predictors across diagnoses may arise through convergence in pathological involvement of structures important for survival. In my study thalamic, pontine and midbrain atrophy were key transdiagnostic survival predictors. Shared survival predictors may also occur at a network level (Seeley, 2017), with similar patterns of network connectivity relevant to survival occurring in PSP and CBS despite difference in distribution of pathology. The accumulation of connectivity differences associated with poor survival over longitudinal imaging suggests active network change in the presence of pathology, rather than the identified patterns solely representing pre-existing cognitive reserve (Stern et al., 2020).

The relationship between network connectivity and clinical severity is in keeping with findings that connectivity changes are closely associated with cognitive status in aging (Chan et al., 2014) and in presymptomatic carriers of dementia-causing mutations (Rittman et al., 2019; Tsvetanov et al., 2020). The whole brain approach adopted here shows that connectivity changes that predict survival similarly represent disruption to functional organisation rather than simply connectivity loss. Between-network connectivity was predominantly decreased in participants with CBS and PSP, with increased connectivity also occurring across network hierarchies (Gotts et al., 2020; Margulies et al., 2016).

Greater connectivity increased scores of a component with covariance maximised to predict survival, notably between task-positive multimodal networks, from the thalamus to sensorimotor regions and from the default mode network to visual regions. The finding that relative regional increases in connectivity contribute to poor survival supports studies demonstrating an association between increased connectivity of higher cognitive networks in health and poor cognitive function (Chan et al., 2014; Geerlings et al., 2017), and suggests that these connectivity differences indicate network inefficiency rather than compensatory changes. Cell death and the widespread cortical synaptic loss in PSP and CBS (Holland et al., 2020) may cause loss of segregation between distinct networks, such as the dorsal and ventral attention networks, with network segregation important in maintaining performance on cognitive tasks despite pathological change (Ewers et al., 2021; Tsvetanov et al., 2020). Functional brain organisation at rest relates to task-based network changes (Cole et al., 2016, 2014). Altered connectivity between multimodal networks at rest in PSP and CBS may indicate task-based network dysfunction, with behavioural and cognitive consequences relevant for disease progression (Lansdall et al., 2019; Murley et al., 2021).

Cortical atrophy and cortical network connectivity are interconnected, demonstrated by the finding that ‘epicenter’ regions of maximal atrophy can be used as seeds to select functional networks associated with neurodegenerative disease (Seeley et al., 2009; Zhou et al., 2012). These findings support this observation, suggesting that connectivity change potentially mediates the survival effects of cortical atrophy. Since greater network segregation is associated with attenuated accumulation of neuropathology (Steward et al., 2023), a vicious circle may arise where greater pathology causes network dysfunction that is cognitively detrimental, which itself results in a faster rate of pathological spread. The largest effects on connectivity for structural measures were for the thalamus, pons and midbrain. The importance of thalamic atrophy may be surprising given that in PSP cortical pathology defines the later stage of PSP tauopathy (Kovacs et al., 2020) while in CBS cortical rather than thalamic atrophy is a major imaging correlate (Boxer et al., 2006; Whitwell et al., 2010). The thalamus, pons, and midbrain contain fibres and nuclei important in diverse neuronal systems (Roy et al., 2022), including in core motor functions that have been linked to survival in PSP and CBS (Glasmacher et al., 2017; Murley et al., 2021). While thalamocortical connections have been shown to be disrupted in primary tauopathies (Whitwell et al., 2011) this data suggests that the majority of the effect of subcortical atrophy on survival is not mediated by disruption to between-network connectivity. Instead,

the contribution of subcortical atrophy to survival is relatively independent of cortical atrophy or connectivity.

The differential effects of subcortical and cortical atrophy on survival show the importance of different methodologies in selecting survival predictors, and the ability to recognise regional effects. Connectivity components were included as significant predictors of survival and longitudinal change in clinical/neuropsychological assessments beyond total grey matter volumes. Stepwise regression and standard regression models are not well suited to large number of collinear structural features, with differential regional effects identified by partial least squares regression. I also used post-hoc selected regions to show that collinearity is not significantly worsening cross-validation performance, and to determine how regional atrophy (as a marker of pathology) predicts longitudinal connectivity change.

My work highlights some of the barriers that limit between-network connectivity from resting state functional MRI as a dementia biomarker. Network connectivity satisfies criteria for a biomarker of progression, anticipating clinical deterioration with a mechanistic rationale for a causal relationship (Eimeren et al., 2019). Yet even when adopting a methodology designed to increase reliability, the failure of connections to appear repeatedly in imaging means that results are insufficiently robust to provide accurate single-subject survival predictions or to operate as an intermediate endpoint for clinical trials (D'Esposito, 2019). I selected a small number of independent components to assess between-network connectivity, but this approach may fail to identify important functional connectivity or activation patterns relevant for survival. There are a range of alternative approaches to analysing functional data, including graph metric, dynamic connectivity, voxel-wise, and gradient based analyses which may also capture characteristic differences predictive of survival. Further work is needed to determine whether these methods are more robust and with better test-retest reliability in neurodegenerative conditions with diffuse connectivity change and synaptic loss. One important consideration is the relevance of brainstem and thalamic structures in survival in PSP and CBS. Estimates of functional connectivity in these regions are affected by high physiological noise and other analytic approaches may be considered (Beissner et al., 2014).

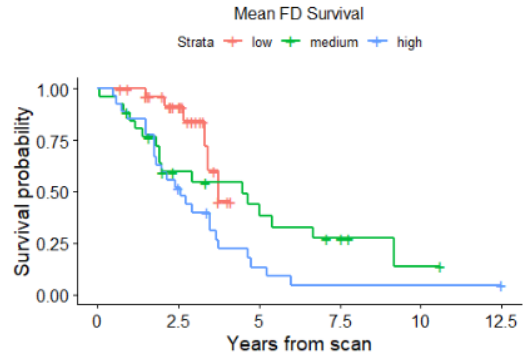
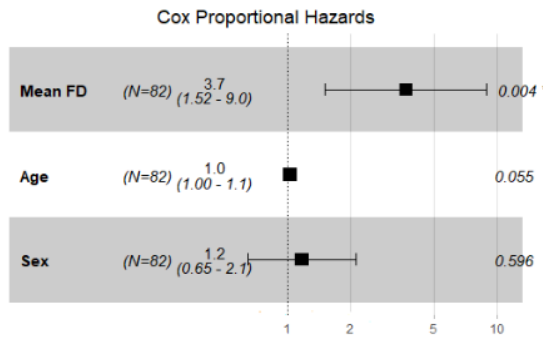
There are other limitations to this study. I found that in-scanner motion itself predicts survival in PSP and CBS. Despite adopting a principled preprocessing pipeline and not

including motion confounds as a regressor in higher-order regressions (Geerligs et al., 2017), there is an inevitable compromise between over-zealous preprocessing removing connectivity indicative of poor survival, and the failure to remove spurious connectivity deriving from motion (Power et al., 2012). To reduce the risk of motion biasing our assessments of connectivity I excluded significant numbers of participants, so it is possible that our conclusions do not apply to the excluded members of the cohort. I have used cross-validation to assess the accuracy of our survival predictions across sites but have not tested results in a third, out-of-sample, cohort that varies by scanner and protocol (Yu et al., 2018). Although I present data from a sizeable cohort of participants, increasing study power would allow for model fine-tuning and to compare machine learning approaches. I found only uncorrected differences between PSP and CBS and differential effects of connectivity on cognitive performance. I adopted an approach to analysis designed to detect diffuse changes in connectivity that might be associated with poor survival. Alternative methodological choices, such as completing analysis only with patient groups, may better capture between-group differences and be useful to test if these differences are important in predicting survival. Recent developments (Horie et al., 2022) in fluid biomarkers may help improve in vivo prediction of pathological aetiology in tauopathies, which has the potential to assist prognostication.

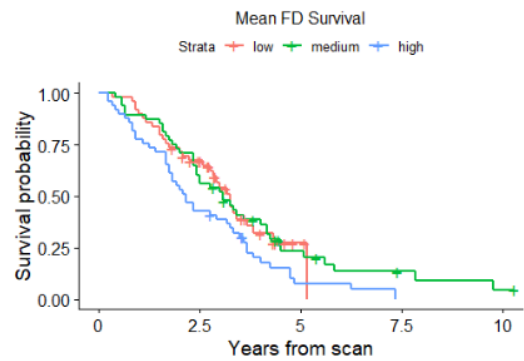
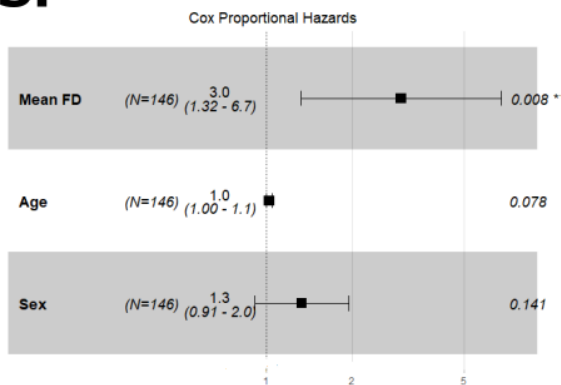
In conclusion, between-network functional brain connectivity predicts clinical deterioration and survival in PSP and CBS, with prediction in terms of cross validation and in terms of future changes after baseline scanning. However, functional connectivity provides less accurate predictions of survival than simpler measures of focal subcortical atrophy and baseline clinical severity.

6.5 Supplementary materials for chapter 6

CBS



PSP



Supplementary Figure 6-1. Mean framewise displacement from resting state functional MRI is a significant predictor of survival in both PSP and CBS. Here all participants are considered prior to any exclusion for excess motion.

	Control	PSP	CBS	F	p
Mean framewise displacement	0.19 (0.12)	0.18 (0.13)	0.26 (0.22)	7.5	0.0007
Median spike percentage	3.9 (2.6)	3.5 (2.5)	3.5 (3.5)	0.5	0.59
Max spike percentage	14.2 (9.0)	18.3 (11.2)	13.8 (10.4)	5.2	0.006
Max DVARS	7.8 (1.1)	7.9 (1.1)	7.6 (1.3)	1.1	0.33

Supplementary Table 6-1. Motion parameters by group at baseline scan

	Intercept	years	t	P
ACER	80.1	-4.3	-8.2	4×10^{-12}
CBIR	42.2	8.0	5.1	5×10^{-6}
PSPRS	32.6	6.8	10.6	2×10^{-11}

*Supplementary Table 6-2. Fixed effects for mixed linear models for different neuropsychological tests. *t* and *p*-values for the years terms calculated using Satterthwaite's method*

Predictor	PLSR standardised coefficients	P value
PSPRS	0.20	3.1×10^{-8}
CBIR	0.10	5.1×10^{-4}
ACER	-0.056	0.058
Age	0.067	0.013

Supplementary Table 6-3. PLSR coefficients for a one component PLSR Cox model

7 Discussion

In this thesis I have assessed imaging changes throughout the disease course in the syndromes associated with frontotemporal lobar degeneration. Here, I relate findings to the aims and hypotheses outlined in section 1.10, highlighting common themes across chapters. I discuss how focal changes to structure in FTLD result in widespread disruption to functional networks, how imaging biomarkers can be used to improve predictions of prognosis across the disease course, and the benefits of using functional connectivity as an explanatory tool and intermediate outcome measure. I comment on the utility and limits of task-free fMRI in neurodegenerative conditions. The chapter ends with an overview of the developments required to introduce advanced imaging biomarkers in supporting precision medicine and trials of experimental therapeutics in FTLD.

7.1 A summary of key findings

7.1.1 Diffuse network changes occur in FTLD and correlate with severity.

Using various methodological approaches, I have found that functional networks are disrupted in FTLD syndromes. In sporadic and familial FTD, and in PSP, functional network dynamics are altered, with increased time in heteromodal large-scale networks, and a decrease in proportion of time spent in the primary cortices and subcortical regions. In PSP and CBS, I found reductions, compared to healthy controls, in weighted degree across cortical and subcortical regions, and reduced connectivity between multiple large-scale networks.

While network disruption is diffuse in FTLD syndromes, there is variation in network involvement associated with phenotypic heterogeneity across diagnostic entities. In FTD the largest change in network dynamics was in occupancy of the salience network. Patterns of atrophy in behavioural variant FTD mirror the salience network (Seeley et al., 2009), changes which correlate with post-mortem pathological change in the insular cortex (Pasquini et al., 2020). Attenuation in salience network connectivity (Dopper et al., 2013; Zhou et al., 2010) is associated with the cardinal social and behavioural dysfunction of bvFTD (Toller et al., 2018). In CBS there were uncorrected greater reductions in connectivity in posterior components, including the dorsal attention network, which has

been found to be a focus of network localisation in meta-analyses of task-free fMRI studies (Darby et al., 2019).

Network disruption is associated with clinical severity. In PSP, scores on a network dynamic component correlated with the standard multidomain rating scale, the PSPRS. In sporadic and familial FTD time-varying network markers from hidden Markov modelling were associated with executive dysfunction and cognitive impairment. Broad changes in between-network connectivity were associated with severity in both PSP and CBS, with an interaction in the relationship between greater posterior connectivity change and diagnosis for cognitive impairment measured by the ACE-R.

These results demonstrate the advantages of adopting whole brain approaches to analyses of neurodegenerative disease, rather than regional- or edge- level analyses. In healthy adults brain-behaviour effect sizes are larger with multivariate techniques (Marek et al., 2022) and these relationships are more likely to be detected using methods that assess significance across the whole brain (Noble et al., 2022). It is plausible that outcomes such as survival, or rating scales and neuropsychological assessments that capture highly varied functions and cognitive domains, would be associated with widespread (rather than focal) disruption to brain function. Considering both temporal and spatial information in a time-varying analysis of functional networks provides an effective technique to characterise brain-wide functional change in FTLN, in keeping with the finding that dynamic functional connectivity improves group classification in dementia (Moguilner et al., 2021). While alterations to analyses may be needed to capture different features of a syndrome, such as motor, behavioural, executive, or visuospatial impairment, all are likely best captured by methods that consider the whole brain.

7.1.2 Connectivity loss both co-localises and occurs remotely from atrophy and synaptic loss.

Functional connectivity differences in the FTLN syndromes occur both at the site of structural change and remotely from it. In chapter 4 I showed that subcortical atrophy in PSP is associated with dynamic network dysfunction of both cortical and subcortical regions. In chapter 5 regional variation in synaptic density spatially covaried with functional connectivity in topographically distinct regions, with frontal synaptic loss associated with reduced connectivity in posterior hubs of the default mode network. In

chapter 6 cortical atrophy at baseline predicted future accumulation of disparate between-network differences.

These results demonstrate that clinicoanatomical convergence (Seeley, 2017) can arise at a network level, with regionally distinct pathological change involving a single network. Therefore, although two pathologies (e.g. 3-R or 4-R tauopathy) may preferentially affect different brain regions, they can both cause behavioural and executive disturbance by involvement of relevant networks (e.g. salience or frontoparietal networks). Using hidden Markov modelling I have shown that regional pathology causes global perturbation in non-stationary brain dynamics. This is in keeping with the observation that certain brain nodes are key in orchestrating brain state changes (Gu et al., 2015), with pathology in distinct regions causing similar changes to brain dynamics. Convergence in clinical symptoms may only be temporary (Murley et al., 2020a), since pathological processes would then follow different regional patterns and involve different networks. Task-free fMRI, in combination with other imaging modalities, is therefore useful in understanding when clinical symptoms might be predictive of outcome.

7.1.3 Imaging biomarkers predict outcomes across the disease course.

A key motivation in biomarker research in neurodegeneration is to enhance understanding of the factors that determine outcome and to improve prognostication, both to support clinical practice and in a trial setting. In chapters 3 and 6 I tested the ability of imaging markers to predict disease outcomes at different stages of the disease course. In chapter 3 I showed that dynamic network changes are associated with conversion to symptomatic disease and cognitive decline in familial FTD. In chapter 6 I found that in PSP and CBS, both structural and functional imaging metrics were associated with faster rate of clinical decline and shorter survival, with best predictions of survival combining clinical and structural imaging metrics.

These findings provide mechanistic insight. In presymptomatic patients in familial FTD hyperconnectivity has also been observed (Lee et al., 2019), with increased coupling between functional connectivity and cognition close to symptom onset (Tsvetanov et al., 2020), suggestive of early compensatory processes (Figure 1-4, (Gregory et al., 2017)). Network integrity is relatively maintained in presymptomatic patients prior to network breakdown in the symptomatic phase (Rittman et al., 2019). This thesis adds the finding that large-scale network disruption occurs around the point of symptom onset. Given the

difficulties in determining clinically when someone has entered the symptomatic stage of familial FTD (Moore et al., 2020), characterising large-scale network changes typical of disease provides a useful objective marker. In PSP and CBS thalamic, pontine, and midbrain atrophy predict poor survival, potentially a consequence of the central role of these structures and their connections in varied core functions (Hwang et al., 2017; Roy et al., 2022; Sherman, 2016).

The cross-validation in chapter 6 is informative as to biomarker utility in predicting outcome (functional imaging v structural imaging v clinical metrics). There are multiple contributory factors that account for between-network connectivity being only a moderate predictor of survival in PSP and CBS. Functional MRI has poor signal-to-noise ratio from subcortical and brainstem structures (Beissner et al., 2014). It may be that the connectivity of these regions is important in survival. This is suggested by the poor prognosis associated with subcortical atrophy and with clinical features associated with subcortical disease, such as falls and dysphagia (Glasmacher et al., 2017). I found that between-network connectivity was a mediator of cortical rather than subcortical atrophy.

Consideration of the neurodegenerative cascade in Figure 1-1 offers further insight. Connectivity loss in regions or networks important for an outcome would be prognostically relevant if associated with future disturbance in the same system in a manner that worsens symptoms. Connectivity change that occurs in synchrony with symptom development would not be predictive of outcome (correlating rather than anticipating outcome, using the framework in Figure 1-3). Correlative but non-predictive changes have been found in PSP using longitudinal imaging over a 6 month time frame (Brown et al., 2017). Multi-modal imaging may be helpful to differentiate associative and anticipatory measures, if we construct disease models that estimate when prognostically important networks become affected. In chapter 3 I showed that large-scale changes in dynamic network activation are non-linear. Prognostic accuracy of functional connectivity (and other imaging makers) may be greater for moderate rather than severe change, or instead when peak compensatory processes can be detected (Gregory et al., 2017).

In sections 7.2 and 7.3 I discuss the clinical situations in which biomarkers predictive of outcome may be useful, and the challenges of implementing task-free fMRI in a trial or clinical setting.

7.1.4 Transdiagnostic analyses demonstrate shared imaging features in FTLD.

A common finding across the chapters of this thesis are shared imaging phenotypes in the syndromes associated with FTLD in multiple modalities. Using [¹¹C]UCB-J positron emission tomography, I found partially overlapping distributions of reduced synaptic density, but with disease specific effects. With task-free fMRI, large-scale network dynamic differences in familial FTD from non-carriers were observed across mutations and between those with behavioural predominant symptoms and primary progressive aphasia. The primary component of dynamic network change in familial FTD showed similarities with the pattern I found in PSP, recognising that differences in model order choices limit the ability to make direct comparisons of fractional occupancy for individual states. Between-network connectivity differences from controls were broadly comparable in PSP and CBS.

This is not to argue that differences are not found depending on the diagnostic label – indeed I describe some such differences above. Other choices of analysis may bring these to the fore. For instance, I would expect to find differences from task-free fMRI in familial FTD between PPA and bvFTD by focusing on specific states, perhaps with a higher model order (Reyes et al., 2018). But crucially, transdiagnostic analyses demonstrate overlap in disease physiology and determinants of outcomes. PSP and CBS share the same between-network connectivity survival predictors, suggesting convergence in factors that influence survival, in keeping with transdiagnostic approaches in FTLD using clinical metrics (Murley et al., 2021). In chapter 5, I show how synaptic loss results in associated topographical distributions of connectivity loss across diagnostic labels, with similar consequences for cognition and clinical severity. These findings imply that therapies, such as to limit synapse loss, could be applied across the FTLD spectrum. I discuss how transdiagnostic approaches can lead to precision medicine and support novel trial designs below.

7.1.5 Functional connectivity and modelling the neurodegenerative cascade.

The utility of a biomarker can be considered and assessed against its usefulness in clinical medicine by the criteria described in Figure 1-3 (Eimeren et al., 2019), or by whether it allows us to test hypothesis relevant to neurodegenerative pathogenesis or treatment. In chapter 6 I use both approaches; between-network connectivity is a less accurate predictor of survival than clinical and structural measurements, with the observed changes in

connectivity associated with cortical (versus subcortical) atrophy. In chapter 5 functional connectivity acts both as an explanatory biomarker and as an outcome measure. Synaptic loss, atrophy, and neurotransmitter receptor/transporter distributions explain non-overlapping variance in functional connectivity. Functional connectivity both adds to and moderates the effect of synaptic loss on survival.

In health there is divergence between network patterns derived from structural imaging and from task-free fMRI (Honey et al., 2009; Mišić et al., 2016). Structural connectomes partially predict their functional counterparts with variable overlap (Mišić et al., 2016). Moreover a structural connectome can be associated with multiple configurations of functional networks (Deco et al., 2017; Honey et al., 2007; Vidaurre et al., 2017), even within short scanning windows and in a single subject (Poldrack et al., 2015). Functional connectivity, a statistical dependency between two brain regions, is determined by complex direct and indirect influences and does not imply causality or influence (Friston, 1994).

Similarly, I have shown that in neurodegeneration structural changes (cell loss or synapse loss) partially but incompletely explain functional network differences. Modelling functional connectivity as a dependent variable allows us to test other important factors that may explain variance. In chapter 5 I show the importance of noradrenaline transporter distributions, beyond structural determinates, to functional connectivity loss in FTLD. That the strength of the connectivity-noradrenaline transporter distribution relationship is associated with locus coeruleus integrity provides validation for this methodology and shows how it may be possible to limit number of modalities when characterising brain change in disease. It does not follow from these results that noradrenaline is necessarily depleted, given the complexity of determinants of any neural system (Hansen et al., 2022). A further challenge in using functional connectivity as an outcome measure is ascertaining which connectivity changes observed at rest relate to behaviour and cognition, particularly given that task-induced changes in functional connectivity show differential effects and improve predictions of phenotype (Greene et al., 2020, 2018).

How do we further improve modelling of functional changes from task-free fMRI? Using diffusion tensor imaging enables characterisation of the structural connectome and the relationship with functional connectivity (Honey et al., 2009, 2007; Mišić et al., 2016), important in FTLD where there are extensive structural connectivity changes (Mahoney et al., 2015; Whitwell et al., 2011). Direct measurement of neurotransmitter deficits in

individual patients (e.g. using MR spectroscopy or PET ligands) would provide more precise information about the effects of pathology than from using transporter/receptor maps from healthy populations. Whole brain modelling which considers causal pathways, interactions, non-linear effects, and regionally distant effects of structural change on function may explain a larger proportion of variance (Jancke et al., 2022). In addition, there remains the possibility of unaccounted for artefactual influences on connectivity. Delineating these components is important to maximise use of task-free fMRI as an intermediate outcome or endpoint.

7.2 The utility of task-free fMRI in neurodegeneration

In the introductory chapter I discussed doubts regarding the merits of research using task-free fMRI in neurological diseases or in understanding brain-behaviour relationships (Kullmann, 2020). Drivers of this scepticism included the limited clinical applications of fMRI (including task-based fMRI) and uncertainty as to the relationship between the blood-oxygen-level-dependent signal and neuronal activity (Kullmann, 2020). The effect sizes of brain-behaviour relationships are small (Marek et al., 2022), which in combination with high degree of freedom in analysis risks unreproducible research (Carp, 2012; Ioannidis, 2008; Poldrack et al., 2017). Subject motion results in spurious and systemic increases in correlation without careful pre-processing (Power et al., 2012; Satterthwaite et al., 2012), a problem made more challenging in FTLD where motion itself predicts survival (chapter 6).

Despite these problems, which are variably surmountable, I suggest that task-free fMRI remains a useful research tool where appropriately targeted. In keeping with the model of the neurodegenerative cascade introduced in chapter 1, task-free fMRI is best considered a near-cognition imaging marker. It is not therefore plausible to suggest that it would be helpful in determining the underlying pathology of a clinical presentation, or to detect very early accumulation of pathology long before symptom onset. In keeping with the hypothesised utility of task-free fMRI, I have shown that it can act as an upstream outcome marker of neuropathological change (chapter 5), can predict important outcomes for patients with FTLD (chapters 3 and 6), and can support understanding of how various physiological changes in neurodegeneration result in behavioural and cognitive symptoms. Functional MRI also has advantages over other biomarkers of function and neural activity,

such as magnetoencephalography; it is scalable and widely available, with excellent spatial resolution including for subcortical structures.

Task-free functional MRI should therefore not be discarded as a research tool, although its limitations must be recognised and taken into consideration when designing analysis strategies. Key requirements for obtaining robust results include formal pre-registration of analysis plans, the use of external or hold-out datasets for validation, and full reporting of analyses, including those that did not produce significant results (Poldrack et al., 2017). There are significant challenges in using task-free fMRI in clinical practice or a clinical trial setting. Pre- and post-processing is complex and would require technical innovation to implement (see Leuthardt et al., 2018 for an example of how this might be achieved). In chapters 3 and 4 I have shown that results can be replicated across sites, albeit with research-grade scanning and harmonisation of acquisition protocols. Collaboration and benchmarking research are also required to develop analysis and pre-processing standards that could theoretically support task-free fMRI use in trial settings (Bijsterbosch et al., 2021; Botvinik-Nezer et al., 2020).

A more fundamental problem is that the effect sizes of task-free fMRI changes may be too small to use in clinical practice. In chapter 6, although between-network connectivity was associated with poor survival in PSP and CBS, it did not improve survival predictions beyond clinical and structural imaging metrics. Assessment of biomarker utility needs to replicate true clinical practice as closely as possible. For instance, it would be of interest to compare the predictive power of task-free fMRI changes in presymptomatic familial FTD, as described in chapter 3, with clinical predictions of time to disease onset. Only with such data can we test if effect-sizes are sufficiently large to support clinical practice and trials of experimental medications, or to determine if task-free fMRI should primarily remain a research tool to probe disease mechanisms in neurodegeneration.

There are promising experimental advances in task-free fMRI that may help overcome these challenges and provide additional insights into the neurodegenerative cascade in FTLD. Developments include functional MRI with millisecond temporal precision (Toi et al., 2022), potentially allowing exploration of rapid brain dynamics and testing of causal relationships, presuming such methods can be applied to humans. Spatial precision and mapping of mesoscale brain functions in humans has been shown to be possible with ultra-high field functional MRI (Jia et al., 2021). However sequence acquisition currently

requires longer scanning times than at 3-Tesla and it may be that using optical pumping magnetometers for magneto-encephalography mean that the latter is a better option for detailed spatial and temporal resolution of the whole brain in neurodegeneration (Qin and Gao, 2021). Low demand tasks during fMRI scanning, such as movie watching, provide a richer and better defined array of brain states than resting state acquisition protocols (Meer et al., 2020).

Novel computation modelling techniques allow prediction of disease spread through the brain (Iturria-Medina et al., 2014; Oxtoby et al., 2018; Pandya et al., 2019), comparison of different components of the neurodegenerative cascade to ascertain their relative importance (Meisl et al., 2021), and characterisation individual disease profiles by combining multiple modalities (Khan et al., 2022). I have showed how functional connectivity may be used as an outcome marker to quantify contribution of synaptic density, atrophy, and neurotransmitter deficits to function. This approach uses parcellation and modelling of the connectome defined at the group level. Individualised representations of functional connectivity are possible from task-free fMRI (Poldrack et al., 2015; Wang et al., 2015) and may assist in characterising participant variability in disease (Bijsterbosch et al., 2021), including when assessing longitudinal change.

In the next section I place the work in this thesis, together with developments such as described here, in the context of precision medicine and supporting clinical trials.

7.3 Towards precision medicine and supporting clinical trials

Throughout this thesis I have emphasised shared features and heterogeneity in the clinical syndromes associated with FTLD. I have leveraged heterogeneity to understand disease mechanisms and combined patients across diagnoses to detect transdiagnostic outcome predictors. This is not to suggest that diagnostic labels should be abandoned, or that diagnostic entities should be further sub-divided in a finer-grained classification system. Debates on the relative merits of ‘lumping’ and ‘splitting’ in disease nosology tend to highlight scenarios when these respective approaches are beneficial (Höglinger, 2018; Ling and Macerollo, 2018). Transdiagnostic disease modelling and biomarker design can accommodate both perspectives and is essential for the development of precision or personalised medicine.

Precision medicine in neurodegeneration refers to the use of clinical, genetic, and imaging and fluid biomarker information to generate a complete risk profile of a patient with dementia, and to tailor treatment accordingly (Kosik, 2015; Schork, 2015). This approach is motivated by the complex multifactorial nature of neurodegenerative diseases. Focusing on single disease factors is likely a contributor to the (at best) small-moderate effect sizes found in trials of disease-modifying therapies (Khan et al., 2022). Traditional large-scale phase III studies are inefficient at detecting subgroups who may respond most effectively to a treatment, relying on post-hoc analysis (Schork, 2015). Patient-customised treatments are most advanced in oncology, but examples exist of design, manufacture, and delivery of tailored drugs for single rare neurodegenerative diseases such as Batten’s disease (Kim et al., 2019). Figure 7-1 provides a schematic representation of how precision medicine might be developed and applied in a clinical setting for patients with FTLD syndromes. There are varying degrees to which trial design might be personalised, from using biomarkers in inclusion criteria to select and assess patients at tightly defined disease stages (see for instance Mintun et al., 2021), to drawing inferences from commonalities in multiple N-of-1 studies.

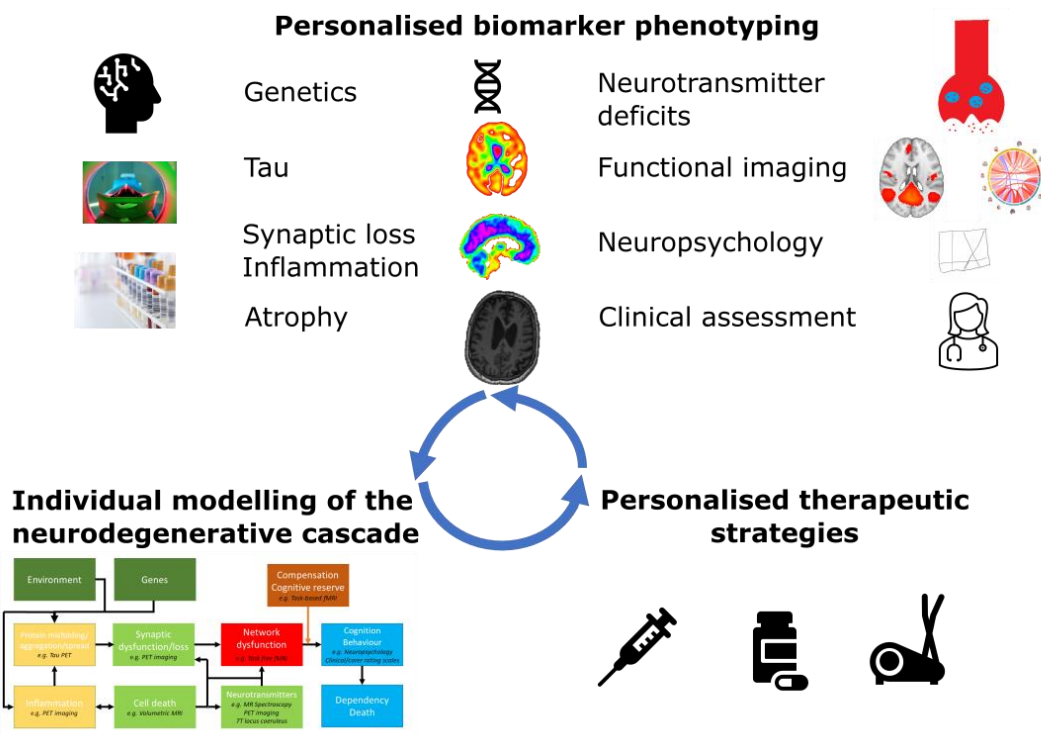


Figure 7-1. A schematic representation of personalised approach to medicine in FTLD. The neurodegenerative cascade is characterised using multiple imaging and other biomarkers, with modelling of disease processes leading to individualised treatment. Longitudinal biomarker assessment is used for feedback and refining treatment.

How realistic is personalised medicine in dementia care? In the NHS patients with neurodegeneration have long and growing waits for review and diagnosis in memory clinics (Royal College of Psychiatrists, 2022). Access to different imaging modalities is variable, with a proportion of memory services performing no imaging at all (Cook et al., 2020). Clinicians in the majority of memory services are unable to view scans (Cook et al., 2020). Personalised medicine requires significant upfront and on-going costs, even with growing availability of genetic sequencing and affordable wearable technologies to collect health data (Schork, 2015). Acquisition of multiple biomarkers, including repeated imaging, is challenging in dementia, and may be refused by patients, particularly if they do not lead to treatments which substantially improve quality of life. Given that wholesale reform would be needed for these approaches to be implemented, developments are most likely in specific trial settings. I discuss two such scenarios, namely trials in presymptomatic patients and basket trials in FTLD, particularly for symptomatic management.

As discussed in chapter 1, pathophysiological processes in dementia start many years before disease onset. A potential therapeutic needs to be aimed at the right target at the optimum point in the disease course, which may be in the asymptomatic or prodromal phase of the disease (Sperling et al., 2011). There is particular interest in presymptomatic trials in familial dementias, given the possibility of identifying trial participants and the development of targeted genetic treatments. Novel imaging and fluid biomarkers have a crucial role in this group for both inclusion criteria and as outcome measures, where relying on clinical or neuropsychological tests would require unfeasibly large numbers of participants (Staffaroni et al., 2022). For instance, a trial in a genetic variant in FTD might use neurofilament light chain, neuropsychological performance, and brain volume to predict proximity to onset and as endpoints. Dynamic network changes in FTD may improve disease age modelling and act as secondary endpoints. Progress is needed in identifying presymptomatic individuals in sporadic FTLD, with large population databases such as the UK Biobank providing insight into this group (Street et al., 2022; Swaddiwudhipong et al., 2022). Presymptomatic patients are more likely to be able to tolerate collection of multiple and repeated biomarkers and combination therapies, which would allow precision targeting of trial treatments.

Transdiagnostic characterisation of the FTLD syndromes emphasises the possibility of basket trials, where multiple diseases are included in a single trial design (Boxer et al., 2020; Woodcock and LaVange, 2017). Possible trials include those for symptoms common

in multiple FTLD syndromes, such as apathy, or for common mechanistic targets, such as tau or inflammation. This approach increases the recruitment population for these rare or uncommon conditions, with results that would be applicable to a larger patient cohort. Here greater biomarker use is essential to ensure that disease mechanisms or molecular aetiologies are shared between trial participants. An example trial for noradrenaline replacement in FTLD syndromes could use combination imaging, including 7-Tesla imaging to assess locus coeruleus integrity, structural and synaptic PET imaging to select patients with sufficiently mild disease to benefit from treatment, and functional imaging to refine selection and as an intermediate outcome marker. A clinical trial setting allows more resource intensive biomarker selection, although results could not then be easily applied in clinical practice. Trialists may consider multiple staged trials, with an initial stage with higher numbers of biomarkers followed by a stage using biomarkers selected as more readily available for ‘real-world’ populations. For instance, blood or CSF biomarkers of synaptic degeneration (Ashton et al., 2019) may be used instead of the PET ligand, presuming a similar cohort is selected.

To progress to greater use of imaging biomarkers in clinical trials and precision medicine in FTLD we need to advance understanding of the factors that dictate imaging change, extending the work of this thesis. How neurodegenerative processes cause atrophy, as observed on structural imaging, is only partially understood (Fung et al., 2020; Planche et al., 2022). Consequently, structural imaging findings in experimental drug trials in dementia can be difficult to explain. Drugs that remove amyloid in Alzheimer’s disease have in some studies been associated with greater rates of atrophy than in placebo groups (Cummings, 2019), including lecanemab (Swanson et al., 2021). It is uncertain whether similar effects might be observed in FTLD, impacting on the use of structural MRI as a trial endpoint.

Significant work is also required to progress imaging modalities apart from volumetric MRI in a clinical trial setting, particularly in characterising longitudinal imaging changes (Sperling, 2011). I have shown in chapter 6 how longitudinal task-free fMRI can be used to understand how atrophy determines functional connectivity. Effect sizes of longitudinal fMRI in early PSP appears too small for clinical trial use (Brown et al., 2017). It is possible larger effect sizes might be seen in FTLD syndromes with a greater proportion of cortical pathological burden, given the low signal-to-noise ratio in brainstem regions (Beissner et al., 2014), or by using participant specific connectomes. Integrating data across modalities

captures greater information about an individual patient's biology (Calhoun and Sui, 2016; Khan et al., 2022; Uludağ and Roebroek, 2014). However, care is needed to ensure that common effects of artefact are not amplified in multi-modal imaging studies. Given the complexities of inference and analysis when using multiple sequences, I suggest that pre-registered approaches with strong theoretical grounding are essential if modalities are to be combined to support personalised brain models in FTLD syndromes.

One incentive for developing precision medicine in neurodegeneration is that experimental drug trials are frequently biased to white Western populations (Padala and Yarns, 2022), resulting in uncertainty as to whether effects replicate in other ethnicities. Theoretically, personalised medicine may support trials in under-represented groups, helping to direct treatment to individual risk factors and remove concerns that trial participants are 'guinea pigs' (Schork, 2015), a particular concern for groups that have been historically mistreated by research (Buseh et al., 2013; Wolinetz and Collins, 2020). An important caveat is that biomarker development has also often excluded the same groups. This is evidenced in racial disparities in biomarkers for Alzheimer's disease pathology, with lower rates of positive PET and cerebrospinal fluid biomarkers in African American participants with a clinical diagnosis of mild cognitive impairment or Alzheimer's disease (Garrett et al., 2019; Morris et al., 2019). Biomarkers must be designed and tested in diverse groups to improve dementia care for all patients.

7.4 Conclusions

I have shown how imaging biomarkers are useful in understanding heterogeneity in phenotypic presentation and progression in syndromes associated with frontotemporal lobar degeneration. Adopting transdiagnostic approaches to analyses provides insight into how heterogeneity arises, enhanced by combining multiple modalities in single studies. Task-free fMRI has a role in mechanistic understanding of disease mechanisms and in predicting progression throughout the disease course, but its usefulness in clinical settings is limited by low signal-to-noise ratio and small-moderate effect sizes. I have sketched a path for how we progress to personalised medicine and support trials in presymptomatic patients. These developments will be essential to introduce new symptomatic and disease-modifying treatments to improve outcomes for patients, families, and carers.

8 References

- Achard, S., Bullmore, E., 2007. Efficiency and cost of economical brain functional networks. *PLoS computational biology*.
<https://doi.org/10.1371/journal.pcbi.0030017>
- Adams, N.E., Hughes, L.E., Rouse, M.A., Phillips, H.N., Shaw, A.D., Murley, A.G., Cope, T.E., Bevan-Jones, W.R., Passamonti, L., Street, D., Holland, N., Nesbitt, D., Friston, K., Rowe, J.B., 2021. GABAergic cortical network physiology in frontotemporal lobar degeneration. *Brain* 144, 2135–2145.
<https://doi.org/10.1093/brain/awab097>
- Adams, N.E., Jafarian, A., Perry, A., Rouse, M.A., Shaw, A.D., Murley, A.G., Cope, T.E., Bevan-Jones, W.R., Passamonti, L., Street, D., Holland, N., Nesbitt, D., Hughes, L.E., Friston, K.J., Rowe, J.B., 2022. Neurophysiological consequences of synapse loss in progressive supranuclear palsy. *Brain*.
<https://doi.org/10.1093/brain/awac471>
- Aghourian, M., Legault-Denis, C., Soucy, J.-P., Rosa-Neto, P., Gauthier, S., Kostikov, A., Gravel, P., Bédard, M.-A., 2017. Quantification of brain cholinergic denervation in Alzheimer's disease using PET imaging with [18F]-FEOBV. *Mol Psychiatry* 22, 1531–1538. <https://doi.org/10.1038/mp.2017.183>
- Ahmed, R.M., Devenney, E.M., Strikwerda-Brown, C., Hodges, J.R., Piguet, O., Kiernan, M.C., 2020. Phenotypic variability in ALS-FTD and effect on survival. *Neurology* 94, e2005–e2013. <https://doi.org/10.1212/WNL.0000000000009398>
- Ahmed, R.M., Highton-Williamson, E., Caga, J., Thornton, N., Ramsey, E., Zoing, M., Kim, W.S., Halliday, G.M., Piguet, O., Hodges, J.R., Farooqi, I.S., Kiernan, M.C., 2017. Lipid Metabolism and Survival Across the Frontotemporal Dementia-Amyotrophic Lateral Sclerosis Spectrum: Relationships to Eating Behavior and Cognition. *JAD* 61, 773–783. <https://doi.org/10.3233/JAD-170660>
- Ahmed, R.M., Irish, M., Kam, J., van Keizerswaard, J., Bartley, L., Samaras, K., Hodges, J.R., Piguet, O., 2014. Quantifying the Eating Abnormalities in Frontotemporal Dementia. *JAMA Neurol* 71, 1540. <https://doi.org/10.1001/jamaneurol.2014.1931>
- Ahmed, Z., Cooper, J., Murray, T.K., Garn, K., McNaughton, E., Clarke, H., Parhizkar, S., Ward, M.A., Cavallini, A., Jackson, S., Bose, S., Clavaguera, F., Tolnay, M., Lavenir, I., Goedert, M., Hutton, M.L., O'Neill, M.J., 2014. A novel in vivo model of tau propagation with rapid and progressive neurofibrillary tangle pathology: the pattern of spread is determined by connectivity, not proximity. *Acta Neuropathol*.
<https://doi.org/10.1007/s00401-014-1254-6>
- Alafuzoff, I., Pikkarainen, M., Neumann, M., Arzberger, T., Al-Sarraj, S., Bodi, I., Bogdanovic, N., Bugiani, O., Ferrer, I., Gelpi, E., Gentleman, S., Giaccone, G., Graeber, M.B., Hortobagyi, T., Ince, P.G., Ironside, J.W., Kavantzias, N., King, A., Korkolopoulou, P., Kovács, G.G., Meyronet, D., Monoranu, C., Nilsson, T., Parchi, P., Patsouris, E., Revesz, T., Roggendorf, W., Rozemuller, A., Seilhean, D., Streichenberger, N., Thal, D.R., Wharton, S.B., Kretzschmar, H., 2015. Neuropathological assessments of the pathology in frontotemporal lobar degeneration with TDP43-positive inclusions: an inter-laboratory study by the BrainNet Europe consortium. *J Neural Transm* 122, 957–972.
<https://doi.org/10.1007/s00702-014-1304-1>

- Albert, M.L., Feldman, R.G., Willis, A.L., 1974. The 'subcortical dementia' of progressive supranuclear palsy. *Journal of Neurology, Neurosurgery & Psychiatry* 37, 121–130. <https://doi.org/10.1136/jnnp.37.2.121>
- Alexander, S.K., Rittman, T., Xuereb, J.H., Bak, T.H., Hodges, J.R., Rowe, J.B., 2014. Validation of the new consensus criteria for the diagnosis of corticobasal degeneration. *Journal of Neurology, Neurosurgery & Psychiatry*. <https://doi.org/10.1136/jnnp-2013-307035>
- Alfaro-Almagro, F., Jenkinson, M., Bangerter, N.K., Andersson, J.L.R., Griffanti, L., Douaud, G., Sotiropoulos, S.N., Jbabdi, S., Hernandez-Fernandez, M., Vallee, E., Vidaurre, D., Webster, M., McCarthy, P., Rorden, C., Daducci, A., Alexander, D.C., Zhang, H., Dragonu, I., Matthews, P.M., Miller, K.L., Smith, S.M., 2018. Image processing and Quality Control for the first 10,000 brain imaging datasets from UK Biobank. *NeuroImage*. <https://doi.org/10.1016/j.neuroimage.2017.10.034>
- Appel, S.H., 1981. A unifying hypothesis for the cause of amyotrophic lateral sclerosis, parkinsonism, and alzheimer disease. *Ann Neurol*. 10, 499–505. <https://doi.org/10.1002/ana.410100602>
- Arbabshirani, M.R., Plis, S., Sui, J., Calhoun, V.D., 2017. Single subject prediction of brain disorders in neuroimaging: Promises and pitfalls. *NeuroImage*. <https://doi.org/10.1016/j.neuroimage.2016.02.079>
- Armstrong, M.J., Litvan, I., Lang, A.E., Bak, T.H., Bhatia, K.P., Borroni, B., Boxer, A.L., Dickson, D.W., Grossman, M., Hallett, M., Josephs, K.A., Kertesz, A., Lee, S.E., Miller, B.L., Reich, S.G., Riley, D.E., Tolosa, E., Troster, A.I., Vidailhet, M., Weiner, W.J., 2013. Criteria for the diagnosis of corticobasal degeneration. *Neurology* 80, 496–503. <https://doi.org/10.1212/WNL.0b013e31827f0fd1>
- Arrant, A.E., Onyilo, V.C., Unger, D.E., Roberson, E.D., 2018. Progranulin Gene Therapy Improves Lysosomal Dysfunction and Microglial Pathology Associated with Frontotemporal Dementia and Neuronal Ceroid Lipofuscinosis. *J. Neurosci.* 38, 2341–2358. <https://doi.org/10.1523/JNEUROSCI.3081-17.2018>
- Ashton, N.J., Höglund, K., Leuzy, A., Heurling, K., Hugon, J., Dumurgier, J., Cognat, E., Paquet, C., Hansson, O., Schöll, M., Zetterberg, H., Blennow, K., 2019. O2-05-01: CEREBROSPINAL FLUID SYNAPTIC VESICLE GLYCOPROTEIN 2A IN ALZHEIMER'S DISEASE. *Alzheimer's & Dementia* 15, P545–P545. <https://doi.org/10.1016/j.jalz.2019.06.4475>
- Ashton, N.J., Janelidze, S., Al Khleifat, A., Leuzy, A., van der Ende, E.L., Karikari, T.K., Benedet, A.L., Pascoal, T.A., Lleó, A., Parnetti, L., Galimberti, D., Bonanni, L., Pilotto, A., Padovani, A., Lycke, J., Novakova, L., Axelsson, M., Velayudhan, L., Rabinovici, G.D., Miller, B., Pariante, C., Nikkheslat, N., Resnick, S.M., Thambisetty, M., Schöll, M., Fernández-Eulate, G., Gil-Bea, F.J., López de Munain, A., Al-Chalabi, A., Rosa-Neto, P., Strydom, A., Svenningsson, P., Stomrud, E., Santillo, A., Aarsland, D., van Swieten, J.C., Palmqvist, S., Zetterberg, H., Blennow, K., Hye, A., Hansson, O., 2021. A multicentre validation study of the diagnostic value of plasma neurofilament light. *Nat Commun* 12, 3400. <https://doi.org/10.1038/s41467-021-23620-z>
- Azevedo, T., Bethlehem, R.A.I., Whiteside, D.J., Swaddiwudhipong, N., Rowe, J.B., Lió, P., Rittman, T., 2022. Identifying healthy individuals with Alzheimer neuroimaging phenotypes in the UK Biobank (preprint). *Neurology*. <https://doi.org/10.1101/2022.01.05.22268795>
- Bak, T.H., Caine, D., Hearn, V.C., Hodges, J.R., 2006. Visuospatial functions in atypical parkinsonian syndromes. *J Neurol Neurosurg Psychiatry* 77, 454–456. <https://doi.org/10.1136/jnnp.2005.068239>

- Bak, T.H., Crawford, L.M., Berrios, G., Hodges, J.R., 2010. Behavioural symptoms in progressive supranuclear palsy and frontotemporal dementia. *Journal of Neurology, Neurosurgery & Psychiatry* 81, 1057–1059. <https://doi.org/10.1136/jnnp.2008.157974>
- Ballarini, T., Albrecht, F., Mueller, K., Jech, R., Diehl-Schmid, J., Fließbach, K., Kassubek, J., Lauer, M., Fassbender, K., Schneider, A., Synofzik, M., Wiltfang, J., Otto, M., Schroeter, M.L., 2020. Disentangling brain functional network remodeling in corticobasal syndrome – A multimodal MRI study. *NeuroImage: Clinical* 25, 102112. <https://doi.org/10.1016/j.nicl.2019.102112>
- Bandettini, P.A., 2012. Twenty years of functional MRI: The science and the stories. *NeuroImage* 62, 575–588. <https://doi.org/10.1016/j.neuroimage.2012.04.026>
- Bang, J., Lobach, I.V., Lang, A.E., Grossman, M., Knopman, D.S., Miller, B.L., Schneider, L.S., Doody, R.S., Lees, A., Gold, M., Morimoto, B.H., Boxer, A.L., Investigators, A.L., 2016. Predicting disease progression in progressive supranuclear palsy in multicenter clinical trials. *Parkinsonism & related disorders*. <https://doi.org/10.1016/j.parkreldis.2016.04.014>
- Bassett, D.S., Bullmore, E.T., 2016. Small-World Brain Networks Revisited. *The Neuroscientist*. <https://doi.org/10.1177/1073858416667720>
- Bastien, P., 2008. Deviance residuals based PLS regression for censored data in high dimensional setting. *Chemometrics and Intelligent Laboratory Systems* 91, 78–86. <https://doi.org/10.1016/j.chemolab.2007.09.009>
- Bastien, P., Bertrand, F., Meyer, N., Maumy-Bertrand, M., 2015. Deviance residuals-based sparse PLS and sparse kernel PLS regression for censored data. *Bioinformatics* 31, 397–404. <https://doi.org/10.1093/bioinformatics/btu660>
- Bastien, P., Vinzi, V.E., Tenenhaus, M., 2005. PLS generalised linear regression. *Computational Statistics & Data Analysis* 48, 17–46. <https://doi.org/10.1016/j.csda.2004.02.005>
- Bateman, R.J., Xiong, C., Benzinger, T.L.S., Fagan, A.M., Goate, A., Fox, N.C., Marcus, D.S., Cairns, N.J., Xie, X., Blazey, T.M., Holtzman, D.M., Santacruz, A., Buckles, V., Oliver, A., Moulder, K., Aisen, P.S., Ghetti, B., Klunk, W.E., McDade, E., Martins, R.N., Masters, C.L., Mayeux, R., Ringman, J.M., Rossor, M.N., Schofield, P.R., Sperling, R.A., Salloway, S., Morris, J.C., 2012. Clinical and Biomarker Changes in Dominantly Inherited Alzheimer’s Disease. *N Engl J Med* 367, 795–804. <https://doi.org/10.1056/NEJMoa1202753>
- Bates, D., Mächler, M., Bolker, B., Walker, S., 2015. Fitting Linear Mixed-Effects Models Using **lme4**. *J. Stat. Soft.* 67. <https://doi.org/10.18637/jss.v067.i01>
- Beach, T.G., 2017. A Review of Biomarkers for Neurodegenerative Disease: Will They Swing Us Across the Valley? *Neurol Ther* 6, 5–13. <https://doi.org/10.1007/s40120-017-0072-x>
- Beach, T.G., Monsell, S.E., Phillips, L.E., Kukull, W., 2012. Accuracy of the Clinical Diagnosis of Alzheimer Disease at National Institute on Aging Alzheimer Disease Centers, 2005–2010. *J Neuropathol Exp Neurol* 71, 266–273. <https://doi.org/10.1097/NEN.0b013e31824b211b>
- Beaty, R.E., Kenett, Y.N., Christensen, A.P., Rosenberg, M.D., Benedek, M., Chen, Q., Fink, A., Qiu, J., Kwapił, T.R., Kane, M.J., Silvia, P.J., 2018. Robust prediction of individual creative ability from brain functional connectivity. *Proceedings of the National Academy of Sciences*.
- Beckmann, C.F., DeLuca, M., Devlin, J.T., Smith, S.M., 2005. Investigations into resting-state connectivity using independent component analysis. *Philos Trans R Soc Lond B Biol Sci* 360, 1001–1013. <https://doi.org/10.1098/rstb.2005.1634>

- Beckmann, C.F., Smith, S.M., 2004. Probabilistic Independent Component Analysis for Functional Magnetic Resonance Imaging. *IEEE Trans. Med. Imaging* 23, 137–152. <https://doi.org/10.1109/TMI.2003.822821>
- Beissner, F., Schumann, A., Brunn, F., Eisenträger, D., Bär, K.-J., 2014. Advances in functional magnetic resonance imaging of the human brainstem. *NeuroImage* 86, 91–98. <https://doi.org/10.1016/j.neuroimage.2013.07.081>
- Beliveau, V., Ganz, M., Feng, L., Ozenne, B., Højgaard, L., Fisher, P.M., Svarer, C., Greve, D.N., Knudsen, G.M., 2017. A High-Resolution *In Vivo* Atlas of the Human Brain’s Serotonin System. *J. Neurosci.* 37, 120–128. <https://doi.org/10.1523/JNEUROSCI.2830-16.2016>
- Belliveau, J.W., Kennedy, D.N., McKinstry, R.C., Buchbinder, B.R., Weisskoff, R.M., Cohen, M.S., Vevea, J.M., Brady, T.J., Rosen, B.R., 1991. Functional Mapping of the Human Visual Cortex by Magnetic Resonance Imaging. *Science* 254, 716–719. <https://doi.org/10.1126/science.1948051>
- Benjamini, Y., Hochberg, Y., 1995. Controlling the False Discovery Rate: A Practical and Powerful Approach to Multiple Testing. *Journal of the Royal Statistical Society: Series B (Methodological)* 57, 289–300. <https://doi.org/10.1111/j.2517-6161.1995.tb02031.x>
- Berkes, P., Orbán, G., Lengyel, M., Fiser, J., 2011. Spontaneous Cortical Activity Reveals Hallmarks of an Optimal Internal Model of the Environment. *Science* 331, 83–87. <https://doi.org/10.1126/science.1195870>
- Berrios, G.E., Girling, D.M., 1994. Introduction: Pick’s disease and the “frontal lobe” dementias. *Hist Psychiatry* 5, 539–541. <https://doi.org/10.1177/0957154X9400502006>
- Bertoux, M., O’Callaghan, C., Flanagan, E., Hodges, J.R., Hornberger, M., 2015. Fronto-Striatal Atrophy in Behavioral Variant Frontotemporal Dementia and Alzheimer’s Disease. *Front. Neurol.* 6. <https://doi.org/10.3389/fneur.2015.00147>
- Bertrand, F., Maumy-Bertrand, M., 2021. Fitting and Cross-Validating Cox Models to Censored Big Data With Missing Values Using Extensions of Partial Least Squares Regression Models. *Frontiers in Big Data* 4, 91. <https://doi.org/10.3389/fdata.2021.684794>
- Bharti, K., Bologna, M., Upadhyay, N., Piattella, M.C., Suppa, A., Petsas, N., Giannì, C., Tona, F., Berardelli, A., Pantano, P., 2017. Abnormal Resting-State Functional Connectivity in Progressive Supranuclear Palsy and Corticobasal Syndrome. *Front Neurol* 8. <https://doi.org/10.3389/fneur.2017.00248>
- Bigio, E.H., Vono, M.B., Satumtira, S., Adamson, J., Sontag, E., Hynan, L.S., White, C.L., Baker, M., Hutton, M., 2001. Cortical Synapse Loss in progressive Supranuclear palsy. *J Neuropathol Exp Neurol* 60, 403–410. <https://doi.org/10.1093/jnen/60.5.403>
- Bijsterbosch, J., 2017. Introduction to resting state fMRI functional connectivity, First edition. ed, Oxford neuroimaging primers. Oxford University Press, Oxford, United Kingdom ; New York, NY.
- Bijsterbosch, J.D., Valk, S.L., Wang, D., Glasser, M.F., 2021. Recent developments in representations of the connectome. *NeuroImage* 243, 118533. <https://doi.org/10.1016/j.neuroimage.2021.118533>
- Biswal, B., Zerrin Yetkin, F., Haughton, V.M., Hyde, J.S., 1995. Functional connectivity in the motor cortex of resting human brain using echo-planar mri. *Magn. Reson. Med.* 34, 537–541. <https://doi.org/10.1002/mrm.1910340409>
- Bluett, B., Pantelyat, A.Y., Litvan, I., Ali, F., Apetauerova, D., Bega, D., Bloom, L., Bower, J., Boxer, A.L., Dale, M.L., Dhall, R., Duquette, A., Fernandez, H.H., Fleisher, J.E.,

- Grossman, M., Howell, M., Kerwin, D.R., Leegwater-Kim, J., Lepage, C., Ljubenkov, P.A., Mancini, M., McFarland, N.R., Moretti, P., Myrick, E., Patel, P., Plummer, L.S., Rodriguez-Porcel, F., Rojas, J., Sidiropoulos, C., Sklerov, M., Sokol, L.L., Tuite, P.J., VandeVrede, L., Wilhelm, J., Wills, A.-M.A., Xie, T., Golbe, L.I., 2021. Best Practices in the Clinical Management of Progressive Supranuclear Palsy and Corticobasal Syndrome: A Consensus Statement of the CurePSP Centers of Care. *Front. Neurol.* 12, 694872. <https://doi.org/10.3389/fneur.2021.694872>
- Bocchetta, M., Gordon, E., Cardoso, M.J., Modat, M., Ourselin, S., Warren, J.D., Rohrer, J.D., 2018. Thalamic atrophy in frontotemporal dementia — Not just a C9orf72 problem. *NeuroImage: Clinical* 18, 675–681. <https://doi.org/10.1016/j.nicl.2018.02.019>
- Boeve, B.F., 2022. Behavioral Variant Frontotemporal Dementia. *CONTINUUM: Lifelong Learning in Neurology* 28, 702–725. <https://doi.org/10.1212/CON.0000000000001105>
- Boeve, B.F., Dickson, D., Duffy, J., Bartleson, J., Trenerry, M., Petersen, R., 2003a. Progressive Nonfluent Aphasia and Subsequent Aphasic Dementia Associated with Atypical Progressive Supranuclear Palsy Pathology. *Eur Neurol* 49, 72–78. <https://doi.org/10.1159/000068502>
- Boeve, B.F., Lang, A.E., Litvan, I., 2003b. Corticobasal degeneration and its relationship to progressive supranuclear palsy and frontotemporal dementia. *Ann Neurol* 54, S15–S19. <https://doi.org/10.1002/ana.10570>
- Boeve, B.F., Maraganore, D.M., Parisi, J.E., Ahlskog, J.E., Graff-Radford, N., Caselli, R.J., Dickson, D.W., Kokmen, E., Petersen, R.C., 1999. Pathologic heterogeneity in clinically diagnosed corticobasal degeneration. *Neurology* 53, 795–795. <https://doi.org/10.1212/WNL.53.4.795>
- Bonnelle, V., Ham, T.E., Leech, R., Kinnunen, K.M., Mehta, M.A., Greenwood, R.J., Sharp, D.J., 2012. Salience network integrity predicts default mode network function after traumatic brain injury. *Proceedings of the National Academy of Sciences* 109, 4690–4695. <https://doi.org/10.1073/pnas.1113455109>
- Borchert, R.J., Rittman, T., Rae, C.L., Passamonti, L., Jones, S.P., Vatansever, D., Vázquez Rodríguez, P., Ye, Z., Nombela, C., Hughes, L.E., Robbins, T.W., Rowe, J.B., 2019. Atomoxetine and citalopram alter brain network organization in Parkinson's disease. *Brain Communications*. <https://doi.org/10.1093/braincomms/fcz013>
- Botha, H., Josephs, K.A., 2019. Primary Progressive Aphasias and Apraxia of Speech: *CONTINUUM: Lifelong Learning in Neurology* 25, 101–127. <https://doi.org/10.1212/CON.0000000000000699>
- Botvinik-Nezer, R., Holzmeister, F., Camerer, C.F., Dreber, A., Huber, J., Johannesson, M., Kirchler, M., Iwanir, R., Mumford, J.A., Adcock, R.A., Avesani, P., Baczkowski, B.M., Bajracharya, A., Bakst, L., Ball, S., Barilari, M., Bault, N., Beaton, D., Beitner, J., Benoit, R.G., Berkers, R.M.W.J., Bhanji, J.P., Biswal, B.B., Bobadilla-Suarez, S., Bortolini, T., Bottenhorn, K.L., Bowering, A., Braem, S., Brooks, H.R., Brudner, E.G., Calderon, C.B., Camilleri, J.A., Castellon, J.J., Cecchetti, L., Cieslik, E.C., Cole, Z.J., Collignon, O., Cox, R.W., Cunningham, W.A., Czoschke, S., Dadi, K., Davis, C.P., Luca, A.D., Delgado, M.R., Demetriou, L., Dennison, J.B., Di, X., Dickie, E.W., Dobryakova, E., Donnat, C.L., Dukart, J., Duncan, N.W., Durnez, J., Eed, A., Eickhoff, S.B., Erhart, A., Fontanesi, L., Fricke, G.M., Fu, S., Galván, A., Gau, R., Genon, S., Glatard, T., Glerean, E., Goeman, J.J., Golowin, S.A.E., González-García, C., Gorgolewski, K.J., Grady, C.L., Green, M.A., Guassi Moreira, J.F., Guest, O., Hakimi, S., Hamilton, J.P., Hancock, R.,

- Handjaras, G., Harry, B.B., Hawco, C., Herholz, P., Herman, G., Heunis, S., Hoffstaedter, F., Hogeveen, J., Holmes, S., Hu, C.-P., Huettel, S.A., Hughes, M.E., Iacovella, V., Jordan, A.D., Isager, P.M., Isik, A.I., Jahn, A., Johnson, M.R., Johnstone, T., Joseph, M.J.E., Juliano, A.C., Kable, J.W., Kassinopoulos, M., Koba, C., Kong, X.-Z., Kosciak, T.R., Kucukboyaci, N.E., Kuhl, B.A., Kupek, S., Laird, A.R., Lamm, C., Langner, R., Lauharatanahirun, N., Lee, H., Lee, S., Leemans, A., Leo, A., Lesage, E., Li, F., Li, M.Y.C., Lim, P.C., Lintz, E.N., Liphardt, S.W., Losecaat Vermeer, A.B., Love, B.C., Mack, M.L., Malpica, N., Marins, T., Maumet, C., McDonald, K., McGuire, J.T., Melero, H., Méndez Leal, A.S., Meyer, B., Meyer, K.N., Mihai, G., Mitsis, G.D., Moll, J., Nielson, D.M., Nilsonne, G., Notter, M.P., Olivetti, E., Onicas, A.I., Papale, P., Patil, K.R., Peelle, J.E., Pérez, A., Pischedda, D., Poline, J.-B., Prystauka, Y., Ray, S., Reuter-Lorenz, P.A., Reynolds, R.C., Ricciardi, E., Rieck, J.R., Rodriguez-Thompson, A.M., Romy, A., Salo, T., Samanez-Larkin, G.R., Sanz-Morales, E., Schlichting, M.L., Schultz, D.H., Shen, Q., Sheridan, M.A., Silvers, J.A., Skagerlund, K., Smith, A., Smith, D.V., Sokol-Hessner, P., Steinkamp, S.R., Tashjian, S.M., Thirion, B., Thorp, J.N., Tinghög, G., Tisdall, L., Tompson, S.H., Toro-Serey, C., Torre Tresols, J.J., Tozzi, L., Truong, V., Turella, L., van 't Veer, A.E., Verguts, T., Vettel, J.M., Vijayarajah, S., Vo, K., Wall, M.B., Weeda, W.D., Weis, S., White, D.J., Wisniewski, D., Xifra-Porxas, A., Yearling, E.A., Yoon, S., Yuan, R., Yuen, K.S.L., Zhang, L., Zhang, X., Zosky, J.E., Nichols, T.E., Poldrack, R.A., Schonberg, T., 2020. Variability in the analysis of a single neuroimaging dataset by many teams. *Nature* 582, 84–88. <https://doi.org/10.1038/s41586-020-2314-9>
- Boxer, A.L., Geschwind, M.D., Belfor, N., Gorno-Tempini, M.L., Schauer, G.F., Miller, B.L., Weiner, M.W., Rosen, H.J., 2006. Patterns of Brain Atrophy That Differentiate Corticobasal Degeneration Syndrome From Progressive Supranuclear Palsy. *Arch Neurol* 63, 81. <https://doi.org/10.1001/archneur.63.1.81>
- Boxer, A.L., Gold, M., Feldman, H., Boeve, B.F., Dickinson, S.L.-J., Fillit, H., Ho, C., Paul, R., Pearlman, R., Sutherland, M., Verma, A., Arneric, S.P., Alexander, B.M., Dickerson, B.C., Dorsey, E.R., Grossman, M., Huey, E.D., Irizarry, M.C., Marks, W.J., Masellis, M., McFarland, F., Niehoff, D., Onyike, C.U., Paganoni, S., Panzara, M.A., Rockwood, K., Rohrer, J.D., Rosen, H., Schuck, R.N., Soares, H.D., Tatton, N., 2020. New directions in clinical trials for frontotemporal lobar degeneration: Methods and outcome measures. *Alzheimer's Dement.* 16, 131–143. <https://doi.org/10.1016/j.jalz.2019.06.4956>
- Boyd Taylor, H.G., Puckett, A.M., Isherwood, Z.J., Schira, M.M., 2019. Vascular effects on the BOLD response and the retinotopic mapping of hV4. *PLoS ONE* 14, e0204388. <https://doi.org/10.1371/journal.pone.0204388>
- Braak, H., Thal, D.R., Ghebremedhin, E., Del Tredici, K., 2011. Stages of the Pathologic Process in Alzheimer Disease: Age Categories From 1 to 100 Years. *J Neuropathol Exp Neurol* 70, 960–969. <https://doi.org/10.1097/NEN.0b013e318232a379>
- Bradburn, M.J., Clark, T.G., Love, S.B., Altman, D.G., 2003. Survival Analysis Part II: Multivariate data analysis – an introduction to concepts and methods. *Br J Cancer* 89, 431–436. <https://doi.org/10.1038/sj.bjc.6601119>
- Bradford, A., Kunik, M.E., Schulz, P., Williams, S.P., Singh, H., 2009. Missed and Delayed Diagnosis of Dementia in Primary Care: Prevalence and Contributing Factors. *Alzheimer Disease & Associated Disorders* 23, 306–314. <https://doi.org/10.1097/WAD.0b013e3181a6bebc>
- Breakspear, M., 2017. Dynamic models of large-scale brain activity. *Nat Neurosci* 20, 340–352. <https://doi.org/10.1038/nn.4497>

- Breevoort, S., Gibson, S., Figueroa, K., Bromberg, M., Pulst, S., 2022. Expanding Clinical Spectrum of *C9ORF72* -Related Disorders and Promising Therapeutic Strategies: A Review. *Neurol Genet* 8, e670. <https://doi.org/10.1212/NXG.0000000000000670>
- Brown, F.S., Rowe, J.B., Passamonti, L., Rittman, T., 2020. Falls in Progressive Supranuclear Palsy. *Mov Disord Clin Pract* 7, 16–24. <https://doi.org/10.1002/mdc3.12879>
- Brown, J.A., Hua, A.Y., Trujillo, A., Attygalle, S., Binney, R.J., Spina, S., Lee, S.E., Kramer, J.H., Miller, B.L., Rosen, H.J., Boxer, A.L., Seeley, W.W., 2017. Advancing functional dysconnectivity and atrophy in progressive supranuclear palsy. *NeuroImage: Clinical*. <https://doi.org/10.1016/j.nicl.2017.09.008>
- Bruun, M., Koikkalainen, J., Rhodius-Meester, H.F.M., Baroni, M., Gjerum, L., van Gils, M., Soinen, H., Remes, A.M., Hartikainen, P., Waldemar, G., Mecocci, P., Barkhof, F., Pijnenburg, Y., van der Flier, W.M., Hasselbalch, S.G., Lötjönen, J., Frederiksen, K.S., 2019. Detecting frontotemporal dementia syndromes using MRI biomarkers. *NeuroImage: Clinical* 22, 101711. <https://doi.org/10.1016/j.nicl.2019.101711>
- Bullmore, E., Sporns, O., 2009. Complex brain networks: graph theoretical analysis of structural and functional systems. *Nature Reviews Neuroscience* 10, 186–198. <https://doi.org/10.1038/nrn2575>
- Burgos, N., Cardoso, M.J., Thielemans, K., Modat, M., Pedemonte, S., Dickson, J., Barnes, A., Ahmed, R., Mahoney, C.J., Schott, J.M., Duncan, J.S., Atkinson, D., Arridge, S.R., Hutton, B.F., Ourselin, S., 2014. Attenuation Correction Synthesis for Hybrid PET-MR Scanners: Application to Brain Studies. *IEEE Trans. Med. Imaging* 33, 2332–2341. <https://doi.org/10.1109/TMI.2014.2340135>
- Burrell, J.R., Hodges, J.R., Rowe, J.B., 2014. Cognition in corticobasal syndrome and progressive supranuclear palsy: a review. *Mov Disord*. <https://doi.org/10.1002/mds.25872>
- Burt, J.B., Helmer, M., Shinn, M., Anticevic, A., Murray, J.D., 2020. Generative modeling of brain maps with spatial autocorrelation. *NeuroImage* 220, 117038. <https://doi.org/10.1016/j.neuroimage.2020.117038>
- Buseh, A.G., Stevens, P.E., Millon-Underwood, S., Townsend, L., Kelber, S.T., 2013. Community leaders' perspectives on engaging African Americans in biobanks and other human genetics initiatives. *J Community Genet* 4, 483–494. <https://doi.org/10.1007/s12687-013-0155-z>
- Caballero-Gaudes, C., Reynolds, R.C., 2017. Methods for cleaning the BOLD fMRI signal. *NeuroImage* 154, 128–149. <https://doi.org/10.1016/j.neuroimage.2016.12.018>
- Cairns, N.J., Bigio, E.H., Mackenzie, I.R.A., Neumann, M., Lee, V.M.-Y., Hatanpaa, K.J., White, C.L., Schneider, J.A., Grinberg, L.T., Halliday, G., Duyckaerts, C., Lowe, J.S., Holm, I.E., Tolnay, M., Okamoto, K., Yokoo, H., Murayama, S., Woulfe, J., Munoz, D.G., Dickson, D.W., Ince, P.G., Trojanowski, J.Q., Mann, D.M.A., 2007. Neuropathologic diagnostic and nosologic criteria for frontotemporal lobar degeneration: consensus of the Consortium for Frontotemporal Lobar Degeneration. *Acta Neuropathol* 114, 5–22. <https://doi.org/10.1007/s00401-007-0237-2>
- Calhoun, V.D., Miller, R., Pearlson, G., Adali, T., 2014. The chronnectome: time-varying connectivity networks as the next frontier in fMRI data discovery. *Neuron* 84, 262–274. <https://doi.org/10.1016/j.neuron.2014.10.015>
- Calhoun, V.D., Sui, J., 2016. Multimodal Fusion of Brain Imaging Data: A Key to Finding the Missing Link(s) in Complex Mental Illness. *Biological Psychiatry: Cognitive*

- Neuroscience and Neuroimaging 1, 230–244.
<https://doi.org/10.1016/j.bpsc.2015.12.005>
- Capozzo, R., Sassi, C., Hammer, M.B., Arcuti, S., Zecca, C., Barulli, M.R., Tortelli, R., Gibbs, J.R., Crews, C., Seripa, D., Carnicella, F., Dell’Aquila, C., Rossi, M., Tamma, F., Valluzzi, F., Brancasi, B., Panza, F., Singleton, A.B., Logroscino, G., 2017. Clinical and genetic analyses of familial and sporadic frontotemporal dementia patients in Southern Italy. *Alzheimer’s & Dementia* 13, 858–869.
<https://doi.org/10.1016/j.jalz.2017.01.011>
- Carp, J., 2012. On the Plurality of (Methodological) Worlds: Estimating the Analytic Flexibility of fMRI Experiments. *Front. Neurosci.* 6.
<https://doi.org/10.3389/fnins.2012.00149>
- Chan, D., Anderson, V., Pijnenburg, Y., Whitwell, J., Barnes, J., Scahill, R., Stevens, J.M., Barkhof, F., Scheltens, P., Rossor, M.N., Fox, N.C., 2009. The clinical profile of right temporal lobe atrophy. *Brain* 132, 1287–1298.
<https://doi.org/10.1093/brain/awp037>
- Chan, M.Y., Park, D.C., Savalia, N.K., Petersen, S.E., Wig, G.S., 2014. Decreased segregation of brain systems across the healthy adult lifespan. *Proc Natl Acad Sci USA* 111, E4997–E5006. <https://doi.org/10.1073/pnas.1415122111>
- Chang, C., Glover, G.H., 2010. Time–frequency dynamics of resting-state brain connectivity measured with fMRI. *NeuroImage* 50, 81–98.
<https://doi.org/10.1016/j.neuroimage.2009.12.011>
- Chen, A.L., Riley, D.E., King, S.A., Joshi, A.C., Serra, A., Liao, K., Cohen, M.L., Otero-Millan, J., Martinez-Conde, S., Strupp, M., Leigh, R.J., 2010. The Disturbance of Gaze in Progressive Supranuclear Palsy: Implications for Pathogenesis. *Front. Neur.* 1. <https://doi.org/10.3389/fneur.2010.00147>
- Chen, J.A., Wang, Q., Davis-Turak, J., Li, Y., Karydas, A.M., Hsu, S.C., Sears, R.L., Chatzopoulou, D., Huang, A.Y., Wojta, K.J., Klein, E., Lee, J., Beekly, D.L., Boxer, A., Faber, K.M., Haase, C.M., Miller, J., Poon, W.W., Rosen, A., Rosen, H., Sapozhnikova, A., Shapira, J., Varpetian, A., Foroud, T.M., Levenson, R.W., Levey, A.I., Kukull, W.A., Mendez, M.F., Ringman, J., Chui, H., Cotman, C., DeCarli, C., Miller, B.L., Geschwind, D.H., Coppola, G., 2015. A Multiancestral Genome-Wide Exome Array Study of Alzheimer Disease, Frontotemporal Dementia, and Progressive Supranuclear Palsy. *JAMA Neurol* 72, 414.
<https://doi.org/10.1001/jamaneurol.2014.4040>
- Chiu, W.Z., Kaat, L.D., Seelaar, H., Rosso, S.M., Boon, A.J., Kamphorst, W., van Swieten, J.C., 2010. Survival in progressive supranuclear palsy and frontotemporal dementia. *Journal of Neurology, Neurosurgery & Psychiatry* 81, 441–445.
<https://doi.org/10.1136/jnnp.2009.195719>
- Chow, T.W., Binns, M.A., Cummings, J.L., Lam, I., Black, S.E., Miller, B.L., Freedman, M., Stuss, D.T., van Reekum, R., 2009. Apathy Symptom Profile and Behavioral Associations in Frontotemporal Dementia vs Dementia of Alzheimer Type. *Arch Neurol* 66. <https://doi.org/10.1001/archneurol.2009.92>
- Cividini, C., Basaia, S., Spinelli, E.G., Canu, E., Castelnovo, V., Riva, N., Cecchetti, G., Caso, F., Magnani, G., Falini, A., Filippi, M., Agosta, F., 2022. Amyotrophic Lateral Sclerosis–Frontotemporal Dementia: Shared and Divergent Neural Correlates Across the Clinical Spectrum. *Neurology* 98, e402–e415.
<https://doi.org/10.1212/WNL.00000000000013123>
- Clark, H.M., Stierwalt, J.A.G., Tosakulwong, N., Botha, H., Ali, F., Whitwell, J.L., Josephs, K.A., 2020. Dysphagia in Progressive Supranuclear Palsy. *Dysphagia* 35, 667–676. <https://doi.org/10.1007/s00455-019-10073-2>

- Clark, T.G., Bradburn, M.J., Love, S.B., Altman, D.G., 2003. Survival Analysis Part I: Basic concepts and first analyses. *Br J Cancer* 89, 232–238. <https://doi.org/10.1038/sj.bjc.6601118>
- Clavaguera, F., Bolmont, T., Crowther, R.A., Abramowski, D., Frank, S., Probst, A., Fraser, G., Stalder, A.K., Beibel, M., Staufenbiel, M., Jucker, M., Goedert, M., Tolnay, M., 2009. Transmission and spreading of tauopathy in transgenic mouse brain. *Nat Cell Biol.* <https://doi.org/10.1038/ncb1901>
- Cole, M.W., Bassett, D.S., Power, J.D., Braver, T.S., Petersen, S.E., 2014. Intrinsic and Task-Evoked Network Architectures of the Human Brain. *Neuron.* <https://doi.org/10.1016/j.neuron.2014.05.014>
- Cole, M.W., Ito, T., Bassett, D.S., Schultz, D.H., 2016. Activity flow over resting-state networks shapes cognitive task activations. *Nat Neurosci* 19, 1718–1726. <https://doi.org/10.1038/nn.4406>
- Constantinides, V.C., Paraskevas, G.P., Paraskevas, P.G., Stefanis, L., Kapaki, E., 2019. Corticobasal degeneration and corticobasal syndrome: A review. *Clinical Parkinsonism & Related Disorders* 1, 66–71. <https://doi.org/10.1016/j.prdoa.2019.08.005>
- Cook, L., Souris, H., Isaacs, J., 2020. The 2019 national memory service audit. NHS London Clinical Networks.
- Cooper-Knock, J., Shaw, P.J., Kirby, J., 2014. The widening spectrum of C9ORF72-related disease; genotype/phenotype correlations and potential modifiers of clinical phenotype. *Acta Neuropathol* 127, 333–345. <https://doi.org/10.1007/s00401-014-1251-9>
- Cope, T.E., Rittman, T., Borchert, R.J., Jones, P.S., Vatansever, D., Allinson, K., Passamonti, L., Vazquez Rodriguez, P., Bevan-Jones, W.R., O'Brien, J.T., Rowe, J.B., 2018. Tau burden and the functional connectome in Alzheimer's disease and progressive supranuclear palsy. *Brain* 141, 550–567. <https://doi.org/10.1093/brain/awx347>
- Cope, T.E., Weil, R.S., Düzel, E., Dickerson, B.C., Rowe, J.B., 2021. Advances in neuroimaging to support translational medicine in dementia. *J Neurol Neurosurg Psychiatry* 92, 263–270. <https://doi.org/10.1136/jnnp-2019-322402>
- Cordato, N.J., Halliday, G.M., McCann, H., Davies, L., Williamson, P., Fulham, M., Morris, J.G.L., 2001. Corticobasal syndrome with tau pathology. *Mov Disord.* 16, 656–667. <https://doi.org/10.1002/mds.1124>
- Cosottini, M., Ceravolo, R., Faggioni, L., Lazzarotti, G., Michelassi, M.C., Bonuccelli, U., Murri, L., Bartolozzi, C., 2007. Assessment of midbrain atrophy in patients with progressive supranuclear palsy with routine magnetic resonance imaging. *Acta Neurol Scand* 116, 37–42. <https://doi.org/10.1111/j.1600-0404.2006.00767.x>
- Costa, M., Goldberger, A.L., Peng, C.K., 2005. Multiscale entropy analysis of biological signals. *Phys Rev E Stat Nonlin Soft Matter Phys.* <https://doi.org/10.1103/PhysRevE.71.021906>
- Cousins, K.A.Q., Shaw, L.M., Chen-Plotkin, A., Wolk, D.A., Van Deerlin, V.M., Lee, E.B., McMillan, C.T., Grossman, M., Irwin, D.J., 2022. Distinguishing Frontotemporal Lobar Degeneration Tau From TDP-43 Using Plasma Biomarkers. *JAMA Neurol* 79, 1155. <https://doi.org/10.1001/jamaneurol.2022.3265>
- Cox, D.R., 1972. Regression Models and Life-Tables. *Journal of the Royal Statistical Society: Series B (Methodological)* 34, 187–202. <https://doi.org/10.1111/j.2517-6161.1972.tb00899.x>
- Coyle-Gilchrist, I.T.S., Dick, K.M., Patterson, K., Vázquez Rodríguez, P., Wehmann, E., Wilcox, A., Lansdall, C.J., Dawson, K.E., Wiggins, J., Mead, S., Brayne, C., Rowe,

- J.B., 2016. Prevalence, characteristics, and survival of frontotemporal lobar degeneration syndromes. *Neurology* 86, 1736–1743. <https://doi.org/10.1212/WNL.0000000000002638>
- Crossley, N.A., Mechelli, A., Scott, J., Carletti, F., Fox, P.T., McGuire, P., Bullmore, E.T., 2014. The hubs of the human connectome are generally implicated in the anatomy of brain disorders. *Brain*. <https://doi.org/10.1093/brain/awu132>
- Cui, S.-S., Ling, H.-W., Du, J.-J., Lin, Y.-Q., Pan, J., Zhou, H.-Y., Wang, G., Wang, Y., Xiao, Q., Liu, J., Tan, Y.-Y., Chen, S.-D., 2020. Midbrain/pons area ratio and clinical features predict the prognosis of progressive Supranuclear palsy. *BMC Neurol* 20, 114. <https://doi.org/10.1186/s12883-020-01692-6>
- Cummings, J., 2019. The Role of Biomarkers in Alzheimer’s Disease Drug Development, in: Guest, P.C. (Ed.), *Reviews on Biomarker Studies in Psychiatric and Neurodegenerative Disorders, Advances in Experimental Medicine and Biology*. Springer International Publishing, Cham, pp. 29–61. https://doi.org/10.1007/978-3-030-05542-4_2
- Cummings, J., Lee, G., Zhong, K., Fonseca, J., Taghva, K., 2021. Alzheimer’s disease drug development pipeline: 2021. *A&D Transl Res & Clin Interv* 7. <https://doi.org/10.1002/trc2.12179>
- Dale, A.M., Fischl, B., Sereno, M.I., 1999. Cortical surface-based analysis. I. Segmentation and surface reconstruction. *Neuroimage*. <https://doi.org/10.1006/nimg.1998.0395>
- Dam, T., Boxer, A.L., Golbe, L.I., Höglinger, G.U., Morris, H.R., Litvan, I., Lang, A.E., Corvol, J.-C., Aiba, I., Grundman, M., Yang, L., Tidemann-Miller, B., Kupferman, J., Harper, K., Kamisoglu, K., Wald, M.J., Graham, D.L., Gedney, L., O’Gorman, J., Haeberlein, S.B., PASSPORT Study Group, 2021. Safety and efficacy of anti-tau monoclonal antibody gosuranemab in progressive supranuclear palsy: a phase 2, randomized, placebo-controlled trial. *Nat Med* 27, 1451–1457. <https://doi.org/10.1038/s41591-021-01455-x>
- Damoiseaux, J.S., Rombouts, S.A.R.B., Barkhof, F., Scheltens, P., Stam, C.J., Smith, S.M., Beckmann, C.F., 2006. Consistent resting-state networks across healthy subjects. *Proceedings of the National Academy of Sciences* 103, 13848–13853. <https://doi.org/10.1073/pnas.0601417103>
- Darby, R.R., Joutsa, J., Fox, M.D., 2019. Network localization of heterogeneous neuroimaging findings. *Brain* 142, 70–79. <https://doi.org/10.1093/brain/awy292>
- Darricau, M., Katsinelos, T., Raschella, F., Milekovic, T., Crochemore, L., Li, Q., Courtine, G., McEwan, W.A., Dehay, B., Bezard, E., Planche, V., 2022. Tau seeds from patients induce progressive supranuclear palsy pathology and symptoms in primates. *Brain* awac428. <https://doi.org/10.1093/brain/awac428>
- Day, G.S., Lim, T.S., Hassenstab, J., Goate, A.M., Grant, E.A., Roe, C.M., Cairns, N.J., Morris, J.C., 2017. Differentiating cognitive impairment due to corticobasal degeneration and Alzheimer disease. *Neurology* 88, 1273–1281. <https://doi.org/10.1212/WNL.0000000000003770>
- de Boer, E.M.J., Orié, V.K., Williams, T., Baker, M.R., De Oliveira, H.M., Polvikoski, T., Silsby, M., Menon, P., van den Bos, M., Halliday, G.M., van den Berg, L.H., Van Den Bosch, L., van Damme, P., Kiernan, M.C., van Es, M.A., Vucic, S., 2021. TDP-43 proteinopathies: a new wave of neurodegenerative diseases. *J Neurol Neurosurg Psychiatry* 92, 86–95. <https://doi.org/10.1136/jnnp-2020-322983>
- de Haan, W., Mott, K., van Straaten, E.C.W., Scheltens, P., Stam, C.J., 2012. Activity Dependent Degeneration Explains Hub Vulnerability in Alzheimer’s Disease. *PLoS Comput Biol* 8, e1002582. <https://doi.org/10.1371/journal.pcbi.1002582>

- Deco, G., Kringelbach, M.L., Jirsa, V.K., Ritter, P., 2017. The dynamics of resting fluctuations in the brain: metastability and its dynamical cortical core. *Scientific Reports*. <https://doi.org/10.1038/s41598-017-03073-5>
- DeJesus-Hernandez, M., Mackenzie, I.R., Boeve, B.F., Boxer, A.L., Baker, M., Rutherford, N.J., Nicholson, A.M., Finch, N.A., Flynn, H., Adamson, J., Kouri, N., Wojtas, A., Sengdy, P., Hsiung, G.-Y.R., Karydas, A., Seeley, W.W., Josephs, K.A., Coppola, G., Geschwind, D.H., Szolek, Z.K., Feldman, H., Knopman, D.S., Petersen, R.C., Miller, B.L., Dickson, D.W., Boylan, K.B., Graff-Radford, N.R., Rademakers, R., 2011. Expanded GGGGCC Hexanucleotide Repeat in Noncoding Region of C9ORF72 Causes Chromosome 9p-Linked FTD and ALS. *Neuron* 72, 245–256. <https://doi.org/10.1016/j.neuron.2011.09.011>
- DeKosky, S.T., Scheff, S.W., 1990. Synapse loss in frontal cortex biopsies in Alzheimer's disease: Correlation with cognitive severity. *Ann Neurol*. 27, 457–464. <https://doi.org/10.1002/ana.410270502>
- Del Campo, M., Zetterberg, H., Gandy, S., Onyike, C.U., Oliveira, F., Udeh-Momoh, C., Lleó, A., Teunissen, C.E., Pijnenburg, Y., 2022. New developments of biofluid-based biomarkers for routine diagnosis and disease trajectories in frontotemporal dementia. *Alzheimer's & Dementia* 18, 2292–2307. <https://doi.org/10.1002/alz.12643>
- dell'Aquila, C., Zoccolella, S., Cardinali, V., de Mari, M., Iliceto, G., Tartaglione, B., Lamberti, P., Logroscino, G., 2013. Predictors of survival in a series of clinically diagnosed progressive supranuclear palsy patients. *Parkinsonism & Related Disorders* 19, 980–985. <https://doi.org/10.1016/j.parkreldis.2013.06.014>
- Department of Health, 2013. Dementia: a state of the nation report on dementia care and support in England. London.
- D'Esposito, M., 2019. Are individual differences in human brain organization measured with functional MRI meaningful? *Proc Natl Acad Sci USA* 116, 22432–22434. <https://doi.org/10.1073/pnas.1915982116>
- Devenney, E., Hodges, J.R., 2017. The Mini-Mental State Examination: pitfalls and limitations. *Pract Neurol* 17, 79–80. <https://doi.org/10.1136/practneurol-2016-001520>
- Di Stasio, F., Suppa, A., Marsili, L., Upadhyay, N., Ascì, F., Bologna, M., Colosimo, C., Fabbrini, G., Pantano, P., Berardelli, A., 2019. Corticobasal syndrome: neuroimaging and neurophysiological advances. *Eur J Neurol* 26, 701. <https://doi.org/10.1111/ene.13928>
- Dickerson, B.C., 2006. Functional MRI in the early detection of dementias. *Revue Neurologique* 162, 941–944. [https://doi.org/10.1016/S0035-3787\(06\)75103-7](https://doi.org/10.1016/S0035-3787(06)75103-7)
- Dickson, D.W., Kouri, N., Murray, M.E., Josephs, K.A., 2011. Neuropathology of Frontotemporal Lobar Degeneration-Tau (FTLD-Tau). *J Mol Neurosci* 45, 384–389. <https://doi.org/10.1007/s12031-011-9589-0>
- Ding, Y.-S., Singhal, T., Planeta-Wilson, B., Gallezot, J.-D., Nabulsi, N., Labaree, D., Ropchan, J., Henry, S., Williams, W., Carson, R.E., Neumeister, A., Malison, R.T., 2010. PET imaging of the effects of age and cocaine on the norepinephrine transporter in the human brain using (S,S)-[¹¹C]O-methylreboxetine and HRRT. *Synapse* 64, 30–38. <https://doi.org/10.1002/syn.20696>
- Dopper, E.G.P., Rombouts, S.A.R.B., Jiskoot, L.C., Heijer, T. d., Graaf, J.R.A. d., Koning, I. d., Hammerschlag, A.R., Seelaar, H., Seeley, W.W., Veer, I.M., van Buchem, M.A., Rizzu, P., van Swieten, J.C., 2013. Structural and functional brain connectivity in presymptomatic familial frontotemporal dementia. *Neurology* 80, 814–823. <https://doi.org/10.1212/WNL.0b013e31828407bc>

- Dubois, B., Slachevsky, A., Litvan, I., Pillon, B., 2000. The FAB: A frontal assessment battery at bedside. *Neurology* 55, 1621–1626. <https://doi.org/10.1212/WNL.55.11.1621>
- Ducharme, S., Bajestan, S., Dickerson, B.C., Voon, V., 2017. Psychiatric Presentations of *C9orf72* Mutation: What Are the Diagnostic Implications for Clinicians? *JNP* 29, 195–205. <https://doi.org/10.1176/appi.neuropsych.16090168>
- Duff, E., Zelaya, F., Almagro, F.A., Miller, K.L., Martin, N., Nichols, T.E., Taschler, B., Griffanti, L., Arthofer, C., Douaud, G., Wang, C., Okell, T.W., Bethlehem, R.A.I., Eickel, K., Günther, M., Menon, D.K., Williams, G., Facer, B., Lythgoe, D.J., Dell'Acqua, F., Wood, G.K., Williams, S.C.R., Houston, G., Keller, S.S., Holden, C., Hartmann, M., George, L., Breen, G., Michael, B.D., Jezzard, P., Smith, S.M., Bullmore, E.T., on behalf of the COVID-CNS Consortium, 2022. Reliability of multi-site UK Biobank MRI brain phenotypes for the assessment of neuropsychiatric complications of SARS-CoV-2 infection: The COVID-CNS travelling heads study. *PLoS ONE* 17, e0273704. <https://doi.org/10.1371/journal.pone.0273704>
- Dugger, B.N., Dickson, D.W., 2017. Pathology of Neurodegenerative Diseases. *Cold Spring Harb Perspect Biol* 9, a028035. <https://doi.org/10.1101/cshperspect.a028035>
- Dutt, S., Binney, R.J., Heuer, H.W., Luong, P., Attygalle, S., Bhatt, P., Marx, G.A., Eloffson, J., Tartaglia, M.C., Litvan, I., McGinnis, S.M., Dickerson, B.C., Kornak, J., Waltzman, D., Voltarelli, L., Schuff, N., Rabinovici, G.D., Kramer, J.H., Jack, C.R., Miller, B.L., Rosen, H.J., Boxer, A.L., 2016. Progression of brain atrophy in PSP and CBS over 6 months and 1 year. *Neurology* 87, 2016–2025. <https://doi.org/10.1212/WNL.0000000000003305>
- Eddy, S.R., 2004. What is a hidden Markov model? *Nat Biotechnol* 22, 1315–1316. <https://doi.org/10.1038/nbt1004-1315>
- Eimeren, T., Antonini, A., Berg, D., Bohnen, N., Ceravolo, R., Drzezga, A., Höglinger, G.U., Higuchi, M., Lehericy, S., Lewis, S., Monchi, O., Nestor, P., Ondrus, M., Pavese, N., Peralta, M.C., Piccini, P., Pineda-Pardo, J.Á., Rektorová, I., Rodríguez-Oroz, M., Rominger, A., Seppi, K., Stoessl, A.J., Tessitore, A., Thobois, S., Kaasinen, V., Wenning, G., Siebner, H.R., Strafella, A.P., Rowe, J.B., MDS Neuroimaging Study Group and the JPND Working Group ASAP-SynTau, 2019. Neuroimaging biomarkers for clinical trials in atypical parkinsonian disorders: Proposal for a Neuroimaging Biomarker Utility System. *Alzheimer's & Dementia: Diagnosis, Assessment & Disease Monitoring* 11, 301–309. <https://doi.org/10.1016/j.dadm.2019.01.011>
- Elamin, M., Bede, P., Byrne, S., Jordan, N., Gallagher, L., Wynne, B., O'Brien, C., Phukan, J., Lynch, C., Pender, N., Hardiman, O., 2013. Cognitive changes predict functional decline in ALS: A population-based longitudinal study. *Neurology* 80, 1590–1597. <https://doi.org/10.1212/WNL.0b013e31828f18ac>
- Eldar, E., Cohen, J.D., Niv, Y., 2013. The effects of neural gain on attention and learning. *Nature neuroscience*. <https://doi.org/10.1038/nn.3428>
- Elliott, L.T., Sharp, K., Alfaro-Almagro, F., Shi, S., Miller, K.L., Douaud, G., Marchini, J., Smith, S.M., 2018. Genome-wide association studies of brain imaging phenotypes in UK Biobank. *Nature* 562, 210–216. <https://doi.org/10.1038/s41586-018-0571-7>
- Elliott, M.L., Knodt, A.R., Ireland, D., Morris, M.L., Poulton, R., Ramrakha, S., Sison, M.L., Moffitt, T.E., Caspi, A., Hariri, A.R., 2020. What Is the Test-Retest Reliability of Common Task-Functional MRI Measures? *New Empirical Evidence*

- and a Meta-Analysis. *Psychol Sci* 31, 792–806. <https://doi.org/10.1177/0956797620916786>
- Erlandsson, K., Buvat, I., Pretorius, P.H., Thomas, B.A., Hutton, B.F., 2012. A review of partial volume correction techniques for emission tomography and their applications in neurology, cardiology and oncology. *Phys. Med. Biol.* 57, R119–R159. <https://doi.org/10.1088/0031-9155/57/21/R119>
- Esteban, O., Markiewicz, C.J., Blair, R.W., Moodie, C.A., Isik, A.I., Erramuzpe, A., Kent, J.D., Goncalves, M., DuPre, E., Snyder, M., Oya, H., Ghosh, S.S., Wright, J., Durnez, J., Poldrack, R.A., Gorgolewski, K.J., 2019. fMRIPrep: a robust preprocessing pipeline for functional MRI. *Nat Methods* 16, 111–116. <https://doi.org/10.1038/s41592-018-0235-4>
- Ewers, M., Luan, Y., Frontzkowski, L., Neitzel, J., Rubinski, A., Dichgans, M., Hassenstab, J., Gordon, B.A., Chhatwal, J.P., Levin, J., Schofield, P., Benzinger, T.L.S., Morris, J.C., Goate, A., Karch, C.M., Fagan, A.M., McDade, E., Allegri, R., Berman, S., Chui, H., Cruchaga, C., Farlow, M., Graff-Radford, N., Jucker, M., Lee, J.-H., Martins, R.N., Mori, H., Perrin, R., Xiong, C., Rossor, M., Fox, N.C., O'Connor, A., Salloway, S., Danek, A., Buerger, K., Bateman, R.J., Habeck, C., Stern, Y., Franzmeier, N., for the Alzheimer's Disease Neuroimaging Initiative and the Dominantly Inherited Alzheimer Network, 2021. Segregation of functional networks is associated with cognitive resilience in Alzheimer's disease. *Brain* 144, 2176–2185. <https://doi.org/10.1093/brain/awab112>
- Fan, L., Li, H., Zhuo, J., Zhang, Y., Wang, J., Chen, L., Yang, Z., Chu, C., Xie, S., Laird, A.R., Fox, P.T., Eickhoff, S.B., Yu, C., Jiang, T., 2016. The Human Brainnetome Atlas: A New Brain Atlas Based on Connectional Architecture. *Cerebral cortex* (New York, N.Y. : 1991). <https://doi.org/10.1093/cercor/bhw157>
- Fang, X.T., Toyonaga, T., Hillmer, A.T., Matuskey, D., Holmes, S.E., Radhakrishnan, R., Mecca, A.P., van Dyck, C.H., D'Souza, D.C., Esterlis, I., Worhunsky, P.D., Carson, R.E., 2021. Identifying brain networks in synaptic density PET (11C-UCB-J) with independent component analysis. *NeuroImage* 237, 118167. <https://doi.org/10.1016/j.neuroimage.2021.118167>
- FDA-NIH Biomarker Working Group, 2016. BEST (Biomarkers, EndpointS, and other Tools) Resource [Internet]. Silver Spring (MD): Food and Drug Administration (US); 2016-. Co-published by National Institutes of Health (US), Bethesda (MD).
- Ferrari, R., Manzoni, C., Hardy, J., 2019. Genetics and molecular mechanisms of frontotemporal lobar degeneration: an update and future avenues. *Neurobiology of Aging* 78, 98–110. <https://doi.org/10.1016/j.neurobiolaging.2019.02.006>
- Filippi, M., Spinelli, E.G., Cividini, C., Agosta, F., 2019. Resting State Dynamic Functional Connectivity in Neurodegenerative Conditions: A Review of Magnetic Resonance Imaging Findings. *Front Neurosci* 13, 657–657. <https://doi.org/10.3389/fnins.2019.00657>
- Filippini, N., MacIntosh, B.J., Hough, M.G., Goodwin, G.M., Frisoni, G.B., Smith, S.M., Matthews, P.M., Beckmann, C.F., Mackay, C.E., 2009. Distinct patterns of brain activity in young carriers of the *APOE* -ε4 allele. *Proc. Natl. Acad. Sci. U.S.A.* 106, 7209–7214. <https://doi.org/10.1073/pnas.0811879106>
- Finnema, S.J., Nabulsi, N.B., Eid, T., Detyniecki, K., Lin, S., Chen, M.-K., Dhaher, R., Matuskey, D., Baum, E., Holden, D., Spencer, D.D., Mercier, J., Hannestad, J., Huang, Y., Carson, R.E., 2016. Imaging synaptic density in the living human brain. *Sci. Transl. Med.* 8. <https://doi.org/10.1126/scitranslmed.aaf6667>
- Finnema, S.J., Scheinin, M., Shahid, M., Lehto, J., Borroni, E., Bang-Andersen, B., Sallinen, J., Wong, E., Farde, L., Halldin, C., Grimwood, S., 2015. Application of

- cross-species PET imaging to assess neurotransmitter release in brain. *Psychopharmacology* 232, 4129–4157. <https://doi.org/10.1007/s00213-015-3938-6>
- Folstein, M.F., Folstein, S.E., McHugh, P.R., 1975. “Mini-mental state.” *Journal of Psychiatric Research* 12, 189–198. [https://doi.org/10.1016/0022-3956\(75\)90026-6](https://doi.org/10.1016/0022-3956(75)90026-6)
- Forrest, S.L., Kril, J.J., Stevens, C.H., Kwok, J.B., Hallupp, M., Kim, W.S., Huang, Y., McGinley, C.V., Werka, H., Kiernan, M.C., Götz, J., Spillantini, M.G., Hodges, J.R., Ittner, L.M., Halliday, G.M., 2018. Retiring the term FTDP-17 as MAPT mutations are genetic forms of sporadic frontotemporal tauopathies. *Brain* 141, 521–534. <https://doi.org/10.1093/brain/awx328>
- Fournier, C., Barbier, M., Camuzat, A., Anquetil, V., Lattante, S., Clot, F., Cazeneuve, C., Rinaldi, D., Couratier, P., Deramecourt, V., Sabatelli, M., Belliard, S., Vercelletto, M., Forlani, S., Jornea, L., Leguern, E., Brice, A., Le Ber, I., Brice, A., Auriacombe, S., Belliard, S., Blanc, F., Bouteleau-Bretonnière, C., Ceccaldi, M., Couratier, P., Didic, M., Dubois, B., Duyckaerts, C., Etcharry-Bouix, F., Golfier, V., Hannequin, D., Lacomblez, L., Le Ber, I., Levy, R., Michel, B.-F., Pasquier, F., Thomas-Anterion, C., Pariente, J., Sellal, F., Vercelletto, M., Benchetrit, E., Bertin, H., Bertrand, A., Bissery, A., Bombois, S., Boncoeur, M.-P., Cassagnaud, P., Chastan, M., Chen, Y., Chupin, M., Colliot, O., Couratier, P., Delbecq, X., Deramecourt, V., Delmaire, C., Gerardin, E., Hossein-Foucher, C., Dubois, B., Habert, M.-O., Hannequin, D., Lautrette, G., Lebouvier, T., Le Ber, I., Lehericy, S., Le Toullec, B., Levy, R., Martineau, K., Mackowiak, M.-A., Monteil, J., Pasquier, F., Petyt, G., Pradat, P.-F., Oya, A.-H., Rinaldi, D., Rollin-Sillaire, A., Salachas, F., Sayah, S., Wallon, D., 2019. Relations between C9orf72 expansion size in blood, age at onset, age at collection and transmission across generations in patients and presymptomatic carriers. *Neurobiology of Aging* 74, 234.e1-234.e8. <https://doi.org/10.1016/j.neurobiolaging.2018.09.010>
- Fox, M.D., Raichle, M.E., 2007. Spontaneous fluctuations in brain activity observed with functional magnetic resonance imaging. *Nat Rev Neurosci* 8, 700–711. <https://doi.org/10.1038/nrn2201>
- Franzmeier, N., Brendel, M., Beyer, L., Slemann, L., Kovacs, G.G., Arzberger, T., Kurz, C., Respondek, G., Lukic, M.J., Biel, D., Rubinski, A., Frontzkowski, L., Hummel, S., Müller, A., Finze, A., Palleis, C., Joseph, E., Weidinger, E., Katzdobler, S., Song, M., Biechele, G., Kern, M., Scheifele, M., Rauchmann, B.-S., Perneczky, R., Rullman, M., Patt, M., Schildan, A., Barthel, H., Sabri, O., Rumpf, J.J., Schroeter, M.L., Classen, J., Villemagne, V., Seibyl, J., Stephens, A.W., Lee, E.B., Coughlin, D.G., Giese, A., Grossman, M., McMillan, C.T., Gelpi, E., Molina-Porcel, L., Compta, Y., van Swieten, J.C., Laatsch, L.D., Troakes, C., Al-Sarraj, S., Robinson, J.L., Xie, S.X., Irwin, D.J., Roeber, S., Herms, J., Simons, M., Bartenstein, P., Lee, V.M., Trojanowski, J.Q., Levin, J., Höglinger, G., Ewers, M., 2022. Tau deposition patterns are associated with functional connectivity in primary tauopathies. *Nat Commun* 13, 1362. <https://doi.org/10.1038/s41467-022-28896-3>
- Friston, K., Breakspear, M., Deco, G., 2012. Perception and self-organized instability. *Frontiers in Computational Neuroscience*. <https://doi.org/10.3389/fncom.2012.00044>
- Friston, K.J., 1994. Functional and effective connectivity in neuroimaging: A synthesis. *Hum. Brain Mapp.* 2, 56–78. <https://doi.org/10.1002/hbm.460020107>
- Frost, B., Diamond, M.I., 2010. Prion-like mechanisms in neurodegenerative diseases. *Nat Rev Neurosci* 11, 155–159. <https://doi.org/10.1038/nrn2786>
- Fu, Z., Iraj, A., Turner, J.A., Sui, J., Miller, R., Pearlson, G.D., Calhoun, V.D., 2021. Dynamic state with covarying brain activity-connectivity: On the pathophysiology

- of schizophrenia. *NeuroImage* 224, 117385.
<https://doi.org/10.1016/j.neuroimage.2020.117385>
- Fung, C.W., Guo, J., Fu, H., Figueroa, H.Y., Konofagou, E.E., Duff, K.E., 2020. Atrophy associated with tau pathology precedes overt cell death in a mouse model of progressive tauopathy. *Sci. Adv.* 6, eabc8098.
<https://doi.org/10.1126/sciadv.abc8098>
- Galvin, J.E., Howard, D.H., Denny, S.S., Dickinson, S., Tatton, N., 2017. The social and economic burden of frontotemporal degeneration. *Neurology* 89, 2049–2056.
<https://doi.org/10.1212/WNL.0000000000004614>
- Gardner, R.C., Boxer, A.L., Trujillo, A., Mirsky, J.B., Guo, C.C., Gennatas, E.D., Heuer, H.W., Fine, E., Zhou, J., Kramer, J.H., Miller, B.L., Seeley, W.W., 2013. Intrinsic connectivity network disruption in progressive supranuclear palsy. *Ann Neurol* 73, 603–616. <https://doi.org/10.1002/ana.23844>
- Garrett, S.L., McDaniel, D., Obideen, M., Trammell, A.R., Shaw, L.M., Goldstein, F.C., Hajjar, I., 2019. Racial Disparity in Cerebrospinal Fluid Amyloid and Tau Biomarkers and Associated Cutoffs for Mild Cognitive Impairment. *JAMA Netw Open* 2, e1917363. <https://doi.org/10.1001/jamanetworkopen.2019.17363>
- Geerligs, L., Tsvetanov, K.A., Cam-CAN, Henson, R.N., 2017. Challenges in measuring individual differences in functional connectivity using fMRI: The case of healthy aging: Measuring Individual Differences Using fMRI. *Hum. Brain Mapp.* 38, 4125–4156. <https://doi.org/10.1002/hbm.23653>
- Gelman, A., 2005. Analysis of variance—why it is more important than ever. *Ann. Statist.* 33. <https://doi.org/10.1214/009053604000001048>
- Ghanbari, Y., Bloy, L., Christopher Edgar, J., Blaskey, L., Verma, R., Roberts, T.P.L., 2015. Joint analysis of band-specific functional connectivity and signal complexity in autism. *Journal of autism and developmental disorders.*
<https://doi.org/10.1007/s10803-013-1915-7>
- Ghisletta, P., Renaud, O., Jacot, N., Courvoisier, D., 2015. Linear Mixed-Effects and Latent Curve Models for Longitudinal Life Course Analyses, in: Burton-Jeangros, C., Cullati, S., Sacker, A., Blane, D. (Eds.), *A Life Course Perspective on Health Trajectories and Transitions, Life Course Research and Social Policies.* Springer International Publishing, Cham, pp. 155–178. https://doi.org/10.1007/978-3-319-20484-0_8
- Gilman, S., Wenning, G.K., Low, P.A., Brooks, D.J., Mathias, C.J., Trojanowski, J.Q., Wood, N.W., Colosimo, C., Durr, A., Fowler, C.J., Kaufmann, H., Klockgether, T., Lees, A., Poewe, W., Quinn, N., Revesz, T., Robertson, D., Sandroni, P., Seppi, K., Vidailhet, M., 2008. Second consensus statement on the diagnosis of multiple system atrophy. *Neurology* 71, 670–676.
<https://doi.org/10.1212/01.wnl.0000324625.00404.15>
- Glasmacher, S.A., Leigh, P.N., Saha, R.A., 2017. Predictors of survival in progressive supranuclear palsy and multiple system atrophy: a systematic review and meta-analysis. *J Neurol Neurosurg Psychiatry* 88, 402–411. <https://doi.org/10.1136/jnnp-2016-314956>
- Goedert, M., 2015. Alzheimer’s and Parkinson’s diseases: The prion concept in relation to assembled A β , tau, and α -synuclein. *Science.*
<https://doi.org/10.1126/science.1255555>
- Golbe, L.I., Ohman-Strickland, P.A., 2007. A clinical rating scale for progressive supranuclear palsy. *Brain* 130, 1552–1565. <https://doi.org/10.1093/brain/awm032>

- Gómez-Tortosa, E., Serrano, S., Toledo, M., Pérez-Pérez, J., Sainz, M.J., 2014. Familial benign frontotemporal deterioration with *C9ORF72* hexanucleotide expansion. *Alzheimer's & Dementia* 10. <https://doi.org/10.1016/j.jalz.2013.09.013>
- Gordon, E., Rohrer, J.D., Fox, N.C., 2016. Advances in neuroimaging in frontotemporal dementia. *J. Neurochem.* 138, 193–210. <https://doi.org/10.1111/jnc.13656>
- Gordon, E.M., Laumann, T.O., Gilmore, A.W., Newbold, D.J., Greene, D.J., Berg, J.J., Ortega, M., Hoyt-Drazen, C., Gratton, C., Sun, H., Hampton, J.M., Coalson, R.S., Nguyen, A.L., McDermott, K.B., Shimony, J.S., Snyder, A.Z., Schlaggar, B.L., Petersen, S.E., Nelson, S.M., Dosenbach, N.U.F., 2017. Precision Functional Mapping of Individual Human Brains. *Neuron* 95, 791-807.e7. <https://doi.org/10.1016/j.neuron.2017.07.011>
- Gorno-Tempini, M.L., Brambati, S.M., Ginex, V., Ogar, J., Dronkers, N.F., Marcone, A., Perani, D., Garibotto, V., Cappa, S.F., Miller, B.L., 2008. The logopenic/phonological variant of primary progressive aphasia. *Neurology* 71, 1227–1234. <https://doi.org/10.1212/01.wnl.0000320506.79811.da>
- Gorno-Tempini, M.L., Hillis, A.E., Weintraub, S., Kertesz, A., Mendez, M., Cappa, S.F., Ogar, J.M., Rohrer, J.D., Black, S., Boeve, B.F., Manes, F., Dronkers, N.F., Vandenberghe, R., Rascovsky, K., Patterson, K., Miller, B.L., Knopman, D.S., Hodges, J.R., Mesulam, M.M., Grossman, M., 2011. Classification of primary progressive aphasia and its variants. *Neurology* 76, 1006–1014. <https://doi.org/10.1212/WNL.0b013e31821103e6>
- Gotts, S.J., Gilmore, A.W., Martin, A., 2020. Brain networks, dimensionality, and global signal averaging in resting-state fMRI: Hierarchical network structure results in low-dimensional spatiotemporal dynamics. *NeuroImage* 205, 116289. <https://doi.org/10.1016/j.neuroimage.2019.116289>
- Gousias, I.S., Rueckert, D., Heckemann, R.A., Dyet, L.E., Boardman, J.P., Edwards, A.D., Hammers, A., 2008. Automatic segmentation of brain MRIs of 2-year-olds into 83 regions of interest. *NeuroImage* 40, 672–684. <https://doi.org/10.1016/j.neuroimage.2007.11.034>
- Graham, N.L., Leonard, C., Tang-Wai, D.F., Black, S., Chow, T.W., Scott, C.J.M., McNeely, A.A., Masellis, M., Rochon, E., 2016. Lack of Frank Agrammatism in the Nonfluent Agrammatic Variant of Primary Progressive Aphasia. *Dement Geriatr Cogn Disord Extra* 6, 407–423. <https://doi.org/10.1159/000448944>
- Grandy, T.H., Garrett, D.D., Schmiedek, F., Werkle-Bergner, M., 2016. On the estimation of brain signal entropy from sparse neuroimaging data. *Scientific Reports*. <https://doi.org/10.1038/srep23073>
- Greaves, C.V., Rohrer, J.D., 2019. An update on genetic frontotemporal dementia. *J Neurol* 266, 2075–2086. <https://doi.org/10.1007/s00415-019-09363-4>
- Greene, A.S., Gao, S., Noble, S., Scheinost, D., Constable, R.T., 2020. How Tasks Change Whole-Brain Functional Organization to Reveal Brain-Phenotype Relationships. *Cell Reports* 32, 108066. <https://doi.org/10.1016/j.celrep.2020.108066>
- Greene, A.S., Gao, S., Scheinost, D., Constable, R.T., 2018. Task-induced brain state manipulation improves prediction of individual traits. *Nat Commun* 9, 2807. <https://doi.org/10.1038/s41467-018-04920-3>
- Gregory, S., Long, J.D., Klöppel, S., Razi, A., Scheller, E., Minkova, L., Johnson, E.B., Durr, Alexandra, Roos, R.A.C., Leavitt, B.R., Mills, J.A., Stout, J.C., Scahill, R.I., Tabrizi, S.J., Rees, G., Track-On investigators, Coleman, A., Decolongon, J., Fan, M., Koren, T., Leavitt, B., Durr, A., Jauffret, C., Justo, D., Lehericy, S., Nigaud, K., Valabrègue, R., Roos, R., Hart, E.P. 't, Schoonderbeek, A., Berna, C., Crawford, H., Ghosh, R., Hensman, D., Johnson, E., McColgan, P., Papoutsis, M., Read, J.,

- Owen, G., Craufurd, D., Reilmann, R., Weber, N., Labuschagne, I., Landwehrmeyer, B., Orth, M., 2018. Testing a longitudinal compensation model in premanifest Huntington's disease. *Brain* 141, 2156–2166. <https://doi.org/10.1093/brain/awy122>
- Gregory, S., Long, J.D., Klöppel, S., Razi, A., Scheller, E., Minkova, L., Papoutsis, M., Mills, J.A., Durr, A., Leavitt, B.R., Roos, R.A.C., Stout, J.C., Scahill, R.I., Langbehn, D.R., Tabrizi, S.J., Rees, G., 2017. Operationalizing compensation over time in neurodegenerative disease. *Brain* 140, 1158–1165. <https://doi.org/10.1093/brain/awx022>
- Greicius, M.D., Krasnow, B., Reiss, A.L., Menon, V., 2003. Functional connectivity in the resting brain: A network analysis of the default mode hypothesis. *Proc. Natl. Acad. Sci. U.S.A.* 100, 253–258. <https://doi.org/10.1073/pnas.0135058100>
- Greicius, M.D., Srivastava, G., Reiss, A.L., Menon, V., 2004. Default-mode network activity distinguishes Alzheimer's disease from healthy aging: Evidence from functional MRI. *Proc. Natl. Acad. Sci. U.S.A.* 101, 4637–4642. <https://doi.org/10.1073/pnas.0308627101>
- Griffanti, L., Douaud, G., Bijsterbosch, J., Evangelisti, S., Alfaro-Almagro, F., Glasser, M.F., Duff, E.P., Fitzgibbon, S., Westphal, R., Carone, D., Beckmann, C.F., Smith, S.M., 2017. Hand classification of fMRI ICA noise components. *NeuroImage* 154, 188–205. <https://doi.org/10.1016/j.neuroimage.2016.12.036>
- Griffanti, L., Salimi-Khorshidi, G., Beckmann, C.F., Auerbach, E.J., Douaud, G., Sexton, C.E., Zsoldos, E., Ebmeier, K.P., Filippini, N., Mackay, C.E., Moeller, S., Xu, J., Yacoub, E., Baselli, G., Ugurbil, K., Miller, K.L., Smith, S.M., 2014. ICA-based artefact removal and accelerated fMRI acquisition for improved resting state network imaging. *NeuroImage* 95, 232–247. <https://doi.org/10.1016/j.neuroimage.2014.03.034>
- Grijalva, R.M., Pham, N.T.T., Huang, Q., Martin, P.R., Ali, F., Clark, H.M., Duffy, J.R., Utianski, R.L., Botha, H., Machulda, M.M., Weigand, S.D., Ahlskog, J.E., Dickson, D.W., Josephs, K.A., Whitwell, J.L., 2022. Brainstem Biomarkers of Clinical Variant and Pathology in Progressive Supranuclear Palsy. *Movement Disorders* 37, 702–712. <https://doi.org/10.1002/mds.28901>
- Grimm, M., Respondek, G., Stamelou, M., Arzberger, T., Ferguson, L., Gelpi, E., Giese, A., Grossman, M., Irwin, D.J., Pantelyat, A., Rajput, A., Roeber, S., Swieten, J.C., Troakes, C., Antonini, A., Bhatia, K.P., Colosimo, C., Eimeren, T., Kassubek, J., Levin, J., Meissner, W.G., Nilsson, C., Oertel, W.H., Piot, I., Poewe, W., Wenning, G.K., Boxer, A., Golbe, L.I., Josephs, K.A., Litvan, I., Morris, H.R., Whitwell, J.L., Compta, Y., Corvol, J., Lang, A.E., Rowe, J.B., Höglinger, G.U., for the Movement Disorder Society-endorsed PSP Study Group, 2019. How to apply the movement disorder society criteria for diagnosis of progressive supranuclear palsy. *Mov Disord* 34, 1228–1232. <https://doi.org/10.1002/mds.27666>
- Grossman, M., 2021. Lessons learned from a progressive supranuclear palsy trial. *The Lancet Neurology* 20, 162–163. [https://doi.org/10.1016/S1474-4422\(21\)00035-1](https://doi.org/10.1016/S1474-4422(21)00035-1)
- Grossman, M., 2012. The non-fluent/agrammatic variant of primary progressive aphasia. *The Lancet Neurology* 11, 545–555. [https://doi.org/10.1016/S1474-4422\(12\)70099-6](https://doi.org/10.1016/S1474-4422(12)70099-6)
- Grubbs, F.E., 1969. Procedures for Detecting Outlying Observations in Samples. *Technometrics* 11, 1–21. <https://doi.org/10.1080/00401706.1969.10490657>
- Gu, S., Pasqualetti, F., Cieslak, M., Telesford, Q.K., Yu, A.B., Kahn, A.E., Medaglia, J.D., Vettel, J.M., Miller, M.B., Grafton, S.T., Bassett, D.S., 2015. Controllability of

- structural brain networks. *Nature Communications*.
<https://doi.org/10.1038/ncomms9414>
- Gu, Z., Gu, L., Eils, R., Schlesner, M., Brors, B., 2014. circlize implements and enhances circular visualization in R. *Bioinformatics* 30, 2811–2812.
<https://doi.org/10.1093/bioinformatics/btu393>
- Hagberg, A., Swart, P., S Chult, D., 2008. Exploring network structure, dynamics, and function using networkx. Research Org.: Los Alamos National Lab. (LANL), Los Alamos, NM (United States).
- Hammers, A., Allom, R., Koepp, M.J., Free, S.L., Myers, R., Lemieux, L., Mitchell, T.N., Brooks, D.J., Duncan, J.S., 2003. Three-dimensional maximum probability atlas of the human brain, with particular reference to the temporal lobe. *Hum. Brain Mapp.* 19, 224–247. <https://doi.org/10.1002/hbm.10123>
- Hampton, O.L., Buckley, R.F., Manning, L.K., Scott, M.R., Properzi, M.J., Peña-Gómez, C., Jacobs, H.I.L., Chhatwal, J.P., Johnson, K.A., Sperling, R.A., Schultz, A.P., 2020. Resting-state functional connectivity and amyloid burden influence longitudinal cortical thinning in the default mode network in preclinical Alzheimer’s disease. *NeuroImage: Clinical* 28, 102407.
<https://doi.org/10.1016/j.nicl.2020.102407>
- Hansen, J.Y., Shafiei, G., Markello, R.D., Smart, K., Cox, S.M.L., Nørgaard, M., Beliveau, V., Wu, Y., Gallezot, J.-D., Aumont, É., Servaes, S., Scala, S.G., DuBois, J.M., Wainstein, G., Bezgin, G., Funck, T., Schmitz, T.W., Spreng, R.N., Galovic, M., Koepp, M.J., Duncan, J.S., Coles, J.P., Fryer, T.D., Aigbirhio, F.I., McGinnity, C.J., Hammers, A., Soucy, J.-P., Baillet, S., Guimond, S., Hietala, J., Bédard, M.-A., Leyton, M., Kobayashi, E., Rosa-Neto, P., Ganz, M., Knudsen, G.M., Palomero-Gallagher, N., Shine, J.M., Carson, R.E., Tuominen, L., Dagher, A., Misic, B., 2022. Mapping neurotransmitter systems to the structural and functional organization of the human neocortex.
- Hardwick, A., Rucker, J.C., Cohen, M.L., Friedland, R.P., Gustaw-Rothenberg, K., Riley, D.E., Leigh, R.J., 2009. EVOLUTION OF OCULOMOTOR AND CLINICAL FINDINGS IN AUTOPSY-PROVEN RICHARDSON SYNDROME. *Neurology* 73, 2122–2124. <https://doi.org/10.1212/WNL.0b013e3181c67ba2>
- Harrell, F.E., 1982. Evaluating the Yield of Medical Tests. *JAMA* 247, 2543.
<https://doi.org/10.1001/jama.1982.03320430047030>
- Heagerty, P.J., Lumley, T., Pepe, M.S., 2000. Time-Dependent ROC Curves for Censored Survival Data and a Diagnostic Marker. *Biometrics* 56, 337–344.
<https://doi.org/10.1111/j.0006-341X.2000.00337.x>
- Hebb, D.O., 1949. The organization of behavior; a neuropsychological theory., The organization of behavior; a neuropsychological theory. Wiley, Oxford, England.
- Heuer, H.W., Wang, P., Rascovsky, K., Wolf, A., Appleby, B., Bove, J., Bordelon, Y., Brannelly, P., Brushaber, D.E., Caso, C., Coppola, G., Dickerson, B., Dickinson, S., Domoto-Reilly, K., Faber, K., Ferrall, J., Fields, J., Fishman, A., Fong, J., Foroud, T., Forsberg, L.K., Gearhart, D., Ghazanfari, B., Ghoshal, N., Goldman, J., Graff-Radford, J., Graff-Radford, N., Grant, I., Grossman, M., Haley, D., Hsiung, G.-Y., Huey, E., Irwin, D., Jones, D., Kantarci, K., Karydas, A., Kaufer, D., Kerwin, D., Knopman, D., Kornak, J., Kramer, J.H., Kraft, R., Kremers, W.K., Kukull, W., Litvan, I., Ljubenkov, P., Mackenzie, I.R., Maldonado, M., Manoochchri, M., McGinnis, S., McKinley, E., Mendez, M.F., Miller, B.L., Onyike, C., Pantelyat, A., Pearlman, R., Petrucelli, L., Potter, M., Rademakers, R., Ramos, E.M., Rankin, K.P., Roberson, E.D., Rogalski, E., Sengdy, P., Shaw, L., Syrjanen, J., Tartaglia, M.C., Tatton, N., Taylor, J., Toga, A., Trojanowski, J., Weintraub, S., Wong, B.,

- Wszolek, Z., Boeve, B.F., Rosen, H.J., Boxer, A.L., on behalf of the ARTFL and LEFFTDS consortia, 2020. Comparison of sporadic and familial behavioral variant frontotemporal dementia (FTD) in a North American cohort. *Alzheimer's Dement.* 16, 60–70. <https://doi.org/10.1002/alz.12046>
- Hindriks, R., Adhikari, M.H., Murayama, Y., Ganzetti, M., Mantini, D., Logothetis, N.K., Deco, G., 2016. Can sliding-window correlations reveal dynamic functional connectivity in resting-state fMRI? *NeuroImage* 127, 242–256. <https://doi.org/10.1016/j.neuroimage.2015.11.055>
- Hodges, J.R., Martinos, M., Woollams, A.M., Patterson, K., Adlam, A.-L.R., 2008. Repeat and Point: Differentiating semantic dementia from progressive non-fluent aphasia. *Cortex* 44, 1265–1270. <https://doi.org/10.1016/j.cortex.2007.08.018>
- Hodges, J.R., Patterson, K., 2007. Semantic dementia: a unique clinicopathological syndrome. *The Lancet Neurology* 6, 1004–1014. [https://doi.org/10.1016/S1474-4422\(07\)70266-1](https://doi.org/10.1016/S1474-4422(07)70266-1)
- Hodges, J.R., Patterson, K., Oxbury, S., Funnell, E., 1992. SEMANTIC DEMENTIA: PROGRESSIVE FLUENT APHASIA WITH TEMPORAL LOBE ATROPHY. *Brain* 115, 1783–1806. <https://doi.org/10.1093/brain/115.6.1783>
- Höglinger, G.U., 2018. Is it Useful to Classify Progressive Supranuclear Palsy and Corticobasal Degeneration as Different Disorders? *No. Mov Disord Clin Pract* 5, 141–144. <https://doi.org/10.1002/mdc3.12582>
- Höglinger, G.U., Litvan, I., Mendonca, N., Wang, D., Zheng, H., Rendenbach-Mueller, B., Lon, H.-K., Jin, Z., Fisseha, N., Budur, K., Gold, M., Ryman, D., Florian, H., Ahmed, A., Aiba, I., Albanese, A., Bertram, K., Bordelon, Y., Bower, J., Brosch, J., Claassen, D., Colosimo, C., Corvol, J.-C., Cudia, P., Daniele, A., Defebvre, L., Driver-Dunckley, E., Duquette, A., Eleopra, R., Eusebio, A., Fung, V., Geldmacher, D., Golbe, L., Grandas, F., Hall, D., Hatano, T., Höglinger, G.U., Honig, L., Hui, J., Kerwin, D., Kikuchi, A., Kimber, T., Kimura, T., Kumar, R., Litvan, I., Ljubenkov, P., Lorenzl, S., Ludolph, A., Mari, Z., McFarland, N., Meissner, W., Mir Rivera, P., Mochizuki, H., Morgan, J., Munhoz, R., Nishikawa, N., O'Sullivan, J., Oeda, T., Oizumi, H., Onodera, O., Ory-Magne, F., Peckham, E., Postuma, R., Quattrone, A., Quinn, J., Ruggieri, S., Sarna, J., Schulz, P.E., Slevin, J., Tagliati, M., Wile, D., Wszolek, Z., Xie, T., Zesiewicz, T., 2021. Safety and efficacy of tilavonemab in progressive supranuclear palsy: a phase 2, randomised, placebo-controlled trial. *The Lancet Neurology* 20, 182–192. [https://doi.org/10.1016/S1474-4422\(20\)30489-0](https://doi.org/10.1016/S1474-4422(20)30489-0)
- Höglinger, G.U., Respondek, G., Stamelou, M., Kurz, C., Josephs, K.A., Lang, A.E., Mollenhauer, B., Müller, U., Nilsson, C., Whitwell, J.L., Arzberger, T., Englund, E., Gelpi, E., Giese, A., Irwin, D.J., Meissner, W.G., Pantelyat, A., Rajput, A., van Swieten, J.C., Troakes, C., Antonini, A., Bhatia, K.P., Bordelon, Y., Compta, Y., Corvol, J.-C., Colosimo, C., Dickson, D.W., Dodel, R., Ferguson, L., Grossman, M., Kassubek, J., Krismer, F., Levin, J., Lorenzl, S., Morris, H.R., Nestor, P., Oertel, W.H., Poewe, W., Rabinovici, G., Rowe, J.B., Schellenberg, G.D., Seppi, K., van Eimeren, T., Wenning, G.K., Boxer, A.L., Golbe, L.I., Litvan, I., Movement Disorder Society-endorsed PSP Study Group, 2017. Clinical diagnosis of progressive supranuclear palsy: The movement disorder society criteria. *Mov Disord* 32, 853–864. <https://doi.org/10.1002/mds.26987>
- Holland, N., Jones, P.S., Savulich, G., Wiggins, J.K., Hong, Y.T., Fryer, T.D., Manavaki, R., Sephton, S.M., Boros, I., Malpetti, M., Hezemans, F.H., Aigbirhio, F.I., Coles, J.P., O'Brien, J., Rowe, J.B., 2020. Synaptic Loss in Primary Tauopathies Revealed

- by [¹¹C] UCB-J Positron Emission Tomography. *Mov Disord* 35, 1834–1842. <https://doi.org/10.1002/mds.28188>
- Holmes, S.E., Scheinost, D., Finnema, S.J., Naganawa, M., Davis, M.T., DellaGioia, N., Nabulsi, N., Matuskey, D., Angarita, G.A., Pietrzak, R.H., Duman, R.S., Sanacora, G., Krystal, J.H., Carson, R.E., Esterlis, I., 2019. Lower synaptic density is associated with depression severity and network alterations. *Nat Commun* 10, 1529. <https://doi.org/10.1038/s41467-019-09562-7>
- Honey, C.J., Kötter, R., Breakspear, M., Sporns, O., 2007. Network structure of cerebral cortex shapes functional connectivity on multiple time scales. *Proceedings of the National Academy of Sciences*. <https://doi.org/10.1073/pnas.0701519104>
- Honey, C.J., Sporns, O., Cammoun, L., Gigandet, X., Thiran, J.P., Meuli, R., Hagmann, P., 2009. Predicting human resting-state functional connectivity from structural connectivity. *Proc. Natl. Acad. Sci. U.S.A.* 106, 2035–2040. <https://doi.org/10.1073/pnas.0811168106>
- Hong, S., Beja-Glasser, V.F., Nfonoyim, B.M., Frouin, A., Li, S., Ramakrishnan, S., Merry, K.M., Shi, Q., Rosenthal, A., Barres, B.A., Lemere, C.A., Selkoe, D.J., Stevens, B., 2016. Complement and microglia mediate early synapse loss in Alzheimer mouse models. *Science* 352, 712–716. <https://doi.org/10.1126/science.aad8373>
- Hoover, B.R., Reed, M.N., Su, J., Penrod, R.D., Kotilinek, L.A., Grant, M.K., Pitstick, R., Carlson, G.A., Lanier, L.M., Yuan, L.-L., Ashe, K.H., Liao, D., 2010. Tau Mislocalization to Dendritic Spines Mediates Synaptic Dysfunction Independently of Neurodegeneration. *Neuron* 68, 1067–1081. <https://doi.org/10.1016/j.neuron.2010.11.030>
- Horie, K., Barthélemy, N.R., Spina, S., VandeVrede, L., He, Y., Paterson, R.W., Wright, B.A., Day, G.S., Davis, A.A., Karch, C.M., Seeley, W.W., Perrin, R.J., Koppiseti, R.K., Shaikh, F., Lago, A.L., Heuer, H.W., Ghoshal, N., Gabelle, A., Miller, B.L., Boxer, A.L., Bateman, R.J., Sato, C., 2022. CSF tau microtubule-binding region identifies pathological changes in primary tauopathies. *Nat Med*. <https://doi.org/10.1038/s41591-022-02075-9>
- Hornberger, M., Piguet, O., Graham, A.J., Nestor, P.J., Hodges, J.R., 2010. How preserved is episodic memory in behavioral variant frontotemporal dementia? *Neurology* 74, 472–479. <https://doi.org/10.1212/WNL.0b013e3181cef85d>
- Hornberger, M., Piguet, O., Kipps, C., Hodges, J.R., 2008. Executive function in progressive and nonprogressive behavioral variant frontotemporal dementia. *Neurology* 71, 1481–1488. <https://doi.org/10.1212/01.wnl.0000334299.72023.c8>
- Hsieh, S., Schubert, S., Hoon, C., Mioshi, E., Hodges, J.R., 2013. Validation of the Addenbrooke’s Cognitive Examination III in Frontotemporal Dementia and Alzheimer’s Disease. *Dementia and Geriatric Cognitive Disorders*. <https://doi.org/10.1159/000351671>
- Hu, W.T., Shelnutt, M., Wilson, A., Yarab, N., Kelly, C., Grossman, M., Libon, D.J., Khan, J., Lah, J.J., Levey, A.I., Glass, J., 2013. Behavior Matters—Cognitive Predictors of Survival in Amyotrophic Lateral Sclerosis. *PLoS ONE* 8, e57584. <https://doi.org/10.1371/journal.pone.0057584>
- Huber, N., Korhonen, S., Hoffmann, D., Leskelä, S., Rostalski, H., Remes, A.M., Honkakoski, P., Solje, E., Haapasalo, A., 2022. Deficient neurotransmitter systems and synaptic function in frontotemporal lobar degeneration—Insights into disease mechanisms and current therapeutic approaches. *Mol Psychiatry* 27, 1300–1309. <https://doi.org/10.1038/s41380-021-01384-8>
- Hudson, A.J., 1981. AMYOTROPHIC LATERAL SCLEROSIS AND ITS ASSOCIATION WITH DEMENTIA, PARKINSONISM AND OTHER

- NEUROLOGICAL DISORDERS: A REVIEW. *Brain* 104, 217–247.
<https://doi.org/10.1093/brain/104.2.217>
- Hunter, C.A., Kirson, N.Y., Desai, U., Cummings, A.K.G., Faries, D.E., Birnbaum, H.G., 2015. Medical costs of Alzheimer’s disease misdiagnosis among US Medicare beneficiaries. *Alzheimer’s & Dementia* 11, 887–895.
<https://doi.org/10.1016/j.jalz.2015.06.1889>
- Hutchinson, A.D., Mathias, J.L., 2007. Neuropsychological deficits in frontotemporal dementia and Alzheimer’s disease: a meta-analytic review. *Journal of Neurology, Neurosurgery & Psychiatry* 78, 917–928.
<https://doi.org/10.1136/jnnp.2006.100669>
- Hutton, M., Lendon, C.L., Rizzu, P., Baker, M., Froelich, S., Houlden, H., Pickering-Brown, S., Chakraverty, S., Isaacs, A., Grover, A., Hackett, J., Adamson, J., Lincoln, S., Dickson, D., Davies, P., Petersen, R.C., Stevens, M., de Graaff, E., Wauters, E., van Baren, J., Hillebrand, M., Joosse, M., Kwon, J.M., Nowotny, P., Che, L.K., Norton, J., Morris, J.C., Reed, L.A., Trojanowski, J., Basun, H., Lannfelt, L., Neystat, M., Fahn, S., Dark, F., Tannenberg, T., Dodd, P.R., Hayward, N., Kwok, J.B.J., Schofield, P.R., Andreadis, A., Snowden, J., Craufurd, D., Neary, D., Owen, F., Oostra, B.A., Hardy, J., Goate, A., van Swieten, J., Mann, D., Lynch, T., Heutink, P., 1998. Association of missense and 5'-splice-site mutations in tau with the inherited dementia FTDP-17. *Nature* 393, 702–705.
<https://doi.org/10.1038/31508>
- Hwang, K., Bertolero, M.A., Liu, W.B., D’Esposito, M., 2017. The Human Thalamus Is an Integrative Hub for Functional Brain Networks. *J. Neurosci.* 37, 5594–5607.
<https://doi.org/10.1523/JNEUROSCI.0067-17.2017>
- Hyvarinen, A., 1999. Fast and robust fixed-point algorithms for independent component analysis. *IEEE Trans. Neural Netw.* 10, 626–634.
<https://doi.org/10.1109/72.761722>
- Iglesias, J.E., Van Leemput, K., Bhatt, P., Casillas, C., Dutt, S., Schuff, N., Truran-Sacrey, D., Boxer, A., Fischl, B., 2015. Bayesian segmentation of brainstem structures in MRI. *Neuroimage*. <https://doi.org/10.1016/j.neuroimage.2015.02.065>
- Ikeda, M., 2002. Changes in appetite, food preference, and eating habits in frontotemporal dementia and Alzheimer’s disease. *Journal of Neurology, Neurosurgery & Psychiatry* 73, 371–376. <https://doi.org/10.1136/jnnp.73.4.371>
- Illán-Gala, I., Nigro, S., VandeVrede, L., Falgàs, N., Heuer, H.W., Painous, C., Compta, Y., Martí, M.J., Montal, V., Pagonabarraga, J., Kulisevsky, J., Lleó, A., Fortea, J., Logroscino, G., Quattrone, Andrea, Quattrone, Aldo, Perry, D.C., Gorno-Tempini, M.L., Rosen, H.J., Grinberg, L.T., Spina, S., La Joie, R., Rabinovici, G.D., Miller, B.L., Rojas, J.C., Seeley, W.W., Boxer, A.L., 2022. Diagnostic Accuracy of Magnetic Resonance Imaging Measures of Brain Atrophy Across the Spectrum of Progressive Supranuclear Palsy and Corticobasal Degeneration. *JAMA Netw Open* 5, e229588. <https://doi.org/10.1001/jamanetworkopen.2022.9588>
- Ioannidis, J.P.A., 2008. Why Most Discovered True Associations Are Inflated. *Epidemiology* 19, 640–648. <https://doi.org/10.1097/EDE.0b013e31818131e7>
- Irwin, D.J., Brettschneider, J., McMillan, C.T., Cooper, F., Olm, C., Arnold, S.E., Van Deerlin, V.M., Seeley, W.W., Miller, B.L., Lee, E.B., Lee, V.M.-Y., Grossman, M., Trojanowski, J.Q., 2016. Deep clinical and neuropathological phenotyping of Pick disease: Deep Phenotype Pick Disease. *Ann Neurol.* 79, 272–287.
<https://doi.org/10.1002/ana.24559>
- Irwin, D.J., Cairns, N.J., Grossman, M., McMillan, C.T., Lee, E.B., Van Deerlin, V.M., Lee, V.M.-Y., Trojanowski, J.Q., 2015. Frontotemporal lobar degeneration:

- defining phenotypic diversity through personalized medicine. *Acta Neuropathol* 129, 469–491. <https://doi.org/10.1007/s00401-014-1380-1>
- Iturria-Medina, Y., Carbonell, F.M., Evans, A.C., 2018. Multimodal imaging-based therapeutic fingerprints for optimizing personalized interventions: Application to neurodegeneration. *NeuroImage* 179, 40–50. <https://doi.org/10.1016/j.neuroimage.2018.06.028>
- Iturria-Medina, Y., Khan, A.F., Adewale, Q., Shirazi, A.H., the Alzheimer’s Disease Neuroimaging Initiative, 2020. Blood and brain gene expression trajectories mirror neuropathology and clinical deterioration in neurodegeneration. *Brain* 143, 661–673. <https://doi.org/10.1093/brain/awz400>
- Iturria-Medina, Y., Sotero, R.C., Toussaint, P.J., Evans, A.C., and the Alzheimer’s Disease Neuroimaging, I., 2014. Epidemic Spreading Model to Characterize Misfolded Proteins Propagation in Aging and Associated Neurodegenerative Disorders. *PLOS Computational Biology*. <https://doi.org/10.1371/journal.pcbi.1003956>
- Jabbari, E., Holland, N., Chelban, V., Jones, P.S., Lamb, R., Rawlinson, C., Guo, T., Costantini, A.A., Tan, M.M.X., Heslegrave, A.J., Roncaroli, F., Klein, J.C., Ansoorge, O., Allinson, K.S.J., Jaunmuktane, Z., Holton, J.L., Revesz, T., Warner, T.T., Lees, A.J., Zetterberg, H., Russell, L.L., Bocchetta, M., Rohrer, J.D., Williams, N.M., Grosset, D.G., Burn, D.J., Pavese, N., Gerhard, A., Kobylecki, C., Leigh, P.N., Church, A., Hu, M.T.M., Woodside, J., Houlden, H., Rowe, J.B., Morris, H.R., 2020. Diagnosis Across the Spectrum of Progressive Supranuclear Palsy and Corticobasal Syndrome. *JAMA Neurol* 77, 377. <https://doi.org/10.1001/jamaneurol.2019.4347>
- Jabbari, E., Koga, S., Valentino, R.R., Reynolds, R.H., Ferrari, R., Tan, M.M.X., Rowe, J.B., Dalgard, C.L., Scholz, S.W., Dickson, D.W., Warner, T.T., Revesz, T., Höglinger, G.U., Ross, O.A., Ryten, M., Hardy, J., Shoai, M., Morris, H.R., Mok, K.Y., Murphy, D.P., Al-Sarraj, S., Troakes, C., Gentleman, S.M., Allinson, K.S.J., Jaunmuktane, Z., Holton, J.L., Lees, A.J., Morris, C.M., Compta, Y., Gelpi, E., van Swieten, J.C., Rajput, A., Ferguson, L., Cookson, M.R., Gibbs, J.R., Blauwendraat, C., Ding, J., Chia, R., Traynor, B.J., Pantelyat, A., Viollet, C., Traynor, B.J., Pletnikova, O., Troncoso, J.C., Rosenthal, L.S., Boxer, A.L., Respondek, G., Arzberger, T., Roeber, S., Giese, A., Burn, D.J., Pavese, N., Gerhard, A., Kobylecki, C., Leigh, P.N., Church, A., T.M. Hu, M., 2021. Genetic determinants of survival in progressive supranuclear palsy: a genome-wide association study. *The Lancet Neurology* 20, 107–116. [https://doi.org/10.1016/S1474-4422\(20\)30394-X](https://doi.org/10.1016/S1474-4422(20)30394-X)
- Jack, C.R., Holtzman, D.M., 2013. Biomarker Modeling of Alzheimer’s Disease. *Neuron* 80, 1347–1358. <https://doi.org/10.1016/j.neuron.2013.12.003>
- Jack, C.R., Knopman, D.S., Jagust, W.J., Shaw, L.M., Aisen, P.S., Weiner, M.W., Petersen, R.C., Trojanowski, J.Q., 2010. Hypothetical model of dynamic biomarkers of the Alzheimer’s pathological cascade. *The Lancet Neurology* 9, 119–128. [https://doi.org/10.1016/S1474-4422\(09\)70299-6](https://doi.org/10.1016/S1474-4422(09)70299-6)
- Jack, C.R., Wiste, H.J., Weigand, S.D., Therneau, T.M., Lowe, V.J., Knopman, D.S., Gunter, J.L., Senjem, M.L., Jones, D.T., Kantarci, K., Machulda, M.M., Mielke, M.M., Roberts, R.O., Vemuri, P., Reyes, D.A., Petersen, R.C., 2017. Defining imaging biomarker cut points for brain aging and Alzheimer’s disease. *Alzheimer’s & Dementia* 13, 205–216. <https://doi.org/10.1016/j.jalz.2016.08.005>
- Jackson, S., Yeh, F.L., Ward, M., Rhinn, H., Huang, J.Y., Pappalardo, J.L., Liao, Y., Hagey, M., Long, H., Paul, R., 2021. Six months interim analysis of the phase 2

- study of AL001 in frontotemporal dementia patients carrying a granulin mutation. *Alzheimer's & Dementia* 17. <https://doi.org/10.1002/alz.054593>
- Jancke, D., Herlitze, S., Kringelbach, M.L., Deco, G., 2022. Bridging the gap between single receptor type activity and whole-brain dynamics. *The FEBS Journal* 289, 2067–2084. <https://doi.org/10.1111/febs.15855>
- Jenkinson, M., Bannister, P., Brady, M., Smith, S., 2002. Improved Optimization for the Robust and Accurate Linear Registration and Motion Correction of Brain Images. *NeuroImage* 17, 825–841. <https://doi.org/10.1006/nimg.2002.1132>
- Jenkinson, M., Beckmann, C.F., Behrens, T.E.J., Woolrich, M.W., Smith, S.M., 2012. FSL. *NeuroImage* 62, 782–790. <https://doi.org/10.1016/j.neuroimage.2011.09.015>
- Jia, K., Zamboni, E., Rua, C., Goncalves, N.R., Kemper, V., Ng, A.K.T., Rodgers, C.T., Williams, G., Goebel, R., Kourtzi, Z., 2021. A protocol for ultra-high field laminar fMRI in the human brain. *STAR Protocols* 2, 100415. <https://doi.org/10.1016/j.xpro.2021.100415>
- Jiang, J., Zhu, Q., Gendron, T.F., Saberi, S., McAlonis-Downes, M., Seelman, A., Stauffer, J.E., Jafar-nejad, P., Drenner, K., Schulte, D., Chun, S., Sun, S., Ling, S.-C., Myers, B., Engelhardt, J., Katz, M., Baughn, M., Platoshyn, O., Marsala, M., Watt, A., Heyser, C.J., Ard, M.C., De Muynck, L., Daugherty, L.M., Swing, D.A., Tessarollo, L., Jung, C.J., Delpoux, A., Utzschneider, D.T., Hedrick, S.M., de Jong, P.J., Edbauer, D., Van Damme, P., Petrucelli, L., Shaw, C.E., Bennett, C.F., Da Cruz, S., Ravits, J., Rigo, F., Cleveland, D.W., Lagier-Tourenne, C., 2016. Gain of Toxicity from ALS/FTD-Linked Repeat Expansions in C9ORF72 Is Alleviated by Antisense Oligonucleotides Targeting GGGGCC-Containing RNAs. *Neuron* 90, 535–550. <https://doi.org/10.1016/j.neuron.2016.04.006>
- Jo, M., Lee, S., Jeon, Y.-M., Kim, S., Kwon, Y., Kim, H.-J., 2020. The role of TDP-43 propagation in neurodegenerative diseases: integrating insights from clinical and experimental studies. *Exp Mol Med* 52, 1652–1662. <https://doi.org/10.1038/s12276-020-00513-7>
- Johnson, W.E., Li, C., Rabinovic, A., 2007. Adjusting batch effects in microarray expression data using empirical Bayes methods. *Biostatistics* 8, 118–127. <https://doi.org/10.1093/biostatistics/kxj037>
- Jones, J.L., Thompson, S.A., Loh, P., Davies, J.L., Tuohy, O.C., Curry, A.J., Azzopardi, L., Hill-Cawthorne, G., Fahey, M.T., Compston, A., Coles, A.J., 2013. Human autoimmunity after lymphocyte depletion is caused by homeostatic T-cell proliferation. *Proc Natl Acad Sci U S A*. <https://doi.org/10.1073/pnas.1313654110>
- Josephs, K.A., 2006. Clinicopathological and imaging correlates of progressive aphasia and apraxia of speech. *Brain* 129, 1385–1398. <https://doi.org/10.1093/brain/awl078>
- Josephs, K.A., Duffy, J.R., Clark, H.M., Utianski, R.L., Strand, E.A., Machulda, M.M., Botha, H., Martin, P.R., Pham, N.T.T., Stierwalt, J., Ali, F., Buciuc, M., Baker, M., Fernandez De Castro, C.H., Spsychalla, A.J., Schwarz, C.G., Reid, R.I., Senjem, M.L., Jack, C.R., Lowe, V.J., Bigio, E.H., Reichard, R.R., Polley, Eric.J., Ertekin-Taner, N., Rademakers, R., DeTure, M.A., Ross, O.A., Dickson, D.W., Whitwell, J.L., 2021. A molecular pathology, neurobiology, biochemical, genetic and neuroimaging study of progressive apraxia of speech. *Nat Commun* 12, 3452. <https://doi.org/10.1038/s41467-021-23687-8>
- Joubert, S., Felician, O., Barbeau, E., Ranjeva, J.-P., Christophe, M., Didic, M., Poncet, M., Ceccaldi, M., 2006. The right temporal lobe variant of frontotemporal dementia: Cognitive and neuroanatomical profile of three patients. *J Neurol* 253, 1447–1458. <https://doi.org/10.1007/s00415-006-0232-x>

- Jucker, M., Walker, L.C., 2018. Propagation and spread of pathogenic protein assemblies in neurodegenerative diseases. *Nat Neurosci* 21, 1341–1349. <https://doi.org/10.1038/s41593-018-0238-6>
- Kaalund, S.S., Passamonti, L., Allinson, K.S.J., Murley, A.G., Robbins, T.W., Spillantini, M.G., Rowe, J.B., 2020. Locus coeruleus pathology in progressive supranuclear palsy, and its relation to disease severity. *Acta Neuropathologica Communications*. <https://doi.org/10.1186/s40478-020-0886-0>
- Kaat, L.D., Boon, A.J.W., Kamphorst, W., Ravid, R., Duivenvoorden, H.J., van Swieten, J.C., 2007. Frontal presentation in progressive supranuclear palsy. *Neurology* 69, 723–729. <https://doi.org/10.1212/01.wnl.0000267643.24870.26>
- Kaller, S., Rullmann, M., Patt, M., Becker, G.-A., Luthardt, J., Girbardt, J., Meyer, P.M., Werner, P., Barthel, H., Bresch, A., Fritz, T.H., Hesse, S., Sabri, O., 2017. Test–retest measurements of dopamine D1-type receptors using simultaneous PET/MRI imaging. *Eur J Nucl Med Mol Imaging* 44, 1025–1032. <https://doi.org/10.1007/s00259-017-3645-0>
- Kaniyappan, S., Chandupatla, R.R., Mandelkow, Eva-Maria, Mandelkow, Eckhard, 2017. Extracellular low-n oligomers of tau cause selective synaptotoxicity without affecting cell viability. *Alzheimer's & Dementia* 13, 1270–1291. <https://doi.org/10.1016/j.jalz.2017.04.002>
- Kantarci, K., Jack, C.R., 2004. Quantitative magnetic resonance techniques as surrogate markers of Alzheimer's disease. *Neurotherapeutics* 1, 196–205. <https://doi.org/10.1602/neurorx.1.2.196>
- Kassambara, A., Kosinski, M., Biecek, P., Fabian, S., 2021. *Survminer: Drawing Survival Curves using 'ggplot2'*.
- Kato, N., Arai, K., Hattori, T., 2003. Study of the rostral midbrain atrophy in progressive supranuclear palsy. *Journal of the Neurological Sciences* 210, 57–60. [https://doi.org/10.1016/S0022-510X\(03\)00014-5](https://doi.org/10.1016/S0022-510X(03)00014-5)
- Kay, K., Jamison, K.W., Vizioli, L., Zhang, R., Margalit, E., Ugurbil, K., 2019. A critical assessment of data quality and venous effects in sub-millimeter fMRI. *NeuroImage* 189, 847–869. <https://doi.org/10.1016/j.neuroimage.2019.02.006>
- Kelly, Jr., R.E., Hoptman, M.J., Lee, S., Alexopoulos, G.S., Gunning, F.M., McKeown, M.J., 2022. Seed-based dual regression: An illustration of the impact of dual regression's inherent filtering of global signal. *Journal of Neuroscience Methods* 366, 109410. <https://doi.org/10.1016/j.jneumeth.2021.109410>
- Kety, S.S., Schmidt, C.F., 1948. THE NITROUS OXIDE METHOD FOR THE QUANTITATIVE DETERMINATION OF CEREBRAL BLOOD FLOW IN MAN: THEORY, PROCEDURE AND NORMAL VALUES 1. *J. Clin. Invest.* 27, 476–483. <https://doi.org/10.1172/JCI101994>
- Khan, A.F., Adewale, Q., Baumeister, T.R., Carbonell, F., Zilles, K., Palomero-Gallagher, N., Iturria-Medina, Y., for the Alzheimer's Disease Neuroimaging Initiative, 2022. Personalized brain models identify neurotransmitter receptor changes in Alzheimer's disease. *Brain* 145, 1785–1804. <https://doi.org/10.1093/brain/awab375>
- Killingsworth, M.A., Gilbert, D.T., 2010. A Wandering Mind Is an Unhappy Mind. *Science* 330, 932–932. <https://doi.org/10.1126/science.1192439>
- Kim, E.-J., Vatsavayai, S., Seeley, W.W., 2016. Neuropathology of dementia, in: Miller, B.L., Boeve, B.F. (Eds.), *The Behavioral Neurology of Dementia*. Cambridge University Press, pp. 94–122. <https://doi.org/10.1017/9781139924771.008>
- Kim, J., Hu, C., Moufawad El Achkar, C., Black, L.E., Douville, J., Larson, A., Pendergast, M.K., Goldkind, S.F., Lee, E.A., Kuniholm, A., Soucy, A., Vaze, J., Belur, N.R.,

- Fredriksen, K., Stojkowska, I., Tsytsykova, A., Armant, M., DiDonato, R.L., Choi, J., Cornelissen, L., Pereira, L.M., Augustine, E.F., Genetti, C.A., Dies, K., Barton, B., Williams, L., Goodlett, B.D., Riley, B.L., Pasternak, A., Berry, E.R., Pflock, K.A., Chu, S., Reed, C., Tyndall, K., Agrawal, P.B., Beggs, A.H., Grant, P.E., Urion, D.K., Snyder, R.O., Waisbren, S.E., Poduri, A., Park, P.J., Patterson, A., Biffi, A., Mazzulli, J.R., Bodamer, O., Berde, C.B., Yu, T.W., 2019. Patient-Customized Oligonucleotide Therapy for a Rare Genetic Disease. *N Engl J Med* 381, 1644–1652. <https://doi.org/10.1056/NEJMoa1813279>
- Kipps, C.M., Hodges, J.R., Fryer, T.D., Nestor, P.J., 2009. Combined magnetic resonance imaging and positron emission tomography brain imaging in behavioural variant frontotemporal degeneration: refining the clinical phenotype. *Brain* 132, 2566–2578. <https://doi.org/10.1093/brain/awp077>
- Klaassens, B.L., van Gerven, J.M.A., Klaassen, E.S., van der Grond, J., Rombouts, S.A.R.B., 2019. Cholinergic and serotonergic modulation of resting state functional brain connectivity in Alzheimer’s disease. *NeuroImage* 199, 143–152. <https://doi.org/10.1016/j.neuroimage.2019.05.044>
- Klöppel, S., Gregory, S., Scheller, E., Minkova, L., Razi, A., Durr, A., Roos, R.A.C., Leavitt, B.R., Papoutsis, M., Landwehrmeyer, G.B., Reilmann, R., Borowsky, B., Johnson, H., Mills, J.A., Owen, G., Stout, J., Scahill, R.I., Long, J.D., Rees, G., Tabrizi, S.J., 2015. Compensation in Preclinical Huntington’s Disease: Evidence From the Track-On HD Study. *EBioMedicine* 2, 1420–1429. <https://doi.org/10.1016/j.ebiom.2015.08.002>
- Klunk, W.E., Engler, H., Nordberg, A., Wang, Y., Blomqvist, G., Holt, D.P., Bergström, M., Savitcheva, I., Huang, G.-F., Estrada, S., Ausén, B., Debnath, M.L., Barletta, J., Price, J.C., Sandell, J., Lopresti, B.J., Wall, A., Koivisto, P., Antoni, G., Mathis, C.A., Långström, B., 2004. Imaging brain amyloid in Alzheimer’s disease with Pittsburgh Compound-B: Imaging Amyloid in AD with PIB. *Ann Neurol* 55, 306–319. <https://doi.org/10.1002/ana.20009>
- Klunk, W.E., Koeppe, R.A., Price, J.C., Benzinger, T.L., Devous, M.D., Jagust, W.J., Johnson, K.A., Mathis, C.A., Minhas, D., Pontecorvo, M.J., Rowe, C.C., Skovronsky, D.M., Mintun, M.A., 2015. The Centiloid Project: Standardizing quantitative amyloid plaque estimation by PET. *Alzheimer’s & Dementia* 11, 1. <https://doi.org/10.1016/j.jalz.2014.07.003>
- Kok, Z.Q., Murley, A.G., Rittman, T., Rowe, J., Passamonti, L., 2021. Co-Occurrence of Apathy and Impulsivity in Progressive Supranuclear Palsy. *Mov Disord Clin Pract* 8, 1225–1233. <https://doi.org/10.1002/mdc3.13339>
- Koole, M., van Aalst, J., Devrome, M., Mertens, N., Serdons, K., Lacroix, B., Mercier, J., Sciberras, D., Maguire, P., Van Laere, K., 2019. Quantifying SV2A density and drug occupancy in the human brain using [11C]UCB-J PET imaging and subcortical white matter as reference tissue. *Eur J Nucl Med Mol Imaging* 46, 396–406. <https://doi.org/10.1007/s00259-018-4119-8>
- Kosik, K.S., 2015. Personalized Medicine for Effective Alzheimer Disease Treatment. *JAMA Neurol* 72, 497. <https://doi.org/10.1001/jamaneurol.2014.3445>
- Kouri, N., Whitwell, J.L., Josephs, K.A., Rademakers, R., Dickson, D.W., 2011. Corticobasal degeneration: a pathologically distinct 4R tauopathy. *Nat Rev Neurol* 7, 263–272. <https://doi.org/10.1038/nrneurol.2011.43>
- Kovacs, G.G., 2015. Invited review: Neuropathology of tauopathies: principles and practice: Neuropathology of tauopathies. *Neuropathol Appl Neurobiol* 41, 3–23. <https://doi.org/10.1111/nan.12208>

- Kovacs, G.G., Lukic, M.J., Irwin, D.J., Arzberger, T., Respondek, G., Lee, E.B., Coughlin, D., Giese, A., Grossman, M., Kurz, C., McMillan, C.T., Gelpi, E., Compta, Y., van Swieten, J.C., Laats, L.D., Troakes, C., Al-Sarraj, S., Robinson, J.L., Roeber, S., Xie, S.X., Lee, V.M.-Y., Trojanowski, J.Q., Höglinger, G.U., 2020. Distribution patterns of tau pathology in progressive supranuclear palsy. *Acta Neuropathol* 140, 99–119. <https://doi.org/10.1007/s00401-020-02158-2>
- Kullmann, D.M., 2020. Editorial. *Brain* 143, 1045–1045. <https://doi.org/10.1093/brain/awaa082>
- Kumfor, F., Landin-Romero, R., Devenney, E., Hutchings, R., Grasso, R., Hodges, J.R., Piguet, O., 2016. On the right side? A longitudinal study of left- versus right-lateralized semantic dementia. *Brain* 139, 986–998. <https://doi.org/10.1093/brain/awv387>
- Kwong, K.K., Belliveau, J.W., Chesler, D.A., Goldberg, I.E., Weisskoff, R.M., Poncelet, B.P., Kennedy, D.N., Hoppel, B.E., Cohen, M.S., Turner, R., 1992. Dynamic magnetic resonance imaging of human brain activity during primary sensory stimulation. *Proc. Natl. Acad. Sci. U.S.A.* 89, 5675–5679. <https://doi.org/10.1073/pnas.89.12.5675>
- Laguerre, R.A., 2021. Evaluating hypotheses with dominance analysis. *Ind. Organ. Psychol.* 14, 514–517. <https://doi.org/10.1017/iop.2021.109>
- Laird, N.M., Ware, J.H., 1982. Random-effects models for longitudinal data. *Biometrics* 38, 963–974.
- Lansdall, C.J., Coyle-Gilchrist, I.T.S., Jones, P.S., Vázquez Rodríguez, P., Wilcox, A., Wehmann, E., Dick, K.M., Robbins, T.W., Rowe, J.B., 2017. Apathy and impulsivity in frontotemporal lobar degeneration syndromes. *Brain* 140, 1792–1807. <https://doi.org/10.1093/brain/awx101>
- Lansdall, C.J., Coyle-Gilchrist, I.T.S., Vázquez Rodríguez, P., Wilcox, A., Wehmann, E., Robbins, T.W., Rowe, J.B., 2019. Prognostic importance of apathy in syndromes associated with frontotemporal lobar degeneration. *Neurology* 92, e1547–e1557. <https://doi.org/10.1212/WNL.0000000000007249>
- Laumann, T.O., Snyder, A.Z., Mitra, A., Gordon, E.M., Gratton, C., Adeyemo, B., Gilmore, A.W., Nelson, S.M., Berg, J.J., Greene, D.J., McCarthy, J.E., Tagliazucchi, E., Laufs, H., Schlaggar, B.L., Dosenbach, N.U.F., Petersen, S.E., 2017. On the Stability of BOLD fMRI Correlations. *Cerebral cortex (New York, N.Y. : 1991)*. <https://doi.org/10.1093/cercor/bhw265>
- Lee, J.S., Jung, N.-Y., Jang, Y.K., Kim, H.J., Seo, S.W., Lee, J., Kim, Y.J., Lee, J.-H., Kim, B.C., Park, K.-W., Yoon, S.J., Jeong, J.H., Kim, S.Y., Kim, S.H., Kim, E.-J., Park, K.-C., Knopman, D.S., Na, D.L., 2017. Prognosis of Patients with Behavioral Variant Frontotemporal Dementia Who have Focal Versus Diffuse Frontal Atrophy. *J Clin Neurol* 13, 234. <https://doi.org/10.3988/jcn.2017.13.3.234>
- Lee, S.E., Khazenzon, A.M., Trujillo, A.J., Guo, C.C., Yokoyama, J.S., Sha, S.J., Takada, L.T., Karydas, A.M., Block, N.R., Coppola, G., Pribadi, M., Geschwind, D.H., Rademakers, R., Fong, J.C., Weiner, M.W., Boxer, A.L., Kramer, J.H., Rosen, H.J., Miller, B.L., Seeley, W.W., 2014. Altered network connectivity in frontotemporal dementia with C9orf72 hexanucleotide repeat expansion. *Brain* 137, 3047–3060. <https://doi.org/10.1093/brain/awu248>
- Lee, S.E., Rabinovici, G.D., Mayo, M.C., Wilson, S.M., Seeley, W.W., DeArmond, S.J., Huang, E.J., Trojanowski, J.Q., Growdon, M.E., Jang, J.Y., Sidhu, M., See, T.M., Karydas, A.M., Gorno-Tempini, M.-L., Boxer, A.L., Weiner, M.W., Geschwind, M.D., Rankin, K.P., Miller, B.L., 2011. Clinicopathological correlations in

- corticobasal degeneration. *Ann Neurol.* 70, 327–340. <https://doi.org/10.1002/ana.22424>
- Lee, S.E., Sias, A.C., Kosik, E.L., Flagan, T.M., Deng, J., Chu, S.A., Brown, J.A., Vidovszky, A.A., Ramos, E.M., Gorno-Tempini, M.L., Karydas, A.M., Coppola, G., Geschwind, D.H., Rademakers, R., Boeve, B.F., Boxer, A.L., Rosen, H.J., Miller, B.L., Seeley, W.W., 2019. Thalamo-cortical network hyperconnectivity in preclinical progranulin mutation carriers. *NeuroImage: Clinical* 22, 101751. <https://doi.org/10.1016/j.nicl.2019.101751>
- Lee, V.M.-Y., Goedert, M., Trojanowski, J.Q., 2001. Neurodegenerative Tauopathies. *Annu. Rev. Neurosci.* 24, 1121–1159. <https://doi.org/10.1146/annurev.neuro.24.1.1121>
- Leonardi, N., Van De Ville, D., 2015. On spurious and real fluctuations of dynamic functional connectivity during rest. *NeuroImage* 104, 430–436. <https://doi.org/10.1016/j.neuroimage.2014.09.007>
- Leslie, F.V.C., Foxe, D., Daveson, N., Flannagan, E., Hodges, J.R., Piguet, O., 2016. FRONTIER Executive Screen: a brief executive battery to differentiate frontotemporal dementia and Alzheimer’s disease. *J Neurol Neurosurg Psychiatry* 87, 831–835. <https://doi.org/10.1136/jnnp-2015-311917>
- Leuthardt, E.C., Guzman, G., Bandt, S.K., Hacker, C., Vellimana, A.K., Limbrick, D., Milchenko, M., Lamontagne, P., Speidel, B., Roland, J., Miller-Thomas, M., Snyder, A.Z., Marcus, D., Shimony, J., Benzinger, T.L.S., 2018. Integration of resting state functional MRI into clinical practice - A large single institution experience. *PLoS ONE* 13, e0198349. <https://doi.org/10.1371/journal.pone.0198349>
- Leuzy, A., Chiotis, K., Lemoine, L., Gillberg, P.-G., Almkvist, O., Rodriguez-Vieitez, E., Nordberg, A., 2019. Tau PET imaging in neurodegenerative tauopathies—still a challenge. *Mol Psychiatry* 24, 1112–1134. <https://doi.org/10.1038/s41380-018-0342-8>
- Lewis-Smith, D.J., Wolpe, N., Ghosh, B.C.P., Rowe, J.B., 2020. Alien limb in the corticobasal syndrome: phenomenological characteristics and relationship to apraxia. *J Neurol* 267, 1147–1157. <https://doi.org/10.1007/s00415-019-09672-8>
- Liang, X., Zou, Q., He, Y., Yang, Y., 2013. Coupling of functional connectivity and regional cerebral blood flow reveals a physiological basis for network hubs of the human brain. *Proc. Natl. Acad. Sci. U.S.A.* 110, 1929–1934. <https://doi.org/10.1073/pnas.1214900110>
- Liddel, S.A., Gattenplan, K.A., Clarke, L.E., Bennett, F.C., Bohlen, C.J., Schirmer, L., Bennett, M.L., Münch, A.E., Chung, W.-S., Peterson, T.C., Wilton, D.K., Frouin, A., Napier, B.A., Panicker, N., Kumar, M., Buckwalter, M.S., Rowitch, D.H., Dawson, V.L., Dawson, T.M., Stevens, B., Barres, B.A., 2017. Neurotoxic reactive astrocytes are induced by activated microglia. *Nature* 541, 481–487. <https://doi.org/10.1038/nature21029>
- Liégeois, R., Li, J., Kong, R., Orban, C., Van De Ville, D., Ge, T., Sabuncu, M.R., Yeo, B.T.T., 2019. Resting brain dynamics at different timescales capture distinct aspects of human behavior. *Nat Commun* 10, 2317. <https://doi.org/10.1038/s41467-019-10317-7>
- Ling, H., Macerollo, A., 2018. Is it Useful to Classify PSP and CBD as Different Disorders? Yes. *Mov Disord Clin Pract* 5, 145–148. <https://doi.org/10.1002/mdc3.12581>
- Ling, H., O’Sullivan, S.S., Holton, J.L., Revesz, T., Massey, L.A., Williams, D.R., Paviour, D.C., Lees, A.J., 2010. Does corticobasal degeneration exist? A clinicopathological re-evaluation. *Brain* 133, 2045–2057. <https://doi.org/10.1093/brain/awq123>

- Ling, H., Silva, R., Massey, L.A., Courtney, R., Hondhamuni, G., Bajaj, N., Lowe, J., Holton, J.L., Lees, A., Revesz, T., 2014. Characteristics of progressive supranuclear palsy presenting with corticobasal syndrome: a cortical variant. *Neuropathol Appl Neurobiol* 40, 149–163. <https://doi.org/10.1111/nan.12037>
- Lipton, A.M., Cullum, C.M., Satumtira, S., Sontag, E., Hynan, L.S., White III, C.L., Bigio, E.H., 2001. Contribution of Asymmetric Synapse Loss to Lateralizing Clinical Deficits in Frontotemporal Dementias. *Arch Neurol* 58, 1233. <https://doi.org/10.1001/archneur.58.8.1233>
- Litvan, I., 1997. Which clinical features differentiate progressive supranuclear palsy (Steele-Richardson-Olszewski syndrome) from related disorders? A clinicopathological study. *Brain* 120, 65–74. <https://doi.org/10.1093/brain/120.1.65>
- Litvan, I., Agid, Y., Calne, D., Campbell, G., Dubois, B., Duvoisin, R.C., Goetz, C.G., Golbe, L.I., Grafman, J., Growdon, J.H., Hallett, M., Jankovic, J., Quinn, N.P., Tolosa, E., Zee, D.S., 1996. Clinical research criteria for the diagnosis of progressive supranuclear palsy (Steele-Richardson-Olszewski syndrome): Report of the NINDS-SPSP International Workshop*. *Neurology* 47, 1–9. <https://doi.org/10.1212/WNL.47.1.1>
- Litvan, I., Lees, P.S.J., Cunningham, C.R., Rai, S.N., Cambon, A.C., Standaert, D.G., Marras, C., Juncos, J., Riley, D., Reich, S., Hall, D., Kluger, B., Bordelon, Y., Shprecher, D.R., for ENGENE-PSP, 2016. Environmental and occupational risk factors for progressive supranuclear palsy: Case-control study: Environmental & Occupational Risks for PSP. *Mov Disord* 31, 644–652. <https://doi.org/10.1002/mds.26512>
- Liu, T.T., 2016. Noise contributions to the fMRI signal: An overview. *NeuroImage* 143, 141–151. <https://doi.org/10.1016/j.neuroimage.2016.09.008>
- Liu, Y., Andreucci, A., Iwamoto, N., Yin, Y., Yang, H., Liu, F., Bulychev, A., Hu, X.S., Lin, X., Lamore, S., Patil, S., Mohapatra, S., Purcell-Estabrook, E., Taborn, K., Dale, E., Vargeese, C., 2022. Preclinical evaluation of WVE-004, an investigational stereopure oligonucleotide for the treatment of C9orf72-associated ALS or FTD. *Molecular Therapy - Nucleic Acids* 28, 558–570. <https://doi.org/10.1016/j.omtn.2022.04.007>
- Livingston, G., Huntley, J., Sommerlad, A., Ames, D., Ballard, C., Banerjee, S., Brayne, C., Burns, A., Cohen-Mansfield, J., Cooper, C., Costafreda, S.G., Dias, A., Fox, N., Gitlin, L.N., Howard, R., Kales, H.C., Kivimäki, M., Larson, E.B., Ogunniyi, A., Orgeta, V., Ritchie, K., Rockwood, K., Sampson, E.L., Samus, Q., Schneider, L.S., Selbæk, G., Teri, L., Mukadam, N., 2020. Dementia prevention, intervention, and care: 2020 report of the Lancet Commission. *The Lancet* 396, 413–446. [https://doi.org/10.1016/S0140-6736\(20\)30367-6](https://doi.org/10.1016/S0140-6736(20)30367-6)
- Logothetis, N.K., 2008. What we can do and what we cannot do with fMRI. *Nature* 453, 869–878. <https://doi.org/10.1038/nature06976>
- Lowe, V.J., Curran, G., Fang, P., Liesinger, A.M., Josephs, K.A., Parisi, J.E., Kantarci, K., Boeve, B.F., Pandey, M.K., Bruinsma, T., Knopman, D.S., Jones, D.T., Petrucelli, L., Cook, C.N., Graff-Radford, N.R., Dickson, D.W., Petersen, R.C., Jack, C.R., Murray, M.E., 2016. An autoradiographic evaluation of AV-1451 Tau PET in dementia. *acta neuropathol commun* 4, 58. <https://doi.org/10.1186/s40478-016-0315-6>
- Lu, C.S., Ikeda, A., Terada, K., Mima, T., Nagamine, T., Fukuyama, H., Kohara, N., Kojima, Y., Yonekura, Y., Chen, R.S., Tsai, C.H., Chu, N.S., Kimura, J., Shibasaki, H., 1998. Electrophysiological studies of early stage corticobasal degeneration. *Mov Disord* 13, 140–146. <https://doi.org/10.1002/mds.870130126>

- Lukic, M.J., Respondek, G., Kurz, C., Compta, Y., Gelpi, E., Ferguson, L.W., Rajput, A., Troakes, C., the MDS-endorsed PSP study group, van Swieten, J.C., Giese, A., Roeber, S., Herms, J., Arzberger, T., Höglinger, G., 2022. Long-Duration Progressive Supranuclear Palsy: Clinical Course and Pathological Underpinnings. *Annals of Neurology* 92, 637–649. <https://doi.org/10.1002/ana.26455>
- Lurie, D.J., Kessler, D., Bassett, D.S., Betzel, R.F., Breakspear, M., Kheilholz, S., Kucyi, A., Liégeois, R., Lindquist, M.A., McIntosh, A.R., Poldrack, R.A., Shine, J.M., Thompson, W.H., Bielczyk, N.Z., Douw, L., Kraft, D., Miller, R.L., Muthuraman, M., Pasquini, L., Razi, A., Vidaurre, D., Xie, H., Calhoun, V.D., 2019. Questions and controversies in the study of time-varying functional connectivity in resting fMRI. *Network Neuroscience* 4, 30–69. https://doi.org/10.1162/netn_a_00116
- Lynch, C.J., Power, J.D., Scult, M.A., Dubin, M., Gunning, F.M., Liston, C., 2020. Rapid Precision Functional Mapping of Individuals Using Multi-Echo fMRI. *Cell Reports* 33, 108540. <https://doi.org/10.1016/j.celrep.2020.108540>
- MacArthur, R.H., 1957. ON THE RELATIVE ABUNDANCE OF BIRD SPECIES. *Proc. Natl. Acad. Sci. U.S.A.* 43, 293–295. <https://doi.org/10.1073/pnas.43.3.293>
- Mackenzie, I.R.A., Neumann, M., 2016. Molecular neuropathology of frontotemporal dementia: insights into disease mechanisms from postmortem studies. *J. Neurochem.* 138, 54–70. <https://doi.org/10.1111/jnc.13588>
- Mackenzie, I.R.A., Neumann, M., Bigio, E.H., Cairns, N.J., Alafuzoff, I., Kril, J., Kovacs, G.G., Ghetti, B., Halliday, G., Holm, I.E., Ince, P.G., Kamphorst, W., Revesz, T., Rozemuller, A.J.M., Kumar-Singh, S., Akiyama, H., Baborie, A., Spina, S., Dickson, D.W., Trojanowski, J.Q., Mann, D.M.A., 2010. Nomenclature and nosology for neuropathologic subtypes of frontotemporal lobar degeneration: an update. *Acta Neuropathol* 119, 1–4. <https://doi.org/10.1007/s00401-009-0612-2>
- Mahoney, C.J., Simpson, I.J.A., Nicholas, J.M., Fletcher, P.D., Downey, L.E., Golden, H.L., Clark, C.N., Schmitz, N., Rohrer, J.D., Schott, J.M., Zhang, H., Ourselin, S., Warren, J.D., Fox, N.C., 2015. Longitudinal diffusion tensor imaging in frontotemporal dementia: Longitudinal DTI in FTD. *Ann Neurol.* 77, 33–46. <https://doi.org/10.1002/ana.24296>
- Malpetti, M., Jones, P.S., Cope, T.E., Holland, N., Naessens, M., Rouse, M.A., Rittman, T., Savulich, G., Whiteside, D.J., Street, D., Fryer, T.D., Hong, Y.T., Sephton, S.M., Aigbirhio, F.I., O'Brien, J.T., Rowe, J.B., 2022. Synaptic loss in frontotemporal dementia revealed by [¹¹C]UCB-J PET. *Annals of Neurology* ana.26543. <https://doi.org/10.1002/ana.26543>
- Malpetti, M., Jones, P.S., Tsvetanov, K.A., Rittman, T., Swieten, J.C., Borroni, B., Sanchez-Valle, R., Moreno, F., Laforce, R., Graff, C., Synofzik, M., Galimberti, D., Masellis, M., Tartaglia, M.C., Finger, E., Vandenberghe, R., Mendonça, A., Tagliavini, F., Santana, I., Ducharme, S., Butler, C.R., Gerhard, A., Levin, J., Danek, A., Otto, M., Frisoni, G.B., Ghidoni, R., Sorbi, S., Heller, C., Todd, E.G., Bocchetta, M., Cash, D.M., Convery, R.S., Peakman, G., Moore, K.M., Rohrer, J.D., Kievit, R.A., Rowe, J.B., Genetic FTD Initiative (GENFI), Afonso, S., Almeida, M.R., Anderl-Straub, S., Andersson, C., Antonell, A., Archetti, S., Arighi, A., Balasa, M., Barandiaran, M., Bargalló, N., Bartha, R., Bender, B., Benussi, A., Benussi, L., Bessi, V., Binetti, G., Black, S., Borrego-Ecija, S., Bras, J., Bruffaerts, R., Cañada, M., Caroppo, P., Castelo-Branco, M., Cope, T., Cosseddu, M., Di Fede, G., Díez, A., Duro, D., Fenoglio, C., Ferrari, C., Ferreira, C.B., Fox, N., Freedman, M., Fumagalli, G., Gabilondo, A., Gasparotti, R., Gauthier, S., Gazzina, S., Giaccone, G., Gorostidi, A., Greaves, C., Guerreiro, R., Hoegen, T., Indakoetxea,

- B., Jelic, V., Jiskoot, L., Karnath, H., Keren, R., Langheinrich, T., Leitão, M.J., Lladó, A., Lombardi, G., Loosli, S., Maruta, C., Mead, S., Meeter, L., Miltenberger, G., van Minkelen, R., Mitchell, S., Nacmias, B., Nicholas, J., Öijerstedt, L., Olives, J., Ourselin, S., Padovani, A., Panman, J., Papma, J., Pievani, M., Pijnenburg, Y., Polito, C., Premi, E., Prioni, S., Prix, C., Rademakers, R., Redaelli, V., Rogaeva, E., Rosa-Neto, P., Rossi, G., Rosser, M., Santiago, B., Scarpini, E., Schönecker, S., Semler, E., Shafei, R., Shoesmith, C., Tábuas-Pereira, M., Tainta, M., Taipa, R., Tang-Wai, D., Thomas, D.L., Thompson, P., Thonberg, H., Timberlake, C., Tiraboschi, P., Van Damme, P., Vandenbulcke, M., Veldsman, M., Verdelho, A., Villanua, J., Warren, J., Wilke, C., Woollacott, I., Wlasich, E., Zetterberg, H., Zulaica, M., 2021a. Apathy in presymptomatic genetic frontotemporal dementia predicts cognitive decline and is driven by structural brain changes. *Alzheimer's & Dementia* 17, 969–983. <https://doi.org/10.1002/alz.12252>
- Malpetti, M., Kievit, R.A., Passamonti, L., Jones, P.S., Tsvetanov, K.A., Rittman, T., Mak, E., Nicastro, N., Bevan-Jones, W.R., Su, L., Hong, Y.T., Fryer, T.D., Aigbirhio, F.I., O'Brien, J.T., Rowe, J.B., 2020. Microglial activation and tau burden predict cognitive decline in Alzheimer's disease. *Brain* 143, 1588–1602. <https://doi.org/10.1093/brain/awaa088>
- Malpetti, M., Passamonti, L., Jones, P.S., Street, D., Rittman, T., Fryer, T.D., Hong, Y.T., Vázquez Rodríguez, P., Bevan-Jones, W.R., Aigbirhio, F.I., O'Brien, J.T., Rowe, J.B., 2021b. Neuroinflammation predicts disease progression in progressive supranuclear palsy. *J Neurol Neurosurg Psychiatry* 92, 769–775. <https://doi.org/10.1136/jnnp-2020-325549>
- Manyara, A.M., Ciani, O., Taylor, R.S., 2022. A call for better reporting of trials using surrogate primary endpoints. *A&D Transl Res & Clin Interv* 8. <https://doi.org/10.1002/trc2.12340>
- Marek, S., Tervo-Clemmens, B., Calabro, F.J., Montez, D.F., Kay, B.P., Hatoum, A.S., Donohue, M.R., Foran, W., Miller, R.L., Hendrickson, T.J., Malone, S.M., Kandala, S., Feczko, E., Miranda-Dominguez, O., Graham, A.M., Earl, E.A., Perrone, A.J., Cordova, M., Doyle, O., Moore, L.A., Conan, G.M., Uriarte, J., Snider, K., Lynch, B.J., Wilgenbusch, J.C., Pengo, T., Tam, A., Chen, J., Newbold, D.J., Zheng, A., Seider, N.A., Van, A.N., Metoki, A., Chauvin, R.J., Laumann, T.O., Greene, D.J., Petersen, S.E., Garavan, H., Thompson, W.K., Nichols, T.E., Yeo, B.T.T., Barch, D.M., Luna, B., Fair, D.A., Dosenbach, N.U.F., 2022. Reproducible brain-wide association studies require thousands of individuals. *Nature* 603, 654–660. <https://doi.org/10.1038/s41586-022-04492-9>
- Marek, S., Tervo-Clemmens, B., Nielsen, A.N., Wheelock, M.D., Miller, R.L., Laumann, T.O., Earl, E., Foran, W.W., Cordova, M., Doyle, O., Perrone, A., Miranda-Dominguez, O., Feczko, E., Sturgeon, D., Graham, A., Hermosillo, R., Snider, K., Galassi, A., Nagel, B.J., Ewing, S.W.F., Eggebrecht, A.T., Garavan, H., Dale, A.M., Greene, D.J., Barch, D.M., Fair, D.A., Luna, B., Dosenbach, N.U.F., 2019. Identifying reproducible individual differences in childhood functional brain networks: An ABCD study. *Developmental Cognitive Neuroscience* 40, 100706. <https://doi.org/10.1016/j.dcn.2019.100706>
- Margulies, D.S., Ghosh, S.S., Goulas, A., Falkiewicz, M., Huntenburg, J.M., Langs, G., Bezgin, G., Eickhoff, S.B., Castellanos, F.X., Petrides, M., Jefferies, E., Smallwood, J., 2016. Situating the default-mode network along a principal gradient of macroscale cortical organization. *Proc Natl Acad Sci USA* 113, 12574–12579. <https://doi.org/10.1073/pnas.1608282113>

- Markello, R.D., Hansen, J.Y., Liu, Z.-Q., Bazinet, V., Shafiei, G., Suárez, L.E., Blostein, N., Seidlitz, J., Baillet, S., Satterthwaite, T.D., Chakravarty, M.M., Raznahan, A., Masic, B., 2022. neuromaps: structural and functional interpretation of brain maps. *Nat Methods* 19, 1472–1479. <https://doi.org/10.1038/s41592-022-01625-w>
- Martin, W.R.W., Miles, M., Zhong, Q., Hartlein, J., Racette, B.A., Norris, S.A., Ushe, M., Maiti, B., Criswell, S., Davis, A.A., Kotzbauer, P.T., Cairns, N.J., Perrin, R.J., Perlmutter, J.S., 2021. Is Levodopa Response a Valid Indicator of Parkinson’s Disease? *Movement Disorders* 36, 948–954. <https://doi.org/10.1002/mds.28406>
- Mateen, F.J., Josephs, K.A., 2009. The clinical spectrum of stereotypies in frontotemporal lobar degeneration: Frontotemporal Lobar Degeneration. *Mov. Disord.* 24, 1237–1240. <https://doi.org/10.1002/mds.22555>
- Mathew, R., Bak, T.H., Hodges, J.R., 2012. Diagnostic criteria for corticobasal syndrome: a comparative study. *J Neurol Neurosurg Psychiatry* 83, 405–410. <https://doi.org/10.1136/jnnp-2011-300875>
- Mathuranath, P.S., Nestor, P.J., Berrios, G.E., Rakowicz, W., Hodges, J.R., 2000. A brief cognitive test battery to differentiate Alzheimer’s disease and frontotemporal dementia. *Neurology* 55, 1613–1620. <https://doi.org/10.1212/01.wnl.0000434309.85312.19>
- Matuskey, D., Tinaz, S., Wilcox, K.C., Naganawa, M., Toyonaga, T., Dias, M., Henry, S., Pittman, B., Ropchan, J., Nabulsi, N., Suridjan, I., Comley, R.A., Huang, Y., Finnema, S.J., Carson, R.E., 2020. Synaptic Changes in Parkinson Disease Assessed with in vivo Imaging. *Ann Neurol* 87, 329–338. <https://doi.org/10.1002/ana.25682>
- McCarthy, J., Collins, D.L., Ducharme, S., 2018. Morphometric MRI as a diagnostic biomarker of frontotemporal dementia: A systematic review to determine clinical applicability. *NeuroImage: Clinical* 20, 685–696. <https://doi.org/10.1016/j.nicl.2018.08.028>
- McColgan, P., Gregory, S., Razi, A., Seunarine, K.K., Gargouri, F., Durr, A., Roos, R.A.C., Leavitt, B.R., Scahill, R.I., Clark, C.A., Tabrizi, S.J., Rees, G., and the Track On-HD Investigators, 2017. White matter predicts functional connectivity in premanifest Huntington’s disease. *Ann Clin Transl Neurol* 4, 106–118. <https://doi.org/10.1002/acn3.384>
- McDonough, I.M., Nashiro, K., 2014. Network complexity as a measure of information processing across resting-state networks: evidence from the Human Connectome Project. *Frontiers in Human Neuroscience*.
- McElreath, R., 2020. *Statistical rethinking: a Bayesian course with examples in R and Stan*, Second edition. ed, Texts in statistical science series. CRC Press, Taylor & Francis Group, Boca Raton London New York.
- McIntosh, A.R., Vakorin, V., Kovacevic, N., Wang, H., Diaconescu, A., Protzner, A.B., 2014. Spatiotemporal dependency of age-related changes in brain signal variability. *Cerebral cortex (New York, N.Y. : 1991)*. <https://doi.org/10.1093/cercor/bht030>
- McNeish, D., Matta, T., 2018. Differentiating between mixed-effects and latent-curve approaches to growth modeling. *Behav Res* 50, 1398–1414. <https://doi.org/10.3758/s13428-017-0976-5>
- Mecca, A.P., Chen, M., O’Dell, R.S., Naganawa, M., Toyonaga, T., Godek, T.A., Harris, J.E., Bartlett, H.H., Zhao, W., Nabulsi, N.B., Wyk, B.C.V., Varma, P., Arnsten, A.F.T., Huang, Y., Carson, R.E., Dyck, C.H., 2020. In vivo measurement of widespread synaptic loss in Alzheimer’s disease with SV2A PET. *Alzheimer’s & Dementia* 16, 974–982. <https://doi.org/10.1002/alz.12097>

- Meer, J.N. van der, Breakspear, M., Chang, L.J., Sonkusare, S., Cocchi, L., 2020. Movie viewing elicits rich and reliable brain state dynamics. *Nature Communications* 11, 5004. <https://doi.org/10.1038/s41467-020-18717-w>
- Meeter, L.H., Kaat, L.D., Rohrer, J.D., van Swieten, J.C., 2017. Imaging and fluid biomarkers in frontotemporal dementia. *Nat Rev Neurol* 13, 406–419. <https://doi.org/10.1038/nrneurol.2017.75>
- Meisl, G., Hidari, E., Allinson, K., Rittman, T., DeVos, S.L., Sanchez, J.S., Xu, C.K., Duff, K.E., Johnson, K.A., Rowe, J.B., Hyman, B.T., Knowles, T.P.J., Klenerman, D., 2021. In vivo rate-determining steps of tau seed accumulation in Alzheimer’s disease. *Sci. Adv.* 7, eabh1448. <https://doi.org/10.1126/sciadv.abh1448>
- Mendez, M.F., Shapira, J.S., 2011. Loss of emotional insight in behavioral variant frontotemporal dementia or “frontal anosodiaphoria.” *Consciousness and Cognition* 20, 1690–1696. <https://doi.org/10.1016/j.concog.2011.09.005>
- Mesulam, M.-M., 2003. Primary Progressive Aphasia — A Language-Based Dementia. *N Engl J Med* 349, 1535–1542. <https://doi.org/10.1056/NEJMra022435>
- Mesulam, M.-M., Coventry, C., Bigio, E.H., Geula, C., Thompson, C., Bonakdarpour, B., Gefen, T., Rogalski, E.J., Weintraub, S., 2021. Nosology of Primary Progressive Aphasia and the Neuropathology of Language, in: Ghetti, B., Buratti, E., Boeve, B., Rademakers, R. (Eds.), *Frontotemporal Dementias, Advances in Experimental Medicine and Biology*. Springer International Publishing, Cham, pp. 33–49. https://doi.org/10.1007/978-3-030-51140-1_3
- Milicevic Sephton, S., Miklovicz, T., Russell, J.J., Doke, A., Li, L., Boros, I., Aigbirhio, F.I., 2020. Automated radiosynthesis of [¹¹C]UCB-J for imaging synaptic density by positron emission tomography. *J Label Compd Radiopharm* 63, 151–158. <https://doi.org/10.1002/jlcr.3828>
- Miller, B.L., Darby, A.L., Swartz, J.R., Yener, G.G., Mena, I., 1995. Dietary Changes, Compulsions and Sexual Behavior in Frontotemporal Degeneration. *Dement Geriatr Cogn Disord* 6, 195–199. <https://doi.org/10.1159/000106946>
- Miller, K.L., Alfaró-Almagro, F., Bangerter, N.K., Thomas, D.L., Yacoub, E., Xu, J., Bartsch, A.J., Jbabdi, S., Sotiropoulos, S.N., Andersson, J.L.R., Griffanti, L., Douaud, G., Okell, T.W., Weale, P., Dragonu, I., Garratt, S., Hudson, S., Collins, R., Jenkinson, M., Matthews, P.M., Smith, S.M., 2016. Multimodal population brain imaging in the UK Biobank prospective epidemiological study. *Nat Neurosci* 19, 1523–1536. <https://doi.org/10.1038/nn.4393>
- Mintun, M.A., Lo, A.C., Duggan Evans, C., Wessels, A.M., Ardayfio, P.A., Andersen, S.W., Shcherbinin, S., Sparks, J., Sims, J.R., Brys, M., Apostolova, L.G., Salloway, S.P., Skovronsky, D.M., 2021. Donanemab in Early Alzheimer’s Disease. *N Engl J Med* 384, 1691–1704. <https://doi.org/10.1056/NEJMoa2100708>
- Mioshi, E., Dawson, K., Mitchell, J., Arnold, R., Hodges, J.R., 2006. The Addenbrooke’s Cognitive Examination Revised (ACE-R): a brief cognitive test battery for dementia screening. *Int. J. Geriatr. Psychiatry* 21, 1078–1085. <https://doi.org/10.1002/gps.1610>
- Mioshi, E., Hsieh, S., Savage, S., Hornberger, M., Hodges, J.R., 2010. Clinical staging and disease progression in frontotemporal dementia. *Neurology* 74, 1591–1597. <https://doi.org/10.1212/WNL.0b013e3181e04070>
- Misdraji, E.L., Gass, C.S., 2010. The Trail Making Test and its neurobehavioral components. *Journal of Clinical and Experimental Neuropsychology* 32, 159–163. <https://doi.org/10.1080/13803390902881942>

- Mišić, B., Betzel, R.F., de Reus, M.A., van den Heuvel, M.P., Berman, M.G., McIntosh, A.R., Sporns, O., 2016. Network-Level Structure-Function Relationships in Human Neocortex. *Cereb. Cortex* 26, 3285–3296. <https://doi.org/10.1093/cercor/bhw089>
- Moguilner, S., García, A.M., Perl, Y.S., Tagliazucchi, E., Piguet, O., Kumfor, F., Reyes, P., Matallana, D., Sedeño, L., Ibáñez, A., 2021. Dynamic brain fluctuations outperform connectivity measures and mirror pathophysiological profiles across dementia subtypes: A multicenter study. *NeuroImage* 225, 117522. <https://doi.org/10.1016/j.neuroimage.2020.117522>
- Mohanty, D., Hay, K.R., Berkowitz, S., Patel, S., Lin, Y.-C., Kang, H., Claassen, D.O., 2021. Clinical implications of photophobia in progressive supranuclear palsy. *Clinical Parkinsonism & Related Disorders* 4, 100097. <https://doi.org/10.1016/j.prdoa.2021.100097>
- Moheb, N., Charuworn, K., Ashla, M.M., Desarant, R., Chavez, D., Mendez, M.F., 2019. Repetitive Behaviors in Frontotemporal Dementia: Compulsions or Impulsions? *JNP* 31, 132–136. <https://doi.org/10.1176/appi.neuropsych.18060148>
- Moore, K.M., Nicholas, J., Grossman, M., McMillan, C.T., Irwin, D.J., Massimo, L., Deerlin, V.M.V., Warren, J.D., Fox, N.C., Rossor, M.N., Mead, S., Bocchetta, M., Boeve, B.F., Knopman, D.S., Graff-Radford, N.R., Forsberg, L.K., Rademakers, R., Wszolek, Z.K., Swieten, J.C. van, Jiskoot, L.C., Meeter, L.H., Dopfer, E.G., Papma, J.M., Snowden, J.S., Saxon, J., Jones, M., Pickering-Brown, S., Ber, I.L., Camuzat, A., Brice, A., Caroppo, P., Ghidoni, R., Pievani, M., Benussi, L., Binetti, G., Dickerson, B.C., Lucente, D., Krivensky, S., Graff, C., Öijerstedt, L., Fallström, M., Thonberg, H., Ghoshal, N., Morris, J.C., Borroni, B., Benussi, A., Padovani, A., Galimberti, D., Scarpini, E., Fumagalli, G.G., Mackenzie, I.R., Hsiung, G.-Y.R., Sengdy, P., Boxer, A.L., Rosen, H., Taylor, J.B., Synofzik, M., Wilke, C., Sulzer, P., Hodges, J.R., Halliday, G., Kwok, J., Sanchez-Valle, R., Lladó, A., Borrego-Ecija, S., Santana, I., Almeida, M.R., Tábuas-Pereira, M., Moreno, F., Barandiaran, M., Indakoetxea, B., Levin, J., Danek, A., Rowe, J.B., Cope, T.E., Otto, M., Anderl-Straub, S., Mendonça, A. de, Maruta, C., Masellis, M., Black, S.E., Couratier, P., Lautrette, G., Huey, E.D., Sorbi, S., Nacmias, B., Laforce, R., Tremblay, M.-P.L., Vandenberghe, R., Damme, P.V., Rogalski, E.J., Weintraub, S., Gerhard, A., Onyike, C.U., Ducharme, S., Papageorgiou, S.G., Ng, A.S.L., Brodtmann, A., Finger, E., Guerreiro, R., Bras, J., Rohrer, J.D., Heller, C., Convery, R.S., Woollacott, I.O., Shafei, R.M., Graff-Radford, J., Jones, D.T., Dheel, C.M., Savica, R., Lapid, M.I., Baker, M., Fields, J.A., Gavrilova, R., Domoto-Reilly, K., Poos, J.M., Ende, E.L.V. der, Panman, J.L., Kaat, L.D., Seelaar, H., Richardson, A., Frisoni, G., Mega, A., Fostinelli, S., Chiang, H.-H., Alberici, A., Arighi, A., Fenoglio, C., Heuer, H., Miller, B., Karydas, A., Fong, J., Leitão, M.J., Santiago, B., Duro, D., Ferreira, Carlos, Gabilondo, A., Arriba, M.D., Tainta, M., Zulaica, M., Ferreira, Catarina, Semler, E., Ludolph, A., Landwehrmeyer, B., Volk, A.E., Miltenberger, G., Verdelho, A., Afonso, S., Tartaglia, M.C., Freedman, M., Rogaeva, E., Ferrari, C., Piaceri, I., Bessi, V., Lombardi, G., St-Onge, F., Doré, M.-C., Bruffaerts, R., Vandebulcke, M., Stock, J.V. den, Mesulam, M.M., Bigio, E., Koros, C., Papatriantafyllou, J., Kroupis, C., Stefanis, L., Shoesmith, C., Robertson, E., Coppola, G., Ramos, E.M.D.S., Geschwind, D., 2020. Age at symptom onset and death and disease duration in genetic frontotemporal dementia: an international retrospective cohort study. *The Lancet Neurology* 19, 145–156. [https://doi.org/10.1016/S1474-4422\(19\)30394-1](https://doi.org/10.1016/S1474-4422(19)30394-1)
- Morris, J.C., Schindler, S.E., McCue, L.M., Moulder, K.L., Benzinger, T.L.S., Cruchaga, C., Fagan, A.M., Grant, E., Gordon, B.A., Holtzman, D.M., Xiong, C., 2019.

- Assessment of Racial Disparities in Biomarkers for Alzheimer Disease. *JAMA Neurol* 76, 264. <https://doi.org/10.1001/jamaneurol.2018.4249>
- Morris, J.C., Weintraub, S., Chui, H.C., Cummings, J., DeCarli, C., Ferris, S., Foster, N.L., Galasko, D., Graff-Radford, N., Peskind, E.R., Beekly, D., Ramos, E.M., Kukull, W.A., 2006. The Uniform Data Set (UDS): Clinical and Cognitive Variables and Descriptive Data From Alzheimer Disease Centers. *Alzheimer Disease & Associated Disorders* 20, 210–216. <https://doi.org/10.1097/01.wad.0000213865.09806.92>
- Mowinckel, A., 2018. Circular plots in R and adding images. URL <https://drmwinkels.io/blog/2018-05-25-circular-plots-in-r-and-adding-images/>
- Murley, A.G., Coyle-Gilchrist, I., Rouse, M.A., Jones, P.S., Li, W., Wiggins, J., Lansdall, C., Rodríguez, P.V., Wilcox, A., Tsvetanov, K.A., Patterson, K., Lambon Ralph, M.A., Rowe, J.B., 2020a. Redefining the multidimensional clinical phenotypes of frontotemporal lobar degeneration syndromes. *Brain* 143, 1555–1571. <https://doi.org/10.1093/brain/awaa097>
- Murley, A.G., Rouse, M.A., Coyle-Gilchrist, I.T.S., Jones, P.S., Li, W., Wiggins, J., Lansdall, C., Vázquez Rodríguez, P., Wilcox, A., Patterson, K., Rowe, J.B., 2021. Predicting loss of independence and mortality in frontotemporal lobar degeneration syndromes. *J Neurol Neurosurg Psychiatry* 92, 737–744. <https://doi.org/10.1136/jnnp-2020-324903>
- Murley, A.G., Rouse, M.A., Jones, P.S., Ye, R., Hezemans, F.H., O’Callaghan, C., Frangou, P., Kourtzi, Z., Rua, C., Carpenter, T.A., Rodgers, C.T., Rowe, J.B., 2020b. GABA and glutamate deficits from frontotemporal lobar degeneration are associated with disinhibition. *Brain* 143, 3449–3462. <https://doi.org/10.1093/brain/awaa305>
- Murley, A.G., Rowe, J.B., 2018. Neurotransmitter deficits from frontotemporal lobar degeneration. *Brain*. <https://doi.org/10.1093/brain/awx327>
- Murphy, K., Fox, M.D., 2017. Towards a consensus regarding global signal regression for resting state functional connectivity MRI. *NeuroImage* 154, 169–173. <https://doi.org/10.1016/j.neuroimage.2016.11.052>
- Musall, S., Kaufman, M.T., Juavinett, A.L., Gluf, S., Churchland, A.K., 2019. Single-trial neural dynamics are dominated by richly varied movements. *Nat Neurosci* 22, 1677–1686. <https://doi.org/10.1038/s41593-019-0502-4>
- Neary, D., Snowden, J.S., Northen, B., Goulding, P., 1988. Dementia of frontal lobe type. *Journal of Neurology, Neurosurgery & Psychiatry* 51, 353–361. <https://doi.org/10.1136/jnnp.51.3.353>
- Nebel, M.B., Lidstone, D.E., Wang, L., Benkeser, D., Mostofsky, S.H., Risk, B.B., 2022. Accounting for motion in resting-state fMRI: What part of the spectrum are we characterizing in autism spectrum disorder? *NeuroImage* 257, 119296. <https://doi.org/10.1016/j.neuroimage.2022.119296>
- Neumann, M., Lee, E.B., Mackenzie, I.R., 2021. Frontotemporal Lobar Degeneration TDP-43-Immunoreactive Pathological Subtypes: Clinical and Mechanistic Significance, in: Ghetti, B., Buratti, E., Boeve, B., Rademakers, R. (Eds.), *Frontotemporal Dementias, Advances in Experimental Medicine and Biology*. Springer International Publishing, Cham, pp. 201–217. https://doi.org/10.1007/978-3-030-51140-1_13
- Neumann, M., Sampathu, D.M., Kwong, L.K., Truax, A.C., Micsenyi, M.C., Chou, T.T., Bruce, J., Schuck, T., Grossman, M., Clark, C.M., McCluskey, L.F., Miller, B.L., Masliah, E., Mackenzie, I.R., Feldman, H., Feiden, W., Kretschmar, H.A., Trojanowski, J.Q., Lee, V.M.-Y., 2006. Ubiquitinated TDP-43 in Frontotemporal

Lobar Degeneration and Amyotrophic Lateral Sclerosis. *Science* 314, 130–133.
<https://doi.org/10.1126/science.1134108>

- Nguyen, L., Laboissonniere, L.A., Guo, S., Pilotto, F., Scheidegger, O., Oestmann, A., Hammond, J.W., Li, H., Hyysalo, A., Peltola, R., Pattamatta, A., Zu, T., Voutilainen, M.H., Gelbard, H.A., Saxena, S., Ranum, L.P.W., 2020. Survival and Motor Phenotypes in FVB C9-500 ALS/FTD BAC Transgenic Mice Reproduced by Multiple Labs. *Neuron* 108, 784-796.e3.
<https://doi.org/10.1016/j.neuron.2020.09.009>
- Nichols, E., Steinmetz, J.D., Vollset, S.E., Fukutaki, K., Chalek, J., Abd-Allah, F., Abdoli, A., Abualhasan, A., Abu-Gharbieh, E., Akram, T.T., Al Hamad, H., Alahdab, F., Alanezi, F.M., Alipour, V., Almustanyir, S., Amu, H., Ansari, I., Arabloo, J., Ashraf, T., Astell-Burt, T., Ayano, G., Ayuso-Mateos, J.L., Baig, A.A., Barnett, A., Barrow, A., Baune, B.T., Béjot, Y., Bezabhe, W.M.M., Bezabih, Y.M., Bhagavathula, A.S., Bhaskar, S., Bhattacharyya, K., Bijani, A., Biswas, A., Bolla, S.R., Bloor, A., Brayne, C., Brenner, H., Burkart, K., Burns, R.A., Cámara, L.A., Cao, C., Carvalho, F., Castro-de-Araujo, L.F.S., Catalá-López, F., Cerin, E., Chavan, P.P., Cherbuin, N., Chu, D.-T., Costa, V.M., Couto, R.A.S., Dadras, O., Dai, X., Dandona, L., Dandona, R., De la Cruz-Góngora, V., Dhamnetiya, D., Dias da Silva, D., Diaz, D., Douiri, A., Edvardsson, D., Ekholuenetale, M., El Sayed, I., El-Jaafary, S.I., Eskandari, K., Eskandarieh, S., Esmailnejad, S., Fares, J., Faro, A., Farooque, U., Feigin, V.L., Feng, X., Fereshtehnejad, S.-M., Fernandes, E., Ferrara, P., Filip, I., Fillit, H., Fischer, F., Gaidhane, S., Galluzzo, L., Ghashghae, A., Ghith, N., Gialluisi, A., Gilani, S.A., Glavan, I.-R., Gnedovskaya, E.V., Golechha, M., Gupta, R., Gupta, V.B., Gupta, V.K., Haider, M.R., Hall, B.J., Hamidi, S., Hanif, A., Hankey, G.J., Haque, S., Hartono, R.K., Hasaballah, A.I., Hasan, M.T., Hassan, A., Hay, S.I., Hayat, K., Hegazy, M.I., Heidari, G., Heidari-Soureshjani, R., Herteliu, C., Househ, M., Hussain, R., Hwang, B.-F., Iacoviello, L., Iavicoli, I., Ilesanmi, O.S., Ilic, I.M., Ilic, M.D., Irvani, S.S.N., Iso, H., Iwagami, M., Jabbarinejad, R., Jacob, L., Jain, V., Jayapal, S.K., Jayawardena, R., Jha, R.P., Jonas, J.B., Joseph, N., Kalani, R., Kandel, A., Kandel, H., Karch, A., Kasa, A.S., Kassie, G.M., Keshavarz, P., Khan, M.A., Khatib, M.N., Khoja, T.A.M., Khubchandani, J., Kim, M.S., Kim, Y.J., Kisa, A., Kisa, S., Kivimäki, M., Koroshetz, W.J., Koyanagi, A., Kumar, G.A., Kumar, M., Lak, H.M., Leonard, M., Li, B., Lim, S.S., Liu, X., Liu, Y., Logroscino, G., Lorkowski, S., Lucchetti, G., Lutzky Saute, R., Magnani, F.G., Malik, A.A., Massano, J., Mehndiratta, M.M., Menezes, R.G., Meretoja, A., Mohajer, B., Mohamed Ibrahim, N., Mohammad, Y., Mohammed, A., Mokdad, A.H., Mondello, S., Moni, M.A.A., Moniruzzaman, M., Mossie, T.B., Nagel, G., Naveed, M., Nayak, V.C., Neupane Kandel, S., Nguyen, T.H., Oancea, B., Otstavnov, N., Otstavnov, S.S., Owolabi, M.O., Panda-Jonas, S., Pashazadeh Kan, F., Pasovic, M., Patel, U.K., Pathak, M., Peres, M.F.P., Perianayagam, A., Peterson, C.B., Phillips, M.R., Pinheiro, M., Piradov, M.A., Pond, C.D., Potashman, M.H., Pottoo, F.H., Prada, S.I., Radfar, A., Raggi, A., Rahim, F., Rahman, M., Ram, P., Ranasinghe, P., Rawaf, D.L., Rawaf, S., Rezaei, N., Rezapour, A., Robinson, S.R., Romoli, M., Roshandel, G., Sahathevan, R., Sahebkar, A., Sahraian, M.A., Sathian, B., Sattin, D., Sawhney, M., Saylan, M., Schiavolin, S., Seylani, A., Sha, F., Shaikh, M.A., Shaji, K., Shannawaz, M., Shetty, J.K., Shigematsu, M., Shin, J.I., Shiri, R., Silva, D.A.S., Silva, J.P., Silva, R., Singh, J.A., Skryabin, V.Y., Skryabina, A.A., Smith, A.E., Soshnikov, S., Spurlock, E.E., Stein, D.J., Sun, J., Tabarés-Seisdedos, R., Thakur, B., Timalina, B., Tovani-Palone, M.R., Tran, B.X., Tsegaye, G.W., Valadan Tahbaz, S., Valdez, P.R.,

- Venkatasubramanian, N., Vlassov, V., Vu, G.T., Vu, L.G., Wang, Y.-P., Wimo, A., Winkler, A.S., Yadav, L., Yahyazadeh Jabbari, S.H., Yamagishi, K., Yang, L., Yano, Y., Yonemoto, N., Yu, C., Yunusa, I., Zadey, S., Zastrozhin, M.S., Zastrozhina, A., Zhang, Z.-J., Murray, C.J.L., Vos, T., 2022. Estimation of the global prevalence of dementia in 2019 and forecasted prevalence in 2050: an analysis for the Global Burden of Disease Study 2019. *The Lancet Public Health* 7, e105–e125. [https://doi.org/10.1016/S2468-2667\(21\)00249-8](https://doi.org/10.1016/S2468-2667(21)00249-8)
- Nielsen, A.N., Greene, D.J., Gratton, C., Dosenbach, N.U.F., Petersen, S.E., Schlaggar, B.L., 2019. Evaluating the Prediction of Brain Maturity From Functional Connectivity After Motion Artifact Denoising. *Cerebral Cortex* 29, 2455–2469. <https://doi.org/10.1093/cercor/bhy117>
- NIH Biomarkers Definition Working Group, 2001. Biomarkers and surrogate endpoints: Preferred definitions and conceptual framework. *Clinical Pharmacology & Therapeutics* 69, 89–95. <https://doi.org/10.1067/mcp.2001.113989>
- Nimon, K., Lewis, M., Kane, R., Haynes, R.M., 2008. An R package to compute commonality coefficients in the multiple regression case: An introduction to the package and a practical example. *Behavior Research Methods* 40, 457–466. <https://doi.org/10.3758/BRM.40.2.457>
- Nimon, K.F., Oswald, F.L., 2013. Understanding the Results of Multiple Linear Regression: Beyond Standardized Regression Coefficients. *Organizational Research Methods* 16, 650–674. <https://doi.org/10.1177/1094428113493929>
- Noble, S., Mejia, A.F., Zalesky, A., Scheinost, D., 2022. Improving power in functional magnetic resonance imaging by moving beyond cluster-level inference. *Proc. Natl. Acad. Sci. U.S.A.* 119, e2203020119. <https://doi.org/10.1073/pnas.2203020119>
- Noble, S., Scheinost, D., Constable, R.T., 2019. A decade of test-retest reliability of functional connectivity: A systematic review and meta-analysis. *NeuroImage* 203, 116157. <https://doi.org/10.1016/j.neuroimage.2019.116157>
- Nørgaard, M., Beliveau, V., Ganz, M., Svarer, C., Pinborg, L.H., Keller, S.H., Jensen, P.S., Greve, D.N., Knudsen, G.M., 2021. A high-resolution in vivo atlas of the human brain’s benzodiazepine binding site of GABAA receptors. *NeuroImage* 232, 117878. <https://doi.org/10.1016/j.neuroimage.2021.117878>
- Nunemann, S., Last, D., Schuster, T., Förstl, H., Kurz, A., Diehl-Schmid, J., 2011. Survival in a German Population with Frontotemporal Lobar Degeneration. *Neuroepidemiology* 37, 160–165. <https://doi.org/10.1159/000331485>
- Ogawa, S., Tank, D.W., Menon, R., Ellermann, J.M., Kim, S.G., Merkle, H., Ugurbil, K., 1992. Intrinsic signal changes accompanying sensory stimulation: functional brain mapping with magnetic resonance imaging. *Proc. Natl. Acad. Sci. U.S.A.* 89, 5951–5955. <https://doi.org/10.1073/pnas.89.13.5951>
- O’Keefe, F.M., Murray, B., Coen, R.F., Dockree, P.M., Bellgrove, M.A., Garavan, H., Lynch, T., Robertson, I.H., 2007. Loss of insight in frontotemporal dementia, corticobasal degeneration and progressive supranuclear palsy. *Brain* 130, 753–764. <https://doi.org/10.1093/brain/awl367>
- Omidvarnia, A., Zalesky, A., Mansour L, S., Van De Ville, D., Jackson, G.D., Pedersen, M., 2021. Temporal complexity of fMRI is reproducible and correlates with higher order cognition. *NeuroImage* 230, 117760. <https://doi.org/10.1016/j.neuroimage.2021.117760>
- O’Rourke, J.G., Bogdanik, L., Yáñez, A., Lall, D., Wolf, A.J., Muhammad, A.K.M.G., Ho, R., Carmona, S., Vit, J.P., Zarrow, J., Kim, K.J., Bell, S., Harms, M.B., Miller, T.M., Dangler, C.A., Underhill, D.M., Goodridge, H.S., Lutz, C.M., Baloh, R.H.,

2016. *C9orf72* is required for proper macrophage and microglial function in mice. *Science* 351, 1324–1329. <https://doi.org/10.1126/science.aaf1064>
- Osaki, Y., Ben-Shlomo, Y., Lees, A.J., Daniel, S.E., Colosimo, C., Wenning, G., Quinn, N., 2004. Accuracy of clinical diagnosis of progressive supranuclear palsy. *Mov Disord.* 19, 181–189. <https://doi.org/10.1002/mds.10680>
- Ossenkuppele, R., Pijnenburg, Y.A.L., Perry, D.C., Cohn-Sheehy, B.I., Scheltens, N.M.E., Vogel, J.W., Kramer, J.H., van der Vlies, A.E., Joie, R.L., Rosen, H.J., van der Flier, W.M., Grinberg, L.T., Rozemuller, A.J., Huang, E.J., van Berckel, B.N.M., Miller, B.L., Barkhof, F., Jagust, W.J., Scheltens, P., Seeley, W.W., Rabinovici, G.D., 2015. The behavioural/dysexecutive variant of Alzheimer's disease: clinical, neuroimaging and pathological features. *Brain* 138, 2732–2749. <https://doi.org/10.1093/brain/awv191>
- Oxtoby, N.P., Young, A.L., Cash, D.M., Benzinger, T.L.S., Fagan, A.M., Morris, J.C., Bateman, R.J., Fox, N.C., Schott, J.M., Alexander, D.C., 2018. Data-driven models of dominantly-inherited Alzheimer's disease progression. *Brain* 141, 1529–1544. <https://doi.org/10.1093/brain/awy050>
- Padala, S.P., Yarns, B.C., 2022. Under-Represented Populations Left Out of Alzheimer's Disease Treatment with Aducanumab: Commentary on Ethics. *ADR* 6, 345–348. <https://doi.org/10.3233/ADR-220023>
- Palmqvist, S., Tideman, P., Cullen, N., Zetterberg, H., Blennow, K., the Alzheimer's Disease Neuroimaging Initiative, Dage, J.L., Stomrud, E., Janelidze, S., Mattsson-Carlsson, N., Hansson, O., 2021. Prediction of future Alzheimer's disease dementia using plasma phospho-tau combined with other accessible measures. *Nat Med* 27, 1034–1042. <https://doi.org/10.1038/s41591-021-01348-z>
- Pandya, S., Zeighami, Y., Freeze, B., Dadar, M., Collins, D.L., Dagher, A., Raj, A., 2019. Predictive model of spread of Parkinson's pathology using network diffusion. *NeuroImage*. <https://doi.org/10.1016/j.neuroimage.2019.03.001>
- Parkes, L., Fulcher, B., Yücel, M., Fornito, A., 2018. An evaluation of the efficacy, reliability, and sensitivity of motion correction strategies for resting-state functional MRI. *NeuroImage* 171, 415–436. <https://doi.org/10.1016/j.neuroimage.2017.12.073>
- Pasquini, L., Nana, A.L., Toller, G., Brown, J.A., Deng, J., Staffaroni, A., Kim, E.-J., Hwang, J.-H.L., Li, L., Park, Y., Gaus, S.E., Allen, I., Sturm, V.E., Spina, S., Grinberg, L.T., Rankin, K.P., Kramer, J.H., Rosen, H.J., Miller, B.L., Seeley, W.W., 2020. Salience Network Atrophy Links Neuron Type-Specific Pathobiology to Loss of Empathy in Frontotemporal Dementia. *Cerebral Cortex* 30, 5387–5399. <https://doi.org/10.1093/cercor/bhaa119>
- Passamonti, L., Tsvetanov, K.A., Jones, P.S., Bevan-Jones, W.R., Arnold, R., Borchert, R.J., Mak, E., Su, L., O'Brien, J.T., Rowe, J.B., 2019. Neuroinflammation and Functional Connectivity in Alzheimer's Disease: Interactive Influences on Cognitive Performance. *J. Neurosci.* 39, 7218–7226. <https://doi.org/10.1523/JNEUROSCI.2574-18.2019>
- Patel, A.X., Kundu, P., Rubinov, M., Jones, P.S., Vértes, P.E., Ersche, K.D., Suckling, J., Bullmore, E.T., 2014. A wavelet method for modeling and despiking motion artifacts from resting-state fMRI time series. *NeuroImage* 95, 287–304. <https://doi.org/10.1016/j.neuroimage.2014.03.012>
- Pedroza, P., Miller-Petrie, M.K., Chen, C., Chakrabarti, S., Chapin, A., Hay, S., Tsakalos, G., Wimo, A., Dieleman, J.L., 2022. Global and regional spending on dementia care from 2000–2019 and expected future health spending scenarios from 2020–2050:

- An economic modelling exercise. *eClinicalMedicine* 45, 101337. <https://doi.org/10.1016/j.eclinm.2022.101337>
- Peterson, K.A., Patterson, K., Rowe, J.B., 2019. Language impairment in progressive supranuclear palsy and corticobasal syndrome. *Journal of Neurology*. <https://doi.org/10.1007/s00415-019-09463-1>
- Pick, A., 1892. Über die Beziehungen der senilen Hirnatrophie zur Aphasie, in: *Prager MedicinischeWochenschnft*. pp. 165–167.
- Piguet, O., Halliday, G.M., Reid, W.G.J., Casey, B., Carman, R., Huang, Y., Xuereb, J.H., Hodges, J.R., Kril, J.J., 2011a. Clinical phenotypes in autopsy-confirmed Pick disease. *Neurology* 76, 253–259. <https://doi.org/10.1212/WNL.0b013e318207b1ce>
- Piguet, O., Hornberger, M., Mioshi, E., Hodges, J.R., 2011b. Behavioural-variant frontotemporal dementia: diagnosis, clinical staging, and management. *The Lancet Neurology* 10, 162–172. [https://doi.org/10.1016/S1474-4422\(10\)70299-4](https://doi.org/10.1016/S1474-4422(10)70299-4)
- Piguet, O., Kumfor, F., Hodges, J., 2017. Diagnosing, monitoring and managing behavioural variant frontotemporal dementia. *Medical Journal of Australia* 207, 303–308. <https://doi.org/10.5694/mja16.01458>
- Pilotto, A., Gazzina, S., Benussi, A., Manes, M., Dell’Era, V., Cristillo, V., Cosseddu, M., Turrone, R., Alberici, A., Padovani, A., Borroni, B., 2017. Mild Cognitive Impairment and Progression to Dementia in Progressive Supranuclear Palsy. *Neurodegener Dis* 17, 286–291. <https://doi.org/10.1159/000479110>
- Pincus, S.M., Goldberger, A.L., 1994. Physiological time-series analysis: what does regularity quantify? *Am J Physiol*. <https://doi.org/10.1152/ajpheart.1994.266.4.H1643>
- Planche, V., Manjon, J.V., Mansencal, B., Lanuza, E., Tourdias, T., Catheline, G., Coupé, P., 2022. Structural progression of Alzheimer’s disease over decades: the MRI staging scheme. *Brain Communications* 4, fcac109. <https://doi.org/10.1093/braincomms/fcac109>
- Poldrack, R.A., Baker, C.I., Durnez, J., Gorgolewski, K.J., Matthews, P.M., Munafò, M.R., Nichols, T.E., Poline, J.-B., Vul, E., Yarkoni, T., 2017. Scanning the horizon: towards transparent and reproducible neuroimaging research. *Nature Reviews Neuroscience*. <https://doi.org/10.1038/nrn.2016.167>
- Poldrack, R.A., Laumann, T.O., Koyejo, O., Gregory, B., Hover, A., Chen, M.-Y., Gorgolewski, K.J., Luci, J., Joo, S.J., Boyd, R.L., Hunicke-Smith, S., Simpson, Z.B., Caven, T., Sochat, V., Shine, J.M., Gordon, E., Snyder, A.Z., Adeyemo, B., Petersen, S.E., Glahn, D.C., Reese Mckay, D., Curran, J.E., Göring, H.H.H., Carless, M.A., Blangero, J., Dougherty, R., Leemans, A., Handwerker, D.A., Frick, L., Marcotte, E.M., Mumford, J.A., 2015. Long-term neural and physiological phenotyping of a single human. *Nat Commun* 6, 8885. <https://doi.org/10.1038/ncomms9885>
- Poorkaj, P., Bird, T.D., Wijsman, E., Nemens, E., Garruto, R.M., Anderson, L., Andreadis, A., Wiederholt, W.C., Raskind, M., Schellenberg, G.D., 1998. Tau is a candidate gene for chromosome 17 frontotemporal dementia. *Ann Neurol*. 43, 815–825. <https://doi.org/10.1002/ana.410430617>
- Power, J.D., 2019. Temporal ICA has not properly separated global fMRI signals: A comment on Glasser et al. (2018). *NeuroImage*. <https://doi.org/10.1016/j.neuroimage.2018.12.051>
- Power, J.D., Barnes, K.A., Snyder, A.Z., Schlaggar, B.L., Petersen, S.E., 2012. Spurious but systematic correlations in functional connectivity MRI networks arise from subject motion. *Neuroimage* 59, 2142–2154. <https://doi.org/10.1016/j.neuroimage.2011.10.018>

- Power, J.D., Lynch, C.J., Silver, B.M., Dubin, M.J., Martin, A., Jones, R.M., 2019. Distinctions among real and apparent respiratory motions in human fMRI data. *NeuroImage* 201, 116041. <https://doi.org/10.1016/j.neuroimage.2019.116041>
- Power, J.D., Plitt, M., Laumann, T.O., Martin, A., 2017. Sources and implications of whole-brain fMRI signals in humans. *NeuroImage* 146, 609–625. <https://doi.org/10.1016/j.neuroimage.2016.09.038>
- Premi, E., Calhoun, V.D., Diano, M., Gazzina, S., Cosseddu, M., Alberici, A., Archetti, S., Paternicò, D., Gasparotti, R., van Swieten, J., Galimberti, D., Sanchez-Valle, R., Laforce, R., Moreno, F., Synofzik, M., Graff, C., Masellis, M., Tartaglia, M.C., Rowe, J., Vandenberghe, R., Finger, E., Tagliavini, F., de Mendonça, A., Santana, I., Butler, C., Ducharme, S., Gerhard, A., Danek, A., Levin, J., Otto, M., Frisoni, G., Cappa, S., Sorbi, S., Padovani, A., Rohrer, J.D., Borroni, B., Almeida, M.R., Anderl-Straub, S., Andersson, C., Antonell, A., Arighi, A., Balasa, M., Barandiaran, M., Bargalló, N., Bartha, R., Bender, B., Benussi, L., Binetti, G., Black, S., Bocchetta, M., Borrego-Ecija, S., Bras, J., Bruffaerts, R., Caroppo, P., Cash, D., Castelo-Branco, M., Convery, R., Cope, T., de Arriba, M., Di Fede, G., Díaz, Z., Dick, K.M., Duro, D., Fenoglio, C., Ferreira, C., Ferreira, C.B., Flanagan, T., Fox, N., Freedman, M., Fumagalli, G., Gabilondo, A., Gauthier, S., Ghidoni, R., Giaccone, G., Gorostidi, A., Greaves, C., Guerreiro, R., Heller, C., Hoegen, T., Indakoetxea, B., Jelic, V., Jiskoot, L., Karnath, H.-O., Keren, R., Leitão, M.J., Lladó, A., Lombardi, G., Loosli, S., Maruta, C., Mead, S., Meeter, L., Miltenberger, G., van Minkelen, R., Mitchell, S., Nacmias, B., Neason, M., Nicholas, J., Öijerstedt, L., Olives, J., Panman, J., Papma, J., Patzig, M., Pievani, M., Prioni, S., Prix, C., Rademakers, R., Redaelli, V., Rittman, T., Rogaeva, E., Rosa-Neto, P., Rossi, G., Rossor, M., Santiago, B., Scarpini, E., Semler, E., Shafei, R., Shoesmith, C., Tábuas-Pereira, M., Tainta, M., Tang-Wai, D., Thomas, D.L., Thonberg, H., Timberlake, C., Tiraboschi, P., Vandamme, P., Vandenbulcke, M., Veldsman, M., Verdelho, A., Villanua, J., Warren, J., Wilke, C., Zetterberg, H., Zulaica, M., 2019. The inner fluctuations of the brain in presymptomatic Frontotemporal Dementia: The chronnectome fingerprint. *NeuroImage* 189, 645–654. <https://doi.org/10.1016/j.neuroimage.2019.01.080>
- Prusiner, S.B., 1984. Some Speculations about Prions, Amyloid, and Alzheimer's Disease. *N Engl J Med* 310, 661–663. <https://doi.org/10.1056/NEJM198403083101021>
- Przewodowska, D., Marzec, W., Madetko, N., 2021. Novel Therapies for Parkinsonian Syndromes—Recent Progress and Future Perspectives. *Front. Mol. Neurosci.* 14, 720220. <https://doi.org/10.3389/fnmol.2021.720220>
- Puonti, O., Iglesias, J.E., Van Leemput, K., 2016. Fast and sequence-adaptive whole-brain segmentation using parametric Bayesian modeling. *NeuroImage* 143, 235–249. <https://doi.org/10.1016/j.neuroimage.2016.09.011>
- Qin, L., Gao, J.-H., 2021. New avenues for functional neuroimaging: ultra-high field MRI and OPM-MEG. *Psychoradiology* 1, 165–171. <https://doi.org/10.1093/psyrad/kkab014>
- Quattrone, A., Nicoletti, G., Messina, D., Fera, F., Condino, F., Pugliese, P., Lanza, P., Barone, P., Morgante, L., Zappia, M., Aguglia, U., Gallo, O., 2008. MR Imaging Index for Differentiation of Progressive Supranuclear Palsy from Parkinson Disease and the Parkinson Variant of Multiple System Atrophy. *Radiology* 246, 214–221. <https://doi.org/10.1148/radiol.2453061703>
- Quinn, A.J., Vidaurre, D., Abeyesuriya, R., Becker, R., Nobre, A.C., Woolrich, M.W., 2018. Task-Evoked Dynamic Network Analysis Through Hidden Markov Modeling. *Frontiers in Neuroscience* 12, 603. <https://doi.org/10.3389/fnins.2018.00603>

- R Core Team, 2018. R: A language and environment for statistical computing. R Foundation for Statistical Computing, Vienna, Austria. URL <https://www.R-project.org/>.
- Rabiner, L., Juang, B., 1986. An introduction to hidden Markov models. *IEEE ASSP Mag.* 3, 4–16. <https://doi.org/10.1109/MASSP.1986.1165342>
- Ramon y Cajal, S., 1894. The Croonian lecture.—La fine structure des centres nerveux. *Proceedings of the Royal Society of London* 55, 444–468. <https://doi.org/10.1098/rspl.1894.0063>
- Ranasinghe, K.G., Rankin, K.P., Lobach, I.V., Kramer, J.H., Sturm, V.E., Bettcher, B.M., Possin, K., Christine You, S., Lamarre, A.K., Shany-Ur, T., Stephens, M.L., Perry, D.C., Lee, S.E., Miller, Z.A., Gorno-Tempini, M.L., Rosen, H.J., Boxer, A., Seeley, W.W., Rabinovici, G.D., Vossel, K.A., Miller, B.L., 2016. Cognition and neuropsychiatry in behavioral variant frontotemporal dementia by disease stage. *Neurology* 86, 600–610. <https://doi.org/10.1212/WNL.0000000000002373>
- Rascovsky, K., Hodges, J.R., Knopman, D., Mendez, M.F., Kramer, J.H., Neuhaus, J., van Swieten, J.C., Seelaar, H., Dopper, E.G.P., Onyike, C.U., Hillis, A.E., Josephs, K.A., Boeve, B.F., Kertesz, A., Seeley, W.W., Rankin, K.P., Johnson, J.K., Gorno-Tempini, M.-L., Rosen, H., Prioleau-Latham, C.E., Lee, A., Kipps, C.M., Lillo, P., Piguet, O., Rohrer, J.D., Rossor, M.N., Warren, J.D., Fox, N.C., Galasko, D., Salmon, D.P., Black, S.E., Mesulam, M., Weintraub, S., Dickerson, B.C., Diehl-Schmid, J., Pasquier, F., Deramecourt, V., Lebert, F., Pijnenburg, Y., Chow, T.W., Manes, F., Grafman, J., Cappa, S.F., Freedman, M., Grossman, M., Miller, B.L., 2011. Sensitivity of revised diagnostic criteria for the behavioural variant of frontotemporal dementia. *Brain* 134, 2456–2477. <https://doi.org/10.1093/brain/awr179>
- Ray, K.L., McKay, D.R., Fox, P.M., Riedel, M.C., Uecker, A.M., Beckmann, C.F., Smith, S.M., Fox, P.T., Laird, A.R., 2013. ICA model order selection of task co-activation networks. *Front. Neurosci.* 7. <https://doi.org/10.3389/fnins.2013.00237>
- Rebeiz, J.J., Kolodny, E.H., Richardson, E.P., 1968. Corticodentatonigral Degeneration With Neuronal Achromasia. *Archives of Neurology* 18, 20–33. <https://doi.org/10.1001/archneur.1968.00470310034003>
- Respondek, G., Stamelou, M., Kurz, C., Ferguson, L.W., Rajput, A., Chiu, W.Z., van Swieten, J.C., Troakes, C., al Sarraj, S., Gelpi, E., Gaig, C., Tolosa, E., Oertel, W.H., Giese, A., Roeber, S., Arzberger, T., Wagenpfeil, S., Höglinger, G.U., for the Movement Disorder Society-endorsed PSP Study Group, 2014. The phenotypic spectrum of progressive supranuclear palsy: A retrospective multicenter study of 100 definite cases: PSP Diagnostic Criteria. *Mov Disord.* 29, 1758–1766. <https://doi.org/10.1002/mds.26054>
- Reyes, P., Ortega-Merchan, M.P., Rueda, A., Uriza, F., Santamaria-García, H., Rojas-Serrano, N., Rodriguez-Santos, J., Velasco-Leon, M.C., Rodriguez-Parra, J.D., Mora-Diaz, D.E., Matallana, D., 2018. Functional Connectivity Changes in Behavioral, Semantic, and Nonfluent Variants of Frontotemporal Dementia. *Behavioural Neurology* 2018, 1–10. <https://doi.org/10.1155/2018/9684129>
- Richman, J.S., Moorman, J.R., 2000. Physiological time-series analysis using approximate entropy and sample entropy. *Am J Physiol Heart Circ Physiol.* <https://doi.org/10.1152/ajpheart.2000.278.6.H2039>
- Rittman, T., 2020. Neurological update: neuroimaging in dementia. *J Neurol* 267, 3429–3435. <https://doi.org/10.1007/s00415-020-10040-0>
- Rittman, T., Borchert, R., Jones, S., van Swieten, J., Borroni, B., Galimberti, D., Masellis, M., Tartaglia, M.C., Graff, C., Tagliavini, F., Frisoni, G.B., Laforce, Jr., Robert,

- Finger, E., Mendonça, A., Sorbi, S., Rohrer, J.D., Rowe, J.B., Genetic Frontotemporal Dementia, I., 2019. Functional network resilience to pathology in presymptomatic genetic frontotemporal dementia. *Neurobiology of aging*. <https://doi.org/10.1016/j.neurobiolaging.2018.12.009>
- Rittman, T., Coyle-Gilchrist, I.T., Rowe, J.B., 2016a. Managing cognition in progressive supranuclear palsy. *Neurodegenerative disease management*. <https://doi.org/10.2217/nmt-2016-0027>
- Rittman, T., Rubinov, M., Vértes, P.E., Patel, A.X., Ginestet, C.E., Ghosh, B.C.P., Barker, R.A., Spillantini, M.G., Bullmore, E.T., Rowe, J.B., 2016b. Regional expression of the MAPT gene is associated with loss of hubs in brain networks and cognitive impairment in Parkinson disease and progressive supranuclear palsy. *Neurobiology of aging*. <https://doi.org/10.1016/j.neurobiolaging.2016.09.001>
- Rizzoli, S.O., Betz, W.J., 2005. Synaptic vesicle pools. *Nat Rev Neurosci* 6, 57–69. <https://doi.org/10.1038/nrn1583>
- Robinson, G., Shallice, T., Cipolotti, L., 2006. Dynamic aphasia in progressive supranuclear palsy: A deficit in generating a fluent sequence of novel thought. *Neuropsychologia* 44, 1344–1360. <https://doi.org/10.1016/j.neuropsychologia.2006.01.002>
- Rogalski, E., Johnson, N., Weintraub, S., Mesulam, M., 2008. Increased Frequency of Learning Disability in Patients With Primary Progressive Aphasia and Their First-Degree Relatives. *Arch Neurol* 65. <https://doi.org/10.1001/archneurol.2007.34>
- Rohrer, J.D., Boxer, A.L., 2021. The Frontotemporal Dementia Prevention Initiative: Linking Together Genetic Frontotemporal Dementia Cohort Studies, in: Ghetti, B., Buratti, E., Boeve, B., Rademakers, R. (Eds.), *Frontotemporal Dementias, Advances in Experimental Medicine and Biology*. Springer International Publishing, Cham, pp. 113–121. https://doi.org/10.1007/978-3-030-51140-1_8
- Rohrer, J.D., Guerreiro, R., Vandrovцова, J., Uphill, J., Reiman, D., Beck, J., Isaacs, A.M., Authier, A., Ferrari, R., Fox, N.C., Mackenzie, I.R.A., Warren, J.D., de Silva, R., Holton, J., Revesz, T., Hardy, J., Mead, S., Rossor, M.N., 2009. The heritability and genetics of frontotemporal lobar degeneration. *Neurology* 73, 1451–1456. <https://doi.org/10.1212/WNL.0b013e3181bf997a>
- Rohrer, J.D., Lashley, T., Schott, J.M., Warren, J.E., Mead, S., Isaacs, A.M., Beck, J., Hardy, J., de Silva, R., Warrington, E., Troakes, C., Al-Sarraj, S., King, A., Borroni, B., Clarkson, M.J., Ourselin, S., Holton, J.L., Fox, N.C., Revesz, T., Rossor, M.N., Warren, J.D., 2011. Clinical and neuroanatomical signatures of tissue pathology in frontotemporal lobar degeneration. *Brain* 134, 2565–2581. <https://doi.org/10.1093/brain/awr198>
- Rohrer, J.D., Nicholas, J.M., Cash, D.M., Swieten, J. van, Dopper, E., Jiskoot, L., Minkelen, R. van, Rombouts, S.A., Cardoso, M.J., Clegg, S., Espak, M., Mead, S., Thomas, D.L., Vita, E.D., Masellis, M., Black, S.E., Freedman, M., Keren, R., MacIntosh, B.J., Rogaeva, E., Tang-Wai, D., Tartaglia, M.C., Laforce, R., Tagliavini, F., Tiraboschi, P., Redaelli, V., Prioni, S., Grisoli, M., Borroni, B., Padovani, A., Galimberti, D., Scarpini, E., Arighi, A., Fumagalli, G., Rowe, J.B., Coyle-Gilchrist, I., Graff, C., Fallström, M., Jelic, V., Ståhlbom, A.K., Andersson, C., Thonberg, H., Lilius, L., Frisoni, G.B., Binetti, G., Pievani, M., Bocchetta, M., Benussi, L., Ghidoni, R., Finger, E., Sorbi, S., Nacmias, B., Lombardi, G., Polito, C., Warren, J.D., Ourselin, S., Fox, N.C., Rossor, M.N., 2015. Presymptomatic cognitive and neuroanatomical changes in genetic frontotemporal dementia in the Genetic Frontotemporal dementia Initiative (GENFI) study: a cross-sectional

- analysis. *The Lancet Neurology* 14, 253–262. [https://doi.org/10.1016/S1474-4422\(14\)70324-2](https://doi.org/10.1016/S1474-4422(14)70324-2)
- Rohrer, J.D., Warren, J.D., 2010. Phenomenology and anatomy of abnormal behaviours in primary progressive aphasia. *Journal of the Neurological Sciences* 293, 35–38. <https://doi.org/10.1016/j.jns.2010.03.012>
- Rojas, J.C., Karydas, A., Bang, J., Tsai, R.M., Blennow, K., Liman, V., Kramer, J.H., Rosen, H., Miller, B.L., Zetterberg, H., Boxer, A.L., 2016. Plasma neurofilament light chain predicts progression in progressive supranuclear palsy. *Ann Clin Transl Neurol* 3, 216–225. <https://doi.org/10.1002/acn3.290>
- Rosen, H.J., Allison, S.C., Ogar, J.M., Amici, S., Rose, K., Dronkers, N., Miller, B.L., Gorno-Tempini, M.L., 2006. Behavioral features in semantic dementia vs other forms of progressive aphasia. *Neurology* 67, 1752–1756. <https://doi.org/10.1212/01.wnl.0000247630.29222.34>
- Rosen, H.J., Gorno-Tempini, M.L., Goldman, W.P., Perry, R.J., Schuff, N., Weiner, M., Feiwell, R., Kramer, J.H., Miller, B.L., 2002. Patterns of brain atrophy in frontotemporal dementia and semantic dementia. *Neurology* 58, 198–208. <https://doi.org/10.1212/WNL.58.2.198>
- Rosenberg, M.D., Finn, E.S., Scheinost, D., Papademetris, X., Shen, X., Constable, R.T., Chun, M.M., 2016. A neuromarker of sustained attention from whole-brain functional connectivity. *Nature Neuroscience* 19, 165–171. <https://doi.org/10.1038/nn.4179>
- Roskopf, J., Gorges, M., Müller, H.-P., Lulé, D., Uttner, I., Ludolph, A.C., Pinkhardt, E., Juengling, F.D., Kassubek, J., 2017. Intrinsic functional connectivity alterations in progressive supranuclear palsy: Differential effects in frontal cortex, motor, and midbrain networks. *Mov Disord* 32, 1006–1015. <https://doi.org/10.1002/mds.27039>
- Rosso, S.M., 2003. Medical and environmental risk factors for sporadic frontotemporal dementia: a retrospective case-control study. *Journal of Neurology, Neurosurgery & Psychiatry* 74, 1574–1576. <https://doi.org/10.1136/jnnp.74.11.1574>
- Rosso, S.M., Roks, G., Stevens, M., de Koning, I., Tanghe, H.L.J., Kamphorst, W., Ravid, R., Niermeijer, M.F., van Swieten, J.C., 2001. Complex compulsive behaviour in the temporal variant of frontotemporal dementia. *Journal of Neurology* 248, 965–970. <https://doi.org/10.1007/s004150170049>
- Rowe, J.B., 2019. Parkinsonism in frontotemporal dementias, in: *International Review of Neurobiology*. Elsevier, pp. 249–275. <https://doi.org/10.1016/bs.irn.2019.10.012>
- Roy, D.S., Zhang, Y., Halassa, M.M., Feng, G., 2022. Thalamic subnetworks as units of function. *Nat Neurosci* 25, 140–153. <https://doi.org/10.1038/s41593-021-00996-1>
- Royal College of Psychiatrists, 2022. National Audit of Dementia Memory Assessment Services Spotlight Audit 2021.
- Rusz, J., Bonnet, C., Klempíř, J., Tykalová, T., Baborová, E., Novotný, M., Rulseh, A., Růžička, E., 2015. Speech disorders reflect differing pathophysiology in Parkinson's disease, progressive supranuclear palsy and multiple system atrophy. *Journal of Neurology*. <https://doi.org/10.1007/s00415-015-7671-1>
- Ryman, D.C., Acosta-Baena, N., Aisen, P.S., Bird, T., Danek, A., Fox, N.C., Goate, A., Frommelt, P., Ghetti, B., Langbaum, J.B.S., Lopera, F., Martins, R., Masters, C.L., Mayeux, R.P., McDade, E., Moreno, S., Reiman, E.M., Ringman, J.M., Salloway, S., Schofield, P.R., Sperling, R., Tariot, P.N., Xiong, C., Morris, J.C., Bateman, R.J., And the Dominantly Inherited Alzheimer Network, 2014. Symptom onset in autosomal dominant Alzheimer disease: A systematic review and meta-analysis. *Neurology* 83, 253–260. <https://doi.org/10.1212/WNL.0000000000000596>

- Sakae, N., Josephs, K.A., Litvan, I., Murray, M.E., Duara, R., Uitti, R.J., Wszolek, Z.K., Graff-Radford, N.R., Dickson, D.W., 2019. Neuropathologic basis of frontotemporal dementia in progressive supranuclear palsy. *Mov Disord* 34, 1655–1662. <https://doi.org/10.1002/mds.27816>
- Salimi-Khorshidi, G., Douaud, G., Beckmann, C.F., Glasser, M.F., Griffanti, L., Smith, S.M., 2014. Automatic denoising of functional MRI data: Combining independent component analysis and hierarchical fusion of classifiers. *NeuroImage* 90, 449–468. <https://doi.org/10.1016/j.neuroimage.2013.11.046>
- Sampathu, D.M., Neumann, M., Kwong, L.K., Chou, T.T., Micsenyi, M., Truax, A., Bruce, J., Grossman, M., Trojanowski, J.Q., Lee, V.M.-Y., 2006. Pathological Heterogeneity of Frontotemporal Lobar Degeneration with Ubiquitin-Positive Inclusions Delineated by Ubiquitin Immunohistochemistry and Novel Monoclonal Antibodies. *The American Journal of Pathology* 169, 1343–1352. <https://doi.org/10.2353/ajpath.2006.060438>
- Sandiego, C.M., Gallezot, J.-D., Lim, K., Ropchan, J., Lin, S., Gao, H., Morris, E.D., Cosgrove, K.P., 2015. Reference Region Modeling Approaches for Amphetamine Challenge Studies with [¹¹C]FLB 457 and PET. *J Cereb Blood Flow Metab* 35, 623–629. <https://doi.org/10.1038/jcbfm.2014.237>
- Santos-Santos, M.A., Mandelli, M.L., Binney, R.J., Ogar, J., Wilson, S.M., Henry, M.L., Hubbard, H.I., Meese, M., Attygalle, S., Rosenberg, L., Pakvasa, M., Trojanowski, J.Q., Grinberg, L.T., Rosen, H., Boxer, A.L., Miller, B.L., Seeley, W.W., Gorno-Tempini, M.L., 2016. Features of Patients With Nonfluent/Agrammatic Primary Progressive Aphasia With Underlying Progressive Supranuclear Palsy Pathology or Corticobasal Degeneration. *JAMA Neurol* 73, 733. <https://doi.org/10.1001/jamaneurol.2016.0412>
- Satterthwaite, T.D., Wolf, D.H., Loughhead, J., Ruparel, K., Elliott, M.A., Hakonarson, H., Gur, R.C., Gur, R.E., 2012. Impact of in-scanner head motion on multiple measures of functional connectivity: Relevance for studies of neurodevelopment in youth. *NeuroImage* 60, 623–632. <https://doi.org/10.1016/j.neuroimage.2011.12.063>
- Savli, M., Bauer, A., Mitterhauser, M., Ding, Y.-S., Hahn, A., Kroll, T., Neumeister, A., Haeusler, D., Ungersboeck, J., Henry, S., Isfahani, S.A., Rattay, F., Wadsak, W., Kasper, S., Lanzenberger, R., 2012. Normative database of the serotonergic system in healthy subjects using multi-tracer PET. *NeuroImage* 63, 447–459. <https://doi.org/10.1016/j.neuroimage.2012.07.001>
- Saxena, S., Caroni, P., 2011. Selective Neuronal Vulnerability in Neurodegenerative Diseases: from Stressor Thresholds to Degeneration. *Neuron* 71, 35–48. <https://doi.org/10.1016/j.neuron.2011.06.031>
- Schork, N.J., 2015. Personalized medicine: Time for one-person trials. *Nature* 520, 609–611. <https://doi.org/10.1038/520609a>
- Seeley, W.W., 2017. Mapping Neurodegenerative Disease Onset and Progression. *Cold Spring Harb Perspect Biol* 9. <https://doi.org/10.1101/cshperspect.a023622>
- Seeley, W.W., Crawford, R.K., Zhou, J., Miller, B.L., Greicius, M.D., 2009. Neurodegenerative diseases target large-scale human brain networks. *Neuron* 62, 42–52. <https://doi.org/10.1016/j.neuron.2009.03.024>
- Serrano, M.E., Kim, E., Petrinovic, M.M., Turkheimer, F., Cash, D., 2022. Imaging Synaptic Density: The Next Holy Grail of Neuroscience? *Front. Neurosci.* 16, 796129. <https://doi.org/10.3389/fnins.2022.796129>
- Shafiei, G., Bazinet, V., Dadar, M., Manera, A.L., Collins, D.L., Dagher, A., Borroni, B., Sanchez-Valle, R., Moreno, F., Laforce, R., Graff, C., Synofzik, M., Galimberti, D., Rowe, J.B., Masellis, M., Tartaglia, M.C., Finger, E., Vandenberghe, R., de

- Mendonça, A., Tagliavini, F., Santana, I., Butler, C., Gerhard, A., Danek, A., Levin, J., Otto, M., Sorbi, S., Jiskoot, L.C., Seelaar, H., van Swieten, J.C., Rohrer, J.D., Misic, B., Ducharme, S., Frontotemporal Lobar Degeneration Neuroimaging Initiative (FTLDNI), Rosen, H., Dickerson, B.C., Domoto-Reilly, K., Knopman, D., Boeve, B.F., Boxer, A.L., Kornak, J., Miller, B.L., Seeley, W.W., Gorno-Tempini, M.-L., McGinnis, S., Mandelli, M.L., GENetic Frontotemporal dementia Initiative (GENFI), Esteve, A.S., Nelson, A., Bouzigues, A., Heller, C., Greaves, C.V., Cash, D., Thomas, D.L., Todd, E., Benotmane, H., Zetterberg, H., Swift, I.J., Nicholas, J., Samra, K., Russell, L.L., Bocchetta, M., Shafei, R., Convery, R.S., Timberlake, C., Cope, T., Rittman, T., Benussi, A., Premi, E., Gasparotti, R., Archetti, S., Gazzina, S., Cantoni, V., Arighi, A., Fenoglio, C., Scarpini, E., Fumagalli, G., Borracci, V., Rossi, G., Giaccone, G., Fede, G.D., Caroppo, P., Tiraboschi, P., Prioni, S., Redaelli, V., Tang-Wai, D., Rogaeve, E., Castelo-Branco, M., Freedman, M., Keren, R., Black, S., Mitchell, S., Shoesmith, C., Bartha, R., Rademakers, R., van der Ende, E., Poos, J., Papma, J.M., Giannini, L., van Minkelen, R., Pijnenburg, Y., Nacmias, B., Ferrari, C., Polito, C., Lombardi, G., Bessi, V., Veldsman, M., Andersson, C., Thonberg, H., Öijerstedt, L., Jelic, V., Thompson, P., Langheinrich, T., Lladó, A., Antonell, A., Olives, J., Balasa, M., Bargalló, N., Borrego-Ecija, S., Verdelho, A., Maruta, C., Ferreira, C.B., Miltenberger, G., do Couto, F.S., Gabilondo, A., Gorostidi, A., Villanua, J., Cañada, M., Tainta, M., Zulaica, M., Barandiaran, M., Alves, P., Bender, B., Wilke, C., Graf, L., Vogels, A., Vandenbulcke, M., Van Damme, P., Bruffaerts, R., Rosa-Neto, P., Gauthier, S., Camuzat, A., Brice, A., Bertrand, A., Funkiewiez, A., Rinaldi, D., Saracino, D., Colliot, O., Sayah, S., Prix, C., Wlasich, E., Wagemann, O., Loosli, S., Schönecker, S., Hoegen, T., Lombardi, J., Anderl-Straub, S., Rollin, A., Kuchcinski, G., Bertoux, M., Lebouvier, T., Deramecourt, V., Santiago, B., Duro, D., Leitão, M.J., Almeida, M.R., Tábuas-Pereira, M., Afonso, S., Engel, A., Polyakova, M., 2023. Network structure and transcriptomic vulnerability shape atrophy in frontotemporal dementia. *Brain* 146, 321–336. <https://doi.org/10.1093/brain/awac069>
- Sheline, Y.I., Raichle, M.E., 2013. Resting State Functional Connectivity in Preclinical Alzheimer's Disease. *Biological Psychiatry* 74, 340–347. <https://doi.org/10.1016/j.biopsych.2012.11.028>
- Sherman, S.M., 2016. Thalamus plays a central role in ongoing cortical functioning. *Nat Neurosci* 19, 533–541. <https://doi.org/10.1038/nn.4269>
- Shi, Y., Zhang, W., Yang, Y., Murzin, A.G., Falcon, B., Kotecha, A., van Beers, M., Tarutani, A., Kametani, F., Garringer, H.J., Vidal, R., Hallinan, G.I., Lashley, T., Saito, Y., Murayama, S., Yoshida, M., Tanaka, H., Kakita, A., Ikeuchi, T., Robinson, A.C., Mann, D.M.A., Kovacs, G.G., Revesz, T., Ghetti, B., Hasegawa, M., Goedert, M., Scheres, S.H.W., 2021. Structure-based classification of tauopathies. *Nature* 598, 359–363. <https://doi.org/10.1038/s41586-021-03911-7>
- Shine, J.M., 2019. Neuromodulatory Influences on Integration and Segregation in the Brain. *Trends in Cognitive Sciences*. <https://doi.org/10.1016/j.tics.2019.04.002>
- Shine, J.M., Breakspear, M., Bell, P.T., Ehgoetz Martens, K.A., Shine, R., Koyejo, O., Sporns, O., Poldrack, R.A., 2019. Human cognition involves the dynamic integration of neural activity and neuromodulatory systems. *Nature Neuroscience*. <https://doi.org/10.1038/s41593-018-0312-0>
- Shine, J.M., van den Brink, R.L., Hernaus, D., Nieuwenhuis, S., Poldrack, R.A., 2018. Catecholaminergic manipulation alters dynamic network topology across cognitive

- states. *Network neuroscience* (Cambridge, Mass.).
https://doi.org/10.1162/netn_a_00042
- Shirer, W.R., Ryali, S., Rykhlevskaia, E., Menon, V., Greicius, M.D., 2012. Decoding Subject-Driven Cognitive States with Whole-Brain Connectivity Patterns. *Cerebral Cortex* 22, 158–165. <https://doi.org/10.1093/cercor/bhr099>
- Shmuel, A., Leopold, D.A., 2008. Neuronal correlates of spontaneous fluctuations in fMRI signals in monkey visual cortex: Implications for functional connectivity at rest. *Hum. Brain Mapp.* 29, 751–761. <https://doi.org/10.1002/hbm.20580>
- Shoeibi, A., Litvan, I., Juncos, J.L., Bordelon, Y., Riley, D., Standaert, D., Reich, S.G., Shprecher, D., Hall, D., Marras, C., Kluger, B., Olfati, N., Jankovic, J., 2019. Are the International Parkinson disease and Movement Disorder Society progressive supranuclear palsy (IPMDS-PSP) diagnostic criteria accurate enough to differentiate common PSP phenotypes? *Parkinsonism & Related Disorders* 69, 34–39. <https://doi.org/10.1016/j.parkreldis.2019.10.012>
- Smart, K., Cox, S.M.L., Scala, S.G., Tippler, M., Jaworska, N., Boivin, M., Séguin, J.R., Benkelfat, C., Leyton, M., 2019. Sex differences in [11C]ABP688 binding: a positron emission tomography study of mGlu5 receptors. *Eur J Nucl Med Mol Imaging* 46, 1179–1183. <https://doi.org/10.1007/s00259-018-4252-4>
- Smith, A.M., Lewis, B.K., Ruttimann, U.E., Ye, F.Q., Sinnwell, T.M., Yang, Y., Duyn, J.H., Frank, J.A., 1999. Investigation of Low Frequency Drift in fMRI Signal. *NeuroImage* 9, 526–533. <https://doi.org/10.1006/nimg.1999.0435>
- Smith, S.M., 2002. Fast robust automated brain extraction. *Hum. Brain Mapp.* 17, 143–155. <https://doi.org/10.1002/hbm.10062>
- Smith, S.M., Beckmann, C.F., Andersson, J., Auerbach, E.J., Bijsterbosch, J., Douaud, G., Duff, E., Feinberg, D.A., Griffanti, L., Harms, M.P., Kelly, M., Laumann, T., Miller, K.L., Moeller, S., Petersen, S., Power, J., Salimi-Khorshidi, G., Snyder, A.Z., Vu, A.T., Woolrich, M.W., Xu, J., Yacoub, E., Uğurbil, K., Van Essen, D.C., Glasser, M.F., 2013a. Resting-state fMRI in the Human Connectome Project. *NeuroImage* 80, 144–168. <https://doi.org/10.1016/j.neuroimage.2013.05.039>
- Smith, S.M., Fox, P.T., Miller, K.L., Glahn, D.C., Fox, P.M., Mackay, C.E., Filippini, N., Watkins, K.E., Toro, R., Laird, A.R., Beckmann, C.F., 2009. Correspondence of the brain’s functional architecture during activation and rest. *Proceedings of the National Academy of Sciences* 106, 13040–13045. <https://doi.org/10.1073/pnas.0905267106>
- Smith, S.M., Miller, K.L., Salimi-Khorshidi, G., Webster, M., Beckmann, C.F., Nichols, T.E., Ramsey, J.D., Woolrich, M.W., 2011. Network modelling methods for FMRI. *NeuroImage* 54, 875–891. <https://doi.org/10.1016/j.neuroimage.2010.08.063>
- Smith, S.M., Vidaurre, D., Beckmann, C.F., Glasser, M.F., Jenkinson, M., Miller, K.L., Nichols, T.E., Robinson, E.C., Salimi-Khorshidi, G., Woolrich, M.W., Barch, D.M., Uğurbil, K., Van Essen, D.C., 2013b. Functional connectomics from resting-state fMRI. *Trends in Cognitive Sciences* 17, 666–682. <https://doi.org/10.1016/j.tics.2013.09.016>
- Smyser, C.D., Inder, T.E., Shimony, J.S., Hill, J.E., Degnan, A.J., Snyder, A.Z., Neil, J.J., 2010. Longitudinal analysis of neural network development in preterm infants. *Cereb Cortex* 20, 2852–2862. <https://doi.org/10.1093/cercor/bhq035>
- Snowden, J.S., Bathgate, D., Varma, A., Blackshaw, A., Gibbons, Z.C., Neary, D., 2001. Distinct behavioural profiles in frontotemporal dementia and semantic dementia. *J Neurol Neurosurg Psychiatry* 70, 323. <https://doi.org/10.1136/jnnp.70.3.323>
- Snowden, J.S., Goulding, P.J., Neary, D., 1989. Semantic dementia: A form of circumscribed cerebral atrophy. *Behavioural Neurology* 2, 167–182.

- Sokoloff, L., Mangold, R., Wechsler, R.L., Kennedy, C., Kety, S.S., 1955. THE EFFECT OF MENTAL ARITHMETIC ON CEREBRAL CIRCULATION AND METABOLISM 1. *J. Clin. Invest.* 34, 1101–1108. <https://doi.org/10.1172/JCI103159>
- Soto, C., Pritzkow, S., 2018. Protein misfolding, aggregation, and conformational strains in neurodegenerative diseases. *Nat Neurosci* 21, 1332–1340. <https://doi.org/10.1038/s41593-018-0235-9>
- Spencer, P.S., Nunn, P.B., Hugon, J., Ludolph, A.C., Ross, S.M., Roy, D.N., Robertson, R.C., 1987. Guam Amyotrophic Lateral Sclerosis-Parkinsonism-Dementia Linked to a Plant Excitant Neurotoxin. *Science* 237, 517–522. <https://doi.org/10.1126/science.3603037>
- Sperling, R., 2011. The potential of functional MRI as a biomarker in early Alzheimer’s disease. *Neurobiology of Aging* 32, S37–S43. <https://doi.org/10.1016/j.neurobiolaging.2011.09.009>
- Sperling, R.A., Aisen, P.S., Beckett, L.A., Bennett, D.A., Craft, S., Fagan, A.M., Iwatsubo, T., Jack, C.R., Kaye, J., Montine, T.J., Park, D.C., Reiman, E.M., Rowe, C.C., Siemers, E., Stern, Y., Yaffe, K., Carrillo, M.C., Thies, B., Morrison-Bogorad, M., Wagster, M.V., Phelps, C.H., 2011. Toward defining the preclinical stages of Alzheimer’s disease: Recommendations from the National Institute on Aging-Alzheimer’s Association workgroups on diagnostic guidelines for Alzheimer’s disease. *Alzheimer’s & Dementia* 7, 280–292. <https://doi.org/10.1016/j.jalz.2011.03.003>
- Spillantini, M.G., Murrell, J.R., Goedert, M., Farlow, M.R., Klug, A., Ghetti, B., 1998. Mutation in the tau gene in familial multiple system tauopathy with presenile dementia. *Proc. Natl. Acad. Sci. U.S.A.* 95, 7737–7741. <https://doi.org/10.1073/pnas.95.13.7737>
- Spina, S., Brown, J.A., Deng, J., Gardner, R.C., Nana, A.L., Hwang, J.-H.L., Gaus, S.E., Huang, E.J., Kramer, J.H., Rosen, H.J., Kornak, J., Neuhaus, J., Miller, B.L., Grinberg, L.T., Boxer, A.L., Seeley, W.W., 2019. Neuropathological correlates of structural and functional imaging biomarkers in 4-repeat tauopathies. *Brain* 142, 2068–2081. <https://doi.org/10.1093/brain/awz122>
- Spinelli, E.G., Mandelli, M.L., Miller, Z.A., Santos-Santos, M.A., Wilson, S.M., Agosta, F., Grinberg, L.T., Huang, E.J., Trojanowski, J.Q., Meyer, M., Henry, M.L., Comi, G., Rabinovici, G., Rosen, H.J., Filippi, M., Miller, B.L., Seeley, W.W., Gorno-Tempini, M.L., 2017. Typical and atypical pathology in primary progressive aphasia variants: Pathology in PPA Variants. *Ann Neurol.* 81, 430–443. <https://doi.org/10.1002/ana.24885>
- Spires-Jones, T.L., Attems, J., Thal, D.R., 2017. Interactions of pathological proteins in neurodegenerative diseases. *Acta Neuropathol* 134, 187–205. <https://doi.org/10.1007/s00401-017-1709-7>
- Spires-Jones, T.L., Hyman, B.T., 2014. The Intersection of Amyloid Beta and Tau at Synapses in Alzheimer’s Disease. *Neuron* 82, 756–771. <https://doi.org/10.1016/j.neuron.2014.05.004>
- Spooner, A., Chen, E., Sowmya, A., Sachdev, P., Kochan, N.A., Trollor, J., Brodaty, H., 2020. A comparison of machine learning methods for survival analysis of high-dimensional clinical data for dementia prediction. *Sci Rep* 10, 20410. <https://doi.org/10.1038/s41598-020-77220-w>
- Sridharan, D., Levitin, D.J., Menon, V., 2008. A critical role for the right fronto-insular cortex in switching between central-executive and default-mode networks.

Proceedings of the National Academy of Sciences 105, 12569–12574.
<https://doi.org/10.1073/pnas.0800005105>

- Staffaroni, A.M., Quintana, M., Wendelberger, B., Heuer, H.W., Russell, L.L., Cobigo, Y., Wolf, A., Goh, S.-Y.M., Petrucelli, L., Gendron, T.F., Heller, C., Clark, A.L., Taylor, Jack Carson, Wise, A., Ong, E., Forsberg, L., Brushaber, D., Rojas, J.C., VandeVrede, L., Ljubenkov, P., Kramer, J., Casaletto, K.B., Appleby, B., Bordelon, Y., Botha, H., Dickerson, B.C., Domoto-Reilly, K., Fields, J.A., Foroud, T., Gavrilova, R., Geschwind, D., Ghoshal, N., Goldman, J., Graff-Radford, J., Graff-Radford, N., Grossman, M., Hall, M.G.H., Hsiung, G.-Y., Huey, E.D., Irwin, D., Jones, D.T., Kantarci, K., Kaufer, D., Knopman, D., Kremers, W., Lago, A.L., Lapid, M.I., Litvan, I., Lucente, D., Mackenzie, I.R., Mendez, M.F., Mester, C., Miller, B.L., Onyike, C.U., Rademakers, R., Ramanan, V.K., Ramos, E.M., Rao, M., Rascovsky, K., Rankin, K.P., Roberson, E.D., Savica, R., Tartaglia, M.C., Weintraub, S., Wong, B., Cash, D.M., Bouzigues, A., Swift, I.J., Peakman, G., Bocchetta, M., Todd, E.G., Convery, R.S., Rowe, J.B., Borroni, B., Galimberti, D., Tiraboschi, P., Masellis, M., Finger, E., van Swieten, J.C., Seelaar, H., Jiskoot, L.C., Sorbi, S., Butler, C.R., Graff, C., Gerhard, A., Langheinrich, T., Laforce, R., Sanchez-Valle, R., de Mendonça, A., Moreno, F., Synofzik, M., Vandenberghe, R., Ducharme, S., Le Ber, I., Levin, J., Danek, A., Otto, M., Pasquier, F., Santana, I., Kornak, J., Boeve, B.F., Rosen, H.J., Rohrer, J.D., Boxer, Adam.L., Frontotemporal Dementia Prevention Initiative (FPI) Investigators, ALLFTD Investigators, Apostolova, L., Barmada, S., Boeve, B., Boxer, A.L., Bozoki, A., Clark, D., Coppola, G., Darby, R., Dickson, D., Faber, K., Fagan, A., Galasko, D.R., Grant, I.M., Huang, E., Kerwin, D., Lapid, M., Lee, S., Leger, G., Masdeux, J.C., McGinnis, S., Mendez, M., Onyike, C., Pascual, M.B., Pressman, P., Rademakers, R., Ramanan, V., Ritter, A., Seeley, W.W., Syrjanen, J., Taylor, Jack C., Weintraub, S., GENFI Investigators, Esteve, A.S., Nelson, A., Greaves, C.V., Thomas, D.L., Benotmane, H., Zetterberg, H., Nicholas, J., Samra, K., Shafei, R., Timberlake, C., Cope, T., Rittman, T., Benussi, A., Premi, E., Gasparotti, R., Archetti, S., Gazzina, S., Cantoni, V., Arighi, A., Fenoglio, C., Scarpini, E., Fumagalli, G., Borracchi, V., Rossi, G., Giaccone, G., Di Fede, G., Caroppo, P., Prioni, S., Redaelli, V., Tang-Wai, D., Rogaeva, E., Castelo-Branco, M., Freedman, M., Keren, R., Black, S., Mitchell, S., Shoosmith, C., Bartha, R., Poos, J., Papma, J.M., Giannini, L., van Minkelen, R., Pijnenburg, Y., Nacmias, B., Ferrari, C., Polito, C., Lombardi, G., Bessi, V., Veldsman, M., Andersson, C., Thonberg, H., Öijerstedt, L., Jelic, V., Thompson, P., Lladó, A., Antonell, A., Olives, J., Balasa, M., Bargalló, N., Borrego-Ecija, S., Verdelho, A., Maruta, C., Ferreira, C.B., Miltenberger, G., Simões do Couto, F., Gabilondo, A., Gorostidi, A., Villanua, J., Cañada, M., Tainta, M., Zulaica, M., Barandiaran, M., Alves, P., Bender, B., Wilke, C., Graf, L., Vogels, A., Vandenbulcke, M., Van Damme, P., Bruffaerts, R., Poesen, K., Rosa-Neto, P., Gauthier, S., Camuzat, A., Brice, A., Bertrand, A., Funkiewiez, A., Rinaldi, D., Saracino, D., Colliot, O., Sayah, S., Prix, C., Wlasich, E., Wagemann, O., Loosli, S., Schönecker, S., Hoegen, T., Lombardi, J., Anderl-Straub, S., Rollin, A., Kuchcinski, G., Bertoux, M., Lebouvier, T., Deramecourt, V., Santiago, B., Duro, D., Leitão, M.J., Almeida, M.R., Tábuas-Pereira, M., Afonso, S., 2022. Temporal order of clinical and biomarker changes in familial frontotemporal dementia. *Nat Med* 28, 2194–2206. <https://doi.org/10.1038/s41591-022-01942-9>
- Stam, C.J., 2014. Modern network science of neurological disorders. *Nat Rev Neurosci* 15, 683–695. <https://doi.org/10.1038/nrn3801>

- Steele, J.C., Richardson, J.C., Olszewski, J., 1964. Progressive Supranuclear Palsy: A Heterogeneous Degeneration Involving the Brain Stem, Basal Ganglia and Cerebellum With Vertical Gaze and Pseudobulbar Palsy, Nuchal Dystonia and Dementia. *Arch Neurol* 10, 333. <https://doi.org/10.1001/archneur.1964.00460160003001>
- Stern, Y., Arenaza-Urquijo, E.M., Bartrés-Faz, D., Belleville, S., Cantilon, M., Chetelat, G., Ewers, M., Franzmeier, N., Kempermann, G., Kremen, W.S., Okonkwo, O., Scarmeas, N., Soldan, A., Udeh-Momoh, C., Valenzuela, M., Vemuri, P., Vuoksima, E., and the Reserve, Resilience and Protective Factors PIA Empirical Definitions and Conceptual Frameworks Workgroup, 2020. Whitepaper: Defining and investigating cognitive reserve, brain reserve, and brain maintenance. *Alzheimer's & Dementia* 16, 1305–1311. <https://doi.org/10.1016/j.jalz.2018.07.219>
- Steward, A., Biel, D., Brendel, M., Dewenter, A., Roemer, S., Rubinski, A., Luan, Y., Dichgans, M., Ewers, M., Franzmeier, N., for the Alzheimer's Disease Neuroimaging Initiative (ADNI), 2023. Functional network segregation is associated with attenuated tau spreading in Alzheimer's disease. *Alzheimer's & Dementia* 19, 2034–2046. <https://doi.org/10.1002/alz.12867>
- Street, D., Malpetti, M., Rittman, T., Ghosh, B.C.P., Murley, A.G., Coyle-Gilchrist, I., Passamonti, L., Rowe, J.B., 2021. Clinical progression of progressive supranuclear palsy: impact of trials bias and phenotype variants. *Brain Communications* 3, fcab206. <https://doi.org/10.1093/braincomms/fcab206>
- Street, D., Whiteside, D., Rittman, T., Rowe, J.B., 2022. Prediagnostic Progressive Supranuclear Palsy – Insights from the UK Biobank. *Parkinsonism & Related Disorders* 95, 59–64. <https://doi.org/10.1016/j.parkreldis.2022.01.004>
- Strimbu, K., Tavel, J.A., 2010. What are biomarkers?: Current Opinion in HIV and AIDS 5, 463–466. <https://doi.org/10.1097/COH.0b013e32833ed177>
- Strong, M.J., Abrahams, S., Goldstein, L.H., Woolley, S., McLaughlin, P., Snowden, J., Mioshi, E., Roberts-South, A., Benatar, M., HortobáGyi, T., Rosenfeld, J., Silani, V., Ince, P.G., Turner, M.R., 2017. Amyotrophic lateral sclerosis - frontotemporal spectrum disorder (ALS-FTSD): Revised diagnostic criteria. *Amyotrophic Lateral Sclerosis and Frontotemporal Degeneration* 18, 153–174. <https://doi.org/10.1080/21678421.2016.1267768>
- Sudlow, C., Gallacher, J., Allen, N., Beral, V., Burton, P., Danesh, J., Downey, P., Elliott, P., Green, J., Landray, M., Liu, B., Matthews, P., Ong, G., Pell, J., Silman, A., Young, A., Sprosen, T., Peakman, T., Collins, R., 2015. UK biobank: an open access resource for identifying the causes of a wide range of complex diseases of middle and old age. *PLoS medicine*. <https://doi.org/10.1371/journal.pmed.1001779>
- Swaddiwudhipong, N., Whiteside, D.J., Hezemans, F.H., Street, D., Rowe, J.B., Rittman, T., 2022. Pre-diagnostic cognitive and functional impairment in multiple sporadic neurodegenerative diseases. *Alzheimer's & Dementia* alz.12802. <https://doi.org/10.1002/alz.12802>
- Swanson, C.J., Zhang, Y., Dhadda, S., Wang, J., Kaplow, J., Lai, R.Y.K., Lannfelt, L., Bradley, H., Rabe, M., Koyama, A., Reyderman, L., Berry, D.A., Berry, S., Gordon, R., Kramer, L.D., Cummings, J.L., 2021. A randomized, double-blind, phase 2b proof-of-concept clinical trial in early Alzheimer's disease with lecanemab, an anti-A β protofibril antibody. *Alz Res Therapy* 13, 80. <https://doi.org/10.1186/s13195-021-00813-8>

- Symms, M., 2004. A review of structural magnetic resonance neuroimaging. *Journal of Neurology, Neurosurgery & Psychiatry* 75, 1235–1244. <https://doi.org/10.1136/jnnp.2003.032714>
- Taoufik, E., Kouroupi, G., Zygogianni, O., Matsas, R., 2018. Synaptic dysfunction in neurodegenerative and neurodevelopmental diseases: an overview of induced pluripotent stem-cell-based disease models. *Open Biol.* 8, 180138. <https://doi.org/10.1098/rsob.180138>
- Tastevin, M., Lavoie, M., de la Sablonnière, J., Carrier-Auclair, J., Laforce, R., 2021. Survival in the Three Common Variants of Primary Progressive Aphasia: A Retrospective Study in a Tertiary Memory Clinic. *Brain Sciences* 11, 1113. <https://doi.org/10.3390/brainsci11091113>
- Terry, R.D., Masliah, E., Salmon, D.P., Butters, N., DeTeresa, R., Hill, R., Hansen, L.A., Katzman, R., 1991. Physical basis of cognitive alterations in alzheimer's disease: Synapse loss is the major correlate of cognitive impairment. *Ann Neurol.* 30, 572–580. <https://doi.org/10.1002/ana.410300410>
- The Lancet, 2022. Lecanemab for Alzheimer's disease: tempering hype and hope. *The Lancet* 400, 1899. [https://doi.org/10.1016/S0140-6736\(22\)02480-1](https://doi.org/10.1016/S0140-6736(22)02480-1)
- Therneau, T.M., 2023. A Package for Survival Analysis in R.
- Thijssen, E.H., La Joie, R., Strom, A., Fonseca, C., Iaccarino, L., Wolf, A., Spina, S., Allen, I.E., Cobigo, Y., Heuer, H., VandeVrede, L., Proctor, N.K., Lago, A.L., Baker, S., Sivasankaran, R., Kieloch, A., Kinhikar, A., Yu, L., Valentin, M.-A., Jeromin, A., Zetterberg, H., Hansson, O., Mattsson-Carlsson, N., Graham, D., Blennow, K., Kramer, J.H., Grinberg, L.T., Seeley, W.W., Rosen, H., Boeve, B.F., Miller, B.L., Teunissen, C.E., Rabinovici, G.D., Rojas, J.C., Dage, J.L., Boxer, A.L., 2021. Plasma phosphorylated tau 217 and phosphorylated tau 181 as biomarkers in Alzheimer's disease and frontotemporal lobar degeneration: a retrospective diagnostic performance study. *The Lancet Neurology* 20, 739–752. [https://doi.org/10.1016/S1474-4422\(21\)00214-3](https://doi.org/10.1016/S1474-4422(21)00214-3)
- Thijssen, E.H., La Joie, R., Wolf, A., Strom, A., Wang, P., Iaccarino, L., Bourakova, V., Cobigo, Y., Heuer, H., Spina, S., VandeVrede, L., Chai, X., Proctor, N.K., Airey, D.C., Shcherbinin, S., Duggan Evans, C., Sims, J.R., Zetterberg, H., Blennow, K., Karydas, A.M., Teunissen, C.E., Kramer, J.H., Grinberg, L.T., Seeley, W.W., Rosen, H., Boeve, B.F., Miller, B.L., Rabinovici, G.D., Dage, J.L., Rojas, J.C., Boxer, A.L., 2020. Diagnostic value of plasma phosphorylated tau181 in Alzheimer's disease and frontotemporal lobar degeneration. *Nat Med* 26, 387–397. <https://doi.org/10.1038/s41591-020-0762-2>
- Tingley, D., Yamamoto, T., Hirose, K., Keele, L., Imai, K., 2014. **mediation** : R Package for Causal Mediation Analysis. *J. Stat. Soft.* 59. <https://doi.org/10.18637/jss.v059.i05>
- Tognoli, E., Kelso, J.A.S., 2014. The Metastable Brain. *Neuron* 81, 35–48. <https://doi.org/10.1016/j.neuron.2013.12.022>
- Toi, P.T., Jang, H.J., Min, K., Kim, S.-P., Lee, S.-K., Lee, J., Kwag, J., Park, J.-Y., 2022. In vivo direct imaging of neuronal activity at high temporospatial resolution. *Science* 378, 160–168. <https://doi.org/10.1126/science.abh4340>
- Toller, G., Brown, J., Sollberger, M., Shdo, S.M., Bouvet, L., Sukhanov, P., Seeley, W.W., Miller, B.L., Rankin, K.P., 2018. Individual differences in socioemotional sensitivity are an index of salience network function. *Cortex* 103, 211–223. <https://doi.org/10.1016/j.cortex.2018.02.012>
- Torralva, T., Roca, M., Gleichgerricht, E., López, P., Manes, F., 2009. INECO Frontal Screening (IFS): A brief, sensitive, and specific tool to assess executive functions

- in dementia—CORRECTED VERSION. *J Int Neuropsychol Soc* 15, 777–786. <https://doi.org/10.1017/S1355617709990415>
- Tsagris, M., Preston, S., Wood, A.T.A., 2016. Improved Classification for Compositional Data Using the α -transformation. *J Classif* 33, 243–261. <https://doi.org/10.1007/s00357-016-9207-5>
- Tsai, R.M., Boxer, A.L., 2014. Treatment of Frontotemporal Dementia. *Curr Treat Options Neurol* 16, 319. <https://doi.org/10.1007/s11940-014-0319-0>
- Tsuboi, Y., Josephs, K.A., Boeve, B.F., Litvan, I., Caselli, R.J., Caviness, J.N., Uitti, R.J., Bott, A.D., Dickson, D.W., 2005. Increased tau burden in the cortices of progressive supranuclear palsy presenting with corticobasal syndrome. *Mov Disord*. 20, 982–988. <https://doi.org/10.1002/mds.20478>
- Tsvetanov, K.A., Gazzina, S., Jones, P.S., Swieten, J., Borroni, B., Sanchez-Valle, R., Moreno, F., Laforce, R., Graff, C., Synofzik, M., Galimberti, D., Masellis, M., Tartaglia, M.C., Finger, E., Vandenberghe, R., Mendonça, A., Tagliavini, F., Santana, I., Ducharme, S., Butler, C., Gerhard, A., Danek, A., Levin, J., Otto, M., Frisoni, G., Ghidoni, R., Sorbi, S., Rohrer, J.D., Rowe, J.B., the Genetic FTD Initiative, GENFI, 2020. Brain functional network integrity sustains cognitive function despite atrophy in presymptomatic genetic frontotemporal dementia. *Alzheimer's & Dementia* alz.12209. <https://doi.org/10.1002/alz.12209>
- Tsvetanov, K.A., Henson, R.N.A., Tyler, L.K., Davis, S.W., Shafto, M.A., Taylor, J.R., Williams, N., Cam-CAN, Rowe, J.B., 2015. The effect of ageing on f MRI: Correction for the confounding effects of vascular reactivity evaluated by joint f MRI and MEG in 335 adults. *Hum. Brain Mapp*. 36, 2248–2269. <https://doi.org/10.1002/hbm.22768>
- Turchi, J., Chang, C., Ye, F.Q., Russ, B.E., Yu, D.K., Cortes, C.R., Monosov, I.E., Duyn, J.H., Leopold, D.A., 2018. The Basal Forebrain Regulates Global Resting-State fMRI Fluctuations. *Neuron*. <https://doi.org/10.1016/j.neuron.2018.01.032>
- Turkheimer, F.E., Leech, R., Expert, P., Lord, L.-D., Vernon, A.C., 2015. The brain's code and its canonical computational motifs. From sensory cortex to the default mode network: A multi-scale model of brain function in health and disease. *Neuroscience & Biobehavioral Reviews*. <https://doi.org/10.1016/j.neubiorev.2015.04.014>
- Uludağ, K., Roebroeck, A., 2014. General overview on the merits of multimodal neuroimaging data fusion. *NeuroImage* 102, 3–10. <https://doi.org/10.1016/j.neuroimage.2014.05.018>
- van den Heuvel, M.P., de Lange, S.C., Zalesky, A., Seguin, C., Yeo, B.T.T., Schmidt, R., 2017. Proportional thresholding in resting-state fMRI functional connectivity networks and consequences for patient-control connectome studies: Issues and recommendations. *NeuroImage* 152, 437–449. <https://doi.org/10.1016/j.neuroimage.2017.02.005>
- van der Ende, E.L., Meeter, L.H., Poos, J.M., Panman, J.L., Jiskoot, L.C., Dopfer, E.G.P., Papma, J.M., de Jong, F.J., Verberk, I.M.W., Teunissen, C., Rizopoulos, D., Heller, C., Convery, R.S., Moore, K.M., Bocchetta, M., Neason, M., Cash, D.M., Borroni, B., Galimberti, D., Sanchez-Valle, R., Laforce, R., Moreno, F., Synofzik, M., Graff, C., Masellis, M., Carmela Tartaglia, M., Rowe, J.B., Vandenberghe, R., Finger, E., Tagliavini, F., de Mendonça, A., Santana, I., Butler, C., Ducharme, S., Gerhard, A., Danek, A., Levin, J., Otto, M., Frisoni, G.B., Cappa, S., Pijnenburg, Y.A.L., Rohrer, J.D., van Swieten, J.C., Rossor, M.N., Warren, J.D., Fox, N.C., Woollacott, I.O.C., Shafei, R., Greaves, C., Guerreiro, R., Bras, J., Thomas, D.L., Nicholas, J., Mead, S., van Minkelen, R., Barandiaran, M., Indakoetxea, B., Gabilondo, A., Tainta, M., de Arriba, M., Gorostidi, A., Zulaica, M., Villanua, J., Diaz, Z., Borrego-Ecija, S.,

- Olives, J., Lladó, A., Balasa, M., Antonell, A., Bargallo, N., Premi, E., Cosseddu, M., Gazzina, S., Padovani, A., Gasparotti, R., Archetti, S., Black, S., Mitchell, S., Rogaeva, E., Freedman, M., Keren, R., Tang-Wai, D., Öijerstedt, L., Andersson, C., Jelic, V., Thonberg, H., Arighi, A., Fenoglio, C., Scarpini, E., Fumagalli, G., Cope, T., Timberlake, C., Rittman, T., Shoesmith, C., Bartha, R., Rademakers, R., Wilke, C., Karnath, H.-O., Bender, B., Bruffaerts, R., Vandamme, P., Vandenbulcke, M., Ferreira, C.B., Miltenberger, G., Maruta, C., Verdelho, A., Afonso, S., Taipa, R., Caroppo, P., Di Fede, G., Giaccone, G., Prioni, S., Redaelli, V., Rossi, G., Tiraboschi, P., Duro, D., Rosario Almeida, M., Castelo-Branco, M., João Leitão, M., Tabuas-Pereira, M., Santiago, B., Gauthier, S., Schonecker, S., Semler, E., Anderl-Straub, S., Benussi, L., Binetti, G., Ghidoni, R., Pievani, M., Lombardi, G., Nacmias, B., Ferrari, C., Bessi, V., 2019. Serum neurofilament light chain in genetic frontotemporal dementia: a longitudinal, multicentre cohort study. *The Lancet Neurology* 18, 1103–1111. [https://doi.org/10.1016/S1474-4422\(19\)30354-0](https://doi.org/10.1016/S1474-4422(19)30354-0)
- van Dyck, C.H., Swanson, C.J., Aisen, P., Bateman, R.J., Chen, C., Gee, M., Kanekiyo, M., Li, D., Reyderman, L., Cohen, S., Froelich, L., Katayama, S., Sabbagh, M., Vellas, B., Watson, D., Dhadda, S., Irizarry, M., Kramer, L.D., Iwatsubo, T., 2022. Lecanemab in Early Alzheimer’s Disease. *N Engl J Med* NEJMoa2212948. <https://doi.org/10.1056/NEJMoa2212948>
- van Wijk, B.C.M., Stam, C.J., Daffertshofer, A., 2010. Comparing Brain Networks of Different Size and Connectivity Density Using Graph Theory. *PLoS ONE* 5, e13701. <https://doi.org/10.1371/journal.pone.0013701>
- Vemuri, P., Jones, D.T., Jack, C.R., 2012. Resting state functional MRI in Alzheimer’s Disease. *Alz Res Therapy* 4, 2. <https://doi.org/10.1186/alzrt100>
- Vermeiren, Y., Janssens, J., Aerts, T., Martin, J.-J., Sieben, A., Van Dam, D., De Deyn, P.P., 2016. Brain Serotonergic and Noradrenergic Deficiencies in Behavioral Variant Frontotemporal Dementia Compared to Early-Onset Alzheimer’s Disease. *JAD* 53, 1079–1096. <https://doi.org/10.3233/JAD-160320>
- Vidaurre, D., Abeyesuriya, R., Becker, R., Quinn, A.J., Alfaro-Almagro, F., Smith, S.M., Woolrich, M.W., 2018. Discovering dynamic brain networks from big data in rest and task. *NeuroImage* 180, 646–656. <https://doi.org/10.1016/j.neuroimage.2017.06.077>
- Vidaurre, D., Llera, A., Smith, S.M., Woolrich, M.W., 2021. Behavioural relevance of spontaneous, transient brain network interactions in fMRI. *NeuroImage* 229, 117713. <https://doi.org/10.1016/j.neuroimage.2020.117713>
- Vidaurre, D., Smith, S.M., Woolrich, M.W., 2017. Brain network dynamics are hierarchically organized in time. *Proceedings of the National Academy of Sciences* 114, 12827. <https://doi.org/10.1073/pnas.1705120114>
- Vivash, L., Malpas, C.B., Churilov, L., Walterfang, M., Brodtmann, A., Piguet, O., Ahmed, R.M., Bush, A.I., Hovens, C.M., Kalincik, T., Darby, D., Velakoulis, D., O’Brien, T.J., 2020. A study protocol for a phase II randomised, double-blind, placebo-controlled trial of sodium selenate as a disease-modifying treatment for behavioural variant frontotemporal dementia. *BMJ Open* 10, e040100. <https://doi.org/10.1136/bmjopen-2020-040100>
- Voevodskaya, O., Simmons, A., Nordenskjöld, R., Kullberg, J., Ahlström, H., Lind, L., Wahlund, L.-O., Larsson, E.-M., Westman, E., Alzheimer’s Disease Neuroimaging Initiative, 2014. The effects of intracranial volume adjustment approaches on multiple regional MRI volumes in healthy aging and Alzheimer’s disease. *Front. Aging Neurosci.* 6. <https://doi.org/10.3389/fnagi.2014.00264>

- Walsh, S., Merrick, R., Richard, E., Nurock, S., Brayne, C., 2022. Lecanemab for Alzheimer's disease. *BMJ* o3010. <https://doi.org/10.1136/bmj.o3010>
- Wang, D., Buckner, R.L., Fox, M.D., Holt, D.J., Holmes, A.J., Stoecklein, S., Langs, G., Pan, R., Qian, T., Li, K., Baker, J.T., Stufflebeam, S.M., Wang, K., Wang, X., Hong, B., Liu, H., 2015. Parcellating cortical functional networks in individuals. *Nat Neurosci* 18, 1853–1860. <https://doi.org/10.1038/nn.4164>
- Wang, D.J.J., Jann, K., Fan, C., Qiao, Y., Zang, Y.-F., Lu, H., Yang, Y., 2018. Neurophysiological Basis of Multi-Scale Entropy of Brain Complexity and Its Relationship With Functional Connectivity. *Frontiers in Neuroscience*.
- Wareham, L.K., Liddelov, S.A., Temple, S., Benowitz, L.I., Di Polo, A., Wellington, C., Goldberg, J.L., He, Z., Duan, X., Bu, G., Davis, A.A., Shekhar, K., Torre, A.L., Chan, D.C., Canto-Soler, M.V., Flanagan, J.G., Subramanian, P., Rossi, S., Brunner, T., Bovenkamp, D.E., Calkins, D.J., 2022. Solving neurodegeneration: common mechanisms and strategies for new treatments. *Mol Neurodegeneration* 17, 23. <https://doi.org/10.1186/s13024-022-00524-0>
- Watts, D.J., Strogatz, S.H., 1998. Collective dynamics of 'small-world' networks. *Nature*. <https://doi.org/10.1038/30918>
- Wear, H.J., Wedderburn, C.J., Mioshi, E., Williams-Gray, C.H., Mason, S.L., Barker, R.A., Hodges, J.R., 2008. The Cambridge Behavioural Inventory revised. *Dement. neuropsychol.* 2, 102–107. <https://doi.org/10.1590/S1980-57642009DN20200005>
- Wedderburn, C., Wear, H., Brown, J., Mason, S.J., Barker, R.A., Hodges, J., Williams-Gray, C., 2008. The utility of the Cambridge Behavioural Inventory in neurodegenerative disease. *Journal of Neurology, Neurosurgery & Psychiatry* 79, 500–503. <https://doi.org/10.1136/jnnp.2007.122028>
- Whitwell, J.L., 2019. FTD spectrum: Neuroimaging across the FTD spectrum, in: *Progress in Molecular Biology and Translational Science*. Elsevier, pp. 187–223. <https://doi.org/10.1016/bs.pmbts.2019.05.009>
- Whitwell, J.L., Avula, R., Master, A., Vemuri, P., Senjem, M.L., Jones, D.T., Jack, C.R., Josephs, K.A., 2011. Disrupted thalamocortical connectivity in PSP: a resting-state fMRI, DTI, and VBM study. *Parkinsonism Relat Disord* 17, 599–605. <https://doi.org/10.1016/j.parkreldis.2011.05.013>
- Whitwell, J.L., Höglinger, G.U., Antonini, A., Bordelon, Y., Boxer, A.L., Colosimo, C., van Eimeren, T., Golbe, L.I., Kassubek, J., Kurz, C., Litvan, I., Pantelyat, A., Rabinovici, G., Respondek, G., Rominger, A., Rowe, J.B., Stamelou, M., Josephs, K.A., for the Movement Disorder Society-endorsed PSP Study Group, 2017. Radiological biomarkers for diagnosis in PSP: Where are we and where do we need to be?: Neuroimaging Biomarkers for Diagnosis in PSP. *Mov Disord.* 32, 955–971. <https://doi.org/10.1002/mds.27038>
- Whitwell, J.L., Jack, C.R., Boeve, B.F., Parisi, J.E., Ahlskog, J.E., Drubach, D.A., Senjem, M.L., Knopman, D.S., Petersen, R.C., Dickson, D.W., Josephs, K.A., 2010. Imaging correlates of pathology in corticobasal syndrome. *Neurology* 75, 1879–1887. <https://doi.org/10.1212/WNL.0b013e3181feb2e8>
- Wicklund, M.R., Duffy, J.R., Strand, E.A., Machulda, M.M., Whitwell, J.L., Josephs, K.A., 2014. Quantitative application of the primary progressive aphasia consensus criteria. *Neurology* 82, 1119–1126. <https://doi.org/10.1212/WNL.0000000000000261>
- Wilkinson, G.N., Rogers, C.E., 1973. Symbolic Description of Factorial Models for Analysis of Variance. *Applied Statistics* 22, 392. <https://doi.org/10.2307/2346786>
- Williams, D.R., de Silva, R., Paviour, D.C., Pittman, A., Watt, H.C., Kilford, L., Holton, J.L., Revesz, T., Lees, A.J., 2005. Characteristics of two distinct clinical phenotypes

- in pathologically proven progressive supranuclear palsy: Richardson's syndrome and PSP-parkinsonism. *Brain* 128, 1247–1258. <https://doi.org/10.1093/brain/awh488>
- Wilson, S.M., Brambati, S.M., Henry, R.G., Handwerker, D.A., Agosta, F., Miller, B.L., Wilkins, D.P., Ogar, J.M., Gorno-Tempini, M.L., 2009. The neural basis of surface dyslexia in semantic dementia. *Brain* 132, 71–86. <https://doi.org/10.1093/brain/awn300>
- Winawer, J., Horiguchi, H., Sayres, R.A., Amano, K., Wandell, B.A., 2010. Mapping hV4 and ventral occipital cortex: The venous eclipse. *Journal of Vision* 10, 1–1. <https://doi.org/10.1167/10.5.1>
- Winkler, A.M., Ridgway, G.R., Webster, M.A., Smith, S.M., Nichols, T.E., 2014. Permutation inference for the general linear model. *NeuroImage*. <https://doi.org/10.1016/j.neuroimage.2014.01.060>
- Wise, R.G., Ide, K., Poulin, M.J., Tracey, I., 2004. Resting fluctuations in arterial carbon dioxide induce significant low frequency variations in BOLD signal. *NeuroImage* 21, 1652–1664. <https://doi.org/10.1016/j.neuroimage.2003.11.025>
- Wolinetz, C.D., Collins, F.S., 2020. Recognition of Research Participants' Need for Autonomy: Remembering the Legacy of Henrietta Lacks. *JAMA* 324, 1027. <https://doi.org/10.1001/jama.2020.15936>
- Wolpe, N., Hezemans, F.H., Rowe, J.B., 2020. Alien limb syndrome: A Bayesian account of unwanted actions. *Cortex* 127, 29–41. <https://doi.org/10.1016/j.cortex.2020.02.002>
- Woodcock, J., LaVange, L.M., 2017. Master Protocols to Study Multiple Therapies, Multiple Diseases, or Both. *N Engl J Med* 377, 62–70. <https://doi.org/10.1056/NEJMra1510062>
- Woolrich, M.W., Ripley, B.D., Brady, M., Smith, S.M., 2001. Temporal Autocorrelation in Univariate Linear Modeling of fMRI Data. *NeuroImage* 14, 1370–1386. <https://doi.org/10.1006/nimg.2001.0931>
- World Health Organization, 2019. ICD-11: International classification of diseases (11th revision). Retrieved from <https://icd.who.int/>.
- Wu, Y., Carson, R.E., 2002. Noise Reduction in the Simplified Reference Tissue Model for Neuroreceptor Functional Imaging. *J Cereb Blood Flow Metab* 22, 1440–1452. <https://doi.org/10.1097/01.WCB.0000033967.83623.34>
- Wylie, G.R., Genova, H., DeLuca, J., Chiaravalloti, N., Sumowski, J.F., 2014. Functional magnetic resonance imaging movers and shakers: Does subject-movement cause sampling bias?: Subject Motion and Sampling Bias. *Hum. Brain Mapp* 35, 1–13. <https://doi.org/10.1002/hbm.22150>
- Xu, L., Groth, K.M., Pearlson, G., Schretlen, D.J., Calhoun, V.D., 2009. Source-based morphometry: The use of independent component analysis to identify gray matter differences with application to schizophrenia. *Hum. Brain Mapp*. 30, 711–724. <https://doi.org/10.1002/hbm.20540>
- Yang, A.C., Huang, C.-C., Yeh, H.-L., Liu, M.-E., Hong, C.-J., Tu, P.-C., Chen, J.-F., Huang, N.E., Peng, C.-K., Lin, C.-P., Tsai, S.-J., 2013. Complexity of spontaneous BOLD activity in default mode network is correlated with cognitive function in normal male elderly: a multiscale entropy analysis. *Neurobiology of Aging*. <https://doi.org/10.1016/j.neurobiolaging.2012.05.004>
- Yang, A.C., Tsai, S.-J., Lin, C.-P., Peng, C.-K., 2018. A Strategy to Reduce Bias of Entropy Estimates in Resting-State fMRI Signals. *Frontiers in Neuroscience*.
- Yang, Y., Schmitt, H.P., 2001. Frontotemporal dementia: evidence for impairment of ascending serotonergic but not noradrenergic innervation: Immunocytochemical

- and quantitative study using a graph method. *Acta Neuropathol* 101, 256–270. <https://doi.org/10.1007/s004010000293>
- Ye, R., O'Callaghan, C., Rua, C., Hezemans, F.H., Holland, N., Malpetti, M., Jones, P.S., Barker, R.A., Williams-Gray, C.H., Robbins, T.W., Passamonti, L., Rowe, J., 2022. Locus Coeruleus Integrity from 7 T MRI Relates to Apathy and Cognition in Parkinsonian Disorders. *Movement Disorders* 37, 1663–1672. <https://doi.org/10.1002/mds.29072>
- Yeo, B.T.T., Krienen, F.M., Sepulcre, J., Sabuncu, M.R., Lashkari, D., Hollinshead, M., Roffman, J.L., Smoller, J.W., Zöllei, L., Polimeni, J.R., Fischl, B., Liu, H., Buckner, R.L., 2011. The organization of the human cerebral cortex estimated by intrinsic functional connectivity. *Journal of Neurophysiology* 106, 1125–1165. <https://doi.org/10.1152/jn.00338.2011>
- Yoo, K., Rosenberg, M.D., Noble, S., Scheinost, D., Constable, R.T., Chun, M.M., 2019. Multivariate approaches improve the reliability and validity of functional connectivity and prediction of individual behaviors. *NeuroImage* 197, 212–223. <https://doi.org/10.1016/j.neuroimage.2019.04.060>
- Yoon, W.T., Chung, E.J., Lee, S.H., Kim, B.J., Lee, W.Y., 2005. Clinical Analysis of Blepharospasm and Apraxia of Eyelid Opening in Patients with Parkinsonism. *J Clin Neurol* 1, 159. <https://doi.org/10.3988/jcn.2005.1.2.159>
- Yoshiyama, Y., Higuchi, M., Zhang, B., Huang, S.-M., Iwata, N., Saido, T.C., Maeda, J., Sahara, T., Trojanowski, J.Q., Lee, V.M.-Y., 2007. Synapse Loss and Microglial Activation Precede Tangles in a P301S Tauopathy Mouse Model. *Neuron* 53, 337–351. <https://doi.org/10.1016/j.neuron.2007.01.010>
- Yoshiyama, Y., Lee, V.M.Y., Trojanowski, J.Q., 2013. Therapeutic strategies for tau mediated neurodegeneration. *Journal of Neurology, Neurosurgery & Psychiatry* 84, 784–795. <https://doi.org/10.1136/jnnp-2012-303144>
- Younes, K., Borghesani, V., Montembeault, M., Spina, S., Mandelli, M.L., Welch, A.E., Weis, E., Callahan, P., Elahi, F.M., Hua, A.Y., Perry, D.C., Karydas, A., Geschwind, D., Huang, E., Grinberg, L.T., Kramer, J.H., Boxer, A.L., Rabinovici, G.D., Rosen, H.J., Seeley, W.W., Miller, Z.A., Miller, B.L., Sturm, V.E., Rankin, K.P., Gorno-Tempini, M.L., 2022. Right temporal degeneration and socioemotional semantics: semantic behavioural variant frontotemporal dementia. *Brain* 145, 4080–4096. <https://doi.org/10.1093/brain/awac217>
- Young, A.L., Vogel, J.W., Robinson, J.L., McMillan, C.T., Ossenkoppele, R., Wolk, D.A., Irwin, D.J., Elman, L., Grossman, M., Lee, V.M.-Y., Lee, E.B., Hansson, O., 2023. Data-driven neuropathological staging and subtyping of TDP-43 proteinopathies (preprint). *Pathology*. <https://doi.org/10.1101/2023.01.31.23285242>
- Yu, M., Linn, K.A., Cook, P.A., Phillips, M.L., McInnis, M., Fava, M., Trivedi, M.H., Weissman, M.M., Shinohara, R.T., Sheline, Y.I., 2018. Statistical harmonization corrects site effects in functional connectivity measurements from multi-site fMRI data. *Hum Brain Mapp* 39, 4213–4227. <https://doi.org/10.1002/hbm.24241>
- Yu, M., Sporns, O., Saykin, A.J., 2021. The human connectome in Alzheimer disease — relationship to biomarkers and genetics. *Nat Rev Neurol* 17, 545–563. <https://doi.org/10.1038/s41582-021-00529-1>
- Zalesky, A., Fornito, A., Bullmore, E., 2012. On the use of correlation as a measure of network connectivity. *NeuroImage* 60, 2096–2106. <https://doi.org/10.1016/j.neuroimage.2012.02.001>
- Zhang, J., Wang, J., Xu, X., You, Z., Huang, Q., Huang, Y., Guo, Q., Guan, Y., Zhao, J., Liu, J., Xu, W., Deng, Y., Xie, F., Li, B., 2023. In vivo synaptic density loss correlates with impaired functional and related structural connectivity in

- Alzheimer's disease. *J Cereb Blood Flow Metab* 0271678X2311537. <https://doi.org/10.1177/0271678X231153730>
- Zhou, J., Gennatas, E.D., Kramer, J.H., Miller, B.L., Seeley, W.W., 2012. Predicting Regional Neurodegeneration from the Healthy Brain Functional Connectome. *Neuron* 73, 1216–1227. <https://doi.org/10.1016/j.neuron.2012.03.004>
- Zhou, J., Greicius, M.D., Gennatas, E.D., Growdon, M.E., Jang, J.Y., Rabinovici, G.D., Kramer, J.H., Weiner, M., Miller, B.L., Seeley, W.W., 2010. Divergent network connectivity changes in behavioural variant frontotemporal dementia and Alzheimer's disease. *Brain* 133, 1352–1367. <https://doi.org/10.1093/brain/awq075>
- Zhou, J., Seeley, W.W., 2014. Network Dysfunction in Alzheimer's Disease and Frontotemporal Dementia: Implications for Psychiatry. *Biological Psychiatry* 75, 565–573. <https://doi.org/10.1016/j.biopsych.2014.01.020>

9 Appendix

9.1 Publications

First author publications arising from my PhD at the time of submission:

Whiteside DJ, Jones PS, Ghosh BCP *et al*, Altered network stability in progressive supranuclear palsy. *Neurobiology of Aging*; 2021 107:109-117

Whiteside DJ, Malpetti M, Jones PS *et al*, Temporal dynamics predict symptom onset and cognitive decline in familial frontotemporal dementia. *Alzheimer's and Dementia*; 2022
doi: 10.1002/alz.12824

Whiteside DJ, Street D, Murley AG *et al*, Network connectivity and structural correlates of survival in progressive supranuclear palsy and corticobasal syndrome. *Human Brain Mapping*; Aug 1;44(11):4239-4255. doi: 10.1002/hbm.26342